The Chemistry of Radical Scavenging Antioxidants at Elevated Temperatures

Gareth John Moody

A thesis submitted for the degree of

Doctor of Philosophy

University of York

Department of Chemistry

April 2013

Abstract

In this study, the autoxidation of squalane inhibited by phenolic and aminic antioxidants was analysed between 160 and 220 °C representing piston assembly temperatures of automotive engines.

The mechanism of the phenolic antioxidant octadecyl 3-(3,5-di-*tert*-butyl-4-hydroxyphenyl) (OHPP) in the presence of oxygen at these temperatures was analysed. It was concluded that OHPP autoxidation formed four products; a hydroxyl-substituted phenolic, octadecyl 3-(3,5-ditert-butyl-4-hydroxy-phenyl)-3-hydroxy-propanoate, a hydroxyl-substituted quinone methide (octadecyl 3-(3,5-ditert-butyl-4-oxo-cyclohexa-2,5-dien-1-ylidene)-2-hydroxy-propanoate), and the previously observed hydroxycinnamate and di-tert-butyl benzoquinone. Quantification of the time development of these products indicates that benzoquinone is formed from hydroxycinnamate and not from the phenoxyl radical as previously thought. Mechanisms are suggested to account for this.

In the presence of alkyl hydroperoxide, the aminic antioxidant octylated diphenylamine (ODPA) was found to be less effective at high temperatures with large amounts of ODPA remaining at the end of the induction period where the substrate started to oxidise significantly. This is contrary to most previous studies where all the ODPA was consumed by the end of the induction period. The suggested reason for this is that autoxidation occurs preferentially by abstraction of tertiary hydrogen atoms, forming

tertiary alkyl peroxy radicals and hydroperoxides. The difference of the O-H bond strength of tertiary alkyl hydroperoxides and the N-H bond strength of ODPA was relatively small resulting in the abstraction of hydrogen atoms from ODPA by tertiary alkyl peroxy radicals being noticeably reversible at higher temperatures.

Aminic antioxidants containing naphthalene rings and heteroatom bridges were found to increase the induction period relative to substituted diphenylamines. The alkylated naphthenic antioxidant N-[4-(1,1,3,3-tetramethylbutyl)phenyl]naphthalen-1-amine could achieve this despite 53% of the reacted antioxidant in the initial stages forming dehydrodimer structures. N-(1-naphthyl)naphthalene-1-amine was investigated and was found to form the product (4E)-4-(1-naphthylimino)-1H-naphthalen-1-ol.

Based on the aminic antioxidants used, (1,1,3,3-tetramethylbutyl)-12H-benzo-α-phenothiazine was synthesised and used as an antioxidant in squalane autoxidation.

Table of Contents

Title Page i

Abstract ii

List of Contents iv

List of Tables ix

List of Figures xi

Abbreviations xviii

Acknowledgements xxi

Author's Declaration xxii

1.0 Introduction 2

1.1 Principles of engine lubrication 2

1.1.1 Introduction 2

1.1.2 Base oil types and composition 3

1.2 Hydrocarbon liquid-phase autoxidation 6

1.2.1 General mechanism of hydrocarbon oxidation 6

1.3 Lubricant additives package 8

1.3.1 Composition of a typical lubricant additive package 8

1.4 Inhibition of autoxidation by radical scavenging antioxidants 10

1.4.1 Inhibition of oxidation by phenolic antioxidants 10

1.4.2 Inhibition of oxidation by aminic antioxidants 15

1.5 Synergistic effects of antioxidants 18

1.5.1 Phenolic and aminic antioxidants 19

1.5.2 Antioxidant and peroxide decomposer 19

1.6 Inhibition of autoxidation by peroxide decomposers 20

1.7 Inhibition of oxidation by metal deactivators 22

1.8 Defining piston ring conditions 23

1.9 Project aims 25

2.0 Experimental 28

2.1 Bench-top continuous flow reactor 28

2.1.1 Bench-top reactor 28

2.1.2 Sample preparation....31
2.1.3 Reactor heating....31
2.1.4 Reactor setup....31
2.1.5 Reaction conditions....33
2.1.6 Reaction start up procedure....34
2.2 Product analysis....35
2.2.1 Gas chromatography (GC)....35
2.2.2 Gas chromatography – Mass spectrometry (GC-MS)....36
2.2.3 Gel permeation chromatography (GPC)....37
2.2.4 UV-VIS spectroscopy....37
2.2.5 Nuclear Magnetic Resonance (NMR)....38
2.2.6 Electron Spin Resonance (ESR)....38
2.2.7 Determination of hydroperoxide concentration....42
2.2.8 Determination of induction period and oxygen uptake....43
2.2.9 Column chromatography....46
2.3 Thermochemical calculations using the computational chemistry software Gaussian09W....47
2.3.1 Principles and uses....47
2.3.2 Method selection....47
2.3.3 Method testing....48
2.3.4 Example Gaussian calculation....50
2.4 Materials....52
3.0 The Antioxidant Mechanisms of a Hindered Phenolic Antioxidant....56
3.1 Introduction....56
3.2 Previous work....58
3.2.1 Mechanistic studies on BHT and OHPP....58
3.3 Results and discussion....62
3.4 GC analysis of a OHPP oxidation run....63
3.4.1 Starting material analysis....63
3.4.2 Antioxidant quantification....65
3.4.3 New product identification....66
3.5 Product identification using GC-MS....69
3.6 Antioxidant intermediate quantification....77
3.7 Hydroxycinnamate synthesis....78

3.7.1 Steglich esterification of antioxidant intermediate 78
3.7.2 Column chromatography purification 79
3.7.3 NMR analysis 80
3.8 Synthesised hydroxycinnamate as a standard 84
3.8.1 GC analysis 84
3.8.2 GC-MS analysis 85
3.8.3 UV-vis analysis 86
3.8.4 GPC analysis 87
3.9 Synthesised hydroxycinnamate as an antioxidant 90
3.9.1 Autoxidation of hydroxycinnamate in squalane 90
3.9.2 Product analysis 91
3.10 Phenolic antioxidant mechanism 94
3.11 Conclusions 98
4.0 Antioxidant properties of an Alkylated Diphenylamine under Piston Ring Conditions 101
4.1 Introduction 101
4.2 Previous work 102
4.2.1 Oxidation work 103
4.2.2 Mechanistic studies of aminic antioxidants 104
4.3 ODPA high temperature oxidation 105
4.3.1 Autoxidation using continuous flow reactor 105
4.3.2 Autoxidation by in situ ESR 107
4.4 GC analysis of ODPA from continuous flow oxidation reaction 109
4.4.1 Antioxidant product identification 110
4.4.2 Antioxidant quantification during oxidation runs 115
4.5 Possible critical antioxidant concentration of ODPA 118
4.6 Alkyl hydroperoxides in autoxidation 120
4.6.1 Alkyl hydroperoxide quantification 121
4.7 The effect of alkyl hydroperoxides on ODPA 124
4.8 Thermodynamics of the alkyl peroxy radical reaction with ODPA ... 132
4.8.1 Enthalpy of reaction 134
4.8.2 Entropy of reaction 136
4.8.3 Gibbs energy from enthalpy and entropy results 137
4.9 Equilibrium constant of the alkyl peroxy radical reaction with ODPA 139

4.10 The effects of peroxide decomposers on the lifetime of radical scavenging antioxidants 141
4.10.1 Selecting a suitable peroxide decomposer 142
4.10.2 The peroxide decomposer TPP as an antioxidant 143
4.10.3 ODPA and peroxide decomposer together 144
4.11 Conclusions 148
4.11.1 ODPA oxidation results 148
4.11.2 Critical concentration of ODPA 148
4.11.3 Peroxide quantification 149
4.11.4 The effect of alkyl hydroperoxides on ODPA 149
4.11.5 Thermodynamics and equilibrium constant of reaction 150
4.11.6 The effect of peroxide decomposers on antioxidants 151
4.11.7 Subsequent work on aminic antioxidants 152
5.0 The Antioxidant properties of other aminic antioxidants under Piston Ring Conditions 155
5.1 Introduction 155
5.1.1 Previous work 155
5.2 Bond dissociation energies of the N-H bond in diphenylamines 156
5.3 Autoxidation of DPAOMe in squalane 160
5.3.1 Oxidation of DPAOMe under piston ring conditions 160
5.3.2 Concentration of DPAOMe during the induction period 162
5.3.3 DPAOMe and peroxide decomposer in squalane 163
5.4 PANA type antioxidant 165
5.5 Oxidation reactions of OPANA under piston ring conditions 166
5.6 Intermediate product formation during oxidation reactions of OPANA at high temperatures 167
5.6.1 Product quantification 169
5.6.2 Product identification 171
5.7 Comparison of diphenylamine with mononaphthalene -monophenyl antioxidants. 175
5.8 Dinaphthalene aminic antioxidants 180
5.8.1 Autoxidation of dinaphthalene antioxidants in squalane 182
5.8.2 Identification of intermediate species for NANA1. 183
5.9 Induction period and N-H bond dissociation energy correlation 187

5.10 Heteroaromatic aminic antioxidants 190
5.10.1 High temperature oxidation of phenothiazine and phenoxazine 192
5.11 New antioxidant synthesis and induction period 195
5.11.1 Synthesis of the new antioxidant (SOPANA) 195
5.11.2 High temperature oxidation of SOPANA 198
5.12 Conclusions 200
5.13 Future work 204
A. Appendix to Chapter 3 206
B Appendix to Chapter 4 212
References 215

List of Tables

Table 1.1 – API mineral base oil classifications 3

Table 1.2 – Overview of the processing of base oil fractions[5,8,9,10] 5

Table 1.3 – Overview of hydrocarbon oxidation reactions,[11,12,16,17] 6

Table 1.4 Typical additives used in an automotive lubricant[7,5] 9

Table 1.5 – Bond dissociation energies of a primary, secondary and tertiary C-H bond compared to the O-H dissociation energy of a typical phenolic antioxidant 12

Table 1.6 – Rate constants of alkyl radicals with oxygen and peroxy radicals with hydrocarbon compared to their reactions with quinone 13

Table 1.7 – Stoichiometric coefficient per phenolic head group of phenolic antioxidants 14

Table 1.8 – Stoichiometric coefficient of aminic antioxidants 18

Table 1.9 – Changes in the V-8 engine over the past seven decades [3] 24

Table 2.1 - Table of reactor equipment used 33

Table 2.2 – Comparison of calculated N-H bond dissociation energies with a known experimental value for 4-methyl-N-(p-tolyl)aniline 49

Table 2.3 – Conversion factors for Gaussain output 51

Table 2.4 – List of materials used 52

Table 3.1 – Accurate mass spec fragmentation of product D of mass 528 71

Table 3.2 – Quinone methide alcohol accurate mass spec fragmentation 75

Table 3.3 – Phenolic antioxidant alcohol accurate mass spec fragmentation 76

Table 3.4 – NMR shifts of hydroxycinnamate compared to expected shifts 83

Table 4.1 – Reaction scheme to test influence of oxidised squalane 126

Table 4.2 – Summary of influence of enthalpy and entropy on gibbs free energy 134

Table 4.3 – Bond dissociation energies of antioxidant and alkyl hydroperoxides with experimental errors 135

Table 4.4 – Entropy change of reaction of antioxidant with alkyl peroxy radicals as shown in Figure 4.20 136

Table 4.5 – Summary of enthalpy and entropy values and the temperature at which the forwards reaction becomes unfavourable 138

Table 4.6 – Examples of ceiling temperatures of reactions 141

Table 5.1 – N-H bond dissociation energies of para substituted diphenylamines 158

Table 5.2 – Comparison of thermodynamic data of ODPA and DPAOMe with alkyl peroxy radicals 160

Table 5.3 – Percentage of antioxidant going on to form intermediates 171

Table 5.4 – Accurate mass spectroscopy of OPANA, SOPANA and benzophenothiazone 198

List of figures

Figure 1.1 – Hydrocarbon oxidation chain step cycle 7

Figure 1.2 – Overview of phenolic antioxidant interaction with an alkane undergoing autoxidation. [11,12,26,27] 11

Figure 1.3 – The well established phenolic antioxidant mechanism 13

Figure 1.4 – Low temperature aminic antioxidant mechanism 16

Figure 1.5 – High temperature (120 °C+) aminic antioxidant mechanism 17

Figure 1.6 – Aminic antioxidant regeneration mechanism 19

Figure 1.7 – Structure of ZDDP 20

Figure 1.8 – Schematic of ZDDP layer 21

Figure 1.9 – Two contrasting film formations of ZDDP (a) progressive thickening (b) progressive coverage 21

Figure 1.10 – Antioxidant mechanism of ZDDP 22

Figure 1.11 – Metal catalysed decomposition of alkyl hydrogen peroxide 23

Figure 1.12 – Example of a triazole metal deactivating compound 23

Figure 1.13 – Diagram showing top piston ring area on an automotive piston of a diesel engine 25

Figure 2.1 – 49 cm^3 stainless steel reactor with magnetic stirrer 29

Figure 2.2 – Reactor lid and base from side 30

Figure 2.3 – Reactor lid schematic 30

Figure 2.4 Schematic of the overall reactor set up 32

Figure 2.5 - Oxidation of squalane at 180 – 220 °C without stirring 34

Figure 2.6 – The three stages of ESR spectra of an in situ oxidation run 40

Figure 2.7 – The Jeol JES-RE1X ESR machine and close up of cavity on the right 41

Figure 2.8 – Reaction between triphenylphosphine and alkyl hydroperoxide 43

Figure 2.9 – Oxygen sensor output 44

Figure 2.10 - Structure of 4-methyl-N-(p-tolyl)aniline 48

Figure 3.1 – Structure of α-tocopherol (vitamin E) 56

Figure 3.2 - octadecyl 3-(3,5-ditert-butyl-4-hydroxy-phenyl)propanoate 57

(OHPP) 57

Figure 3.3 – Recap of Figure 1.3, the well-established phenolic antioxidant mechanism 58

Figure 3.5 – Octadecyl (E)-3-(3,5-ditert-butyl-4-hydroxy-phenyl)prop-2-enoate (Hydroxycinnamate) 60

Figure 3.6 – Quninone methide rearrangement to form hydroxycinnamate 61

Figure 3.7 –Reaction of quinone methide with water 61

Figure 3.8– Oxygen uptake during autoxidation of OHPP in squalane between 180 and 220 °C 63

Figure 3.9 – GC trace of starting material containing 7.5 x10^{-3} mol dm^{-3} of OHPP 64

Figure 3.10 – GC trace of material containing 7.5 x10^{-3} mol dm^{-3} of OHPP after 30 minutes. 65

Figure 3.11– Antioxidant and squalane ketone concentration at 180 °C 66

Figure 3.11 – GC trace of 20 – 30 minute region of the starting material (top) and a sample taken after 20 minutes in to the induction period at 180 °C 67

Figure 3.12 - GC trace of the 50 – 65 minute region of the starting material (top) and a sample taken after 20 minutes in to the induction period at 180 °C 68

Figure 3.13 – Structure of 2,6-ditert-butyl-1,4-benzoquinone (quinone) 69

Figure 3.14 – The two possible structures of product (D) 70

Figure 3.15 – Structures of possible fragments of Di and Dii. 71

Figure 3.16 – Product D fragmentation 72

Figure 3.17 – Decarboxylation mechanism of di-tert butyl coumaric acid 73

Figure 3.18 – Resonance structures of coumaric acid which aid decarboxylation. 74

Figure 3.19 - Octadecyl 3-(3,5-ditert-butyl-4-oxo-cyclohexa-2,5-dien-1-ylidene)-2-hydroxy-propanoate (C) 76

Figure 3.20 - Proposed Phenolic antioxidant alcohol structure octadecyl 3-(3,5-ditert-butyl-4-hydroxy-phenyl)-3-hydroxy-propanoate (B) 77

Figure 3.21 - Concentrations of starting antioxidant and build-up of intermediate products during a run at 180 °C 78

Figure 3.22 – Steglich esterification reaction to make hydroxycinnamate 79

Figure 3.24 – Predicted NMR spectra of hydroxycinnamate 81

Figure 3.25 – Predicted NMR spectra of quinone methide 82

Figure 3.26 – Hydroxycinnamate H^1 NMR shifts at 400 MHz 83

Figure 3.27 – GC traces of Hydroxycinnamate from synthesis, oxidation and a mixture of the two 85

Figure 3.28 - MS traces of Hydroxycinnamate from synthesis, oxidation and a mixture of the two 86

Figure 3.29 – UV spectra of quinone, hydroxycinnamate and OHPP starting antioxidant 87

Figure 3.30 – GPC trace of OHPP in squalane reaction starting material 88

Figure 3.31 – GPC trace of an oxidation run of OHPP in squalane at 180 °C, sampled after 20 minutes 89

Figure 3.32 – GPC trace of an artificial mix of OHPP and synthesised hydroxycinnamate at the same ratios as an oxidation sample as determined by GC 90

Figure 3.33 – Induction periods of hydroxycinnamate and OHPP in squalane at 180 °C 91

Figure 3.34 – Mass spectra of the product C and quinone from hydroxycinnamate oxidation 92

Figure 3.35 – Recap of structures (C) and quinone 92

Figure 3.36 – Quantification of hydroxycinnamate and hydroxycinnamate during the induction period 93

Figure 3.37 – Overview of the products formed and their order of formation during oxidation runs using OHPP 94

Figure 3.38 – Hydrogen abstraction starting points and their relevant bond dissociation energies 95

Figure 4.1 - 4-(1,1,3,3-tetramethylbutyl)-N-[4-(1,1,3,3-tetramethylbutyl) phenyl]aniline aka octylated diphenylamine (ODPA) 102

Figure 4.2 - Structure of N-[4-(1,1,3,3-tetramethylbutyl)phenyl]naphthalen-1-amine (PANA) 103

Figure 4.3 – DPA Antioxidant and alkyl hydroperoxide equilibria 104

Figure 4.4 – Comparison of induction periods of OHPP and ODPA in squalane between 140 and 220 °C 107

Figure 4.5 – Oxygen consumption of squalane containing 100 ppm TEMPO and 100 ppm antioxidant at 170 °C with fixed oxygen volume 108

Figure 4.7 – GC trace of ODPA in squalane starting material 110

Figure 4.8 – GC trace of starting material 39-50 minute region of the GC trace 111

Figure 4.9 – GC trace of 10 minute sample 39-50 minute region of the GC trace 112

Figure 4.10 – Mass spec fragmentation pattern of ODPA and ODPAP 113

Figure 4.11 – Proposed structure for the ODPA product ODPAP 113

Figure 4.12 – Proposed mechanism for the formation of ODPAP 114

Figure 4.13 - Resonance reaction of intermediate species 115

Figure 4.16 – Comparison of GC traces of 7.5 $x10^{-3}$ mol dm^{-3} OHPP after 30 minutes and 7.5 $x10^{-3}$ mol dm^{-3} ODPA after 25 minutes 116

Figure 4.17 – Concentration of ODPA remaining at end of induction period at various temperatures using an initial ODPA concentration of 7.5 $x10^{-3}$ mol dm^{-3} 117

Figure 4.18 – ODPA concentration at induction period end from an initial ODPA concentration of 7.5, 15 and 30 $x10^{-3}$ mol dm^{-3} 119

Figure 4.19 – Induction periods of ODPA with initial concentrations of 5.9 $x10^{-3}$ mol dm^{-3} and 9.6 $x10^{-4}$ mol dm^{-3} at 180 °C 120

Figure 4.20 – Recap of Reactions 1.3.2 and 1.3.3 from Chapter 1 121

Figure 4.21 – Alkyl hydroperoxide quantification during oxidation runs of OHPP and ODPA at a concentration of 7.5 $x10^{-3}$ mol dm^{-3} in squalane at 180 °C 122

Figure 4.22 – Concentrations of alkyl hydroperoxide and ODPA at the end of the induction period 124

Figure 4.23 – The effect of adding oxidised squalane to squalane, OHPP in squalane and ODPA in squalane 127

Figure 4.24 – The Jensen antioxidant regeneration mechanism 129

Figure 4.25 – Summary of the concentration of ODPA and OHPP remaining at the time ODPA stopped working at temperatures between 140 and 220 °C 131

Figure 4.26 – Equilibrium reaction of diphenylamine and cumyl peroxy radicals..... 132

Figure 4.27 – General reaction scheme of substituted diphenylamine antioxidant with alkyl peroxy radicals 134

Figure 4.28 – Graph of K Vs T of theoretical and experimental results 140

Figure 4.29 – The reactions of the phosphite triphenylphosphine with alkyl hydroperoxide, alkyl peroxy radicals and alkoxy radicals 143

Figure 4.30 – Induction period of 0.5 % TPP at 180 °C 144

Figure 4.31 – Synergistic properties of peroxide decomposer and antioxidant compared to the sum of the individual component lifetimes at 180 °C..... 145

Figure 4.32 – TPP, ODPA and hydroperoxide concentration during induction period 147

Figure 5.1 – Structures of ODPA, PAN and phenothiazine..... 156

Figure 5.2 – Recap of the reaction between aminic antioxidant and alkyl peroxy radicals 157

Figure 5.3 – Diphenylamine and para substituent positions 157

Figure 5.4 – Structure of 4-methoxy-N-(4-methoxyphenyl)aniline (DPAOMe)..... 159

Figure 5.5 – Induction periods of DPAOMe in squalane compared to ODPA squalane and squalane without antioxidant from 180 to 220 °C..... 161

Figure 5.6 – DPAOMe concentration and oxygen uptake during the induction period of an oxidation run at 180 °C 162

Figure 5.7 – Synergistic properties of peroxide decomposer and the antioxidants ODPA and DPAOMe and the individual components at 180 ºC..... 164

Figure 5.8 – Structure of N-[4-(1,1,3,3-tetramethylbutyl)phenyl]naphthalen-1-amine (OPANA) 166

Figure 5.9 – Oxygen uptake of 7.55 x10^{-3} mol dm^{-3} concentration of OPANA in squalane between 180 and 220 ºC 166

Figure 5.10 – GC-FID chromatogram of OPANA in squalane starting material using a 5 % -phenyl 95 %-dimethylpolysiloxane column 168

Figure 5.11 - GC trace of OPANA in squalane after 1.5 hours at 180 °C 169

Figure 5.12 – OPANA and intermediate concentration over time at 180 °C 170

Figure 5.13 – GC trace from the GC-MS analysis 172

Figure 5.14 – Mass spectra analysis of OPANA 172

Figure 5.15 – Mass spectra of intermediate species of ODPA oxidation 173

Figure 5.16 – Possible resonance structures of OPANA radical 174

Figure 5.17 – Some possible products by radical-radical combinations of the resonance structures of OPANA 175

Figure 5.18 – Alkyl hydroperoxide concentration and antioxidant concentration of OPANA in squalane at 180 ºC 177

Figure 5.19 – Comparison of alkylhydroperoxide build up in OHPP, ODPA and OPANA 178

Figure 5.20 – Reaction of OPANA with alkyl peroxy radicals 179

Figure 5.21 – Three structures of dinaphthalene aminic antioxidants 181

Figure 5.22 – Induction periods of NANA1 and NANA2 between 180 and 220 °C 182

Figure 5.23 – Colour changes during a N-(1-naphthyl)naphthalene-1-amine run 183

Figure 5.24 – NANA1 sample at the start of the reaction and after 4 hours 184

Figure 5.25 – Mass spectra of starting antioxidant 185

Figure 5.26 – Mass spectra of new intermediate peak at 50.08 minutes 186

Figure 5.28 – Correlation plot between N-H bond dissociation energy and induction period of aminic antioxidants tested 188

Figure 5.29 – Structures of phenothiazine (left) and phenoxazine (right) 190

Figure 5.30 – Reaction of phenothiazine with alkyl hydroperoxide 191

Figure 5.31 – Mechanism of peroxide decomposition by phenothiazine 192

Figure 5.32 – Induction periods of phenothiazine and phenoxazine between 180 and 220 °C 193

Figure 5.33 – Synthesis of the novel aminic antioxidant 196

Figure 5.34 – GC-MS of SOPANA synthesis material post column purification 196

Figure 5.35 – Mass spectra of SOPANA and benzophenothiazine 197

Figure 5.36 – Ratios of material obtained from the reaction of OPANA with sulfur ... 198

Figure 5.37 – Induction periods of SOPANA compared to OPANA at 180, 200 and 220 °C 199

Figure 5.38 – Recap of the aminic antioxidants used in this work and their abbreviations and induction period ranking in brackets when used in squalane at 180 ºC 201

Abbreviations

ADPA	Alkylated diphenylamine
API	American Petroleum Institute
b.p	Temperature of boiling at 1atm pressure
BHP	Brake horse power
BHT	Butylated hydroxy toluene
DPAOME	4-methoxy-N-(4-methoxyphenyl)aniline
ESR	Electron spin resonance
FID	Flame ionisation detector
GC	Gas Chromatography
GC-CI/MS	Gas Chromatography coupled with chemical ionisation mass spectrometry
GC-EI/MS	Gas Chromatography coupled with electron impact ionisation mass spectrometry
GC-FI/MS	Gas Chromatography coupled with field ionisation mass spectrometry
GC-MS	Gas Chromatography coupled with Mass spectrometry
GPC	Gel permeation chromatography
+I	Electron donating inductive effect
-I	Electron withdrawing inductive effect
Irganox L01	4-(1,1,3,3-tetramethylbutyl)-N-[4-(1,1,3,3-tetramethylbutyl)phenyl]aniline
Irganox L06	N-[4-(1,1,3,3-tetramethylbutyl)phenyl]naphthalen-1-amine
Irganox L107	Octadecyl 3-(3,5-ditert-butyl-4-hydroxy-phenyl)propanoate

K	Equilibrium constant
K	Kelvin – unit of temperature
k	Rate constant
+M	Electron donating mesomeric effect
-M	Electron withdrawing mesomeric effect
m.p	Temperature of melting at 1 atm pressure
M_r	Relative molecular mass
N_2	Nitrogen
NANA1	N-(1-naphthyl)naphthalene-1-amine
NANA2	N-(2-naphthyl)naphthalene-2-amine
NMR	Nuclear magnetic resonance
O_2	Oxygen
ODPA	Octylated diphenylamine
OHPP	Octadecyl 3-(3,5-ditert-butyl-4-hydroxy-phenyl)propanoate
OPANA	N-[4-(1,1,3,3-tetramethylbutyl)phenyl]naphthalen-1-amine
PAN	Phenyl alpha naphthylamine
PAO	Polyalphaolefins
Phenolic	Sterically hindered phenol
Quinone	2,6-ditert-butyl-1,4-benzoquinone
R	Molar gas constant, R = 8.314 J mol^{-1} K^{-1}
$R^{\cdot}$	Alkyl radical
RH	Alkane
$RO^{\cdot}$	Alkoxyl radical

ROH	Alcohol
$ROO^{\cdot}$	Alkyl peroxy radical
ROOH	Alkyl hydroperoxide
SOPANA	(1,1,3,3-tetramethylbutyl)-12H-benzo-α-phenothiazine
Squalane	2,6,10,15,19,23-hexamethyltetracosane
TPP	Triphenylphosphine
UV-vis	Ultraviolet and visible spectroscopy
%wt	The weight by % of a reagent relative to the total reaction mixture
ZDDP	Zincdialkyldithiophosphate
λ_{max}	Wavelength at which the maximum UV-vis signal was observed

Acknowledgements

Firstly, I would like to thank my supervisors Dr Moray Stark and Dr Victor Chechik for all their help over the past four years.

I would also like to thank my industrial supervisors Dr Kevin West and Dr Matthias Hof for their support and suggestions throughout the project and also Castrol and BASF for funding the project.

Next, a big thank you to everyone in Green Chemistry for making it such a great place to work and in particular thanks to Bernie and Pete for their ideas and for putting a smile on my face on a daily basis, and also to Jimbo for introducing me to the delights of test match cricket when I had a particularly long reaction going.

Finally, thank you to my family and in particular my parents. Yes it is possible to still be a student in your early 30's! Also, to my wife Joanna for her support and for being my walking thesaurus during the writing of this thesis and more importantly for not giving birth to our first child until I had time to finish writing.

Author’s declaration

The High Resolution Mass Spectrometry with Field Ionisation and Electron Impact were performed by K. Heaton and T. Dransfield (University of York). The High Resolution Proton Nuclear Magnetic Resonance analysis was performed by J. Sherwood (University of York).

Chapter 1

Introduction

1.0 Introduction

1.1 Principles of engine lubrication

Automotive engine lubricants are an essential element to an engine by increasing efficiency through reduced friction and protecting the components from wear and helping to dissipate heat generated by the engine.

1.1.1 Introduction

To protect a lubricant from high temperature, autoxidation antioxidants are used. Antioxidants exist in a variety of forms in a wide range of applications from biological antioxidants found in food such as vitamin E which protects tissue from oxidation[1,2] to synthetic antioxidants such as Zinc dialkyldithiophosphate (ZDDP) which are used in automotive engine oils and industrial applications such as gear oils.[3] Antioxidant containing lubricants are essential in the presence of extreme conditions and moving parts. The study of these interacting surfaces in motion is known as tribology.

The tribological properties of friction and wear are particularly relevant to an automotive engine where surfaces moving at high speed can quickly become damaged. Friction and wear can be significantly reduced by the addition of a substance such as a hydrocarbon fluid which can prevent surfaces from rubbing against each other whilst dissipating heat.[4] This is known as lubrication and the fluid is known as the lubricant.

Early engine lubricants consisted of the residue from the petroleum distillation which when simply refined provided basic lubricant properties.[5] However, advances in engine technology meant that more effective lubricants were required to cope with the increases in surface motion and heat in the engine. This led to improved refining processes and the introduction of additives into lubricants.

1.1.2 Base oil types and composition

A variety of base oils are used in lubricants. As base oils make up the bulk of a lubricant formulation it is important to have consistent material to aid compatibility of formulations. Base oils can be split into one of five classes. Of these, according to the classification produced by the American Petroleum Institute (API), mineral oils make up classes I to III, synthetic are class IV and class V is other.[6] Details of each group are listed in Table 1.1 including viscosity index which is a scale used to assess how the viscosity changes with temperature. The lower the value, the lower the change.

Table 1.1 – API mineral base oil classifications

Group	Saturated (%wt)	Sulfur (%wt)	Viscosity index
I	< 90	> 0.03	≥ 80 but < 120
II	≥ 90	≤ 0.03	≥ 80 but < 120
III	≥ 90	< 0.03	≥ 120

Base oil categorisation will be dependent upon the origin of the crude oil and the extent of the refining process.

Group IV - Base stocks are polyalphaolefins (PAO). According to the API, 'PAOs can be interchanged without additional qualification testing as long as the interchange PAO meets the original PAO manufacturer's specifications in physical and chemical properties.' Key specification parameters that are set by PAO manufacturers are:

1) Kinematic viscosity at 100 °C, 40°C, and -40 °C
2) Viscosity index
3) NOACK volatility (evaporation loss after 1 hour at 250 °C the lower the better)
4) Pour point (the temperature at which the sample stops being pourable)
5) Unsaturates

Group V – These base stocks cover all other base stocks not included in Group I, II, III, or IV and include base oils such as esters.

1.1.2 Base oil refinement

The process of refining is used to purify the base oil and helps standardise base oils which can originate from any one of hundreds of oilfields throughout the world. Prior to the distillation of the crude oil, it is desalted to remove impurities such as salt and clay by washing the crude oil with hot water at 65- 90 °C.[7]

The crude oil is then distilled and fractionated according to the boiling points of the constituents of the crude mixture. Before being suitable to be used as a base oil in a lubricant, the relevant fractions must first be processed further to remove undesirable components from the fraction.

Table 1.2 – Overview of the processing of base oil fractions[5,8,9,10]

Process	Description
Deasphalting	Removal of polar species including some nitrogen and sulfur containing material.
Dewaxing	The removal of wax forming molecules such as straight chain alkanes to improve low temperature stability.
Hydrofinishing	Increasing of oxidative stability of the oil by hydrogenation.
Desulfurization	The removal of sulfur to improve base oil quality and reduce combustion emissions.

Although these processes improve the quality of the base oil and its oxidative stability, they are insufficient to prevent rapid autoxidation at high temperatures such as those seen in an internal combustion engine.

1.2 Hydrocarbon liquid-phase autoxidation

The autoxidation of hydrocarbons is a process where the oxidation steps are self-accelerating. Initiation of an alkane (RH) can occur thermally in the presence of oxygen (Reaction 1.3.1) requiring energy in the region of 125 – 188 kJ mol^{-1}.[11] This is significantly lower than direct thermal cracking of an alkane which requires 293 – 419 kJ mol^{-1}. Once initiated however, the dominant reaction involving the production of alkyl radicals (R·) can be attributed to the radical products formed by the decomposition of peroxide (Reaction 1.3.4).[12] The propagation step (Reaction 1.3.2) has no energy barrier,[13] is highly exothermic[14] and has a rate constant in the region of 1 x10^9 dm^3 mol^{-1} s^{-1} at 373 K.[15]

1.2.1 General mechanism of hydrocarbon oxidation

Table 1.3 – Overview of hydrocarbon oxidation reactions[11,12,16,17]

Phase	Reaction	Reaction Number
Initiation	$RH + O_2 \rightarrow$Products	1.3.1
Propagation	$R\bullet + O_2 \rightarrow ROO\bullet$	1.3.2
	$ROO\bullet + RH \rightarrow ROOH + R\bullet$	1.3.3
Branching	$ROOH \rightarrow RO\bullet + HO\bullet$	1.3.4
	$RO\bullet + RH \rightarrow ROH + R\bullet$	1.3.5
	$HO\bullet + RH \rightarrow H_2O + R\bullet$	1.3.6
Termination	$R\bullet + R'\bullet \rightarrow RR'$	1.3.7
	$R\bullet + R'OO\bullet \rightarrow R'OOR$	1.3.8
	$RCH_2OO\bullet + R'OO\bullet \rightarrow RCHO + R'OH + O_2$	1.3.9

Reaction 1.3.3 of Table 1.3, is also of particular importance to hydrocarbon autoxidation as this is the propagation step which also results in the production of alkyl radicals and resulting in mass oxidation of the hydrocarbon[18] base fluid as shown in Figure 1.1 The formation of alkyl radicals from both this reaction and the peroxide decomposition step are prevented from occurring by the use of radical scavenging antioxidants.

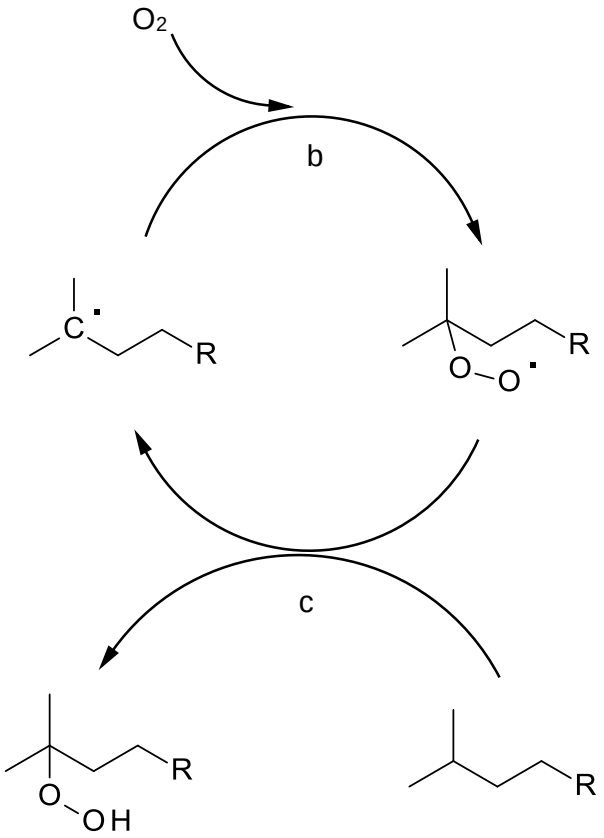

Figure 1.1 – Hydrocarbon oxidation chain step cycle [12]

Alkyl peroxide decomposition reactions (1.3.4) produce two radicals, both of which can initiate further oxidation chain reactions by the production of more alkyl radicals

(Reactions 1.3.5 and 1.3.6). The formation of alkoxy radicals ($RO^{\cdot}$) by the decomposition of peroxides (Reaction number 1.3.4) can also to a lesser extent lead to hydrocarbon cleavage mechanisms and the formation of aldehydes, ketones[19] and carboxylic acids [20,21,22,23] which can cause corrosion.[24] Cross linking reactions are also known to occur[25] which increase the viscosity of the oil, which can in turn lead to the formation of sludge deposits.[7]

1.3 Lubricant additives package

1.3.1 Composition of a typical lubricant additive package

The base fluid typically makes up between 75 and 95% of the oil[7] with the remainder made up of additives, which are functional molecules with specific roles. A typical automotive lubricant composition will contain around 9 different classes of additives, each with a specific role.[3] It is also common for the oil to contain different varieties of any one additive to improve the performance of the lubricant or to increase the lifetime of it.[5] The following is a list (although not comprehensive) of common additives and their typical treat rates in a lubricant.

Table 1.4 Typical additives used in an automotive lubricant[7,5]

Additive type	Typical example	Use	Treat amount
Dispersant	Overbased calcium sulfonate	Disperse oil insoluble material e.g acidic material	~5%
Detergent	Polyisobutylene succinimide	Solublise soot, prevent corrosion	~3%
Primary antioxidant (Radical scavenger)	Phenolic/Aminic Antioxidant	Prevent base oil oxidation	~0.5%
Organic friction modifier	Fatty acid methyl ester (FAME)	Friction reduction	~0.5%
Inorganic friction modifier	MoDTC	Friction reduction	~0.5%
Viscosity modifier	High Mw polymer 10,000+	Reduces temperature dependence of viscosity	~6%
Pour point depressant	Polyalkyl phenols	Prevent wax build up. Maintain low temperature fluidity	~0.5%
Demulsifier	Alkali metal salts	Enhance water separation	~0.05%
Foam inhibitor	Poly siloxanes	Prevent foam build up	~0.0001%
Multi-purpose	Zinc dialkyl dithiophosphate (ZDDP)	Antioxidant, antiwear, corrosion inhibitor	~1.5%

Prevention of lubricant oxidation can be achieved by the use of peroxide decomposers, radical scavenging antioxidants or metal deactivators.

1.4 Inhibition of autoxidation by radical scavenging antioxidants

Antioxidants are radical scavengers that work by preferentially reacting with alkyl peroxy radicals formed during hydrocarbon autoxidation. They are able to achieve this by having a lower bond dissociation energy (BDE) than the corresponding C-H bond of the base oil. The two main examples of bonds with lower BDEs than the C-H of the base oil are O-H of phenolic antioxidants and N-H of aminic antioxidants. The radicals formed by antioxidants are also sufficiently unreactive to react with oxygen or the hydrocarbon.

1.4.1 Inhibition of oxidation by phenolic antioxidants

Phenolic type antioxidants work by preferentially reacting with alkyl peroxy radicals formed during autoxidation and so are classified as radical scavenging antioxidants (step 5 of Figure 1.2). The reaction with alkyl peroxy radicals stops the chain propagation steps in autoxidation, preventing the hydrocarbon from being significantly degraded (step 3 of Figure 1.2).

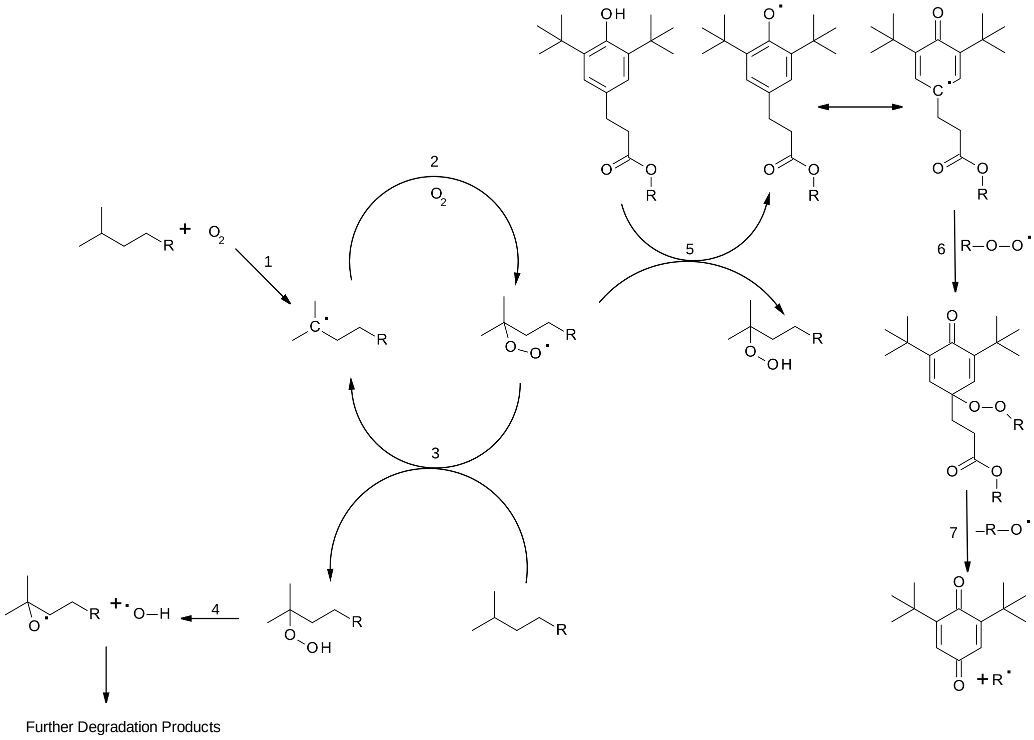

Figure 1.2 – Overview of phenolic antioxidant interaction with an alkane undergoing autoxidation. [11,12,26,27]

A phenolic antioxidant is able to achieve this due to the weak O-H bond of the phenol which is considerably weaker than a primary, secondary or even tertiary C-H bond. The dissociation energy of the O-H bond in phenol is 369.5± 6.3 kJ mol^{-1}. [28] The addition of +I and +M groups to the ortho and para positions of the ring, can significantly lower the O-H bond dissociation energy further. The addition of groups such as hydrocarbon chains will also increase the size of the molecule making it less volatile at high temperatures and will also increase its solubility in non-polar fluids such as automotive lubricants.

Table 1.5 – Bond dissociation energies of a primary, secondary and tertiary C-H bond compared to the O-H dissociation energy of a typical phenolic antioxidant

Compound	Bond type	Dissociation energy kJ mol^{-1} [29,30,31,32]
Octadecyl 3-(3,5-ditert-butyl-4-hydroxy-phenyl)propanoate	O-H	339.6±0.4
Tertiary alkyl C-H	R_3C-H	400.0±2.9
Secondary alkyl C-H	R_2HC-H	411.1±2.2
Primary alkyl C-H	RH_2C-H	425.5±2.1

The abstraction of a hydrogen from the phenolic antioxidant leads to the formation of a phenoxy radical (i of Figure 1.3). This radical is resonance stabilised by the aromatic ring of the phenol (ii of Figure 1.3). The resonance structure can then go on to react with a second alkyl peroxy radical.[27] The peroxide bond will then decompose (iv of Figure 1.3), forming a quinone structure (v of Figure 1.3).[26] The resulting quinone is thought to have an affinity for both alkyl radicals[33] and peroxy radicals.[34] However, due to the relatively low rate constants of these reactions (as shown in Table 1.6) compared to the rate constants of an alkyl radical reacting with oxygen[35] and a peroxy radical abstracting a hydrogen from either the base oil or an antioxidant, these reactions are thought to contribute little in the presence of oxygen.

Table 1.6 – Rate constants of alkyl radicals with oxygen and peroxy radicals with hydrocarbon compared to their reactions with quinone

Radical	Reagent	Rate constant k L mol^{-1} s^{-1}	Temp/K	Ref
$C_6H_{11}^{\cdot}$	O_2	2.0×10^{9}	298	36
$C_6H_{11}^{\cdot}$	p-Quinone	4.6×10^{7}	350	37
$C_6H_{11}O_2^{\cdot}$	C_6H_{12}	0.71	333	38
$C_6H_{11}O_2^{\cdot}$	p-Quinone	1.7×10^{-3}	333	33

Phenolic antioxidants are desirable in automotive lubricants as they are seen as ‘clean’ because the quinone formed will be sufficiently volatile to be removed in the exhaust gases at high temperatures.

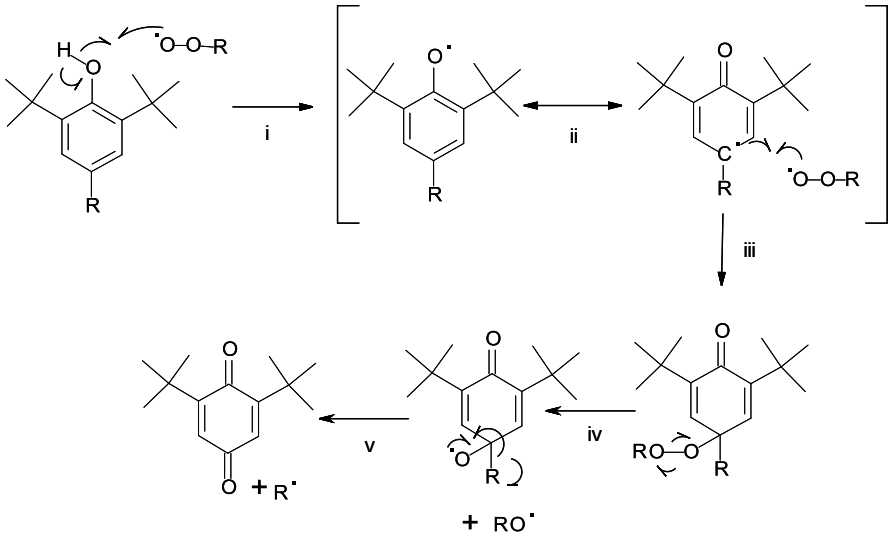

Figure 1.3 – The well established phenolic antioxidant mechanism [26,27,39,40]

The phenolic antioxidant mechanism shows that for this type of antioxidant, every molecule of antioxidant can remove two alkyl peroxy radical molecules, and so can be

said to have a stoichiometric coefficient of two per phenol head group with respect to alkyl peroxy radicals. This stoichiometric coefficient has been previously measured using a range of phenolic antioxidants such as butylated hydroxytoluene (BHT), temperatures and solvents.

Table 1.7 – Stoichiometric coefficient per phenolic head group of phenolic antioxidants

Antioxidant	Solvent	Temp °C	Stoichiometric coefficient	Reference
BHT	Hexadecane	180	2.2	[41]
BHT	Chlorobenzene	62.5	2.0	[26]
4-t-butylcatechol	Chlorobenzene	62.5	2.0	[26]
Phenol	Chlorobenzene	62.5	2.0	[26]
4,4'-methylenebis(2,6-di-tert-butylphenol)	Hexadecane / chlorobenzene	60	2.0*	[42]
BHT	Styrene / chlorobenzene	50	1.7	[43]
BHT	Tetralin	60	2.67	[44]
Vitamin E	Heptanol	60	1.6	[45]

* Antioxidant contains more than one phenolic group and so coefficient quoted was divided by number of phenolic head groups.

Properties such as O-H bond dissociation energy[46,47] and rate constants[48] of phenolic antioxidants in the inhibition of oxidation can differ depending on the substituent groups of the molecule.

1.4.2 Inhibition of oxidation by aminic antioxidants

Aminic antioxidants use a similar underlying principle to phenolic radical scavenging antioxidants. The weak N-H bond in an aminic antioxidant such as diphenylamine has a bond dissociation energy of 364 ± 4 kJ mol^{-1}.[49] Although this is significantly higher than the BDE in a phenolic antioxidant, it is still sufficiently lower than the tertiary alkane C-H bond energy which allows it to act as an antioxidant.

Aminic antioxidants have been proposed to function by two different mechanisms, with different mechanisms dominant at different temperatures. The low temperature mechanism is thought to occur at temperatures below 120 °C.[50] This low temperature mechanism is similar to that of phenolic antioxidants and involves an initial abstraction of the weakest hydrogen (N-H bond in aminic antioxidants) followed by the combination of the aminyl radical resonance structure (ii of Figure 1.4) with an alkyl peroxy radical. The decomposition of the peroxide bond, forms a nitroxyl radical[51] and the molecule then fragments forming quinone and a nitrosobenzene structure.[52]

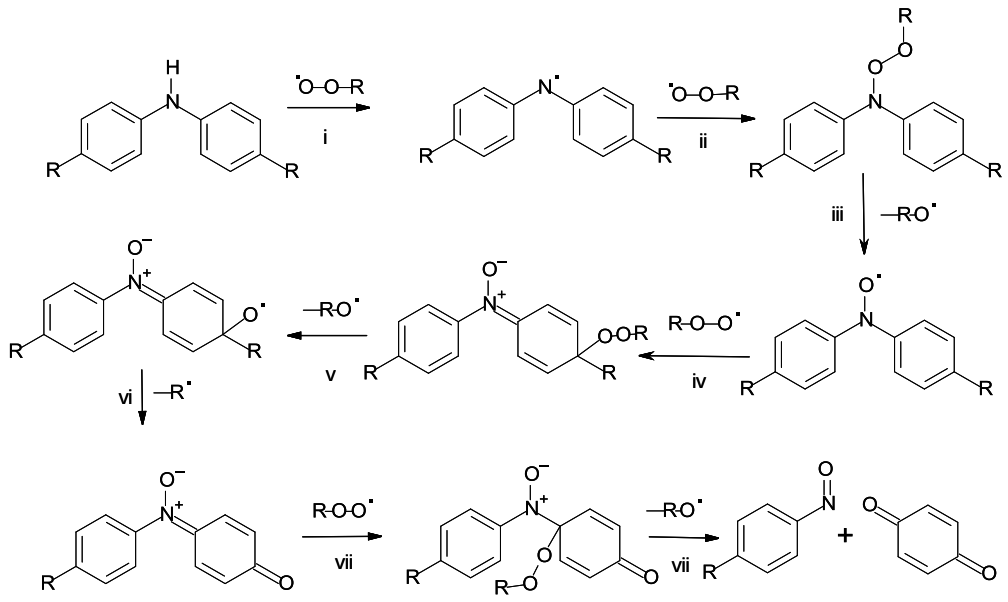

Figure 1.4 – Low temperature aminic antioxidant mechanism[52]

At temperatures above 120 °C, the aminyl and nitroxyl radical are reported to be formed in the same way as in the low temperature mechanism, however the nitroxyl radical formed will react differently at high temperatures. Work by Jensen *et al* 1995 [50] reported that the nitroxyl radical can combine with a secondary alkyl radical to form an hydroxame ether (NOR) (iv of Figure 1.5). This can then either decompose via intramolecular hydrogen abstraction by the nitrogen to regenerate the starting antioxidant (viii of Figure 1.5) and a ketone as a by-product or alternatively form a hydroxylamine by intramolecular abstraction of a hydrogen by the oxygen (v of Figure 1.5) creating an alkene as a by-product.

A slightly different mechanism was proposed by Denisov[53] who proposed that at above 70 °C for alkyl radicals, the NOR can fragment across the O-R bond (iii of Figure 1.5),

followed by abstraction of a hydrogen from an alkyl radical (vii of Figure 1.5), leading to the formation of an alkene and a hydroxylamine structure. This can then reform the nitroxy radical by reacting with an alkyl peroxy radical. This mechanism was suggested to occur despite being below the 120 °C temperature quoted by Jensen[50] for the regeneration reactions to occur.

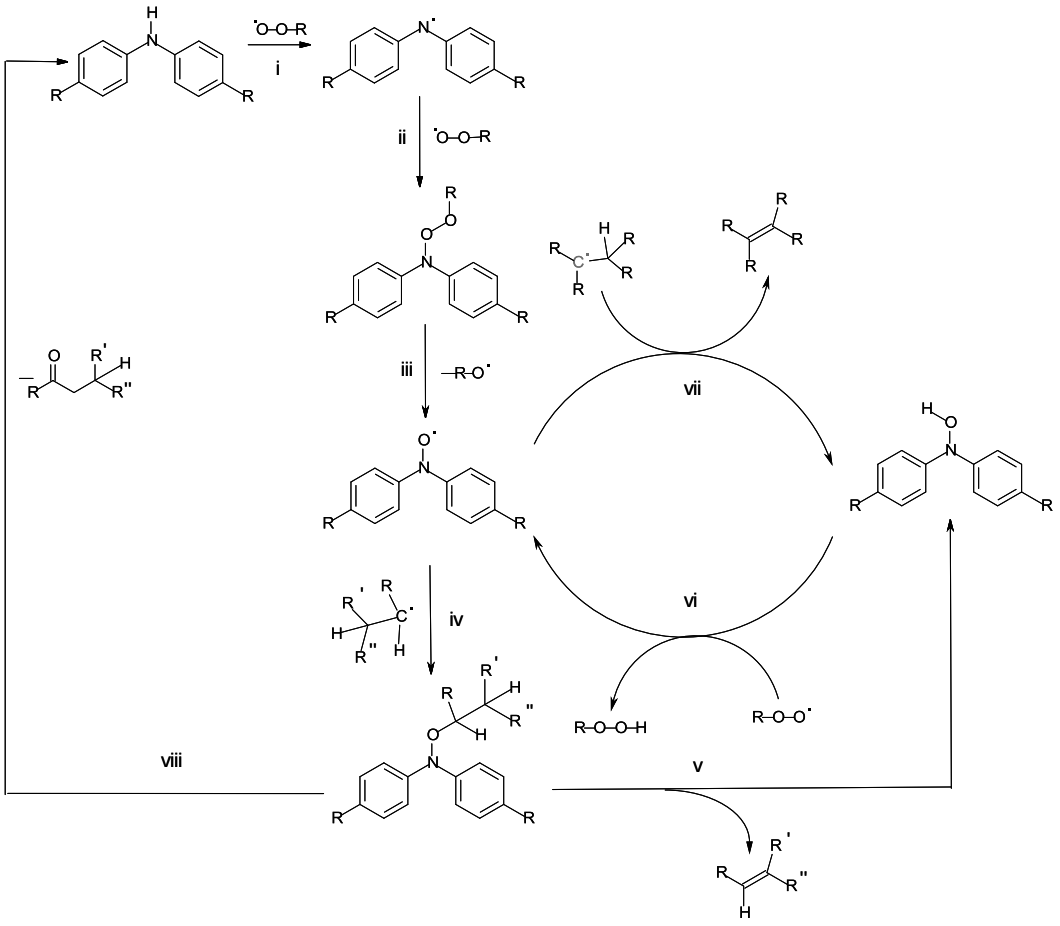

Figure 1.5 – High temperature (120 °C+) aminic antioxidant mechanism[50,59,54]

The quoted stoichiometric coefficients of these antioxidants (Table 1.8) vary much more widely than the phenolic antioxidants. This could potentially be due to the change in

mechanism above 120 °C with the nitroxyl radical regeneration mechanism reacting with multiple alkyl peroxy radicals.

Table 1.8 – Stoichiometric coefficient of aminic antioxidants

Antioxidant	Solvent	Temp °C	Stoichiometric coefficient	Reference
p,p'-dioctylamine	Hexadecane	60	4.0	[42]
Diphenylamine	Chlorobenzene / cumene	57	2.2	[55]
Diphenylamine	Chlorobenzene / cumene	62.5	2.8	[26]
Diphenylamine	Chlorobenzene / tetralin	62.5	3.5	[26]
Diphenylamine	Chlorobenzene / cumene	68.5	2.8	[55]
Diphenylamine	Paraffinic oil	130	41	[56]
Diphenylamine	Isopropyl alcohol	71	23	[53]

1.5 Synergistic effects of antioxidants

When antioxidants are used together they have been reported to have synergistic effects, where their combined effect is greater than the sum of the individual components. This can be using two different classes of radical scavenging antioxidant or a radical scavenging antioxidant with a peroxide decomposer.

1.5.1 Phenolic and aminic antioxidants

Due to the lower bond dissociation energy of the O-H bond of a phenolic antioxidant compared to the N-H of an aminic antioxidant, the phenolic antioxidant can regenerate an aminic antioxidant when used together. As aminic antioxidants are thought to have a higher stoichiometric coefficient than phenolic antioxidants, this regeneration gives a synergistic effect.[57,58,59]

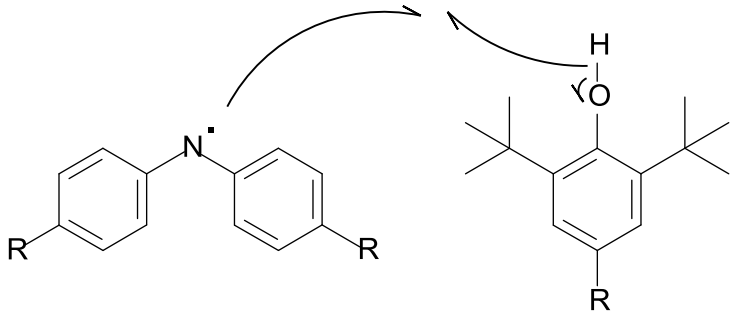

Figure 1.6 – Aminic antioxidant regeneration mechanism[57]

1.5.2 Antioxidant and peroxide decomposer

Although a radical scavenging antioxidant has the ability to prevent further chain abstraction reactions by alkyl peroxy radicals, this still leads to the production of hydroperoxides which produce further radicals. When used in conjunction with a peroxide decomposer, a synergistic effect is observed as the chain branching reactions of oxidation are interrupted by the peroxide decomposer.[11,60,61,62,63]

1.6 Inhibition of autoxidation by peroxide decomposers

Hydroperoxides can decompose to form two highly reactive radical species (Reaction 1.3.4 of Table 1.3) leading to further oxidation reactions. A peroxide decomposer (also known as a secondary antioxidant) promotes decomposition of peroxides in to non-radical species. Some are stoichiometric such as phosphites while others are catalytic such as chelate metal complexes. An example of a peroxide decomposer used extensively in the automotive industry is zinc dialkyldithiophosphate (ZDDP) which acts as both an anti-wear additive and a secondary antioxidant.[64,65,66] A general structure of ZDDP is shown in Figure 1.7. ZDDP is manufactured in two forms, primary and secondary. In a primary ZDDP, the R groups consist of primary alkyl groups. In secondary ZDDPs the R groups consist of secondary alkyl groups. Engine oil formulations will generally consist of a mixture of primary and secondary ZDDP at a ratio of approximately 85% secondary ZDDP, 15% primary ZDDP.[67]

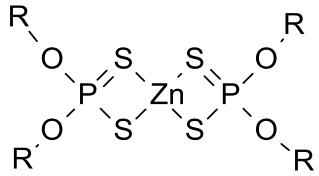

Figure 1.7 – Structure of ZDDP.[66]

To understand the antioxidant properties of ZDDP it is important to first understand the purpose of ZDDP film formation. ZDDP can be activated thermally at temperatures in

excess of 80 °C[68] (thermal film formation) or by rubbing (tribofilm formation). It has the ability to act as an anti-wear additive by forming layers of ZnS on the surface of the metal and in doing so protecting the metal from frictional wear. Glassy phosphate pads form on top of the ZnS films creating thicker tribological films further protecting the metal surface to a thickness of approximately 120 nm.[69,70,71]

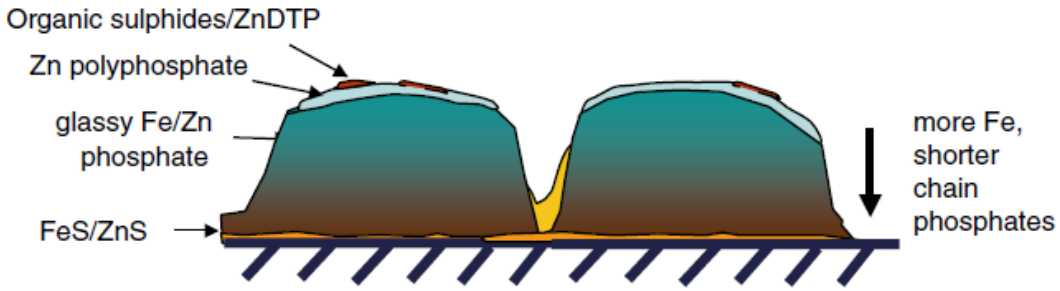

Figure 1.8 – Schematic of ZDDP layer[66]

The rate of activation is dependent upon the type of ZDDP with secondary ZDDPs being more reactive (and so forms layers faster) than primary ZDDPs. A typical ZDDP blend will consist of a mixture of secondary and primary ZDDP. The secondary ZDDP provides rapid protection of metal surfaces and the primary ZDDP provides longevity from the slower layer forming but mechanically stronger films.[72]

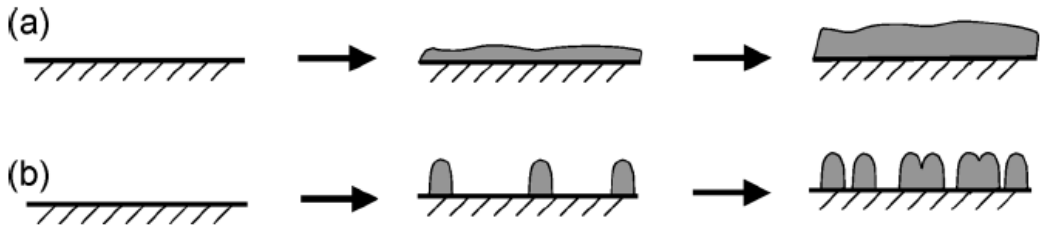

Figure 1.9 – Two contrasting film formations of ZDDP (a) progressive thickening (b) progressive coverage[68]

ZDDP has the ability to act as both a radical scavenger and peroxide decomposer[64,73,74] as well as an anti-wear additive. The mechanism for this was summarised by Willermet *et al.*[75] (Figure 1.10).

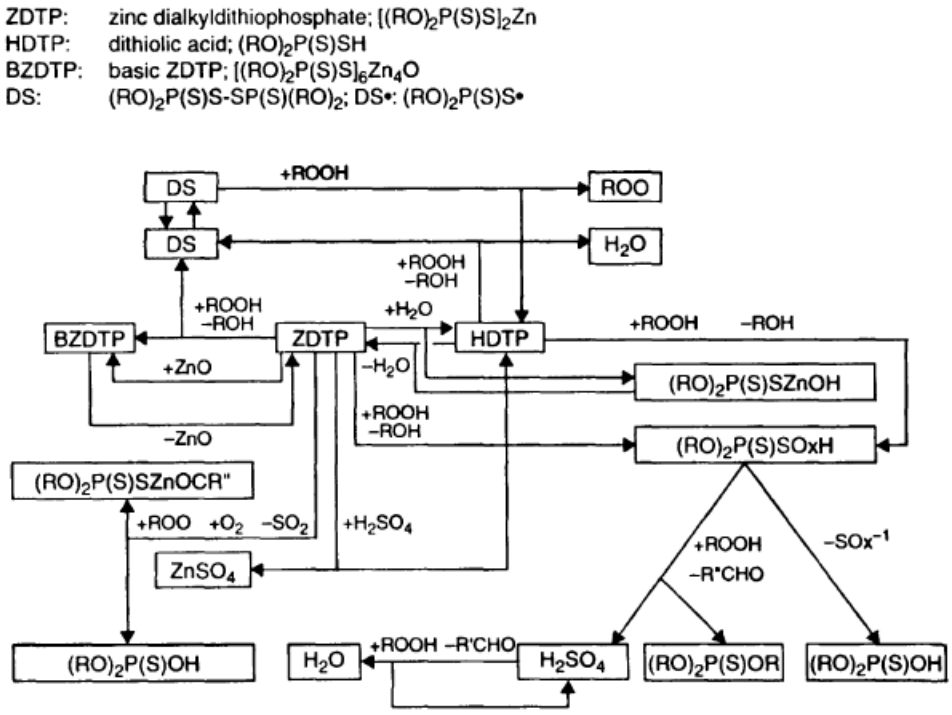

Figure 1.10 – Antioxidant mechanism of ZDDP[75]

1.7 Inhibition of oxidation by metal deactivators

Transition metals such as iron and copper have been reported to have the ability to initiate autoxidation[76,77] and also decompose peroxides into radical species leading to an increase in oxidation.[11,78]

$ROOH + M^{n+} \rightarrow RO\cdot + M^{(n+1)} + OH^-$
$ROOH + M^{(n+1)} \rightarrow ROO\cdot + M^{n+} + H^+$

Figure 1.11 – Metal catalysed decomposition of alkyl hydrogen peroxide

Metal deactivators prevent this catalytic decomposition by interacting with metal ions to form complexes which are inactive with respect to hydroperoxides.[33] Examples of metal deactivator are hydroxyacids and triazole compounds. The structure of a typical triazole is shown below in Figure 1.3. These structures have elements such as nitrogen which can chelate with the metal. The inhibiting ability will vary depending upon the metal involved.[78] They have also been reported to have a synergistic effect when combined with radical scavenging antioxidants.[79]

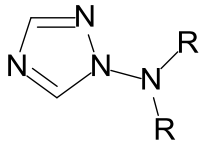

Figure 1.12 – Example of a triazole metal deactivating compound[3]

1.8 Defining piston ring conditions

The previous work on both phenolic and aminic antioxidants has been done over a wide range of temperatures. As this project is concerned with the effects of these antioxidants at high temperatures typical to those seen in the piston chamber, it is important that

these conditions are defined. There has been a trend over the past 70 years to reduce the size of the engine whilst increasing the brake horse power (BHP) output of the engine, leading to an increase in oil stress as the lubricant is subjected to more extreme conditions.[80]

Table 1.9 – Changes in the V-8 engine over the past seven decades [3]

Parameter	1920	1960	1990
Engine capacity (L)	6	2	1.6
Brake horse power	50	70	130
Engine speed (RPM)	1200	5000	7000
Oil temperature (°C/°F)	60/140	90/194	130/266
Oil capacity	14	4.5	3.5
Valve train	Side valves	Overhead valves	Twin overhead camshaft
Fuelling system	Single choke carburettor	Multi choke carburettor	Fuel injected

The increase in oil temperature in 1990 to over double the figure of 1920 has lead to the introduction of more complex mixtures of lubricant additives to protect the lubricant from oxidation. Since 1990, this trend in oil temperature has continued to rise. Recent work by Taylor and Evans[81] and Qian *et al*[82] measuring the temperature of the top

piston ring concluded that this area in a petrol engine reached temperatures of between 150 – 180 °C and between 200 – 230 °C in a diesel engine, as shown in Figure 1.13. This piston-cylinder area is the primary region of antioxidant consumption.[83]

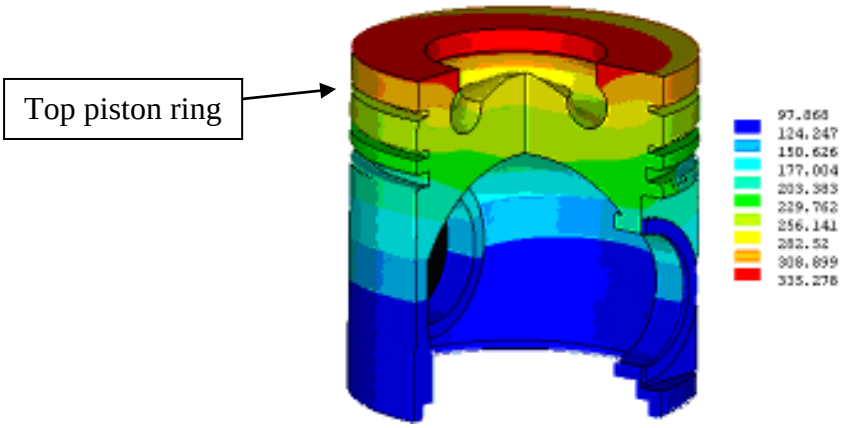

Figure 1.13 – Diagram showing top piston ring area on an automotive piston of a diesel engine[82]

1.9 Project aims

Legislative restrictions on passenger car emissions have put pressure on engine original equipment manufacturers (OEMs) and the lubricant and fuel producers. Since the introduction of the Euro 1 standards in 1992, regulations have been introduced which have significantly reduced the harmful emissions and particulates. Those failing to meet the standards will be penalised €20 per gram of CO_2 over 120g CO_2/km the vehicle produces. This will rise to €95 per gram in 2015.[5] 2014 will see the introduction of the Euro 6 legislation which will further reduce the emission targets for diesel engines by

over 8%, and in particular NOx emissions.[84] It has been found that diesel particulate filters which were fitted by OEMs to meet Euro emission standards can be deteriorated by additive-metals from the consumption of ZDDP containing lubricant oil[85] leading to pressure from OEMs to reduce the oil content of species such as these. As ZDDP is responsible for both anti-wear and antioxidant functions, additives must be used to provide this protection if ZDDP levels are reduced or removed altogether.

The overall aim of the project was to assess the effects and chemistry of established and novel antioxidants in inhibiting lubricant degradation and to examine the chemical mechanisms by which they function, focusing on high temperatures which are representative of engine piston assemblies. A good understanding of antioxidant chemistry under engine conditions will allow targeted synthesis of novel, effective antioxidants, which will in turn allow the formulation of engine lubricants that have extended drain intervals and the retention of fuel economy properties. The experimental reactions were done in a small scale bench-top reactor allowing experiments to be done using single additives in base oil without the need for full or partial additive packs. The benchtop reactor is also a much more rapid and cost effective way of carrying out oxidation chemistry compared to expensive engine testing.

Chapter 2

Experimental

2.0 Experimental

The following chapter contains details of equipment and methods used throughout this work.

2.1 Bench-top continuous flow reactor

To simulate the high temperatures and oxygen rich environment of an engine piston assembly, a continuous flow bench-top reactor setup was used.

2.1.1 Bench-top reactor

The vessel used for this work was a stainless steel reactor (BS304) with an internal volume of 49 cm^3 (Figure 2.1) made in-house at the Department of Chemistry of the University of York.

Figure 2.1 – 49 cm^3 stainless steel reactor with magnetic stirrer.

The lid of the reactor (also made from stainless steel) was attached to the base using a brass ring via a screw thread. A good seal was achieved using a Viton® O-Ring fitted to a groove. Stirring was achieved using a polytetrafluoroethylene coated cross type magnetic stirrer. The lid, complete with a bursting disk and six ports is pictured in Figure 2.2 and schematically in Figure 2.3.

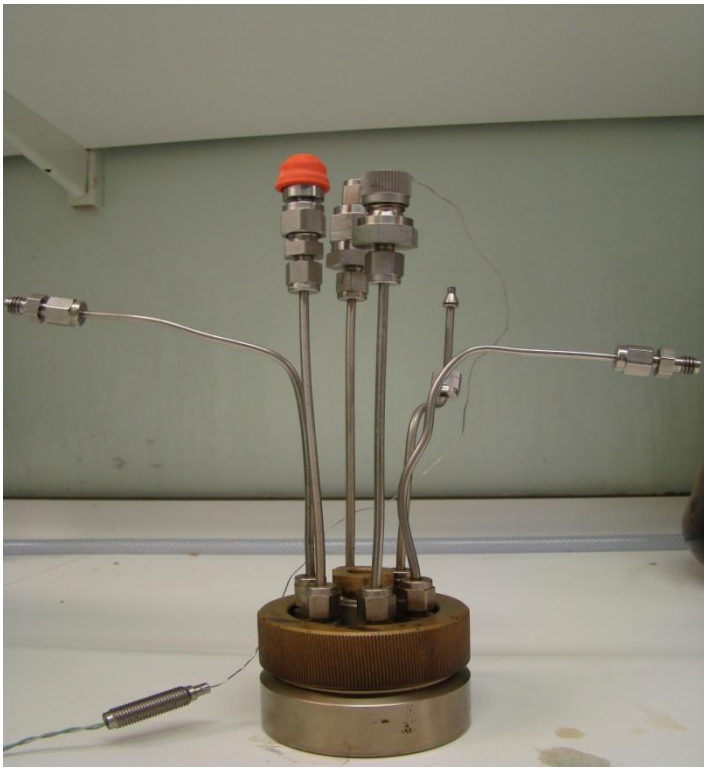

Figure 2.2 – Reactor lid and base from side

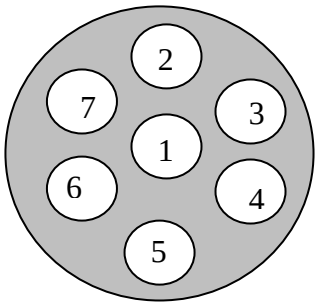

1. 1cm^3 Bursting disk
2. Pressure release valve (2 bar gauge)
3. Pressure sensor
4. Gas outlet
5. Thermocouple
6. Sampling port
7. Gas inlet

Figure 2.3 – Reactor lid schematic

2.1.2 Sample preparation

Samples were prepared on the 10g ± 0.005g scale in a 20ml screw top vial using a 4 figure balance. The antioxidants used in this work were all solids and were dissolved in squalane by gentle heating to 60 °C and holding at this temperature for 5 minutes. Some non-commercial antioxidants used were far less soluble in squalane and required sonification and heating up to 120 °C, again holding at this temperature for 5 minutes. At this temperature, for such a short period of time, it was not believed that oxidation will occur whilst the antioxidant is being dissolved.[41] This was confirmed by GC using a sample soluble at 60 °C and running the same sample after heating up to 120°C.

2.1.3 Reactor heating

The bench top reactor is placed inside a hollow brass block to insulate it and maintain a constant temperature throughout. The brass block (and the reactor inside it) is heated using a stirrer hotplate. A K-type thermocouple of accuracy ± 1.1 °C and calibrated using a digital thermometer with an accuracy of 0.2% was used to measure the temperature of the liquid inside the reactor.

2.1.4 Reactor setup

The reactor was connected to the oxygen inlet and an outlet which led to an oxygen sensor via a cold trap, a squalane bubbler, a filter and a second flow meter. A pressure

sensor is also fitted to the reactor. A schematic of the reactor setup is shown in Figure 2.4.

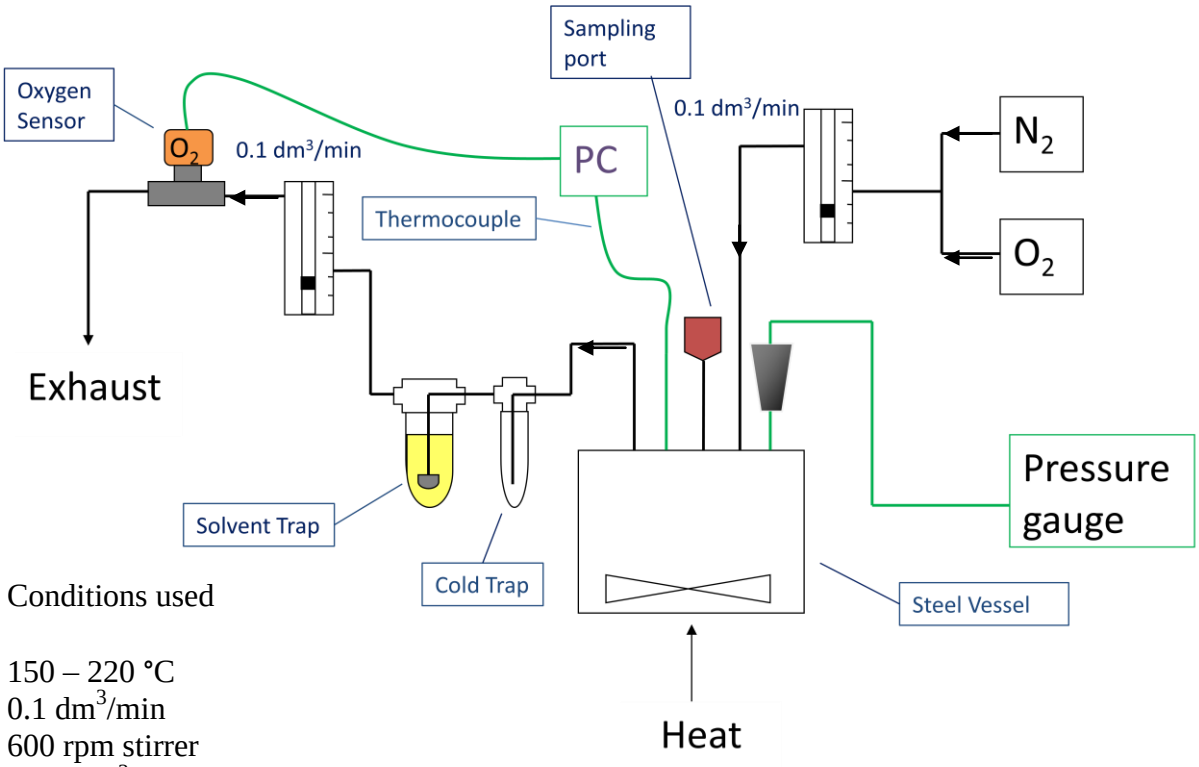

Figure 2.4 Schematic of the overall reactor set up.

The details of the equipment used (other than the reactor) are shown in Table 2.1.

Table 2.1 - Table of reactor equipment used

Equipment	Details
Thermocouple	Type K thermocouple 150mm length and 0.5mm diameter stainless steel (BS316)
Flow meters – suitable for oxygen	Cole Parmer – 0.02-0.5 $dm^3 min^{-1}$ ±5%
Pressure sensor head	Varian model 6543-25-038
Stirrer hotplate	Heidolph – MR-Hei Standard with external temperature controller (EKT-Hei Con)
Oxygen sensor	Monitor - Teledyne AX300i Sensor head - Teledyne R-17a (automotive)
Analogue to Digital Converter	Picotech – ADC-20 running Picolog software on windows XP.
Stirrer bar	Cross head type length 1.5inch

2.1.5 Reaction conditions

The temperature range used throughout this project was 140 – 220 °C. All reactions were completed using an oxygen flow of 0.10 $dm^3 min^{-1}$ ±0.02 $dm^3 min^{-1}$ and stirred at 600rpm. At temperatures between 140 – 200 °C, 7 cm^3 of sample were used and left for 4 minutes to reach the temperature of the reactor. Whilst the stirrer was switched off, no noticeable oxidation of squalane occurred at 200 °C and below for a minimum of 5 minutes (Figure 2.5). At 220 °C, oxidation started to occur (identified by both GC and

oxygen sensor) after approximately 4 minutes and so at 220 °C, the sample size was reduced to 3.5cm^3. This reducing the volume of liquid to be heated and so the hold time could be reduced from 4 minutes to 2 minutes to ensure no oxidation occurs before the reaction starts. The 7.0 cm^3 ±0.1 cm^3 sample size allowed for 6 samples to be taken during the reaction. Although the reduced sample size used at 220 °C only allowed around 3 samples to be taken, this was not problematic because of the short induction periods at this temperature.

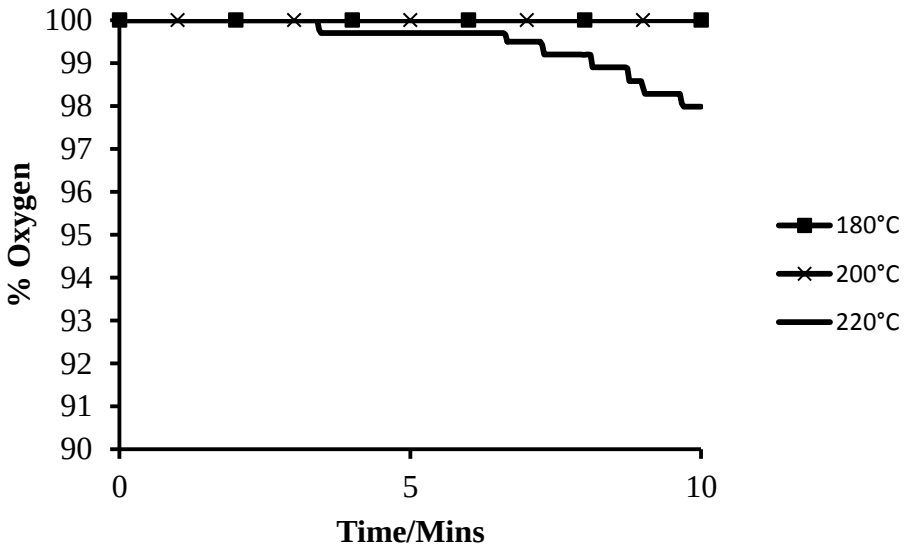

Figure 2.5 - Oxidation of squalane at 180 – 220 °C without stirring.

2.1.6 Reaction start up procedure

Once connected, the reactor was pre-heated in the brass block, and the oxygen flow started at 0.1 dm^3 min^{-1}. Once the temperature and oxygen flow had stabilised at the required value, the squalane sample was injected through the suba-seal into the hot

reactor using a 10ml disposable syringe and stainless steel cannula via the suba-seal sampling port in the lid of the reactor and left to reach the temperature of the reactor with the stirrer switched off (4 minutes at 200 °C and below, 2 minutes at 220 °C). Once up to temperature the stirrer was started to promote the uptake of oxygen by the liquid. This was taken as the start of the reaction. At temperatures of 200 °C and below, the period of time taken to inject the sample and then wait for the sample to heat up to temperature was exactly five minutes. At 220 °C, the total time was three minutes

2.2 Product analysis

A number of samples of 0.6 – 0.7 cm^3 were taken throughout the reaction via the suba-seal port using a 1 ml disposable syringe and stainless steel cannula for subsequent analysis. Samples were stored in a freezer before analysis to preserve them and prevent further oxidation.

2.2.1 Gas chromatography (GC)

Gas chromatography analysis was carried out using a Shimadzu GC-17a with a flame ionisation detector fitted with a Shimadzu AOC-20a autosampler. The column used was a non-polar 5 % phenyl 95 % dimethylpolysiloxane (Zebron ZB-5HT Inferno, Phenomenex) column with dimensions of (30 m length x 0.25 mm bore x 0.25 µm film

thickness) with a temperature operating range of 60 °C – 400 °C. The programme run was 50 °C – 350 °C at a rate of 5 °C per minute and then a 20 minute hold at 350 °C. Quantification of products was achieved using the peak areas of the products in relation to the areas of standardised materials of known concentrations or by using the peak area obtained by GC and calculating concentrations of products using their carbon numbers[86] whilst taking into account the influence to the GC detector of different structures such as aromatic rings compared to branched alkanes.[87] Samples for both GC and GC-MS analysis were prepared by diluting them at a 1:1 ratio in toluene to make injection easier.

2.2.2 Gas chromatography – Mass spectrometry (GC-MS)

Analysis was conducted on one of two GC-MS machines. These were:

Machine 1- Perkin Elmer Clarus 500 GC, fitted with the same type of column as the Shimadzu GC, coupled to a Perkin Elmer Clarus 560s electron impact (EI) mass spectrometer. The run programme was 60 °C – 360 °C at a rate of 8 °C per minute and then a 20 minute hold at 360 °C.

Machine 2 –Agilent 7890A GC and Waters GCT Premier electron impact (EI) mass spectrometer and a ZB5-HT inferno column using the same method as machine 1.

Machine 1 was used on a regular basis to identify possible products and intermediate species. Machine 2 was used to confirm the identity of species found using accurate mass.

2.2.3 Gel permeation chromatography (GPC)

GPC analysis of the substrates was undertaken using a Hewlett Packard 1090 liquid chromatography machine fitted with an auto-sampler. The detector was a photo diode array detector capable of scanning between 280 and 560 nm. The column fitted was a Phenomenex Phenogel gel permeation column with a 5 μm narrow bore 300 mm column with a diameter of 4.6 mm and 50 Angstrom pore size complete with a guard column. The mass separation range of the column was 100-10000 $gmol^{-1}$. Analysis was done at a temperature of 40 ^{o}C and a flow rate of the mobile phase tetrahydrofuran (THF) of 0.35 cm^3 min^{-1}. The total run time was 20 minutes. Samples were diluted with tetrahydrofuran at a ratio of 20:1 solvent:sample and a sample of 25 μm^3. The software used was Chemstation running on Windows 2000.

2.2.4 UV-VIS spectroscopy

UV-VIS was used as a screening method for GPC to ensure the correct wavelengths were measured. The equipment used was a Jasco 550 UV-VIS spectrophotometer with liquid and solid analysis modules capable of scanning between a range of 190 – 900 nm. Samples were diluted in THF at a ratio of 20:1 solvent:sample, and then further diluted

if required. The UV-VIS machine was coupled to a PC running the Jasco analysis software on Windows XP.

2.2.5 Nuclear Magnetic Resonance (NMR)

NMR analysis was achieved using a Bruker 400 MHz spectrometer with the chemical shifts calibrated against the residual solvent signal. Sampled were prepared by dissolving ~10 mg of sample in $CDCl_3$. The analysis done was predominantly ^{1}H NMR, with some ^{13}C and Distortionless Enhancement by Polarization Transfer (DEPT) NMR.

2.2.6 Electron Spin Resonance (ESR)

Electron Spin Resonance (ESR) is a technique used to study species with one or more unpaired electrons, which is of use when studying free radical chemistry. The limitations of the technique to species that are paramagnetic is highly desirable for this research, as hydrocarbons such as squalane which make up over 99 % of the sample will not be detected using the technique meaning that any signal will be due to the antioxidants (assuming oxidation does not occur during the induction period in the presence of antioxidant). The ESR works using a powerful magnet which will make an electron's magnetic moment align either parallel or anti parallel to the magnetic field. The difference in energy between the parallel lower energy state and the higher energy anti parallel state is equal to the energy required to move an unpaired electron between the two energy levels.

The spectra created by the change in the spin state of an unpaired electron is influenced by the interactions that this electron has with its surrounding nuclei creating additional allowed energy states allowing better identification of radical species.

It is also a highly sensitive technique which can detect small changes in oxygen concentration which were not detectable using the flow reactor, for instance during the induction period. This may be of interest when studying the mechanisms of antioxidants as different types of antioxidants may work in different ways. An example of an ESR spectra showing a base oil oxidation reaction is shown in Figure 2.6 along with the structure of the molecule the 2,2,6,6-Tetramethylpiperidine-1-Oxyl (TEMPO) which is a stable radical species[88] which will produce ESR spectra when added to a sample. This is used when it is not possible to detect short lived radical species in reactions such as carbon centered radicals produced during autoxidation.

The ESR signal starts off short and broad (green line of Figure 2.6). It is broad because early in the reaction, the TEMPO is at its highest concentration. It is short because oxygen is also at its highest concentration at this point. The collisions between the oxygen and TEMPO molecules shorten the relaxation time, resulting in the broad spectra. Oxygen is consumed during the reaction resulting in fewer collisions taking place, and the TEMPO peak becoming taller and narrower (blue line of Figure 2.6) but as the concentration of TEMPO does not change, the area of the peak remains the same. Once the oxygen has been consumed, the TEMPO will also be consumed and the signal will reduce in intensity (red line Figure 2.6). The degree of interaction between the

oxygen and TEMPO is shown in Figure 2.6. This shows the oxygen being consumed and the peak becoming sharper (less broad).

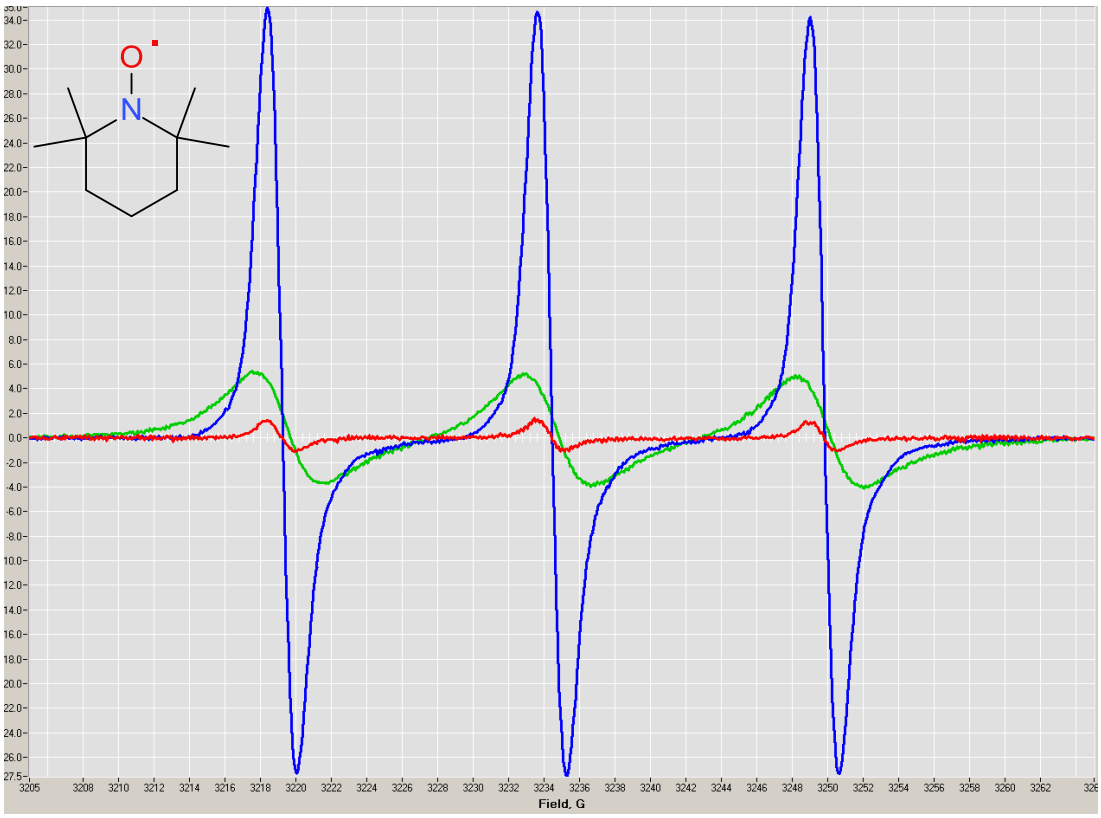

Figure 2.6 – The three stages of ESR spectra of an in situ oxidation run

Typical parameters used were: modulation amplitude = 1.0 Gauss, microwave power = 5.00 mW, acquisition time – 100 seconds and magnetic field of ~3350 Gauss (0.335 Tesla) with a sweep of 50 Gauss.

Three types of analysis were undertaken for this work using two different X-band machines (The Jeol JES-RE1X ESR and the Bruker EMX_{micro} CW-EPR spectrometers) depending on the technique. The *in situ* reactions which involved cavity heating were done on the Jeol, and the cryogenic and lead dioxide work done on the Bruker.

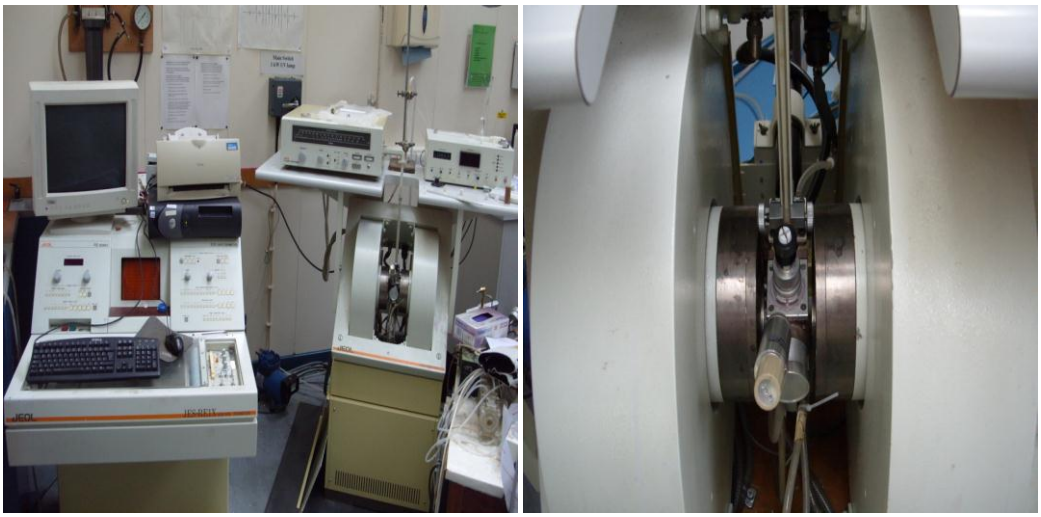

Figure 2.7 – The Jeol JES-RE1X ESR machine and close up of cavity on the right.

The three types of analysis done were:

1. Reactions *in situ*[89] used a sealed melting point tube which contained squalane with and without antioxidant (100 ppm) and 100 ppm of 2,2,6,6-Tetramethylpiperidine-1-Oxyl (TEMPO) which was placed into cavity pre heated to 170 °C. The air in the head space of the cavity was sufficient for oxidation to take place.

2. Cryogenic experiments were done using a Bruker where samples were taken from the continuous flow reactor at intervals where it was believed that radicals may exist. The samples were then crash cooled in liquid nitrogen so the radicals could be observed using ESR before they could react further. The cavity of the Bruker was cooled with liquid nitrogen to preserve the radical species whilst analysis was conducted.

3. Antioxidant products of both radicals and reaction intermediate molecules were also analysed on the Bruker machine. This method involved dissolving a high concentration of antioxidant in dichloromethane and then adding lead dioxide to it to oxidise the antioxidant.[90] The samples were left for 5 minutes for the oxidation to occur before the samples were filtered for analysis by ESR. Scans were done once a minute for one hour. Samples were also sent for analysis by GC-MS. The reactions were done at room temperature.

2.2.7 Determination of hydroperoxide concentration

The concentrations of alkyl hydroperoxides were quantified by adding triphenylphosphine (TPP) to the samples taken from a reaction. This was achieved by making a 0.3 M solution of TPP in toluene which was then used to dilute the samples at a 1:1 ratio for GC analysis in the usual way. Once diluted, samples were shaken and then left for 30 minutes for the TPP to react with the hydroperoxides to form triphenylphosphine oxide (TPPO) before the GC sequence was started. From this, the concentration of the alkyl hydroperoxide could be quantified by the GC peak area of the TPPO which was identified by measuring the retention time of TPPO standard.

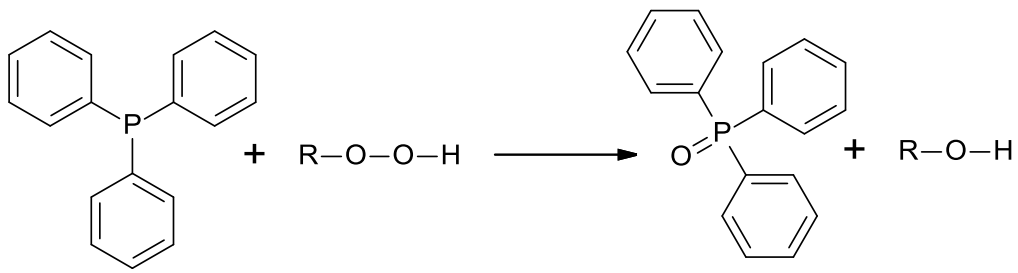

Figure 2.8 – Reaction between triphenylphosphine and alkyl hydroperoxide

Following the work done by West *et al*[91] but using a slightly higher concentration of TPP solution, given the harsh conditions of the continuous flow reactor (detailed in Chapter 1), the conversion of TPP to triphenylphosphine oxide (TPPO) by hydroperoxides is a rapid, accurate, highly convenient method for measuring hydroperoxide concentration.[92] Identification of the TPPO peak was achieved using TPPO from Aldrich as a standard.

2.2.8 Determination of induction period and oxygen uptake

The induction period is the initial time before rapid oxygen uptake begins. The addition of an antioxidant can increase this time. When measuring an induction period, an acceptable level of repeatability throughout this work was 10%. Only one of the antioxidants tested had a greater margin of error than 10%, and the possible reasons for this were outlined (see chapter 4).

The oxygen uptake by the liquid can be defined as the amount of oxygen that has reacted with the sample. This was determined from the data obtained from the oxygen sensor. As autoxidation occurs, the exhaust gas will contain volatile hydrocarbons resulting in a drop in % oxygen detected by the sensor. As pure oxygen was used in this work, the % of oxygen taken in by the sample can be defined as

$$O_2 \text{ taken in } (\%) = 100\% - Oxygen\ sensor\ reading\ (\%)$$

Equation 2.1 – Calculation of % oxygen uptake

An example of the output displayed from this is shown in Figure 2.9. As oxygen is taken in by the sample and volatile hydrocarbons are emitted, the % oxygen will fall. This is an indication that fluid oxidation is occurring.

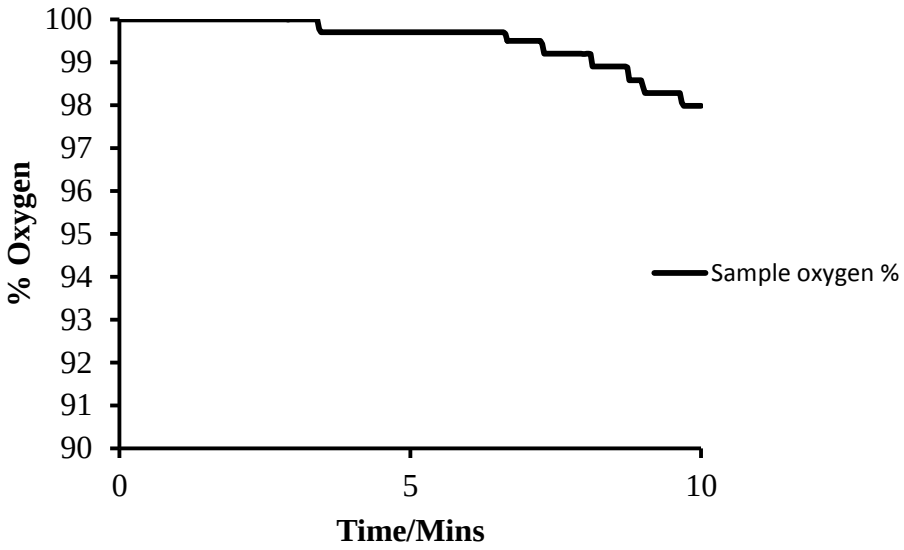

Figure 2.9 – Oxygen sensor output

The flow of oxygen which is measured using a flow meter can then be used to calculate the oxygen uptake in $dm^3\ min^{-1}$.

$$O_2 \text{ taken in } (dm^3\ min^{-1}) = O_2 \text{taken in } (\%) \text{ x } \frac{O_2 \text{ flow rate}(dm^3\ min^{-1})}{100}$$

Equation 2.2 – Calculation of rate of oxygen uptake

The moles of oxygen (n) per minute can then be calculated using the ideal gas equation.

$$O_2 \text{ uptake (mol } \text{min}^{-1}) = (\text{pressure (Pa)}) \text{ x} \frac{O_2 \text{ taken in m}^3 \text{ min}^{-1}}{(\text{R x absolute temperature (K)})}$$

Equation 2.3 – Calculation of moles of oxygen uptake

From this the oxygen uptake per second (integral) can be calculated

$$O_2 \text{ uptake (mol } \text{s}^{-1}) = \frac{O_2 \text{ uptake (mol min}^{-1})}{60}$$

Equation 2.4 – Calculation of oxygen uptake per second

To convert this to a concentration, the number of moles of oxygen uptake is divided by the volume injected into the reactor.

$$O_2 \text{ uptake (mol dm}^{-3} \text{ s}^{-1}) = \frac{O_2 \text{ uptake (mol s}^{-1})}{\text{Volume injected (dm}^{-3})}$$

Equation 2.5 – Calculation of oxygen uptake concentration

By using the sum of these integrals, the total oxygen uptake for a given amount of time can be calculated.

$$O_2 \text{ uptake } (\text{mol dm}^{-3}) = \Sigma\, O_2 \text{ uptake } (\text{mol dm}^{-3}\ \text{s}^{-1})$$

Equation 2.6 – Calculation of total concentration of oxygen uptake

2.2.9 Column chromatography

Separation of products from synthesis reactions was done using column chromatography. A column with dimensions of 40 cm in length and 3cm in diameter was packed with a slurry of silica gel (0.035 – 0.070 mm partial size) using diethyl ether as a solvent. A sand plug of ~1cm was then added to the top of the silica. Samples were dissolved in diethyl ether and pipetted into the column. After elution of the less polar material, ethanol was introduced into the solvent system starting at 75:25 diethyl ether:ethanol and increasing in 25% increments until finishing with pure ethanol. Samples were collected as fractions in test tubes. Eluted sampled were tested by GC and then relevant tubes were combined and the solvent removed using a rotavap.

2.3 Thermochemical calculations using the computational chemistry software Gaussian09W

2.3.1 Principles and uses

Although many parameters such as enthalpy changes (ΔH), entropy changes (ΔS) and bond dissociation energies (BDE) have often been measured experimentally, it is sometimes desirable to be able to calculate parameters using computational software to estimate the favourability of a reaction if experimental work values are not available. This allows the thermodynamics of reactions to be studied in detail. Prediction of the thermochemical values in this work was obtained using Gaussian Software 09.[93]

2.3.2 Method selection

When selecting a method to be used in Gaussian, there is an important trade-off which must be considered. As the level of detail in a method increases, the time it takes for the software to complete the calculations will also increase. It is therefore essential that a method has a high enough degree of complexity to obtain accurate results, but can complete the calculations in a realistic amount of time.

The bond dissociation energy (BDE) is the energy required to break a particular bond. In this work, the BDEs of particular interest are C-H, O-H, and N-H and so the method chosen must be as accurate as is practical in calculating these bond types. A commonly

used hybrid density function recommended in BDE and ΔH calculations is the Becke 3 parameter Lee Yang Parr (B3LYP) along with a density functional theory (DFT) level of theory.[94,95,96,97,98,99] A variety of basis sets were tested to find the best all round method.

2.3.3 Method testing

Different test methods were used to calculate a well-established bond dissociation energy which was relevant to this work. The experimentally determined N-H bond dissociation energy chosen for comparison was that for the molecule 4-methyl-N-(p-tolyl)aniline (shown below). The N-H bond dissociation energy of this molecule was 357.5 kJ mol^{-1} [100]

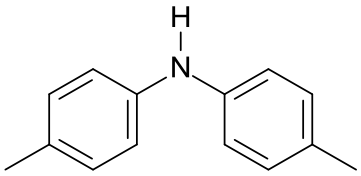

Figure 2.10 - Structure of 4-methyl-N-(p-tolyl)aniline

Using the methods 631g, 631g+, 631g+ d, 6311g, 6311g+ and 6311g+ d, the N-H bond dissociation energy was calculated. This molecule was chosen as the N-H bond dissociation energy of an alkyl substituted diphenylamine type structure is highly relevant to this work but the addition of further steric bulk on the alkyl groups was

deemed unnecessary and although it would dramatically increase the time taken to calculate the data would have a negligible impact on results.[101]

Table 2.2 – Comparison of calculated N-H bond dissociation energies with a known experimental value for 4-methyl-N-(p-tolyl)aniline

Basis set	Experimental value kJmol^{-1}	Calculated value kJ mol^{-1}	Difference kJ mol^{-1}
631g	357.5	374.0	+16.5
631g+	357.5	373.1	+15.6
631g+ d	357.5	354.9	-2.6
6311g	357.5	372.4	+14.9
6311g+	357.5	372.0	+14.5
6311g+ d	357.5	354.9	-2.6

From the data above, it can be seen that either the 631g+ d or 6311g+ d sets give an acceptably accurate figure when compared to the experimental figure. The method selected was 6311g+ d as the extra level of complexity from this method outweighs the small amount of extra time taken for the calculations of this method.

2.3.4 Example Gaussian calculation

The Gaussian output gives various thermochemical information. These include the following:[93]

ε_0 - Total electronic energy

ε_{ZPF} - Zero-point correction

E_{tot} - Thermal correction to energy

H_{corr} - Thermal correction to enthalpy

G_{corr} - Thermal correction to Gibbs free energy

$\varepsilon_0+\varepsilon_{ZPE}$ - Sum of electronic and zero-point energies

ε_0+E_{tot} - Sum of electronic and thermal energies

ε_0+H_{corr} - Sum of electronic and thermal enthalpies

ε_0+G_{corr} - Sum of electronic and thermal free energies

S_{tot} - Total entropy

To calculate the bond dissociation energy, the following calculation must be made:

$$\Delta_r H^o(298K) = \sum_{prod} \Delta_f H^o_{prod}(298K) - \sum_{react} \Delta_f H^o_{react}(298K)$$

Equation 2.7 – Bond dissociation energy calculation

This can be achieved using Gaussian by applying the following formula:

$$\Delta_r H^o(298K) = \sum (\varepsilon_0 + H_{corr})_{prod} - \sum (\varepsilon_0 + H_{corr})_{react}$$

Equation 2.8 – Bond dissociation energy calculation using Gaussian

For example, to calculate the N-H bond dissociation energy of 4-methyl-N-(p-tolyl)aniline the following molecules would be processed using Gaussian to obtain the $\varepsilon_0 + H_{corr}$ values.

$$\Delta_r H^o(298K) = H\cdot + (CH_3C_6H_4)_2N\cdot - (CH_3C6H_4)_2NH$$

Equation 2.9 – Bond dissociation energy species used for calculation

A conversion is also necessary to give a value in kJ mol^{-1} as the output in Gaussian gives a value in Hartrees

Table 2.3 – Conversion factors for Gaussain output

1 Hartree	627.5059 kcal mol^{-1}
1 kcal mol^{-1}	4.1868 kJ mol^{-1}
1 kJ mol^{-1}	0.239005736 kcal mol^{-1}

2.4 Materials

The following is a list of materials used throughout this work along with the suppliers and their purity.

Table 2.4 – List of materials used

Name	Common name	Supplier	Purity(%)
(E)-3-(3,5-ditert-butyl-4-hydroxy-phenyl)prop-2-enoic acid	Hydroxy cinnamic acid	Alfa aesar	98
4-methoxy-N-(4-methoxyphenyl)aniline	DPAOMe	Aldrich	98
4-N,N'-Dimethylaminopyridine	DMAP	Aldrich	98
Dichloromethane	DCM	Fisher	
Diethylether		Fisher	
N,N'-Dicyclohexylcarbodiimide	DCC	Aldrich	99
2,6-ditert-butyl-1,4-benzoquinone	Quinone	Aldrich	98
Ethanol		Aldrich	99
Iodine		Fluka	99
4-(1,1,3,3-tetramethylbutyl)-N-[4-(1,1,3,3-tetramethylbutyl)phenyl]aniline	Irganox L01 (ODPA)	BASF	98
Irganox L01	ODPA	BASF	98
Irganox L06	PANA	BASF	98
Irganox L107	OHPP	BASF	99
Octadecanol		Aldrich	98
Octadecyl (E)-3-(3,5-ditert-butyl-4-hydroxy-phenyl)prop-2-enoate	Hydroxycinnamate		95

Name	Common name	Supplier	Purity(%)
Phenothiazine		Aldrich	99
Phenoxazine		Aldrich	99
2,6,10,15,19,23-Hexamethyltetracosane	Squalane	Aldrich	99
Sulfur		Fluka	99
Toluene	Methyl benzene	Fisher	99
Tetrahydrofuran	THF	Fisher	99
9-(1,1,3,3-tetramethylbutyl)-12H-benzo[a]phenothiazine	PANAS	-	95
Trichloromethane-d	Chloroform-d	Aldrich	99

Chapter 3

The Antioxidant Mechanisms of a Hindered Phenolic Antioxidant

3.0 The Antioxidant Mechanisms of a Hindered Phenolic Antioxidant

3.1 Introduction

The addition of an antioxidant in an automotive lubricant is designed to prevent oxidation caused by the oxygen rich environment and high temperatures.[102] Examples of naturally occurring phenolic antioxidants are abundant in foodstuffs such as fruits and nuts with antioxidants such as α-tocopherol (vitamin E) being an essential radical scavenger in biological systems.[103] Phenolic antioxidants designed for use in automotive lubricants are modified phenol structures which are oil soluble and have low-volatility characteristics at high temperatures.[102]

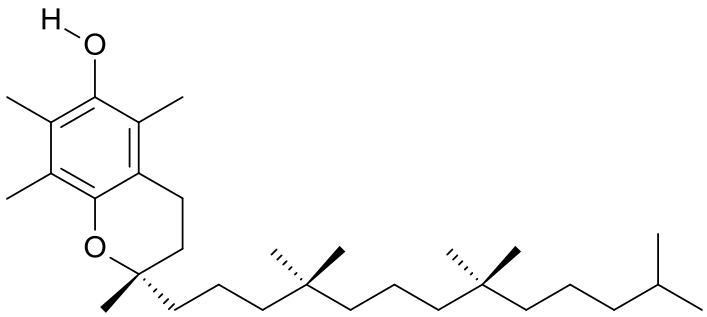

Figure 3.1 – Structure of α-tocopherol (vitamin E)

The work described in this chapter assesses the previous work on phenolic antioxidants and examines the currently widely accepted mechanism for the mode of action for these types of antioxidants as outlined in section1.6 and section 3.2. It also assesses the difference in intermediate product formation between traditional phenolic antioxidants such as 2,6-ditert-butyl-4-methyl-phenol, also known as butylated hydroxytoluene (BHT) and the antioxidant used in this work, which was

octadecyl 3-(3,5-ditert-butyl-4-hydroxy-phenyl)propanoate (OHPP) shown in Figure 3.2. The base oil used was squalane which contains 20% tertiary hydrogen atoms which is comparable to that of a group II mineral oil.[104] This work attempts to indentify mechanisms by identifying products formed from the antioxidant. OHPP was chosen for this reason as this antioxidant is a single structure which aided product analysis when using techniques such as GC. This antioxidant contains substituents in the ortho and para positions which decreases the O-H bond dissociation energy making the reaction between itself and alkyl peroxy radicals more exothermic and therefore more favourable.[105,106,107,108]

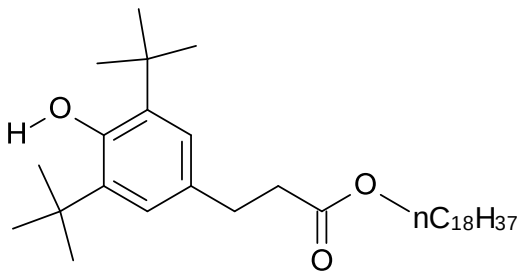

Figure 3.2 - octadecyl 3-(3,5-ditert-butyl-4-hydroxy-phenyl)propanoate (OHPP)

This work focuses on high temperature oxidation using temperatures between 160 and 220 °C to simulate those measured at the ring pack of a piston in an automotive engine.[81,82] The concentration of antioxidant used (unless otherwise stated) was 0.50 %wt (7.5×10^{-3} mol dm^{-3}) which is the treat rate recommended by the supplier for automotive lubricant applications.[109]

3.2 Previous work

3.2.1 Mechanistic studies on BHT and OHPP

Previous studies by Pilař *et al*[110] and Pospíšil *et al*[111] on the reactions of substituted phenols identified the existence of several intermediate antioxidant species in addition to those outlined in Figure 1.3 (recapped in Figure 3.3).

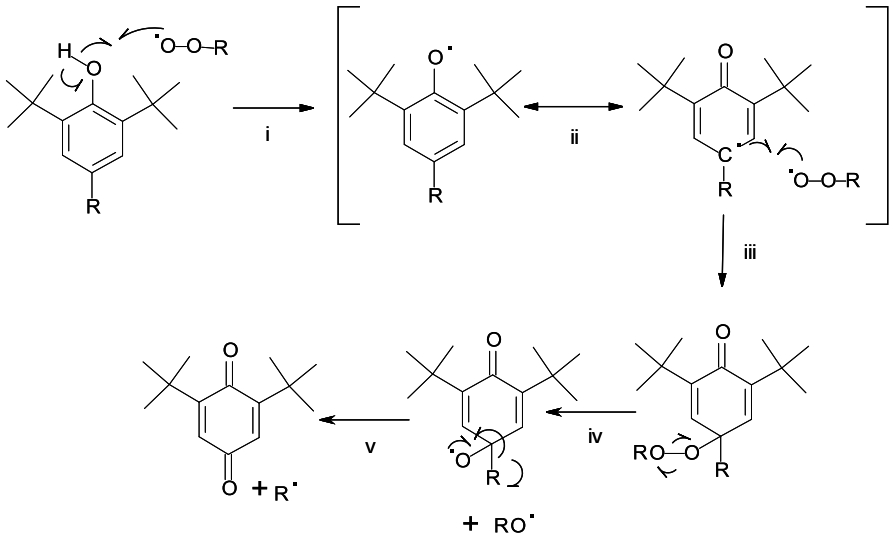

Figure 3.3 – Recap of Figure 1.3, the well-established phenolic antioxidant mechanism

Using BHT, Pilař proposed that the phenolic radical (Species (A) of Figure 3.4) produced by the abstraction of the labile hydrogen of the O-H group, result in two molecules of A reacting with each other to form 2,6-ditert-butyl-4-methylene-cyclohexa-2,5-dien-1-one (Species (B) of Figure 3.4) and BHT in a disproportionation reaction.[40,112,113] The resonance structure of (A) can dimerise in two ways as outlined in Figure 3.4. Analysis of products was carried out using

ESR at 25°C, with oxidation achieved using lead dioxide.

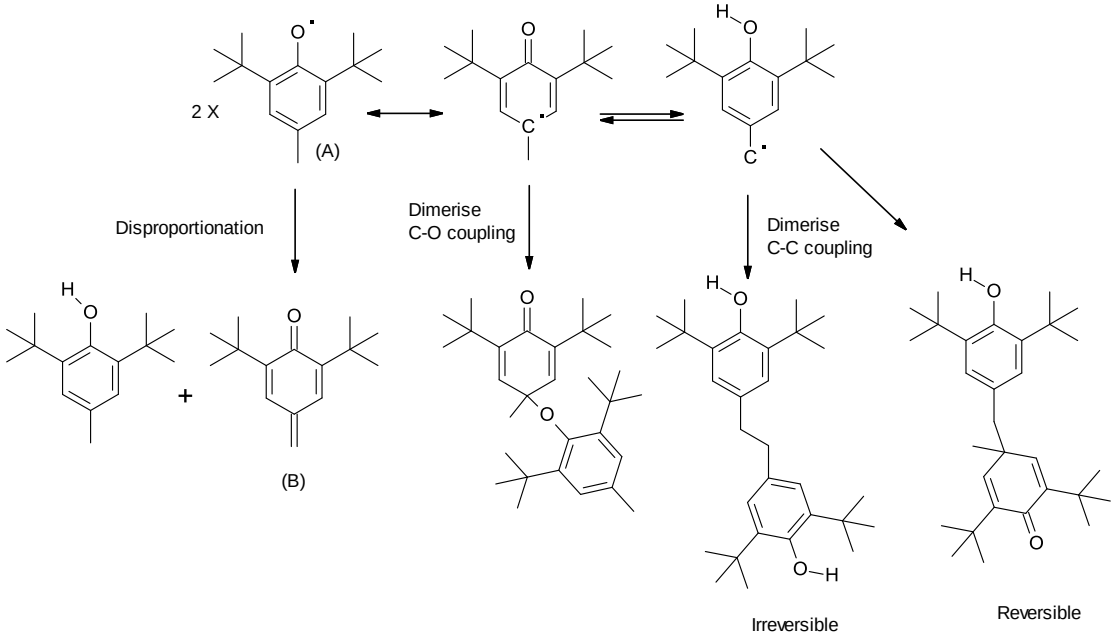

Figure 3.4 - Pilař's oxidation inhibition mechanisms for the antioxidant BHT.

The work done by Pilař[110] on antioxidant mechanisms uses conditions quite different to those found during use in a lubricant (room temperature in the presence of lead oxide instead of high temperature and oxygen). Any lessons drawn from this work may not necessarily be applicable to phenolic antioxidant during use in engine oil lubricants. It also used BHT, which has a flash point temperature of just 127 °C and a boiling point of 265 °C and so significant volatile loss would be expected under piston ring temperatures.

Pospíšil extended this by increasing temperatures to up to 180 °C for 24 hours in a circulation air oven (80 dm^3 $Hour^{-1}$) where samples were placed in an open

vessel in an oven. Amongst the products found from octadecyl 3-(3,5-ditert-butyl-4-hydroxy-phenyl)propanoate (OHPP), which is the same antioxidant is used in this chapter, was octadecyl (E)-3-(3,5-ditert-butyl-4-hydroxy-phenyl)prop-2-enoate (Hydroxycinnamate),[111] which is shown in Figure 3.5.

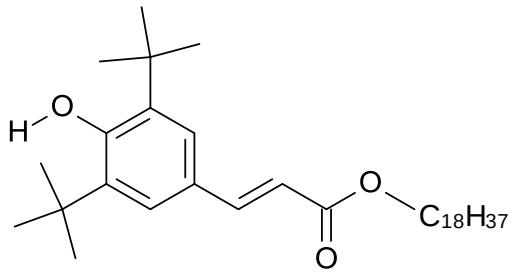

Figure 3.5 – Octadecyl (E)-3-(3,5-ditert-butyl-4-hydroxy-phenyl)prop-2-enoate (Hydroxycinnamate)

The hydroxycinnamate was proposed to be formed by a rearrangement of the relatively unstable quinone methide structure octadecyl 3-(3,5-ditert-butyl-4-oxo-cyclohexa-2,5-dien-1-ylidene)propanoate.[11] The method of detection used was HPLC and so was identified by its UV absorbances. The quinone methide is formed by the abstraction by an alkyl peroxy radical of a hydrogen alpha to the resonance stabilised radical (formed in step ii of Figure 3.3) rather than the combination of this radical with an alkyl peroxy radical. This type of rearrangement mechanism has also been reported in substituted semi-quinone structures that contain an electron withdrawing group such as bromine in the para position, instead of an electron donating alkyl group.[114]

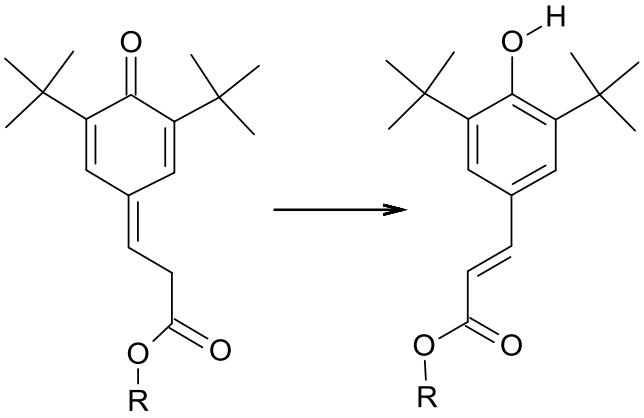

Figure 3.6 – Quninone methide rearrangement to form hydroxycinnamate[111]

An alternative to this rearrangement is a mechanism where the quinone methide structure can react with water to regenerate the phenol ring,[115,116,117,118] as identified by UV-vis analysis by Hemmingson and Leary.[115] This forms an alcohol structure with the alcohol group in the α position of the para positioned alkyl chain, as shown in Figure 3.7.

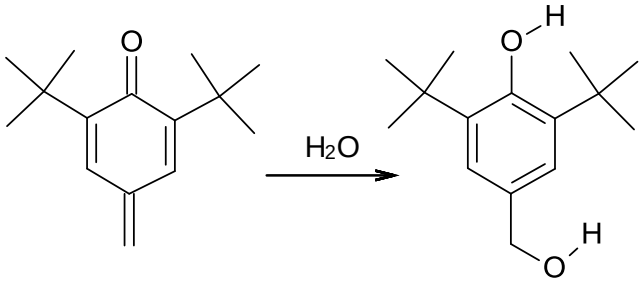

Figure 3.7 –Reaction of quinone methide with water

Although hydroxycinnamate was identified as a product by Pospíšil, it was not determined if the hydroxycinnamate intermediate product could act as a good antioxidant itself. It was also not established if the hydroxycinnamate intermediate went on to form quninone in significant quantities or if the hydroxycinnamate

formation was a small side reaction to the well-established phenolic antioxidant mechanism, which was the aim of this work. The work done in this chapter also adds time development studies to the formation of intermediates with the quantification of these species.

3.3 Results and discussion

The remainder of this chapter shows the results of this work obtained using the continuous flow reactor detailed in chapter 2 and discusses the results in the context of the known mechanisms and intermediate species of phenolic antioxidants.

3.3.1 OHPP high temperature oxidation

Using the continuous flow setup outlined in Figure 2.4, oxidation of squalane containing OHPP was carried out at 180, 200 and 220 °C. As shown in Figure 3.8, at temperatures below 220 °C, the antioxidant prevented squalane oxidation. At 220 °C, little antioxidant protection is provided by OHPP which has an induction period similar to that of just squalane at this temperature. This poor performance of induction periods of 30 minutes and below under piston ring conditions illustrates the extreme conditions of this work as other work at these temperatures using similar antioxidants to OHPP showed much greater antioxidant protection.[119]

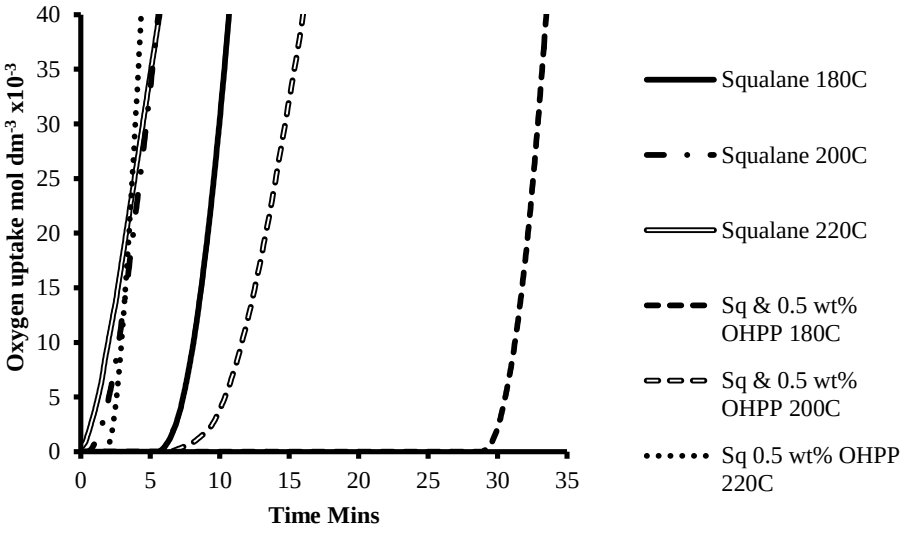

Figure 3.8– Oxygen uptake during autoxidation of OHPP in squalane between 180 and 220 °C

3.4 GC analysis of a OHPP oxidation run

3.4.1 Starting material analysis

By GC, the initial trace shows 4 significant peaks: squalane, antioxidant, squalane impurity which is thought to be 2,6,10,14-Tetramethylpentadecane (pristine) and the toluene which was used as a diluent.

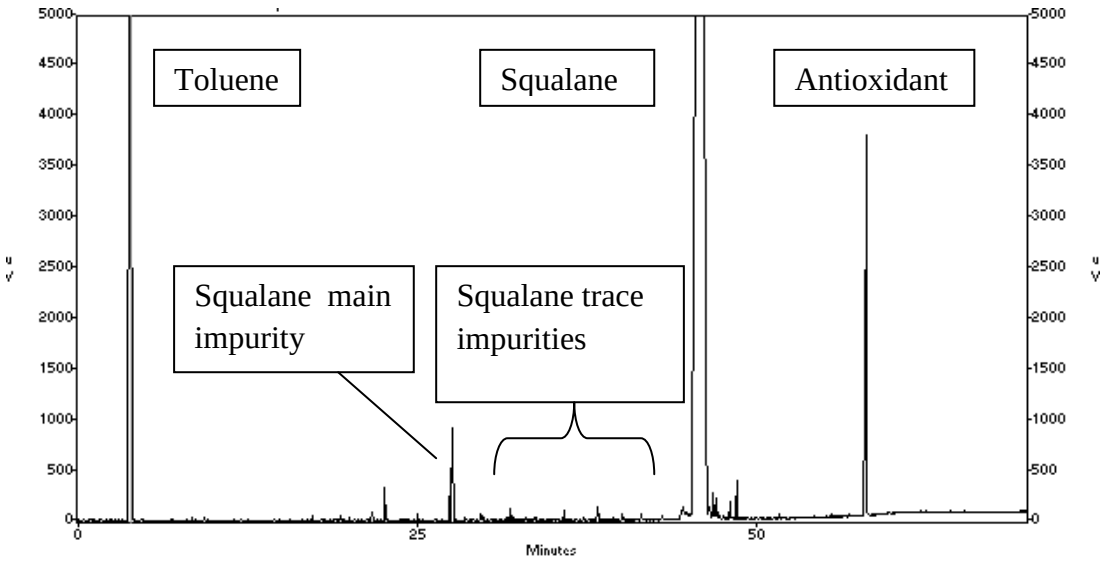

Figure 3.9 – GC trace of starting material containing 7.5 x10^{-3} mol dm^{-3} of OHPP

At the end of the induction period, the antioxidant is consumed and the GC trace contains a number of peaks from the oxidation of squalane including 6,11,15,19,23-pentamethyltetracosan-2-one[120] (ketone).

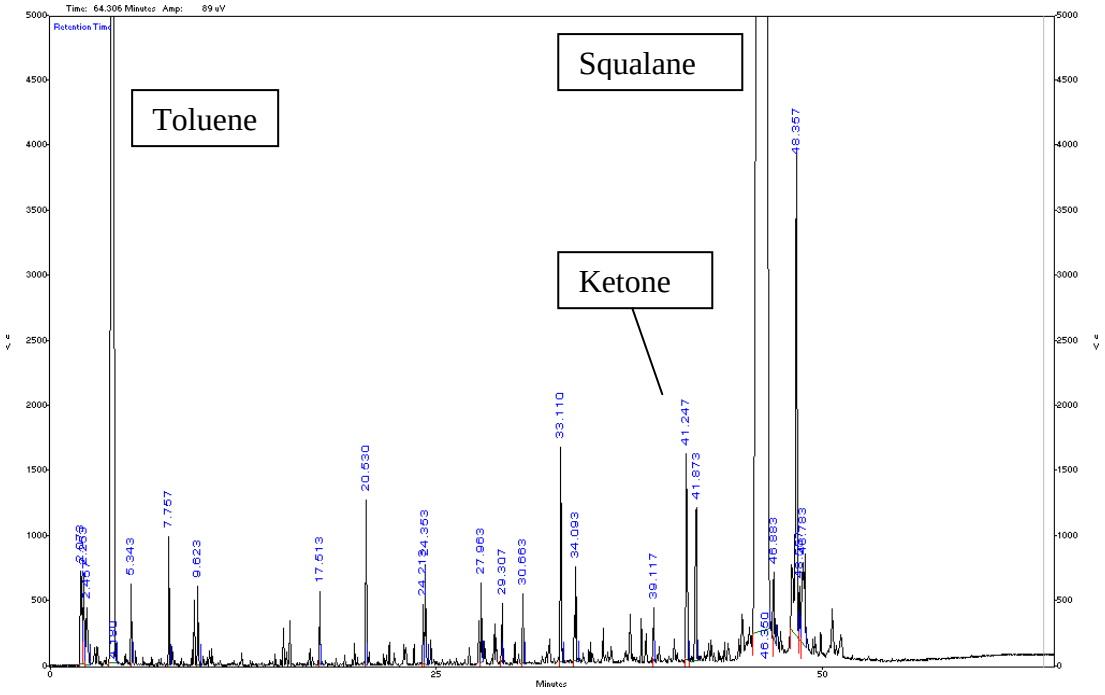

Figure 3.10 – GC trace of material containing 7.5 x10^{-3} mol dm^{-3} of OHPP after 30 minutes.

3.4.2 Antioxidant quantification

At 180 °C, when monitored by GC by taking a sample every 5 minutes, the antioxidant consumption was found to be low in the first 5 minutes and fell by 11 %. This rate of consumption increases over time, and after approximately 30 minutes, the antioxidant was completely consumed. At this point, the squalane began to oxidise as indicated by the build-up of ketone meaning that the phenolic antioxidant protected the base oil from oxidation until it was entirely consumed.[23]

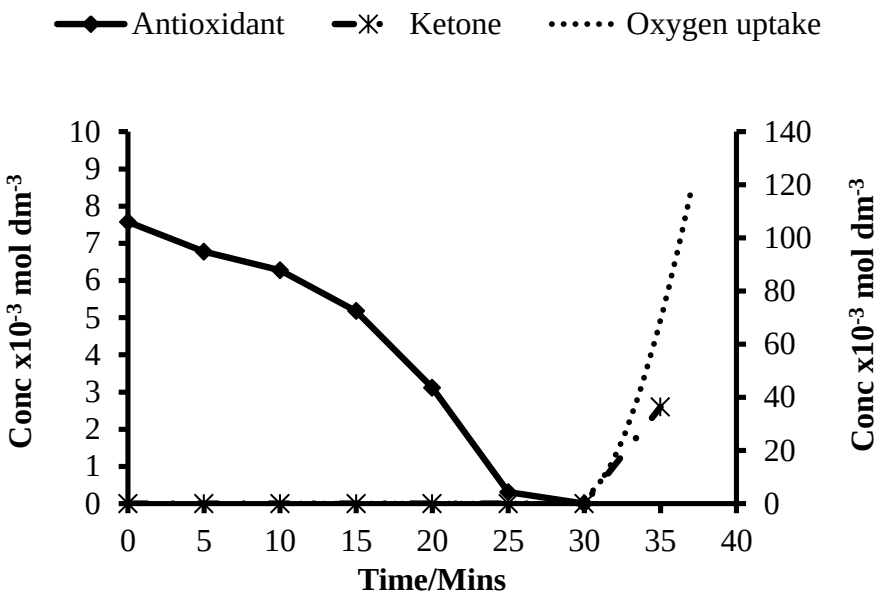

Figure 3.11– Antioxidant and squalane ketone concentration at 180 °C

3.4.3 New product identification

Samples taken during the induction period (0 - 30 minutes) at 180 ºC, confirmed the presence of three new product peaks in the 50 - 65 minute region of the GC trace and one new product peak in the 20 - 30 minute region of the GC trace. Several other new peaks were also found in the 20 - 30 minute region of the GC trace. These are believed to be squalane oxidation products. The peak at 22.017 was believed to be a product peak, as suggested to be 2,6-ditert-butyl-1,4-benzoquinone by the mass spectra library, and so was focused on for further analysis.

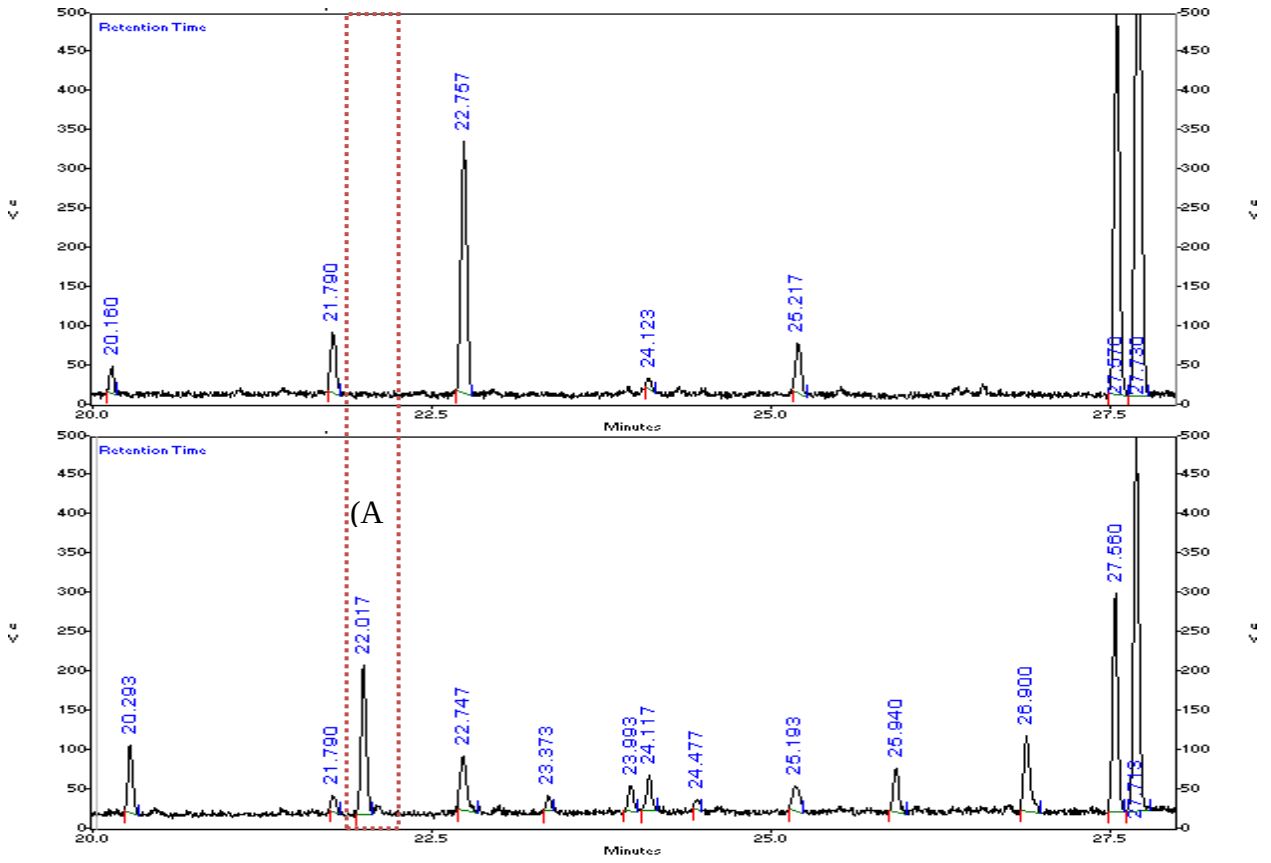

Figure 3.11 – GC trace of 20 – 30 minute region of the starting material (top) and a sample taken after 20 minutes in to the induction period at 180 °C

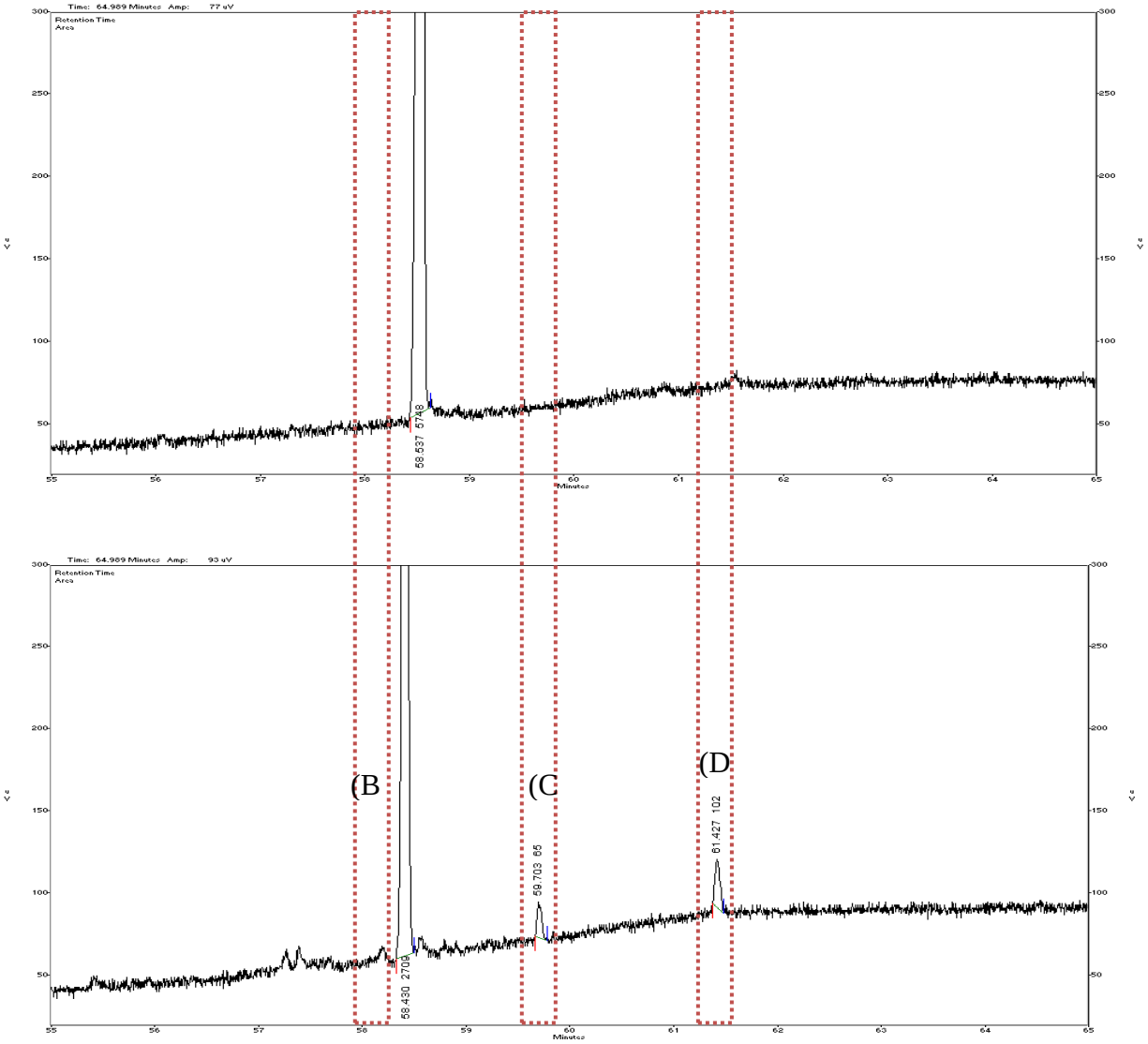

Figure 3.12 - GC trace of the 50 – 65 minute region of the starting material (top) and a sample taken after 20 minutes in to the induction period at 180 °C

3.5 Product identification using GC-MS

Identification of these products was mainly achieved using GC-MS (EI) EI accurate mass spec. Analysis of the product at 22.017 minutes of the GC trace (Figure 3.11) concluded that this was 2,6-ditert-butyl-1,4-benzoquinone (quinone) shown in Figure 3.13, which is the end product of the antioxidant according to the accepted mechanism of phenolic antioxidants. In addition to the mass spec library suggestion, this was confirmed using 2,6-ditert-butyl-1,4-benzoquinone purchased from Sigma Aldrich, which had the same GC retention time as the product peak and eluted a single peak at this retention time when the quinone was added to an oxidation sample containing the intermediate of GC retention time 22.017 minutes.

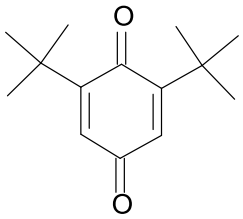

Figure 3.13 – Structure of 2,6-ditert-butyl-1,4-benzoquinone (quinone)

The products in the 50 – 65 minute region of the GC were also identified by GC-MS (EI). These consisted of two quantifiable products (C) and (D) and a third product which was not quantifiable without significant error due to its low concentration.

EI accurate mass spec analysis of the largest product (D) concluded that the largest peak in the 50 – 60 minute region of the GC trace had a molecular ion peak at 528,

which is two less than the starting antioxidant with its nominal mass of 530. From this, two possible structures were deduced (Di) and (Dii) shown below, confirming the previous work of Pospíšil.

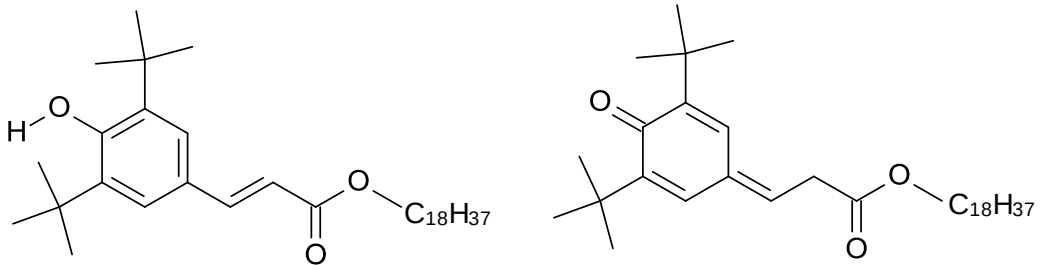

Di Dii

Figure 3.14 – The two possible structures of product (D)

As (Di) and (Dii) are structurally similar, the fragmentation pattern of the mass spectroscopy was analysed for differences. The main difference between the two species is the carbonyl group of (Dii) and the OH group of (Di) but despite this, both molecules can fragment to produce a fragment of m/z 217 as shown below. It was hoped that the absence of a peak of m/z 217 would indicate that the intermediate product was Di as fragmentation of this molecule at the same place would result in a peak of m/z 218 by vinylic cleavage. Unfortunately, this was not the case as no 218 peak was observed.

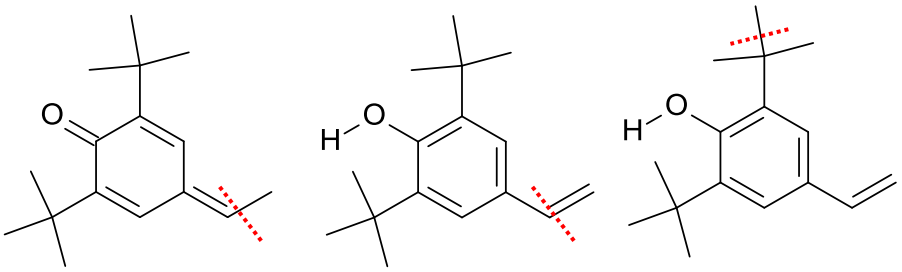

m/z 217 m/z 218 m/z 217

Figure 3.15 – Structures of possible fragments of Di and Dii.

Table 3.1 – Accurate mass spec fragmentation of product D of mass 528

Formula	Formula Mass	Measured Mass	ppm difference
$C_{35}H_{60}O_3^{+\cdot}$	528.4542	528.4597 (100)	10.41
$C_{34}H_{57}O_3^{+}$	513.4302	513.4355 (36)	10.32
$C_{17}H_{24}O_3^{+\cdot}$	276.1720	276.1712 (12)	-2.90
$C_{16}H_{22}O_3^{+}$	261.1485	261.1489 (15)	1.53
$C_{17}H_{23}O_2^{+}$	259.1693	259.1705 (15)	4.63
$C_{16}H_{24}O^{+}$	232.1827	232.1791 (6)	-15.51
$C_{15}H_{23}O^{+}$	219.1734	219.1732 (6)	-0.91
$C_{15}H_{21}O^{+}$	217.1592	217.1478 (5)	-52.50

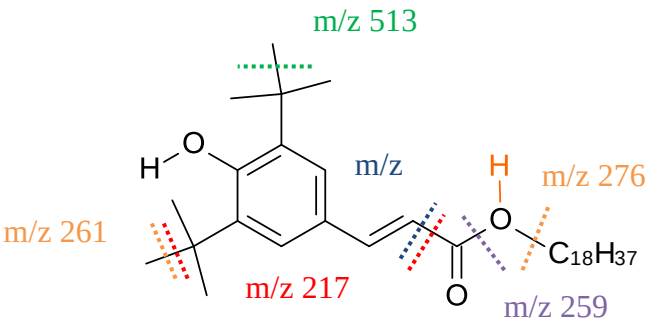

Figure 3.16 – Product D fragmentation

The 217 fragment of the quinone methide occurs via vinylic cleavage, whereas the hydroxycinnamate route involves multiple steps shown in Figure 3.17. It is known that cinnamic acid derivatives such as coumaric acid will undergo thermal decarboxylation.[121] Mass spec analysis done in this work on (E)-3-(3,5-di-tert-butyl-4-hydroxy-phenyl)prop-2-enoic acid (di-tert butyl coumaric acid) concluded that the decarboxylation process occurs to such an extent that the mass ion peak is not observed. Another common fragmentation of tert-butyl substituted phenols is the loss of a methyl group corresponding to a loss of 15 to the observed mass ion peak.[122]

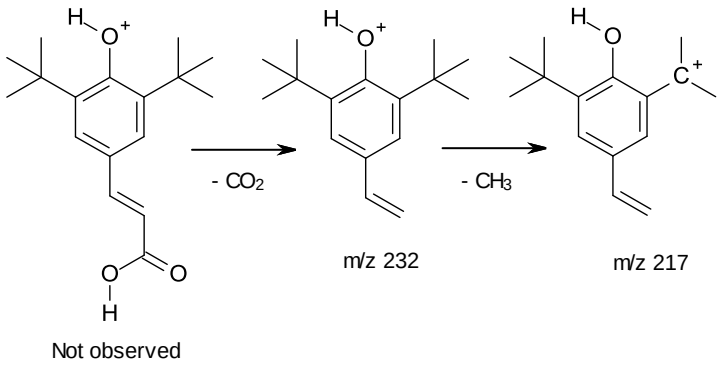

Figure 3.17 – Decarboxylation mechanism of di-tert butyl coumaric acid

The presence of a fragment of m/z 232, of the product of molecular weight 528, indicates that this is structure (Di) as the ester group can form a carboxylic acid via inductive cleavage (McLafferty +1)[123], which can then rapidly decarboxylate. This will not be observed from structure (Dii) as according to Kulik *et al*,[121] the main contribution to the facilitation of coumaric acid decarboxylation is from the +M effect of the hydroxyl group para to the chain which leads to an increase in π-electron density in the -CH=CH- group and the formation of a partical negative charge on the olefin carbon atom bonded to the carboxyl group as shown in Figure 3.18 which cannot as easily be achieved in structure Dii because of the lack of resonance between the -CH=CH- group and the carboxyl group.

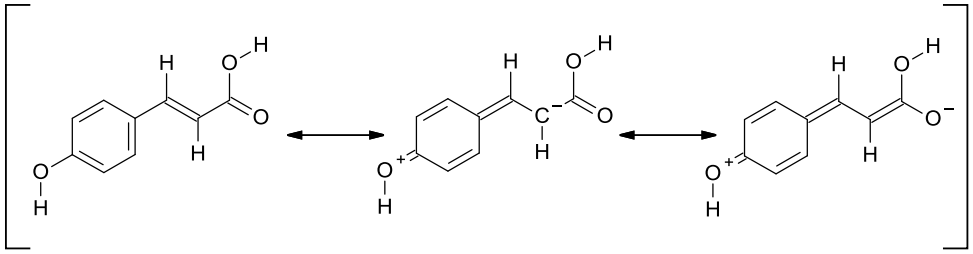

Figure 3.18 – Resonance structures of coumaric acid which aid decarboxylation.

Analysis of the other quantifiable peak (C) by accurate mass EI gave a peak with a molecular mass of 544.4569 ± 15ppm which is +14 to the starting antioxidant and +16 to product (D) which correlates to -H then +OH. In addition to the mass ion peak and the characteristic -15 peak ($-CH_3$) several other fragments could be identified from the mass spec such as loss of 18 ($-H_2O$) which is common in secondary alcohols[124] and occurs by as much as 90% via elimination of the OH and the H attached to the γ carbon resulting in a cyclic structure[125] (m/z 526.4489). Loss of a subsequent methyl group from the tertiary butyl[122] leaves a fragment of $C_{34}H_{56}O_3^+$ m/z 511.4194. The closest formula match for the fragment at m/z 217.1365 is ($C_{14}H_{17}O_2^+$) is contrary to product (D) where the closest formula match for the 217 fragment was ($C_{15}H_{21}O^+$). Also, it is also not acompanied by a decarboxylation fragment of m/z 232, suggesting the product is not a cinnamic acid/ester derivative.

Table 3.2 – Quinone methide alcohol accurate mass spec fragmentation

Formula	Formula Mass	Measured Mass	ppm difference
$C_{35}H_{60}O_4^{+\cdot}$	544.4491	544.4564 (100)	13.41
$C_{34}H_{57}O_4^{+}$	529.4256	529.4196 (23)	-11.33
$C_{35}H_{58}O_3^{+}$	526.4509	526.4478 (5)	-5.89
$C_{34}H_{55}O_3^{+}$	511.4105	511.4185 (42)	15.64
$C_{15}H_{21}O_2^{+}$	233.1504	233.1541 (21)	15.87
$C_{15}H_{21}O^{+}$	217.1587	217.1415 (11)	-79.20

Product (C) was consistent with being octadecyl 3-(3,5-ditert-butyl-4-oxo-cyclohexa-2,5-dien-1-ylidene)-2-hydroxy-propanoate (quinone methide alcohol) shown in Figure 3.19. As the mass (and therefore molecular formula) of the product is consistent with the loss of a hydrogen and the addition of a hydroxyl group, the product was deduced as having an alcohol group. The position of this alcohol group is more likely to be on an alkyl group as abstraction of this hydrogen will require less energy than abstraction of a vinylic hydrogen.[126] This also agrees with the findings of Pospíšil *et al*[112] who believed that abstraction of this hydrogen resulted in antioxidant dimer products from C-C coupling at this point. Analytically, this intermediate was belived to be quinone and methide based and not aromatic becuase the product does not contain fragmentations at m/z 232 or m/z 219 as seen in product Di.

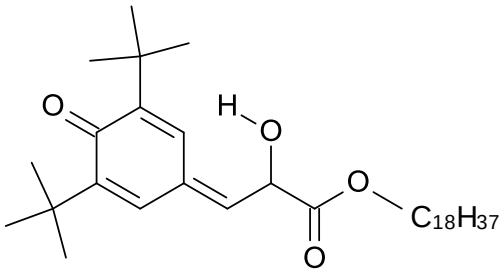

Figure 3.19 - Octadecyl 3-(3,5-ditert-butyl-4-oxo-cyclohexa-2,5-dien-1-ylidene)-2-hydroxy-propanoate (C)

The third, unquantifiable product (B) had a m/z of 546.4618 which is +16 to the starting antioxidant and like all the other products, a fragment at -15. Unlike product (C), this product had a fragmentation peak at 219.1073 and not 217, suggesting that the product is aromatic and not a quinone methide structure, as seen with the minor intermediate peak. As the errors associated with the signficant fragmentation peaks of 235 and 219 were unnacceptably high, the product structure can only be a proposal.

Table 3.3 – Phenolic antioxidant alcohol accurate mass spec fragmentation

Formula	Formula Mass	Measured Mass	ppm difference
$C_{35}H_{62}O_4^+$	546.4648	546.4618 (100)	-5.49
$C_{34}H_{59}O_4^+$	531.4407	531.4380 (20)	-5.08
$C_{15}H_{23}O_2^+$	235.1693	235.1379 (26)	-133.52
$C_{15}H_{23}O^+$	219.1734	219.1073 (15)	-301.59

The intermediate did not have an M -18 peak but as the best formula match to the measured mass was $C_{35}H_{62}O_4$, it is believed to contain an alcohol group. A structure for this molecule is proposed below although this product was observed in very small concentrations and so could not reliably be quantified but was

approximately 10x smaller than product D.

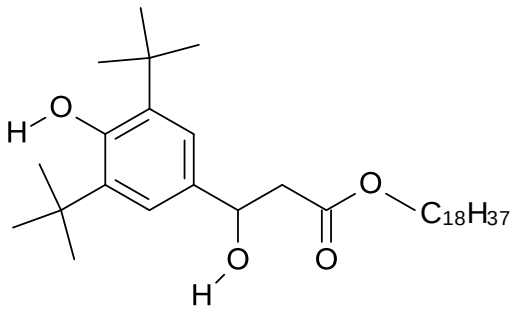

Figure 3.20 - Proposed Phenolic antioxidant alcohol structure octadecyl 3-(3,5-ditert-butyl-4-hydroxy-phenyl)-3-hydroxy-propanoate (B)

3.6 Antioxidant intermediate quantification

The 180 °C run was sampled every 5 minutes for 35 minutes and then analysed using GC FID and GC-MS. Quantification of the antioxidant and product concentration over time was achieved using GC-FID. The products were formed in concentrations of between 1/25 and 1/50 of the starting concentration of the antioxidant. The antioxidant and 6,10,15,19,23-pentamethyltetracosan-2-one (ketone)[120] concentrations are given on the left vertical axis and the product concentration on the right. The ketone is formed from the oxidation of squalane.[127] (D) is the first product to be formed after 5 minutes. The formation of (C) after 10 minutes and the quinone after 15 minutes suggests that both of these are produced from product (D). The squalane ketone is not formed in noticable amounts until all of the antioxidant has been consumed at the 30 minute mark. After this, the concentration increases rapidly. This along with the antioxidant concentration are displayed on the right hand axis below. The

quantifiable intermediates (shown on the left hand axis below) were at their maximum concentration 20 minutes into the 35 minute run. The third product could not be quantified without significant error due to its low concentration.

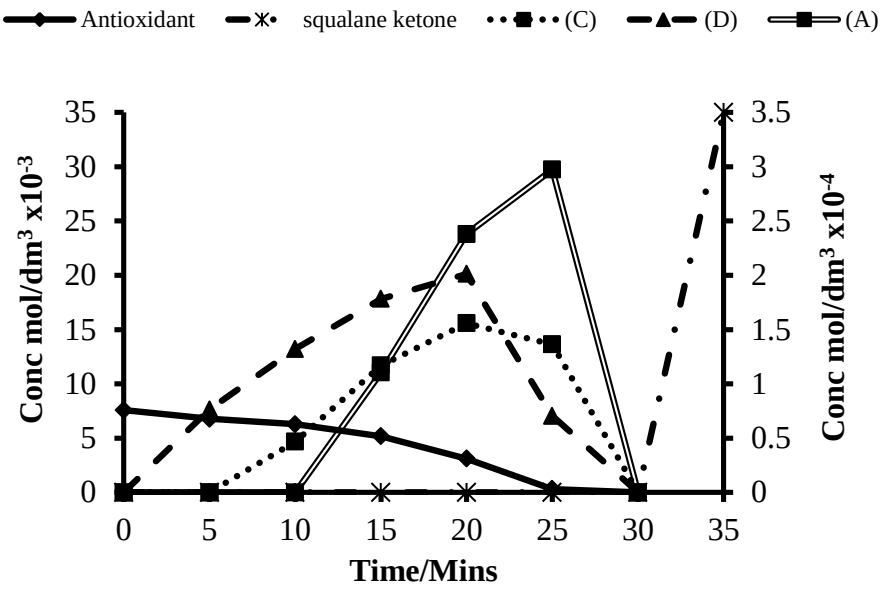

Figure 3.21 - Concentrations of starting antioxidant and build-up of intermediate products during a run at 180 °C

3.7 Hydroxycinnamate synthesis

3.7.1 Steglich esterification of antioxidant intermediate

To further prove the identification of the hydroxycinnamate intermediate and also to assess if hydroxycinnamate was a good antioxidant in its own right, this species was synthesised by Steglich esterification.[128] Although yields of 98 % are quoted for methyl cinnamate by Steglich, the long C_{18} chain of the alcohol may reduce yields and as the starting alcohol was used in excess, the product was

purified using column chromatography giving a product of 95 % purity as analysed by GC.

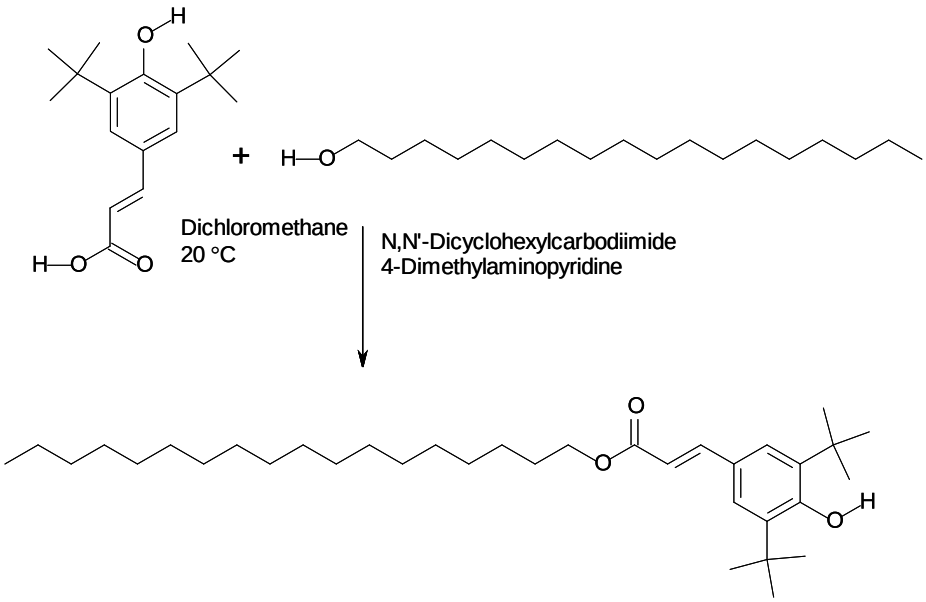

Figure 3.22 – Steglich esterification reaction to make hydroxycinnamate

3.7.2 Column chromatography purification

Using the method outlined in section 2.2.9 the hydroxycinnamate was purified by column chromatography before being analysed by NMR. The hydroxycinnamate fraction was identified using GC and GC-MS.

3.7.3 NMR analysis

The synthesised hydroxycinnamate was analysed by H^1 NMR (400 MHz) in $CDCl_3$ to confirm the synthesis was a success. The chemical shifts obtained from NMR were then compared against the expected shifts using NMR predictor software and the predicted spectra for the quinone methide structure.

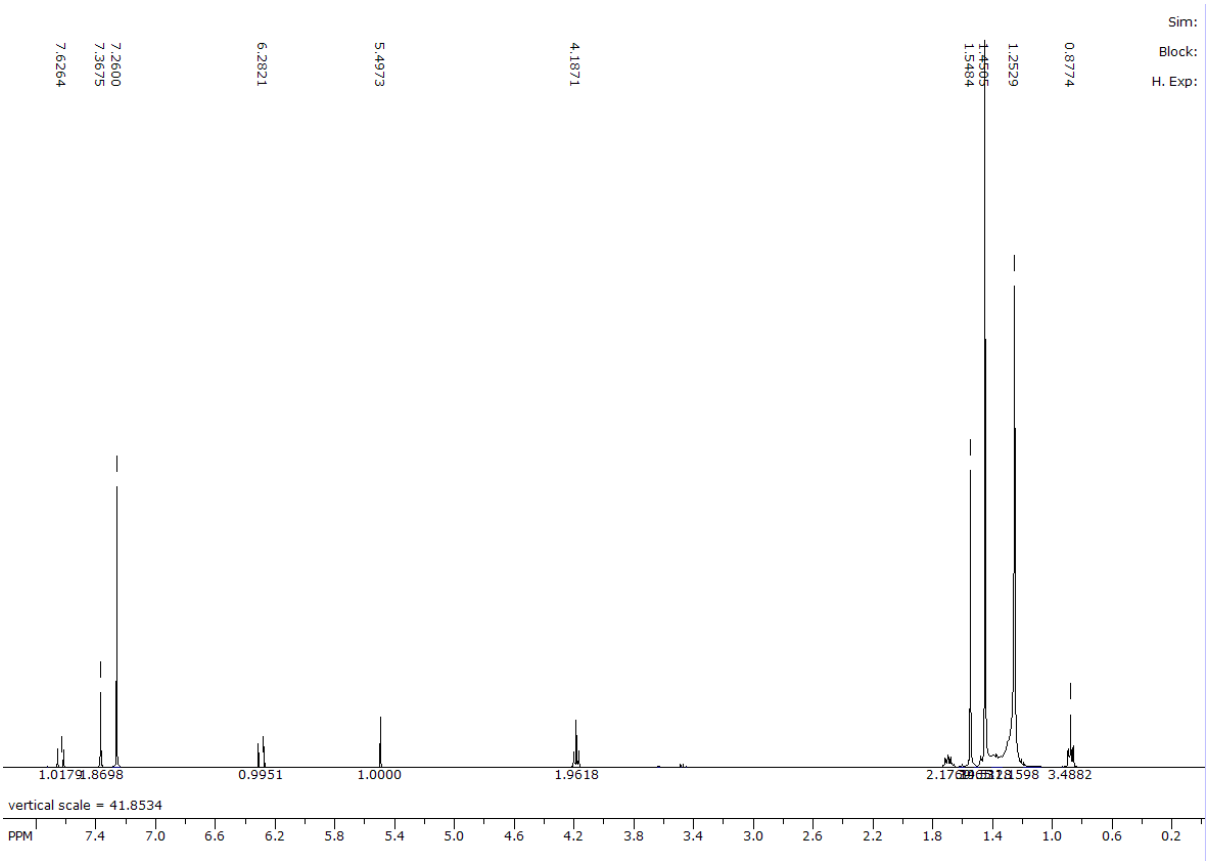

Figure 3.23 – Actual NMR spectra of synthesised hydroxycinnamate

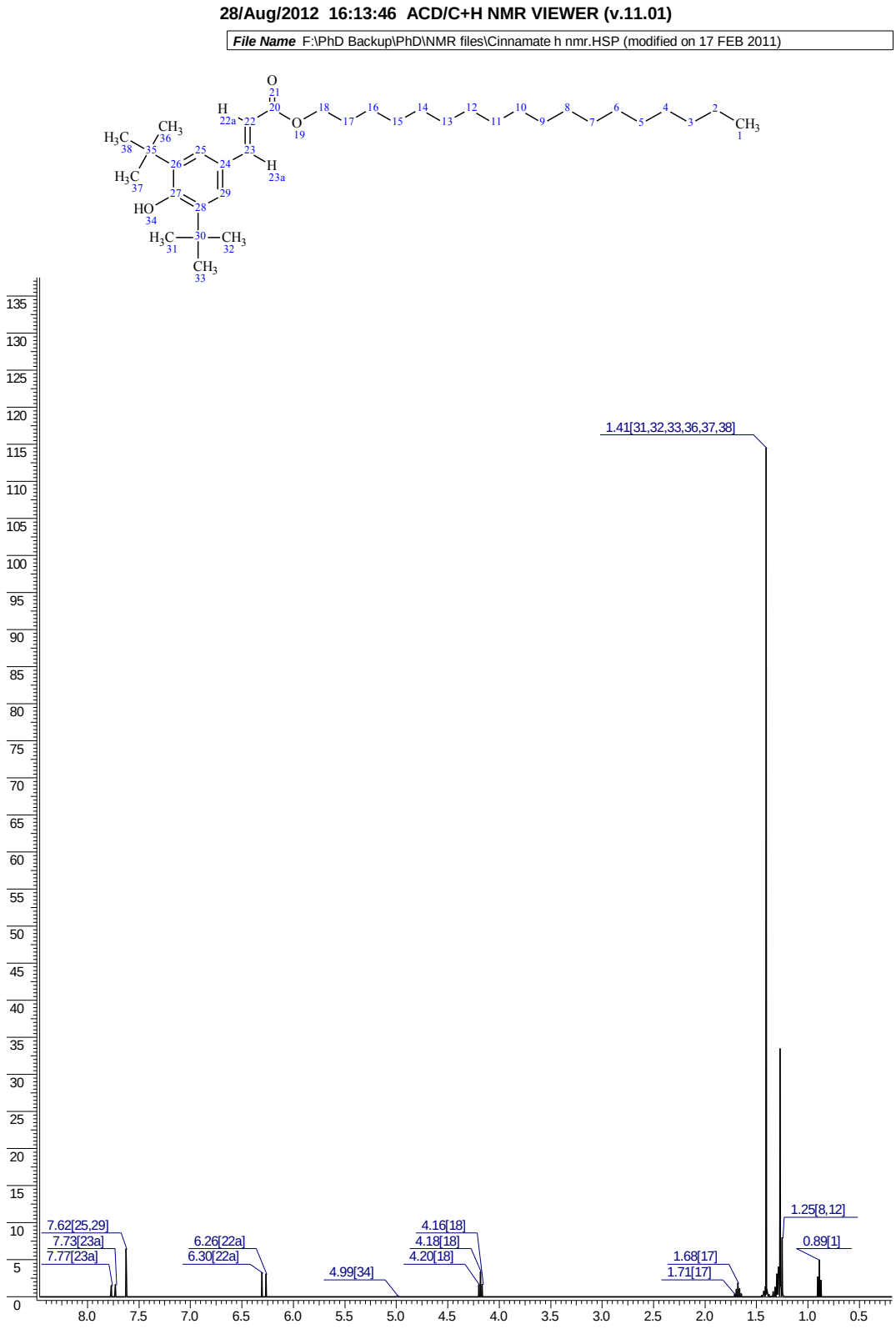

Figure 3.24 – Predicted NMR spectra of hydroxycinnamate

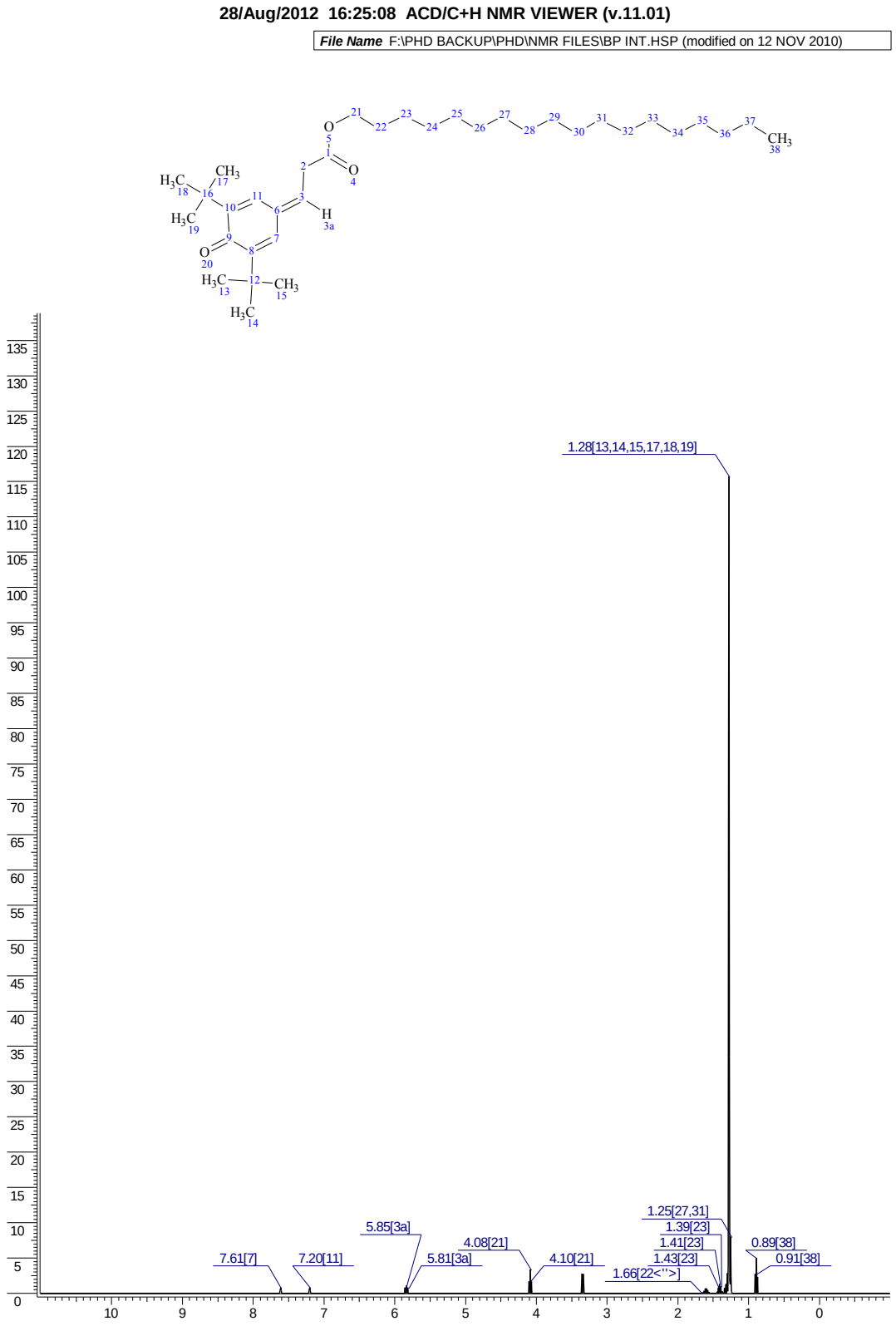

Figure 3.25 – Predicted NMR spectra of quinone methide

Table 3.4 – NMR shifts of hydroxycinnamate compared to expected shifts

Shift	Expected shift	Protons	Identification
0.87 – 1.25	0.89 – 1.25	Alkyl	A
1.45	1.41	18	B
4.18	4.16	2	C
6.28	6.26	1	D
7.36	7.62	2	E
7.62	7.73	1	F

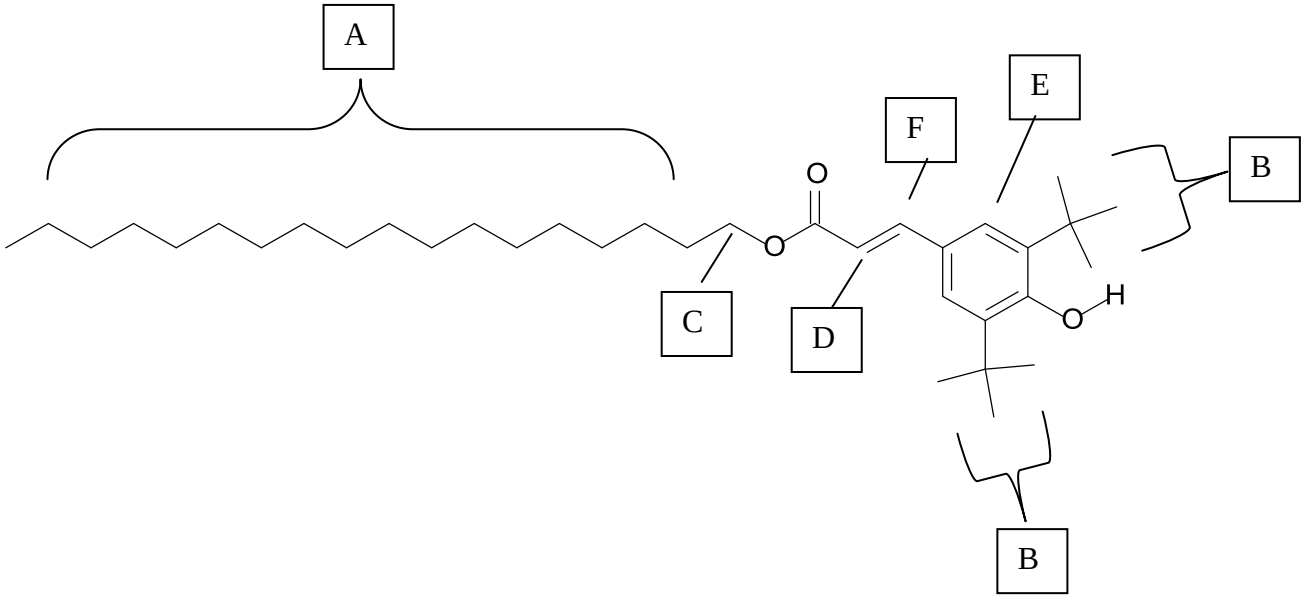

Figure 3.26 – Hydroxycinnamate H^1 NMR shifts at 400 MHz

The chemical shifts were also compared against predicted NMR spectra for both hydroxycinnamate and quinone methide which showed key differences such as both the hydroxycinnamate actual NMR and predicted NMR containing a doublet at 6.2 - 6.3 ppm and a coupling constant of 0.04 ppm (16 Hz) which is a typical coupling constant for trans hydrogen atoms across a C=C bond. This was not present in the quinone methide predicted spectra. The peaks which were present in the NMR of the

sample but not of the predicted software are believed to be from octadecanol (1.5484 ppm), dichloromethane from the synthesis (5.4973 ppm) and from the deuterated chloroform solvent used (7.3675 ppm).

Once the structure of the synthesised hydroxycinnamate was confirmed, it was used as a standard to confirm the structure of the intermediate formed during oxidation and also tested as an antioxidant to assess the antioxidant properties of the intermediate.

3.8 Synthesised hydroxycinnamate as a standard

Using the synthesised hydroxycinnamate as a known standard, several analytical methods were used to help identify the main intermediate of the OHPP oxidation reaction. These were GC, GC-MS, UV-vis and GPC.

3.8.1 GC analysis

When the GC retention times of the synthesised material was compared to that of the hydroxycinnamate intermediate from an oxidation reaction, it was found to have the

same retention time by GC. When the GC vials were mixed together, the sample gave a single GC peak.

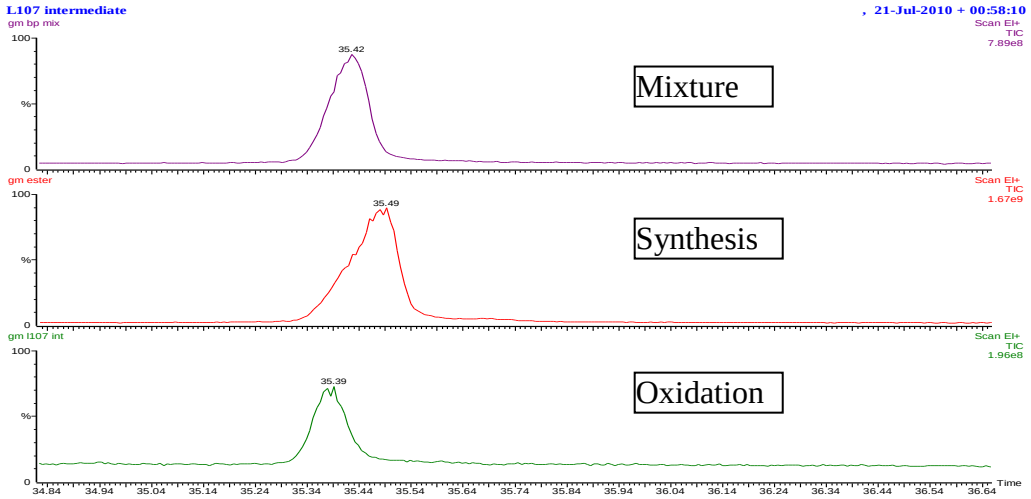

Figure 3.27 – GC traces of Hydroxycinnamate from synthesis, oxidation and a mixture of the two

3.8.2 GC-MS analysis

The mass spectra of the oxidation, synthesis and mixed samples were directly comparable with all spectra showing significant fragment ions of similar intensities at m/z 528, 513, 276, 232, 219 and 187.

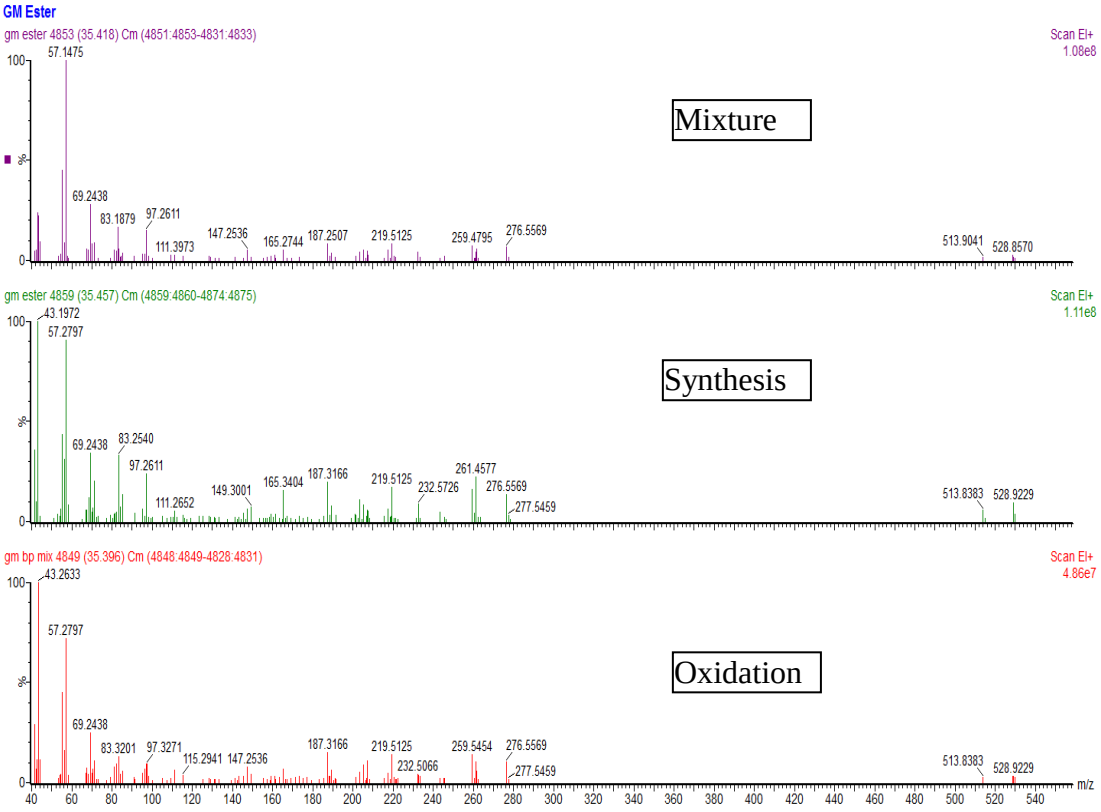

Figure 3.28 - MS traces of Hydroxycinnamate from synthesis, oxidation and a mixture of the two

3.8.3 UV-vis analysis

Due to the highly conjugated structures of the phenolic antioxidant and the products it forms, UV analysis was carried out on the phenolic antioxidant, the synthesised hydroxycinnamate and the end material quinone which was purchased from Aldrich.

The synthesised hydroxycinnamate material had a very similar UV spectum to the starting antioxidant, as both show absorbance at 280 nm however, in addition, the hydroxycinnamate also had a broad absorbance at 316 nm which is a known

characteristic of hydroxycinnamate.[111] The quinone had a maximum absorbance at 258 nm and very little absorbance above 300 nm.

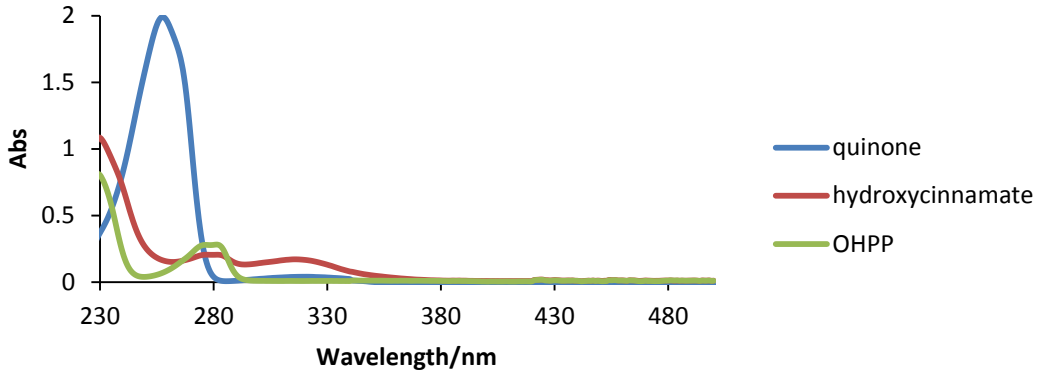

Figure 3.29 – UV spectra of quinone, hydroxycinnamate and OHPP starting antioxidant

3.8.4 GPC analysis

Using the λ_{max} details obtained from UV-vis, a GPC method was developed to assess the UV spectra of species separated by GPC of samples taken during an oxidation run (see section 2.2.4). This is beneficial in this work as squalane is not UV active and so the absorbances of the antioxidant and the products it forms can be assessed more effectively. The starting material had strong absorbances at 260 and 280 nm and a small absorbance at 305 nm shown in the peak at between 8 and 9 minutes. A second much smaller peak was visible between 10 and 11 minutes. After running a sample of 2-6 di-tertbutyl quinone, which had a retention time of 9.8 minutes, it was concluded that this peak was an impurity of the antioxidant of a similar size to BHT. This is not thought to be from the THF solvent as inhibitor free THF was used in this work. As well as the GPC trace, the structure of the molecule

responsible for the largest absorbance is detailed below along with the three greatest absorbance frequencies of those measured for that species.

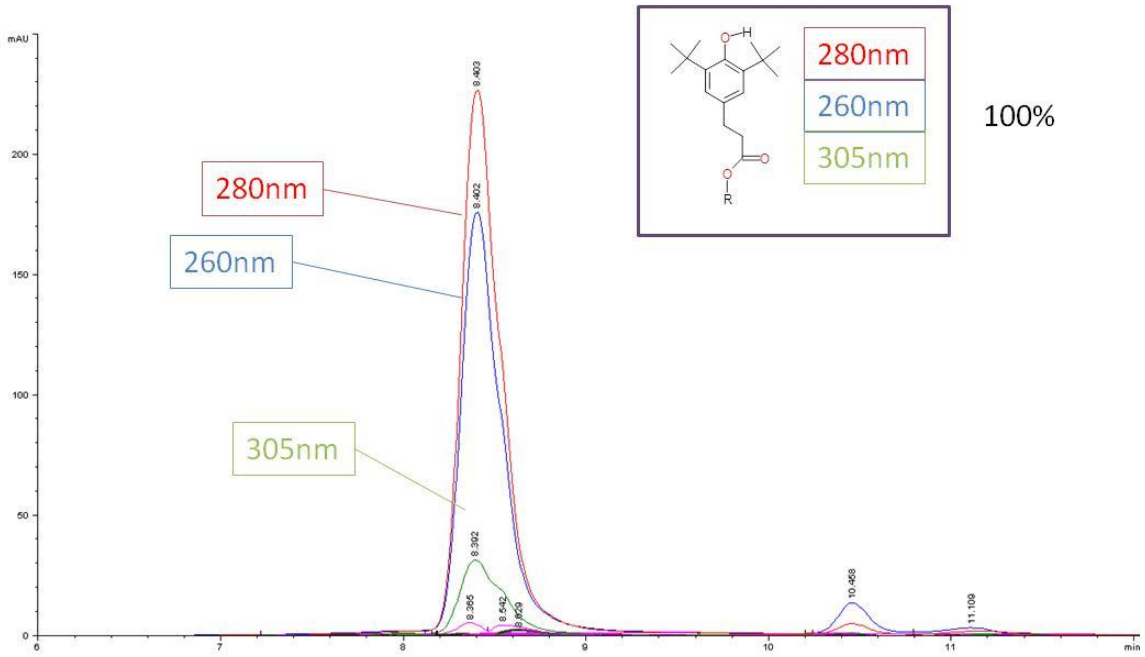

Figure 3.30 – GPC trace of OHPP in squalane reaction starting material

A sample taken after 20 minutes of an oxidation run containing 0.5% w/w OHPP reveals two new GPC peaks and a change to the peak between 8 and 9 minutes, which showed a large increase of absorption between 305 and 320 nm. Absorption at these wavelengths is consistent with the presence of hydroxycinnamate[110] (Figure 3.21) and suggests the co-elution of OHPP and hydroxycinnamate. The peak at 7 – 8 minutes is likely to be antioxidant dimer similar to those observed by Pospíšil[111] and Klemchuk[129] for BHT and the peak at 9 – 10 minutes is quinone (confirmed by running a sample of the quinone material and the presence of a large peak at 260 nm). Using GC data, the ratio of these products is thought to be 25:1 OHPP:hydroxycinnamate.

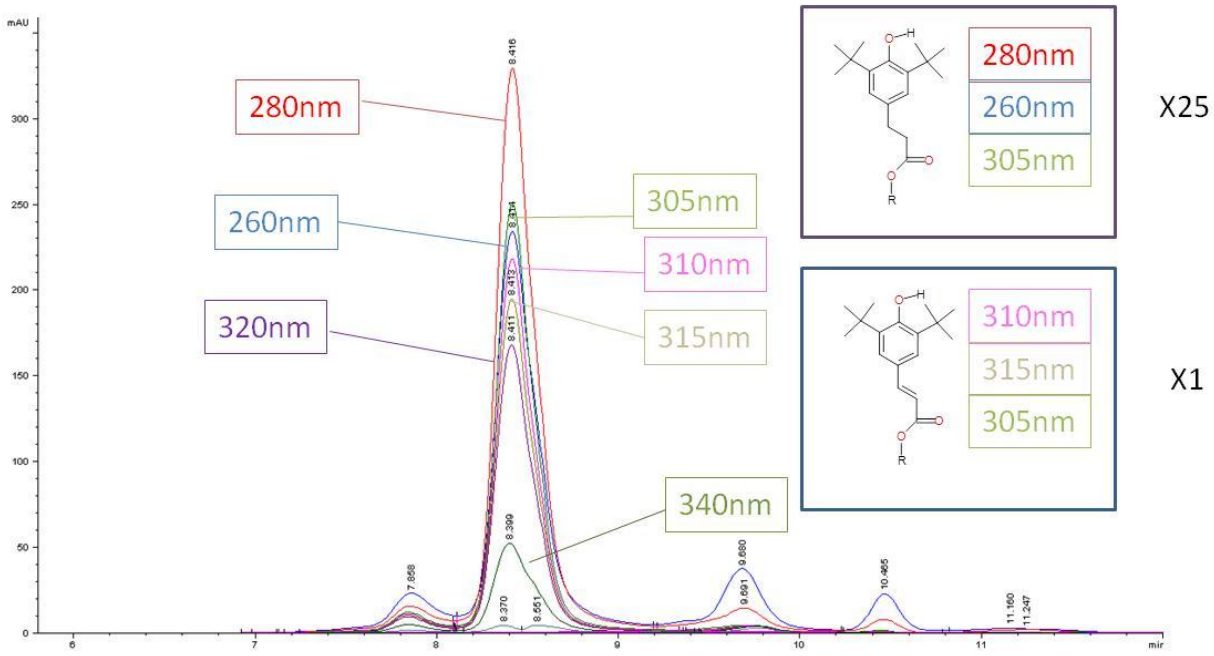

Figure 3.31 – GPC trace of an oxidation run of OHPP in squalane at 180 °C, sampled after 20 minutes

In order to prove this co-elution, a sample was prepared synthetically using synthesised hydroxycinnamate and OHPP in squalane at the concentrations of both species after 20 minutes as measured by GC of 25:1. The peak between 8 – 9 minutes showed the same pattern of absorbances as the sample taken after 20 minutes of oxidation, proving firstly that the OHPP and hydroxycinnamate co-elute and secondly, giving further evidence for the presence of predominantly hydroxycinnamate and not quinone methide, as this is known to show absorptions at a wavelength of 302 nm.[129]

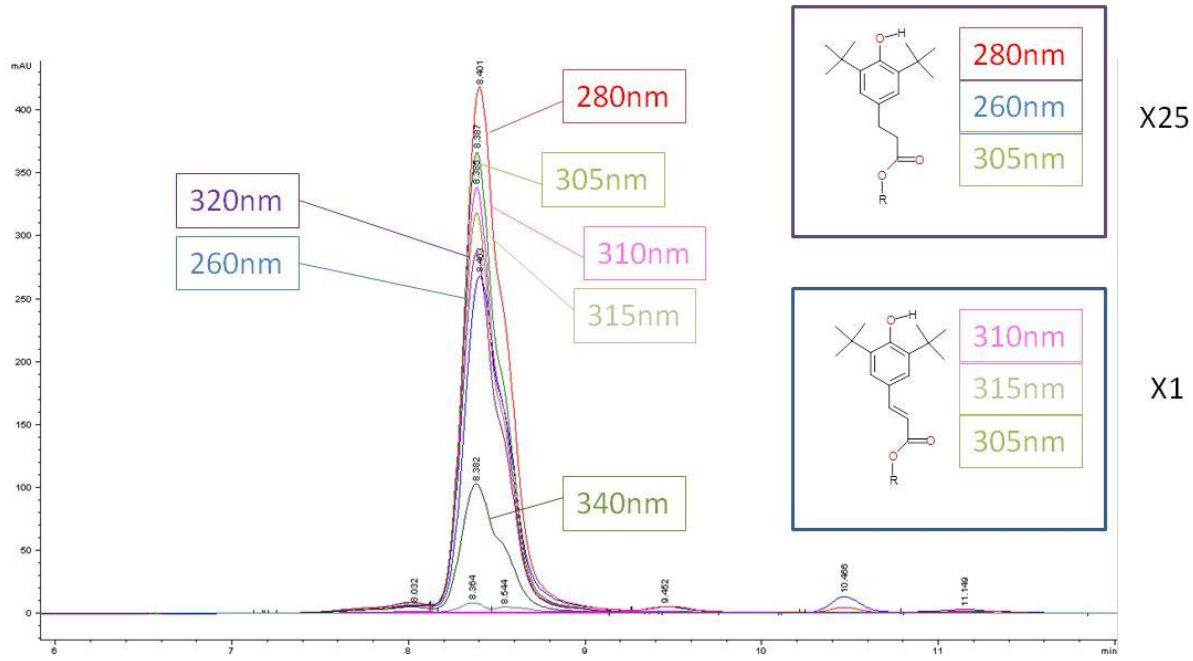

Figure 3.32 – GPC trace of an artificial mix of OHPP and synthesised hydroxycinnamate at the same ratios as an oxidation sample as determined by GC

3.9 Synthesised hydroxycinnamate as an antioxidant

3.9.1 Autoxidation of hydroxycinnamate in squalane

The synthesised hydroxycinnamate was tested at 180 °C in squalane to assess its antioxidant properties. A sample was prepared using a concentration of 7.5 x10^{-3} mol dm^{-3} (the same as used for OHPP). The hydroxycinnamate lasted for approximately 24 minutes, around six minutes less than the OHPP. This was anticipated as in an oxidation reaction using OHPP as a starting antioxidant, hydroxycinnamate was formed which will consume an additional alkyl peroxy radical to form the hydroxycinnamate.

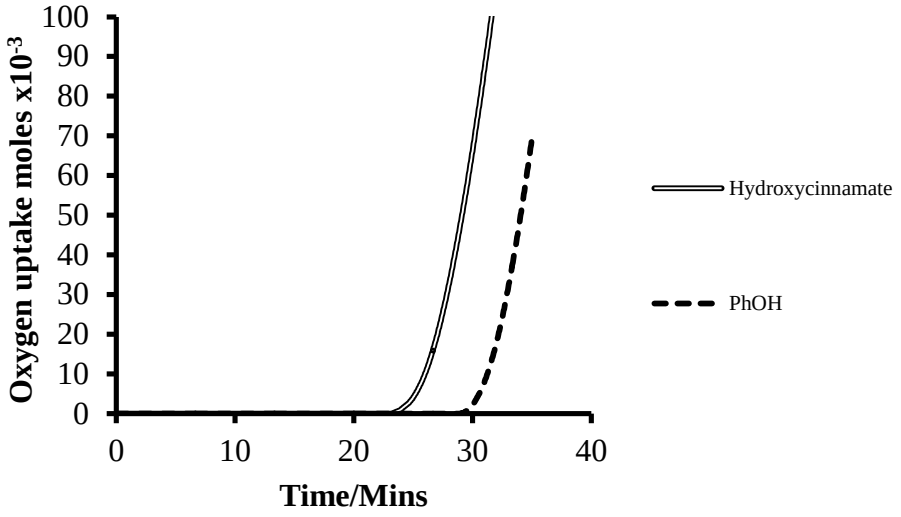

Figure 3.33 – Induction periods of hydroxycinnamate and OHPP in squalane at 180 °C

3.9.2 Product analysis

Samples were taken every 5 minutes during the reaction to test for the presence of intermediates. The same analytical methods were used to identify intermediates from the oxidation of hydroxycinnamate as those used in the oxidation of OHPP. GC-MS identified the presence of two intermediate species from hydroxycinnamate oxidation. These intermediate species were lower in concentration than those seen using OHPP and were difficult to accurately quantify.

Using GC-MS, these were found to be octadecyl 3-(3,5-ditert-butyl-4-hydroxy-phenyl)-3-hydroxy-propanoate (quinone methide alcohol) (product C) and quinone, which were both also found during OHPP oxidation.

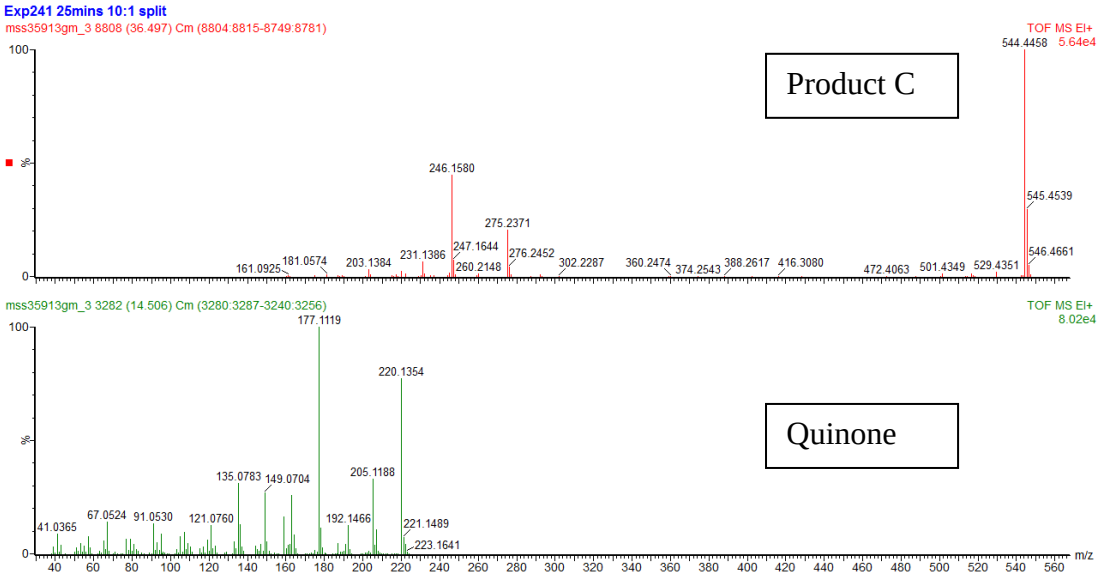

Figure 3.34 – Mass spectra of the product C and quinone from hydroxycinnamate oxidation

The presence of these products confirmed the initial theory that product C and quinone could be formed from hydroxycinnamate.

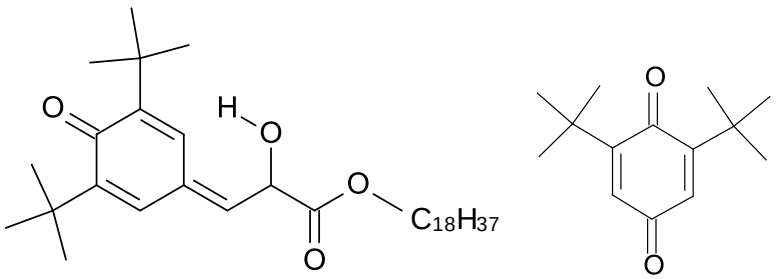

Figure 3.35 – Recap of structures (C) and quinone

Plotting the concentration of these products over time shows the same pattern as seen with OHPP with quinone methide alcohol (C) peaking in concentration before the quinone.

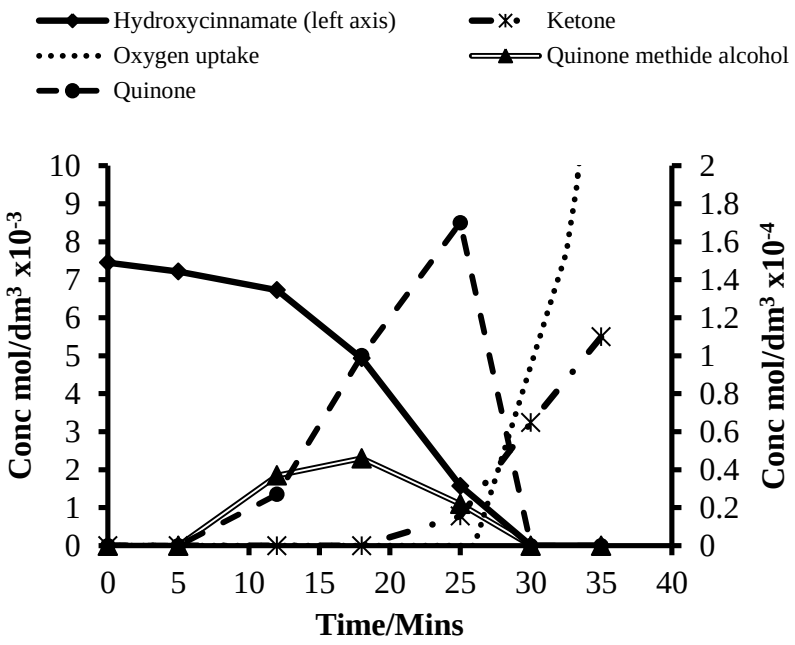

Figure 3.36 – Quantification of hydroxycinnamate and hydroxycinnamate during the induction period

The low concentrations of the two intermediates was unexpected for quinone methide alcohol as it is believed that this product forms directly from hydroxycinnamate. Therefore having a large concentration of hydroxycinnamate at the start of the reaction should therefore produce more quinone methide alcohol. The presence of lower concentrations of quinone was expected as quinone can also be formed from OHPP without first forming hydroxycinnamate. In addition, in order to form quinone from hydroxycinnamate, the long chain in the para position in the molecule must be lost. As this chain is conjugated to the ring system by the double bond in the chain, this is a less favourable reaction than the loss of the alkyl chain in OHPP.[130]

3.10 Phenolic antioxidant mechanism

The previously published chemical mechanisms for the action of phenolic antioxidants cannot completely account for the products and behaviours reported in the previous sections. From the results in this section, a full mechanism was created to account for the products identified. This was achieved using the structures deduced by GC-MS and the order of their formation determined by GC along with the product formation observed during an oxidation run of the intermediate hydroxycinnamate as a starting antioxidant. The order in which they formed was determined as shown below, with the dashed line indicating the well-established mechanism of phenolic antioxidants.

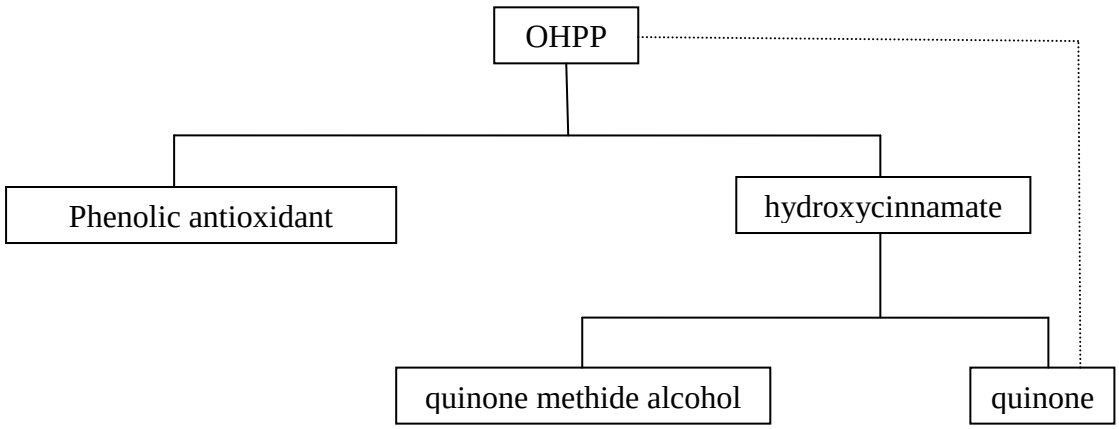

Figure 3.37 – Overview of the products formed and their order of formation during oxidation runs using OHPP

The abstraction of the hydrogen from the weak O-H bond of the phenolic antioxidant is the most plausible starting point due to the low bond dissociation energy of this bond. However, abstraction of a hydrogen between the phenolic aromatic ring and the ester group of the antioxidant does occur as these also have relatively low bond dissociation energies. When calculated using Gaussian and the method outlined in Chapter 2, it was found to be 378 kJ mol^{-1} which is still significantly lower than the bond dissocation energies in squalane (Table 1.5). Although resulting in a very minor product, the abstraction of a hydrogen with a lower bond dissociation energy than that of a tertiary hydrogen in squalane as shown in step 1 of Figure 3.39 results in a radical that can react with oxygen (step 2 of Figure 3.39) and which ultimately produces an alcohol (step 5 of Figure 3.39).

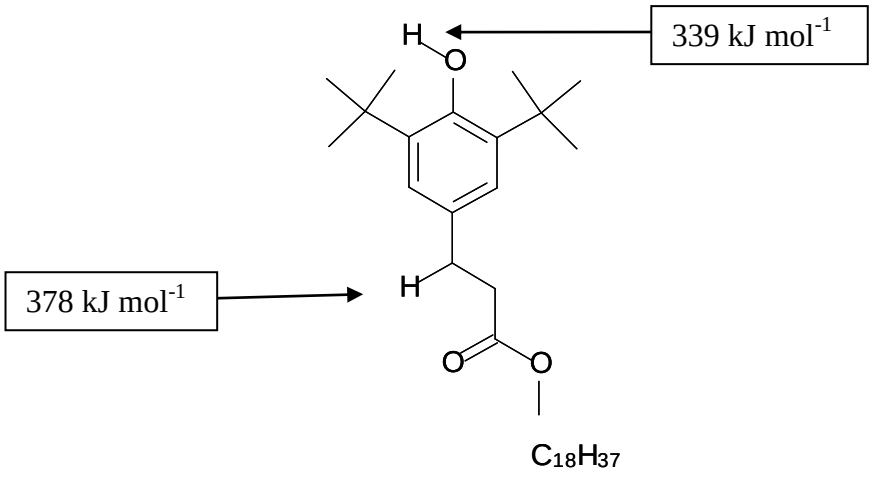

Figure 3.38 – Hydrogen abstraction starting points and their relevant bond dissociation energies

Alternatively, abstraction of the weakest hydrogen (step 6 of Figure 3.39) creates a phenoxy radical which is resonance stabilised. This is the same as the well-

established mechanisms in Figure 3.3. After this point, there are two possible options: either the combination of an alkyl peroxy radical with the antioxidant radical resulting in the loss of the alkyl group as shown in Figure 3.3 or, alternatively abstraction of a second labile hydrogen occurs, as shown in Step 7 of Figure 3.39. The product of step 7 of Figure 3.39 is relatively unstable[111] and so rearranges to form the cinnamate as shown in step 8 of Figure 3.39.

Although it has been observed that hydroxycinnamate will go on to form quinone as shown in Figure 3.36, it is also possible that the hydroxycinnamate can produce an alcohol (C) in the same way as shown in steps 1 to 5 of Figure 3.39, to form the product shown in step 15 of Figure 3.39 (C). This supports the time development of products analysis shown for the oxidation of OHPP in Figure 3.21. Any further reactions involving (C) and (D) are unknown but the concentration data of (C) shown in Figure 3.21 indicates a peak in concentration after 20 minutes and a rapid fall after this time indicating that the product can go on to react further.

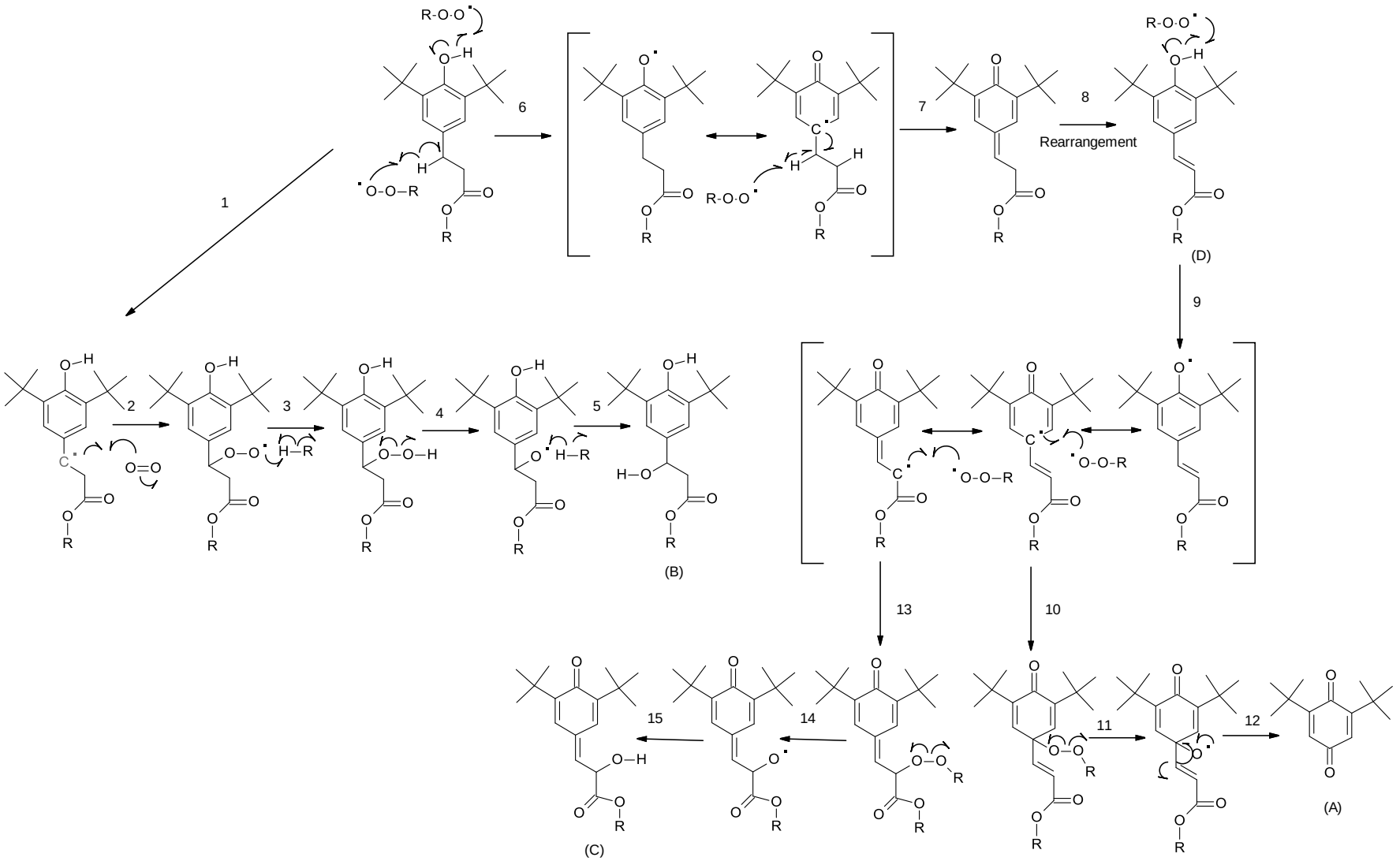

Figure 3.39– The overall mechanism of OHPP reactions and the products formed

3.11 Conclusions

The addition of 0.5% w/w of the phenolic antioxidant OHPP to squalane, at 180 ºC increased the induction period from ~3 minutes with no antioxidant present to ~30 minutes. At temperatures in excess for 200 ºC, the antioxidant becomes relatively ineffective.

During the induction period in the presence of OHPP, four intermediate species were identified. Two of these intermediates (phenolic antioxidant alcohol and quinone methide alcohol) have not been identified in previous work.

From this, an alternate mechanism for the reactions of OHPP was proposed in Figure 3.39. The formation of hydroxycinnamate has been reaffirmed in this work using a combination of mass spectrometry and the synthesis of the intermediate, making identification much more robust than previous work which relied upon GPC analysis. In addition, the reactions and product formation of hydroxycinnamate have also been studied. It was found that the intermediate hydroxycinnamate does itself work well as an antioxidant and reacts further to produce quinone methide alcohol and quinone (Figure 3.33 and 3.36).

It is unknown how the quinone methide alcohol goes on to react further but it is likely that it goes on to react further as the concentration of this product peaks and then diminishes.

The intermediate formed in the highest concentration is quinone. This work has demonstrated that there is an alternative mechanism for the formation of quinone to that shown in Figure 3.3. It remains unclear what the relative proportions of the two mechanisms are for this phenolic antioxidant, although it is apparent from the oxidation work done on the synthesised hydroxycinnamate that the mechanism shown in Figure 3.39 resulting in the formation of quinone is substantial (as shown in Figure 3.33) and should be taken into account when assessing the potential antioxidant properties of phenolic antioxidants.

The OHPP intermediate hydroxycinnamate can itself act as an antioxidant. At 180 ºC, the induction period of 0.5 %wt hydroxycinnamate in squalane was ~23 minutes compared to 30 minutes for OHPP.

Chapter 4

Antioxidant Properties of an Alkylated Diphenylamine under Piston Conditions

4.0 Antioxidant properties of an Alkylated Diphenylamine under Piston Ring Conditions

The second class of primary antioxidants used in engine oils are aminic antioxidants. These are generally based upon diphenylamine structures.[3]

4.1 Introduction

Alkylated diphenylamine antioxidants are modified versions of diphenylamine designed to be used in automotive lubricant formulations as primary antioxidants.[131,132,133] The addition of the alkyl group has the effect of increasing the solubility of diphenylamine in non-polar liquids. They also increase the size of the molecule, reducing the volatile loss of the antioxidant at high temperatures. Aminic antioxidants have been reported to be excellent high temperature antioxidants[134,135,136] and have been described as having significantly larger stoichiometric coefficients than phenolic antioxidants such as BHT. [4, 6,56,136,53]

The work described in this chapter assesses previous work on alkylated diphenylamine antioxidants and examines the limitations and inconsistencies of this work. It reports new experiments and the effectiveness of diphenylamines at elevated temperatures and proposes explanations for the observations seen. The diphenylamine antioxidant used in this chapter was 4-(1,1,3,3-tetramethylbutyl)-N-[4-(1,1,3,3-tetramethylbutyl)phenyl]aniline aka octylated diphenyl amine (ODPA) shown in Figure 4.1 and the base oil used was squalane. This antioxidant was chosen as it is used

extensively in engine lubricant formulations[131] but is a single structure which aided product analysis by GC.

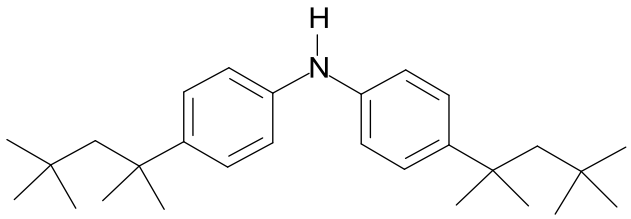

Figure 4.1 - 4-(1,1,3,3-tetramethylbutyl)-N-[4-(1,1,3,3-tetramethylbutyl) phenyl]aniline aka octylated diphenylamine (ODPA)

This work focuses on high temperature oxidation using temperatures between 140 and 220 °C to simulate those measured in the top piston assembly in an automotive engine.[81,82] The concentration of antioxidant used (unless otherwise stated) was 0.37 %wt (7.5×10^{-3} mol dm^{-3}) which is the same as the concentration used for OHPP in the previous chapter to allow for direct comparison of the two. This is within the recommended range of dosage recommended by the manufacturer in this application.[109]

4.2 Previous work

Previous work in this field can be split into two areas. These are oxidation work and mechanistic studies.

4.2.1 Oxidation work

At 130°C, octylated diphenylamine (ODPA) has been reported to give superior antioxidant protection when compared to a phenolic antioxidant such as BHT[136] and octylated phenyl alpha naphthylamine (PANA) in a single additive test.[137] This was also found to be the case for ODPA when compared against phenolic antioxidants at 160 °C.[138] In contrast, it has also been reported to give poorer protection compared to phenolic antioxidants at both 130 °C[139] and 170 °C[61]. On the occasions where ODPA performed worse then OHPP, both sources concluded that aminic antioxidants would work better at higher temperatures and the poor performance in these instances was due to the low temperatures used but gave no reasons for this. A conflicting opinion to the findings of Duangkaewmanee and Petsom (2011)[137] from Hunter and Klaus (1993)[135] states that phenyl alpha naphthylamine (PAN) is a better aminic antioxidant than DPAs especially at high temperatures.

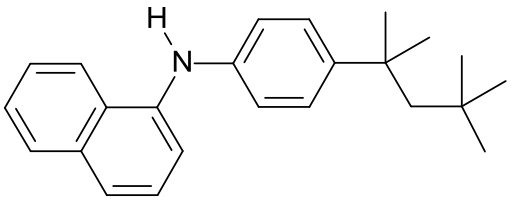

Figure 4.2 - Structure of N-[4-(1,1,3,3-tetramethylbutyl)phenyl]naphthalen-1-amine (PANA)

4.2.2 Mechanistic studies of aminic antioxidants

Two additional factors must be considered in addition to the well understood high and low temperature diphenylamine type antioxidants (DPA) mechanisms detailed in section 1.4.2 of Chapter 1. The first of these is the possibility that diphenylamine type antioxidants can act as peroxide decomposers,[138,140,141] which would make them both radical scavengers and peroxide decomposing antioxidants. The second is that the initial reaction between DPA and peroxy radicals ($ROO^{\cdot}$) in these mechanisms is thought to be reversible,[142] (Figure 4.3) which must be taken into account. At 20 °C, the equilibrium constant of this reversible reaction was measured as 3[142] which implies that, under these conditions (and dependent upon concentrations), the forwards reaction is dominant. Work at higher temperatures which takes into account the backwards reaction done between 120 – 210 °C extends this as full consumption of the antioxidant occurs (because of a dominant forwards reaction), prior to the commencement of base oil oxidation during the induction period. At no point does the backwards reaction become dominant. [140, 143, 144]

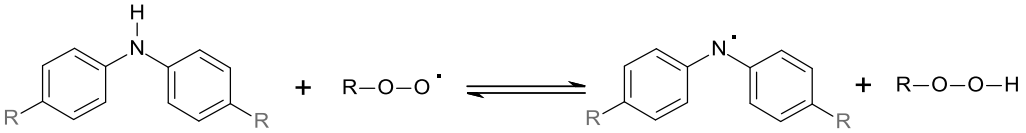

Figure 4.3 – DPA Antioxidant and alkyl hydroperoxide equilibria

To test the contrasting accounts of antioxidant behaviour, the ODPA oxidation work

in this chapter and the phenolic antioxidant work from Chapter 3 will be compared and contrasted throughout the discussion.

4.3 ODPA high temperature oxidation

The autoxidation of squalane containing ODPA was compared using the continuous flow reactor and electron spin resonance (ESR) in situ reactions.

4.3.1 Autoxidation using continuous flow reactor

Oxidation reactions completed between 140 and 220 °C inclusive, at 20 °C intervals, revealed that, ODPA performs significantly worse than the phenolic antioxidant OHPP in a single additive system This is contrary to the current understanding of aminic antioxidants, which are reported to be better antioxidants than phenolics with much greater stoichiometric coefficients especially at higher temperatures.[56, 8,55,53,145,26] The work reported by Becker *et al*, [139] which also concludes that ODPA is a relatively poor antioxidant at a temperature of 130 °C, does not give a reason for the poor performance other than the reaction temperature was too low and that aminic antioxidants would perform better at higher temperatures. However, the source quoted for the good performance at high temperatures was Hunter *et al*[135] who did not use ODPA and used Phenyl-α-naphthylamine (PAN) instead, meaning that the two cannot be directly compared. So although dismissed by the authors, the

findings of a poor performance for diphenylamines appear to be valid for the observation of ODPA as an antioxidant.

In this work the difference between the induction periods of OHPP (from Chapter 3) and ODPA was found to be greater at the low end of the temperature range of 140 and 160 °C (shown on the left hand vertical axis in hours below). As temperature increases, the rate at which antioxidant is consumed also increases and at 220 °C, both OHPP and ODPA offer no antioxidant protection and have an induction period of little over the 1.5 minutes duration of an additive free squalane oxidation run (shown in Figure 4.4). The induction periods between 180 and 220 °C are shown in minutes on the right hand vertical axis in Figure 4.4. The values represent the end of the induction period where oxygen uptake became significant. The OHPP reaction at 140°C was stopped after 9 hours and was found to still contain antioxidant.

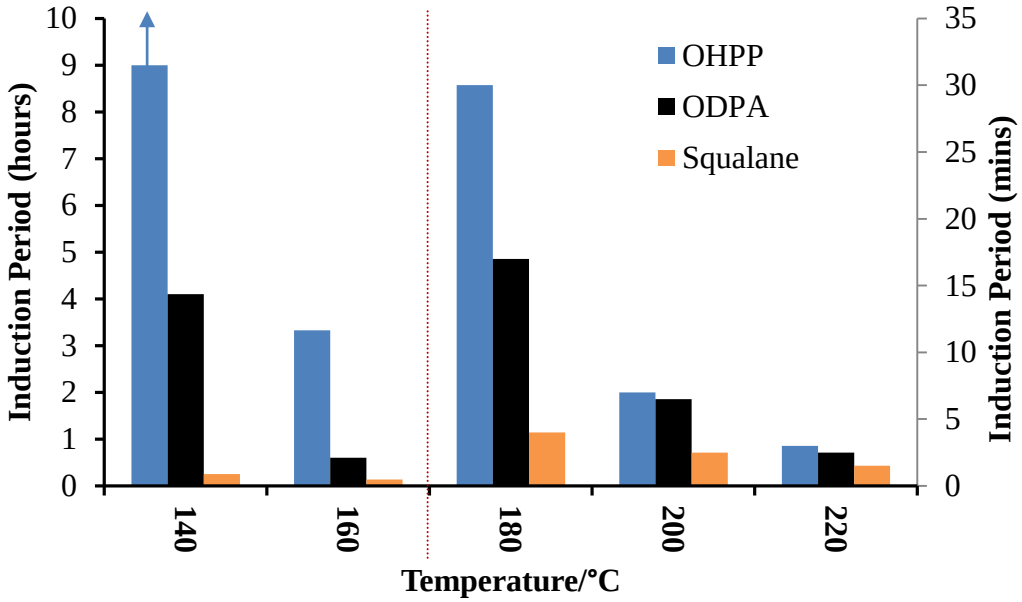

Figure 4.4 – Comparison of induction periods of OHPP and ODPA in squalane between 140 and 220 °C

4.3.2 Autoxidation by in situ ESR

The sample was prepared according to the method in Section 2.2.6 and contained 100ppm of 2,2,6,6-Tetramethylpiperidine-1-Oxyl (TEMPO) and either 100 ppm of antioxidant in squalane or just squalane without antioxidant. It was placed in a sealed melting point tube, with a fixed amount of oxygen contained within the headspace (which was kept constant) and within the liquid. Whilst antioxidant was present, the consumption of oxygen occurred at a slower rate indicating that fewer alkyl radicals were being produced and therefore oxidation was occurring at a slower rate. It was not possible to measure this rate using the continuous flow reactor method but using ESR, two different gradients can be seen for the phenolic antioxidant OHPP as indicated by the dotted black line which showed a slow initial consumption which increased once around half of the antioxidant had been consumed. The same experiment was attempted

using 100ppm of ODPA. This gave little protection to the base oil and the oxygen consumption resembled that of just squalane. As peroxides are formed via the reaction of alkyl radicals and oxygen, the concentration of alkyl hydroperoxide will be inversely proportional to the concentration of oxygen, i.e. as oxygen is consumed, peroxide is formed. The rapid consumption of oxygen in the ODPA system therefore supports previous results that peroxide build-up during the induction period is greater with ODPA than it is for OHPP.

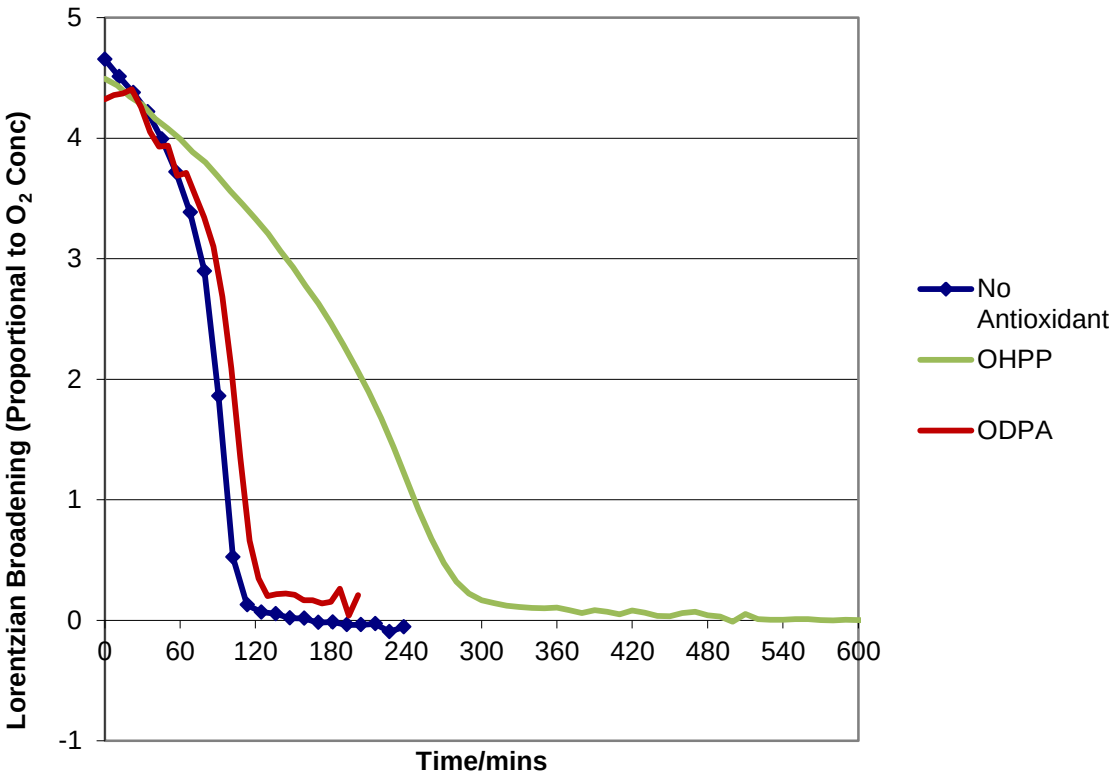

Figure 4.5 – Oxygen consumption of squalane containing 100 ppm TEMPO and 100 ppm antioxidant at 170 °C with fixed oxygen volume

Once the oxygen has been consumed, there can no longer be a reaction between alkyl radicals and oxygen and so any alkyl radicals formed combine with the radical in

TEMPO in a termination step to form a non ESR active species. This can be seen in Figure 4.6 with the initial 360 minutes for OHPP (whilst oxygen is present) shown as a constant signal intensity of TEMPO.

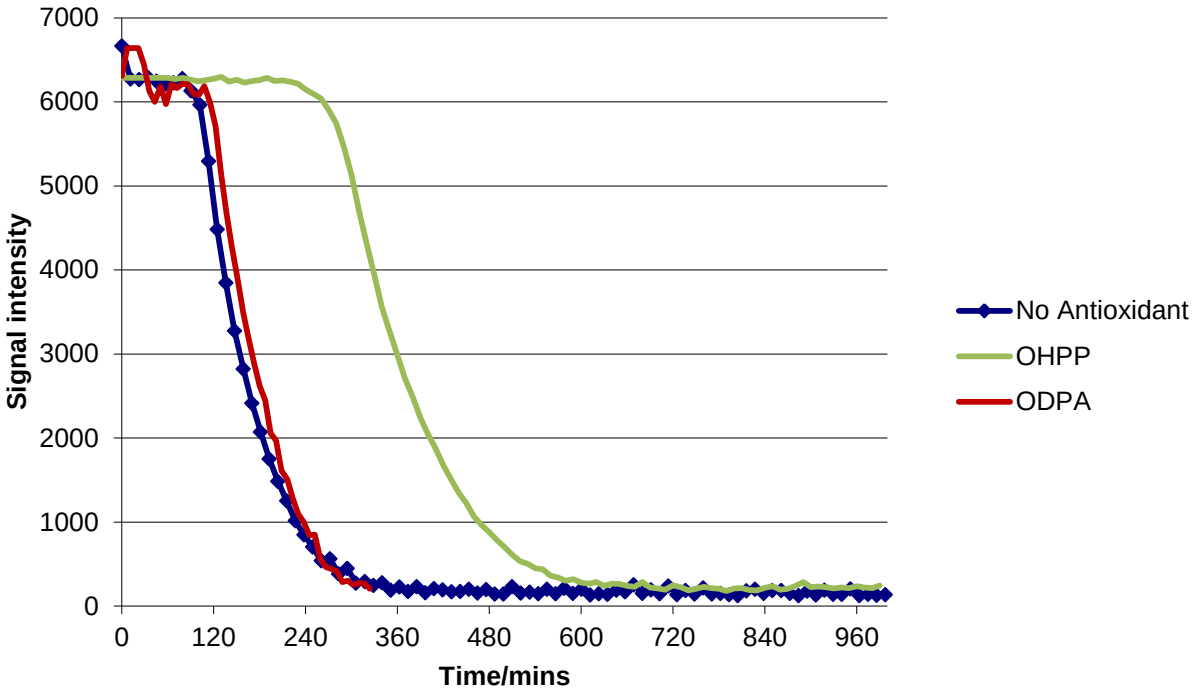

Figure 4.6 – TEMPO signal over time

4.4 GC analysis of ODPA from continuous flow oxidation reaction

In order to explain the poor performance of ODPA at high temperatures, analysis of samples taken during the induction period was conducted by GC and GC-MS (EI).

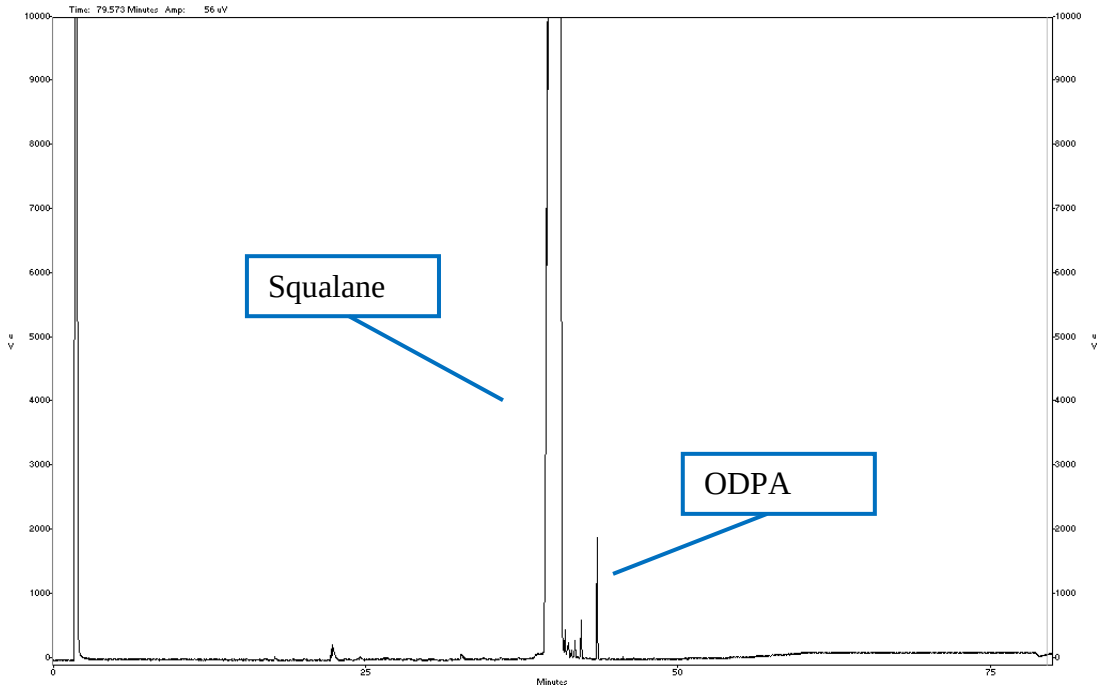

Figure 4.7 – GC trace of ODPA in squalane starting material

4.4.1 Antioxidant product identification

The starting material containing squalane and ODPA also contains a squalane impurity, which is believed to be 2,6,10,15,19,23-hexamethyltetracosanol (squalane alcohol),[120] which is formed by autoxidation of squalane.

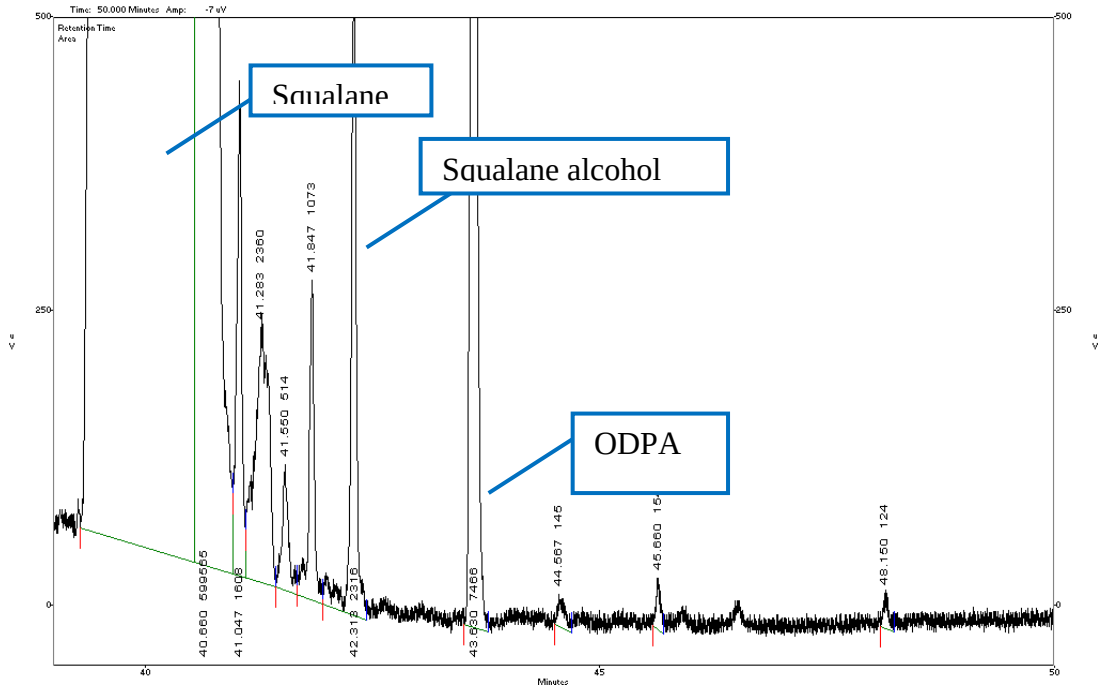

Figure 4.8 – GC trace of starting material 39-50 minute region of the GC trace

One ODPA intermediate product (ODPAP) was found in a sample taken after 10 minutes of an oxidation run at 180 °C when the sample was analysed by GC(FID).

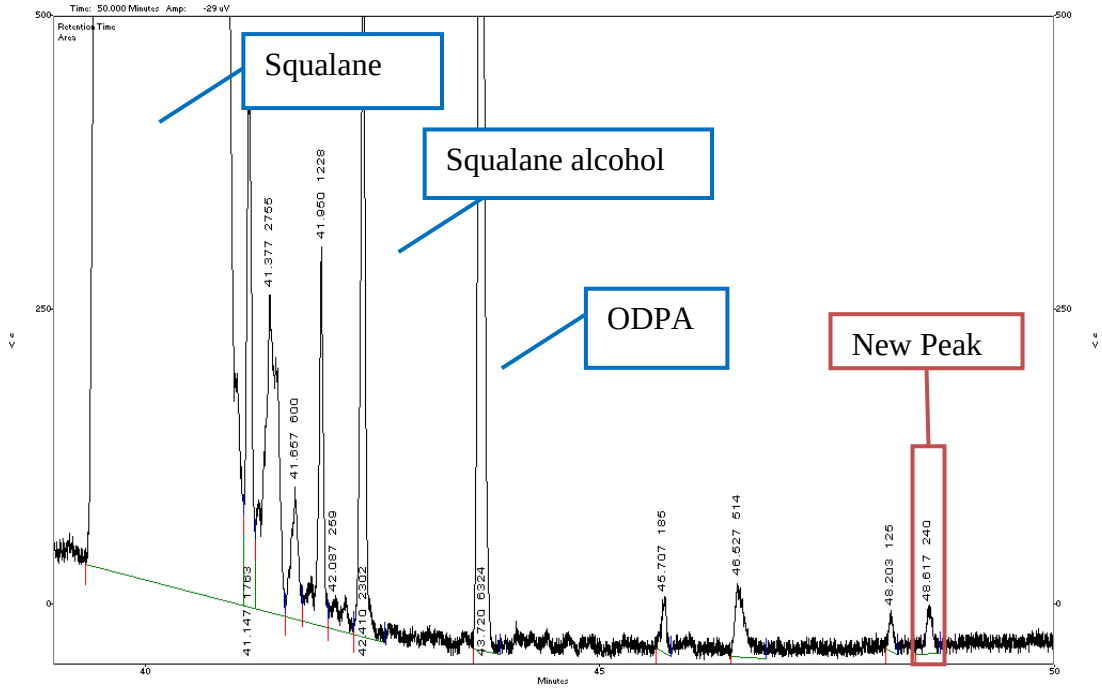

Figure 4.9 – GC trace of 10 minute sample 39-50 minute region of the GC trace

This product was identified using GC-MS (EI). The starting antioxidant ODPA has a molecular weight of 393 and shows significant mass spec fragments at m/z 322 (100), 250 (26) and 236 (10), the structures of which are shown in Figure 4.10, with % relative intensity values shown in brackets.

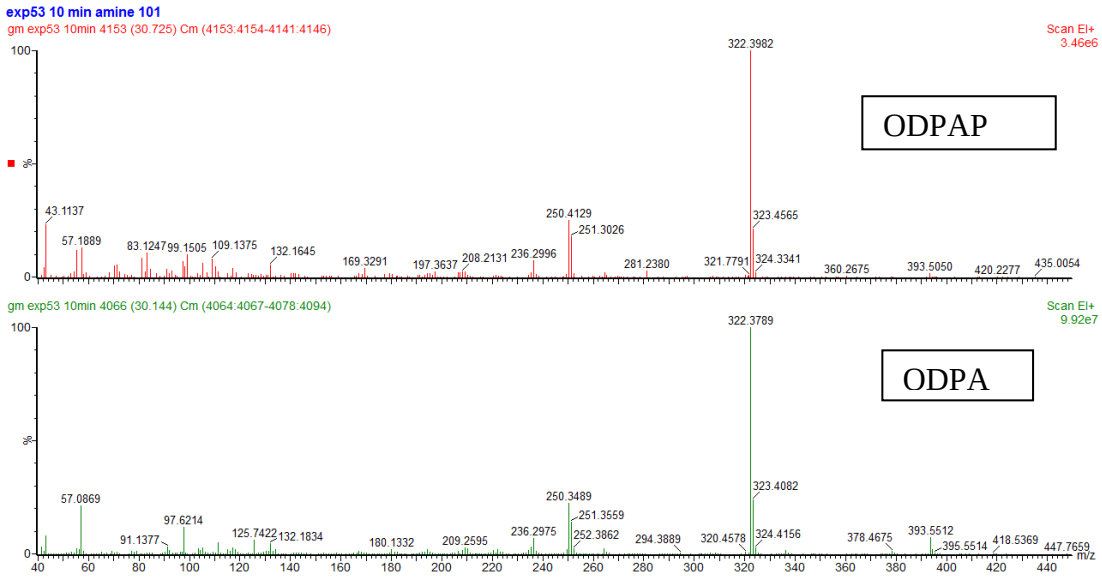

Figure 4.10 – Mass spec fragmentation pattern of ODPA and ODPAP

The product peak followed the same mass spec fragment pattern as the starting antioxidant, showing m/z of 393 (7), 322 (100), 250 (23) and 236 (8). Other fragment peaks such as the one at 207, which can be attributed to siloxanes from the GC column,[146] were subtracted.

The most plausible explanation for this product peak is the rearrangement of the structure, forming the product shown in Figure 4.11

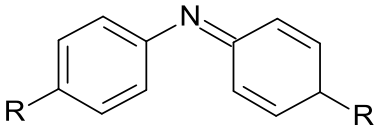

Figure 4.11 – Proposed structure for the ODPA product ODPAP

A possible structure and mechanism for the formation of ODPAP is outlined below in figure 4.12.

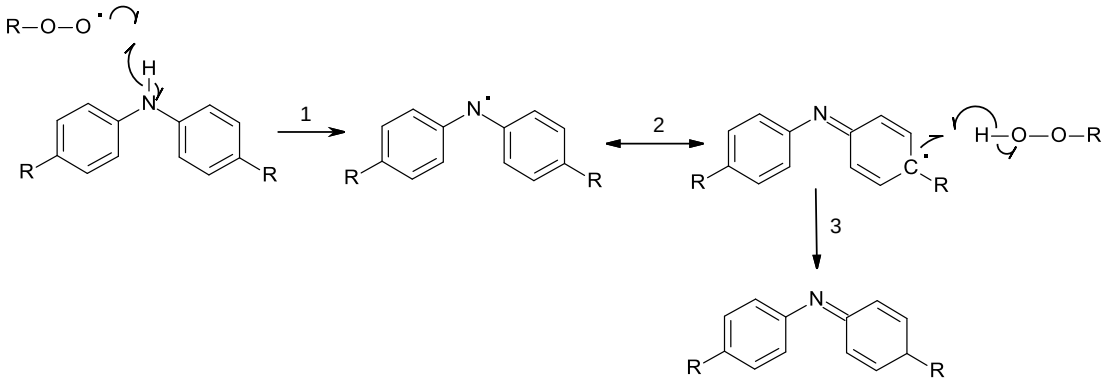

Figure 4.12 – Proposed mechanism for the formation of ODPAP

The intermediate species formed in the oxidation of ODPA (Figure 4.12) was formed in extremely small concentrations. The same mass ion peak of the intermediate to the starting antioxidant is consistent with rearrangement or the loss and gain of a hydrogen atom. As the aminyl radical formed by the abstraction of the hydrogen of the N-H bond has a resonance structure, it is possible that the resonance structure radical abstracts a hydrogen, resulting in the product observed. The C-H bond formed will however, be comparatively weak. Because of this, it is highly likely that the formation of the intermediate is a reversible reaction and so the intermediate is unlikely to play any significant part in the activity of the antioxidant. Concentrations of this product were extremely low (in the region of 4 x10 $^{-5}$ mol dm^{-3}) and were difficult to accurately quantify.

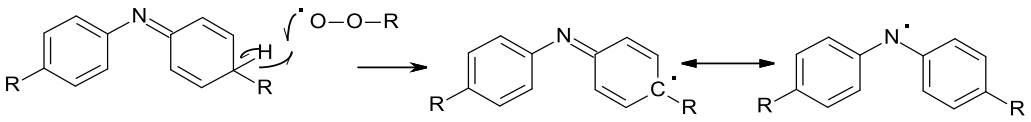

Figure 4.13 - Resonance reaction of intermediate species

4.4.2 Antioxidant quantification during oxidation runs

As well as product identification, GC was used to quantify antioxidant concentration during the reaction. Analysis carried out on samples taken during an oxidation run at 180 °C indicated that initial antioxidant consumption is slow, and after 15 minutes, around 95 % of the starting antioxidant remains. After this, the antioxidant concentration drops rapidly. 18 ± 3 minutes is the end of the induction period represented by oxygen uptake. This is despite the presence of in excess of 73 % of the starting antioxidant still remaining.

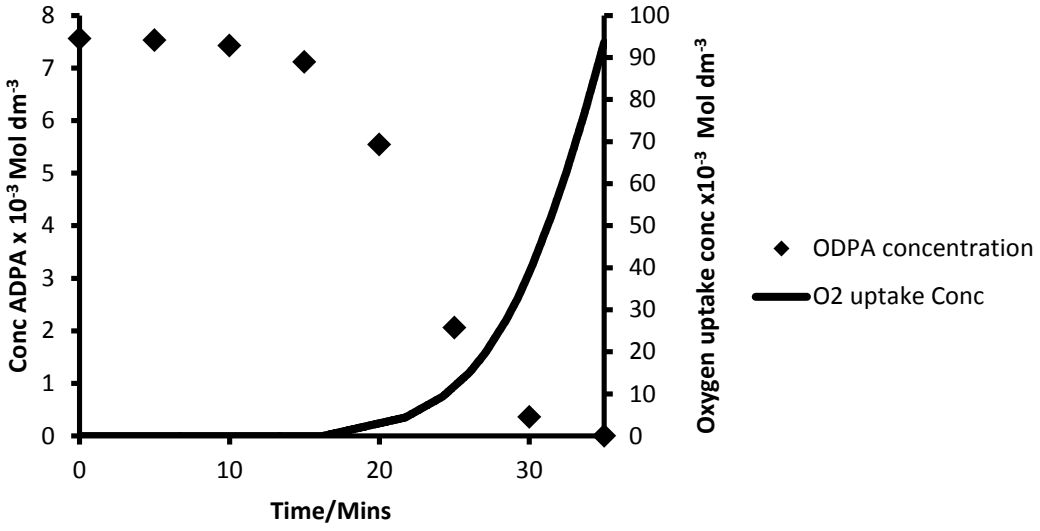

Figure 4.14 – ODPA concentration over time at 180 °C

After 25 minutes, almost all of the antioxidant has been consumed. At this point, the squalane is already heavily oxidised, unlike with the phenolic antioxidant OHPP after 25 minutes, where there was minimal squalane oxidation at the point despite all the antioxidant being consumed as shown in Figure 4.16.

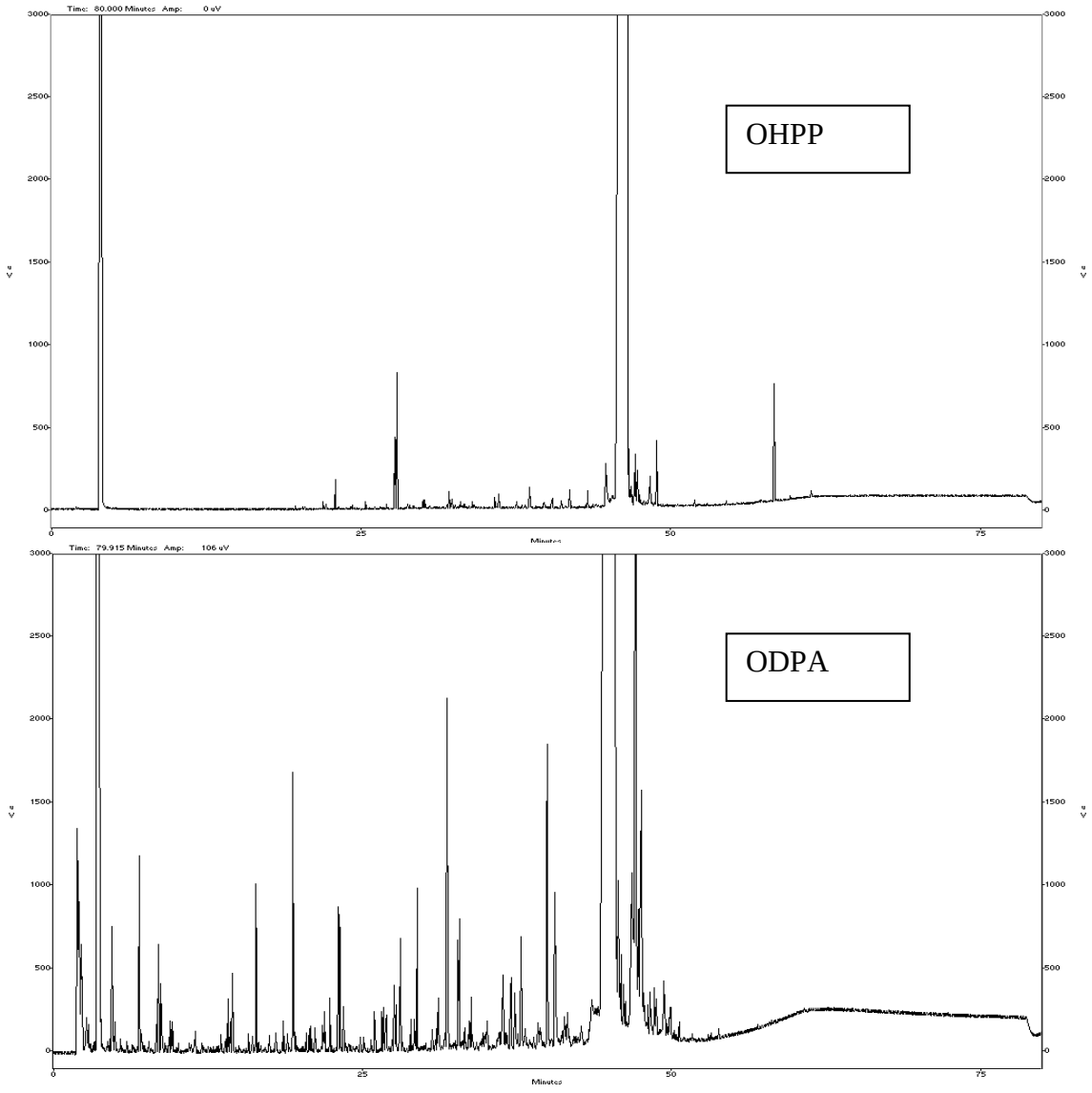

Figure 4.16 – Comparison of GC traces of 7.5 x10^{-3} mol dm^{-3} OHPP after 25 minutes and 7.5 x10^{-3} mol dm^{-3} ODPA after 25 minutes

Following on from the result at 180 °C for ODPA autoxidation, samples were taken during oxidation runs at 140, 160, 180, 200 and 220 °C at the end of the induction period at each of the temperatures. The presence of ODPA at the end of the induction period was observed at all temperatures tested from140 to 220 °C. Once the ODPA had stopped protecting squalane from oxidation, it was quickly consumed entirely.

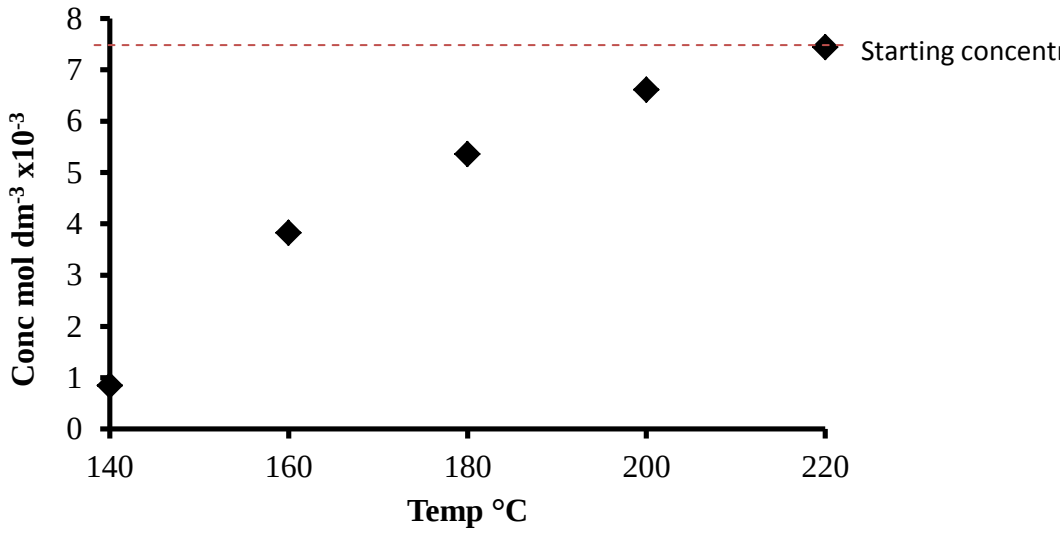

Figure 4.17 – Concentration of ODPA remaining at end of induction period at various temperatures using an initial ODPA concentration of 7.5 x10^{-3} mol dm^{-3}

The amount of antioxidant remaining at the end of the induction period was temperature dependent. At 140 °C, only 11 % of the starting antioxidant remained at the end of the induction period and so it can be said to behave almost like a phenolic antioxidant. As the temperature increased, the percentage of ODPA remaining at the end of the induction period increased At temperatures between 180 and 220 °C, almost all of the starting antioxidant still remains (between 73 and 95 %). In reactions at slightly lower

temperatures of 140-160 °C, much less of the starting antioxidant remained at the end of the induction period and at 140 °C, almost all of the antioxidant had been consumed before squalane oxidation commenced.

Previous work with ODPA showed that autoxidation under piston ring conditions resulted in all of the ODPA being consumed during the induction period at all temperatures tested between 180 and 220 °C.[143] In contrast to this is the work by Alfadhl,[147] which found that antioxidant was present at the end of the reaction at temperatures of 180 – 220 °C and these findings form the basis of this work.

4.5 Possible critical antioxidant concentration of ODPA

The end to antioxidant protection, despite the presence of antioxidant in the squalane, was found not to be due to a critical ODPA concentration. This was despite initial reactions at 180 °C suggesting otherwise, as the induction periods at 180 °C reactions using starting ODPA concentrations of 7.5, 15 and 30 x10 $^{-3}$ mol dm^{-3} all ended with an ODPA concentration of 5.89 ± 0.34 x10 $^{-3}$ mol dm^{-3}.

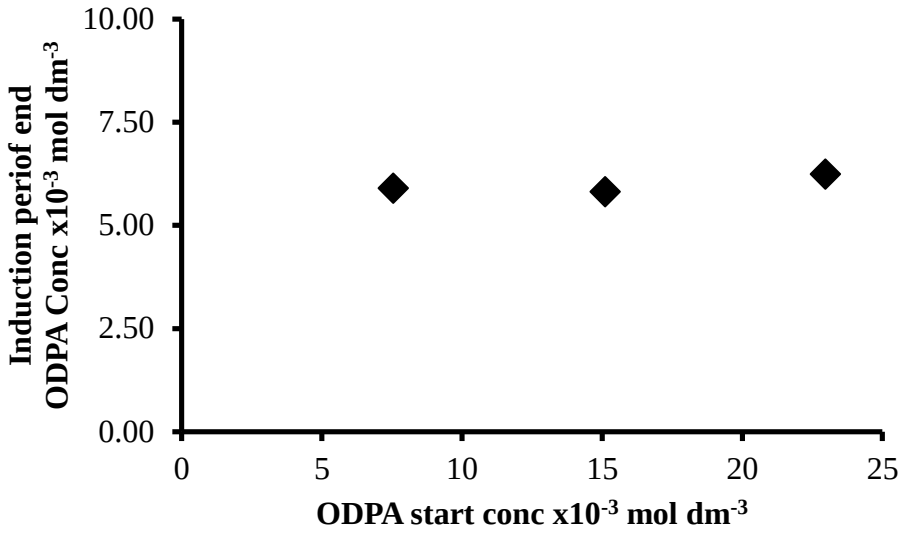

Figure 4.18 – ODPA concentration at induction period end from an initial ODPA concentration of 7.5, 15 and 30 x10^{-3} mol dm^{-3}

As all three starting concentration reactions in Figure 4.18 ended at approximately 5.8 x10^{-3} mol dm^{-3} (0.29 %wt), this concentration and a much smaller concentration (9.6 x10^{-4} mol dm^{-3}) were used as starting concentrations for ODPA oxidation runs at 180 °C. If 5.8 x10^{-3} mol dm^{-3}, these levels should not provide antioxidant protection. When tested, both of these concentrations provided antioxidant protection as shown in Figure 4.19, suggesting that a critical antioxidant concentration is not the cause of the problems seen with ODPA at high temperatures.

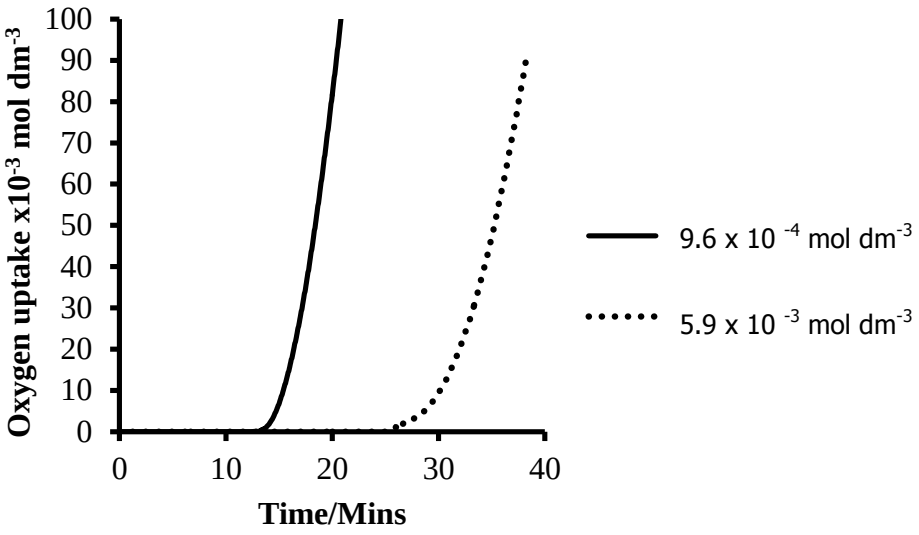

Figure 4.19 – Induction periods of ODPA with initial concentrations of 5.9 x10^{-3} mol dm^{-3} and 9.6 x10^{-4} mol dm^{-3} at 180 °C

Another possible reason for the poor performance of ODPA is the presence of alkyl hydroperoxides (ROOH) produced during squalane oxidation, as proposed by the initial work by Alfadhl.[147] The interaction between alkyl hydroperoxides and aminyl radicals is known[4, 134,144,142,148] but this interaction has not been proven as having a negative effect on the antioxidant.

4.6 Alkyl hydroperoxides in autoxidation

The alkyl radical R˙ formed from the autoxidation initiation reaction will rapidly react with oxygen to form an alkyl peroxy radical (Reaction 1.3.2). Rate constants for this reaction are quoted in the region of 10^9 M^{-1} s^{-1} at 300 K with the tertiary alkyl radical

$(CH_3)_3C^{\cdot}$ measured at $4.93 \times 10^9 \pm 0.12$ M^{-1} s^{-1}.[149] At temperatures below 500 K (this work), this reaction forms an alkyl peroxy radical even in the presence of relatively low concentrations of oxygen,[41] which reacts with hydrocarbon or antioxidant resulting in alkyl hydroperoxide formation (Reaction 1.3.3).[33]

$R\bullet + O_2 \rightarrow ROO\bullet$ Reaction 1.3.2
$ROO\bullet + RH \rightarrow ROOH + R\bullet$ Reaction 1.3.3

Figure 4.20 – Recap of Reactions 1.3.2 and 1.3.3 from Chapter 1

4.6.1 Alkyl hydroperoxide quantification

Using the same method as discussed in Chapter 3 and as outlined in Section 2.7, triphenylphosphine (TPP) was used to quantify alkyl hydroperoxide concentrations for an oxidation using ODPA as an antioxidant. The build up of peroxide followed a similar pattern to that seen using a phenolic antioxidant with large quantities of peroxide being formed at the end of the induction period. However, the levels of peroxide observed during the induction period were higher for a reaction using ODPA as an antioxidant than for a run using OHPP as shown in Figure 4.21.

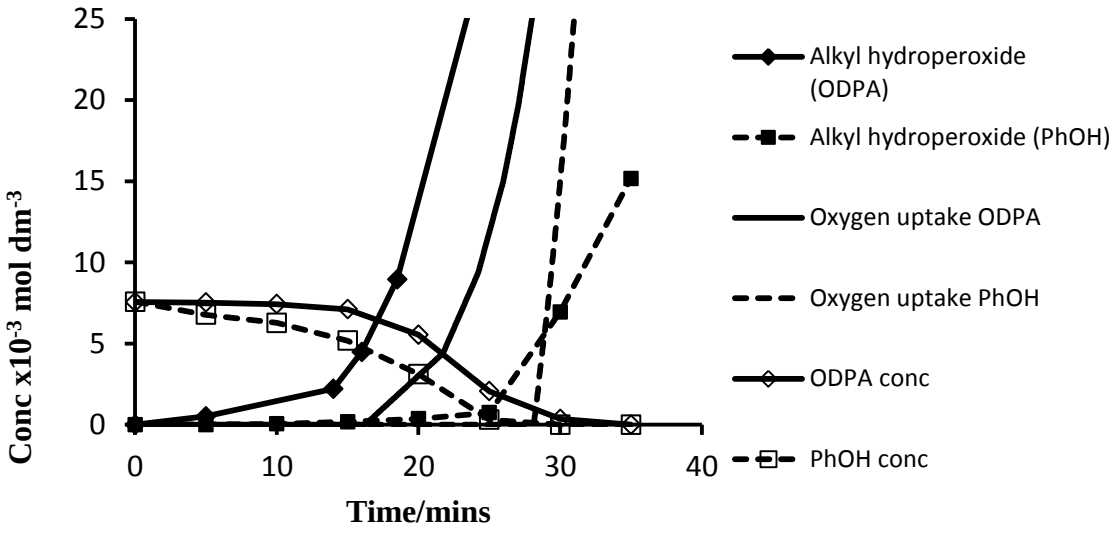

Figure 4.21 – Alkyl hydroperoxide quantification during oxidation runs of OHPP and ODPA at a concentration of 7.5 x10^{-3} mol dm^{-3} in squalane at 180 °C

Contrary to the findings of Capp and Hawkins,[140] this work can find no evidence of the ODPA acting as a peroxide decomposer, turning the hydroperoxide into an alcohol. As the build up of peroxides was higher with ODPA than the phenolic antioxidant OHPP, even after five minutes. It is reported that amines and nitroxyl radicals, and in particular tertiary and secondary amines and nitroxyl radicals, have the ability to decompose peroxides,[150] although the mechanism by which this occurs is not clear.[151] Secondary amines have been found to decompose benzoyl peroxide to form benzoic acid and hydroxylamine benzoate.[152] According to Capp and Hawkins,[140] the decomposition of hydroperoxides such as isopropylnaphthalene hydroperoxide using the secondary amine diisopropylamine at a ratio of 2.5:1 amine:peroxide takes around 1 hour at 110 °C instead of in excess of 17 hours without.

It would be anticipated that under piston ring conditions of 180 °C, the rate of decomposition of hydroperoxide would be greater than at 110 °C and therefore noticeable during the ~20 minute induction period of ODPA autoxidation at 180 °C. This is not the case, with hydroperoxide levels increasing at a similar rate during the induction period of autoxidation runs for both OHPP and ODPA. At the end of the induction period, the concentration of hydroperoxide increases dramatically. This is caused by the chain steps in autoxidation (Figure 4.20). Hydroperoxide build up during the induction period was not observed at 70 °C.[153]

The ratio of peroxide:ODPA at the end of the induction period was also calculated between 140 and 220 °C at 20 °C intervals. In Figure 4.22, the concentration of alkyl hydroperoxide is shown on the left hand vertical axis and is in the order of magnitude of 1 $x10^{-2}$ mol dm^{-3} and the ODPA concentration on the right vertical axis and is in the order of magnitude of 1 $x10^{-3}$ mol dm^{-3}.

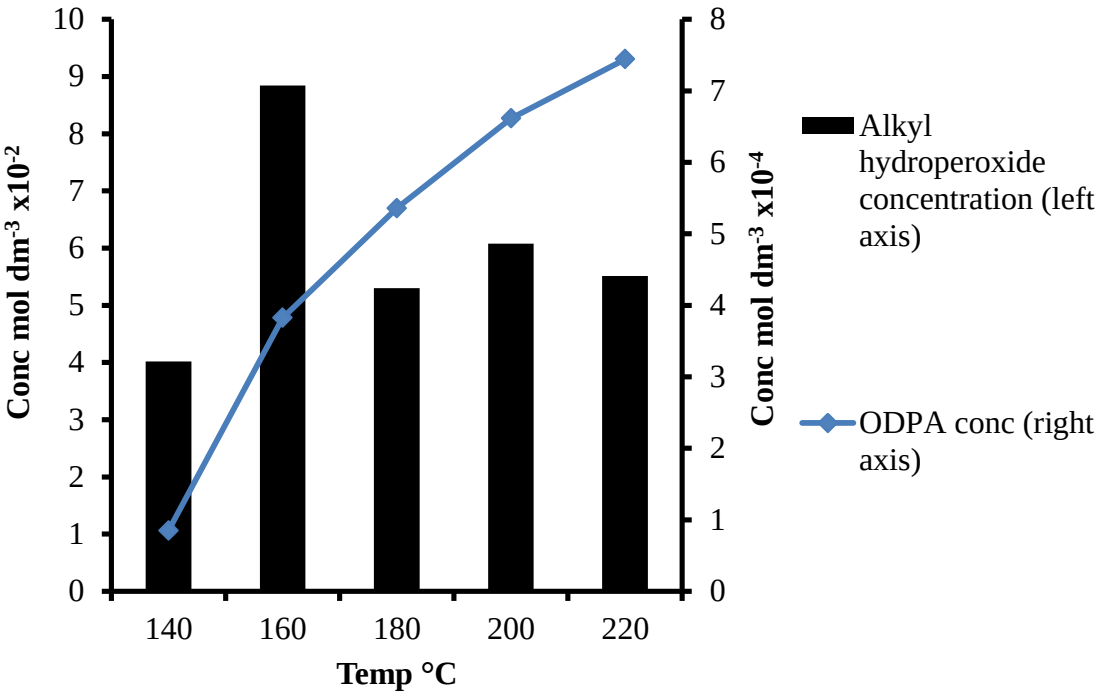

Figure 4.22 – Concentrations of alkyl hydroperoxide and ODPA at the end of the induction period

There was no clear pattern between the ratio of alkyl hydroperoxide:ODPA at the end of the induction period as temperature increased but the amount of alkyl hydroperoxide measured is in the region of 4 – 9 x10^{-2} mol dm^{-3}. This is around 10 times greater than the antioxidant concentration.

4.7 The effect of alkyl hydroperoxides on ODPA

To assess the influence of alkyl hydroperoxides on ODPA, reactions were carried out mixing the fresh unoxidised squalane containing antioxidant with alkyl hydroperoxide. It was not possible to source alkyl hydroperoxides which were sufficiently non-volatile

under piston ring conditions and so squalane, oxidised at 180 °C for 20 minutes was used as the source of alkyl hydroperoxide. Quantification of the alkyl hydroperoxide concentration of the squalane showed that the oxidised squalane oxidised for approximately 20 minutes contained a concentration of around 0.19 mol dm^{-3} alkyl hydroperoxides. To ensure minimum peroxide decomposition, the squalane oxidation and tainting runs were carried out on the same day.

Using oxidised squalane in fresh squalane at a ratio of 6:1 fresh antioxidant free squalane:oxidised squalane as a control, several runs were completed to assess the effect of the alkyl hydroperoxide on both phenolic (OHPP) and aminic (ODPA) antioxidants at a ratio of 6:1 antioxidant in squalane (7.5×10^{-3} mol dm^{-3}):squalane or oxidised squalane. This would also mimic the addition of new engine oil to an engine which contained partially oxidised oil. The sequence below shows the reactions carried out. This volume of oxidised squalane resulted in a starting peroxide concentration of 2.7×10^{-2} mol dm^{-3}, which is an excess of peroxide by a factor of three compared to antioxidant. This accounted for any loss of peroxide between the squalane oxidation and oxidised squalane oxidation runs.

Table 4.1 – Reaction scheme to test influence of oxidised squalane

Reaction Mixture	**OHPP in squalane 7.5 x10^{-3} mol dm^{-3}**	**ODPA in squalane 7.5 x10^{-3} mol dm^{-3}**	**Squalane diluent**	**Oxidised squalane diluent**
Squalane untainted	0 ml	0 ml	7 ml	0 ml
Squalane and oxidised	0 ml	0 ml	6 ml	1 ml
OHPP benchmark	7 ml	0 ml	0 ml	0 ml
OHPP squalane + diluent	6 ml	0 ml	1 ml	0 ml
OHPP squalane + ox dil	6 ml	0 ml	0 ml	1 ml
ODPA benchmark	0 ml	7 ml	0 ml	0 ml
ODPA squalane + diluent	0 ml	6 ml	1 ml	0 ml
ODPA squalane + ox dil	0 ml	6 ml	0 ml	1 ml

The induction period of the squalane benchmark at 180 °C was around four minutes. When spiked with oxidised squalane, the induction period reduced to two minutes, which can be accounted for by the addition of autoxidation promoting species such as radicals from the decomposition of alkyl hydroperoxides upon heating to 180 °C (Figure 4.21)

The addition of squalane as a diluent to the OHPP benchmark had the expected effect of reducing the induction period by roughly 15% from 30.5 minutes to 27 minutes. Adding oxidised squalane as a diluent drastically reduced the induction period of the phenolic antioxidant sample to eight and a half minutes but the antioxidant was still able to protect the squalane from oxidation for six and a half minutes longer than the squalane with oxidised squalane that contained no antioxidant.

Using the ODPA antioxidant, the addition of squalane as a diluent had almost no effect on the induction period, as seen in Section 4.5. This is consistent with the low ODPA concentration results seen in Figure 4.19. The addition of oxidised squalane to the ODPA completely inhibited the activity of the antioxidant resulting in an induction period of two minutes. This was the same as the control sample of squalane and oxidised squalane and so ODPA showed no antioxidant properties and was totally inhibited by oxidised squalane.

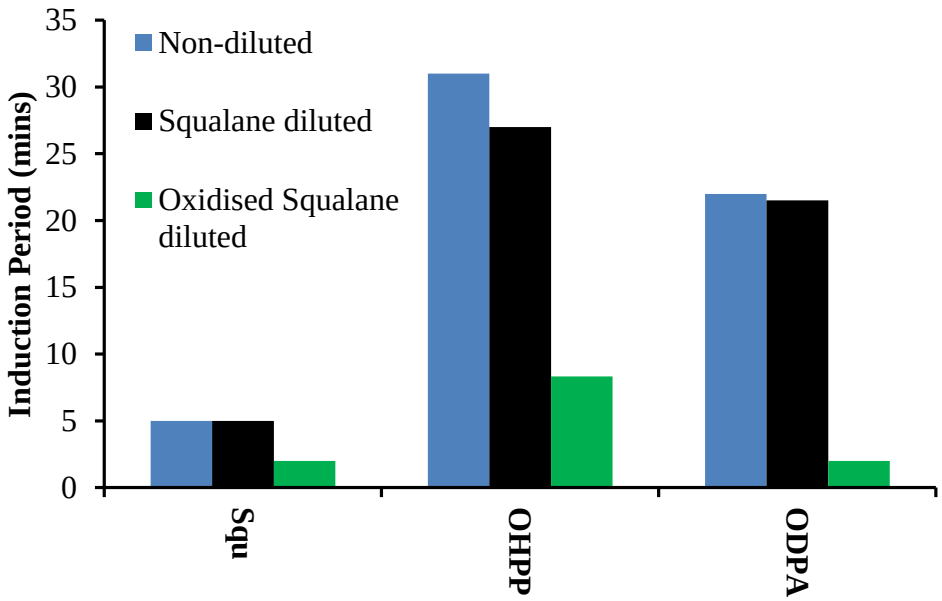

Figure 4.23 – The effect of adding oxidised squalane to squalane, OHPP in squalane and ODPA in squalane

The oxidised squalane runs contained 2.7×10^{-2} moles of alkyl hydroperoxide at the start of the reaction, which was four times higher than the 6.2×10^{-3} moles of OHPP or ODPA antioxidant the mixture contained. Despite the high level of alkyl hydroperoxide present, OHPP still provided some protection to the base oil outperforming the squalane

benchmark, suggesting that it is unhindered by the presence of alkyl hydroperoxide and will continue to act as a radical scavenging antioxidant until it is consumed, unlike ODPA which did not provide any antioxidant protection in the presence of the pre-oxidised squalane.

The inhibition of ODPA by hydroperoxide oxidation products is contrary to the findings of Ekechukwu *et al*[143] and Jensen *et al*[50] using n-dodecane and hexadecane as base fluids at temperatures and antioxidants similar to those used in this work, in the presence of oxygen. This type of hydrocarbon is not representative of all engine lubricants which will contain tertiary hydrogen sites, particularly if they are produced from mineral oil base stocks.[104]

As previously stated, in the autoxidation of squalane, the tertiary hydrogens were 15 ± 1 times more reactive than the corresponding secondary hydrogens[120] and lead to a lower C-H bond dissociation energy than their secondary counterparts.[154] The lack of tertiary hydrogens in the n-dodecane/hexadecane base fluids used by Ekechukwu *et al*[143] and Jensen *et al*[50] will have a considerably reduced rate of oxidation as no tertiary alkyl alkyl peroxy radicals are being formed. Using n-dodecane, the peroxide concentration peaked at around 1.03×10^{-3} mol dm^{-3} (Ekechukwu *et al*[143]), compared to a concentration of 0.19 mol dm^{-3} using squalane. Therefore the concentration of alkyl hydroperoxide in this work is considerably higher than that reported by Ekechukwu at the same temperature.

In addition, in the absence of tertiary hydrogens aminic antioxidants such as ODPA will not be inhibited and appear to be excellent antioxidants. Furthermore, the antioxidant regeneration mechanism from a hydroxame ether proposed by Jensen (Figure 4.24) cannot occur if the hydroxame ether was formed from the combination of a nitroxyl radical and a tertiary alkyl radical (iv of Figure 4.24). This will significantly lower the stoichiometric coefficient of the antioxidant.

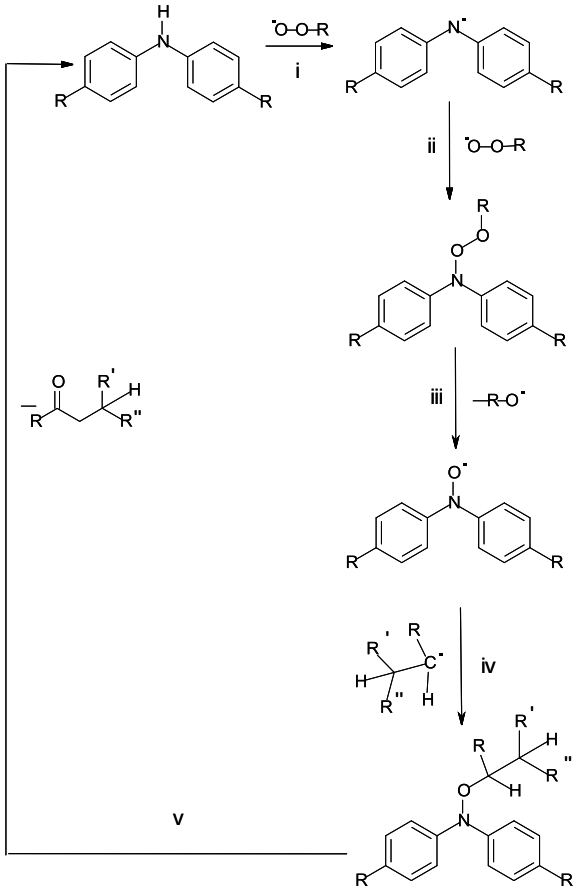

Figure 4.24 – The Jensen antioxidant regeneration mechanism[50]

At 180°C, a sample taken after 17 minutes (which was the time ODPA stopped inhibiting oxidation (Figure 4.14)) showed only 4.5 $x10^{-4}$ moles dm^{-3} of the starting concentration of ODPA had been consumed. A sample is taken during a separate run containing the same starting concentration of OHPP and then after 17 minutes 2.60 $x10^{-3}$ mole dm^{-3} of the OHPP had been consumed. This equates to over a 5 fold difference in concentration. The consumption of less antioxidant over a given time period can be seen as advantageous as generally the presence of antioxidant will prevent autoxidation. The first 17 minutes of the reaction is therefore in agreement with the common belief that aminic antioxidants are superior to phenolic ones.[50,137] By repeating the process of sampling the run at the point at which the ODPA stopped working (and sampling a separate run containing OHPP after the same amount of time, regardless of whether the antioxidant was still preventing autoxidation or not) at different temperatures as shown in Figure 4.25, an estimation of the temperature at which ODPA becomes affected by the presence of alkyl hydroperoxide could be made.

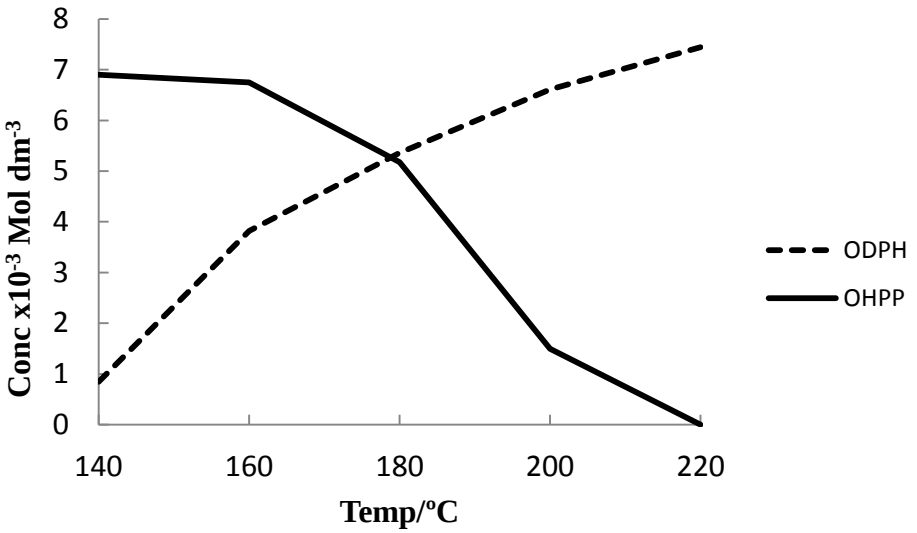

Figure 4.25 – Summary of the concentration of ODPA and OHPP remaining at the time ODPA stopped working at temperatures between 140 and 220 °C

It was found that at temperatures of 180 °C and above, less ODPA was consumed than OHPP in the corresponding phenolic antioxidant run during the period where ODPH still inhibited oxidation. Below 180 °C, this was found not to be the case as ODPA continued to work until the majority of it had been consumed. The graph below suggests that the crossover point of this behaviour is ~178 °C. It is however important to remember that at all temperatures between 140 and 200 °C, the OHPP prevented oxidation for longer than ODPA, which was an unexpected result.

4.8 Thermodynamics of the alkyl peroxy radical reaction with ODPA

To examine the reasons as to why ODPA appears to stop acting as a radical scavenging antioxidant in the presence of alkyl hydroperoxide, the thermodynamics of the equilibrium reaction between ODPA and alkyl peroxy radicals (Figure 4.3) was assessed. Where possible, experimental values for enthalpy (H) and entropy (S) were used. Other values were calculated using the computational software Gaussian, using the method outlined in the experimental section.

The forwards reaction between diphenylamine and cumyl peroxy radicals has been measured as having a forwards rate constant (k_1) of 3.4 x10^5 dm^3 mol^{-1} s^{-1} [142] and the reverse (k_{-1})as 0.2 – 1.1 x10^5 dm^3 mol^{-1} s^{-1} at 293 K, which give an equilibrium constant of between 3 and 17 at this temperature.

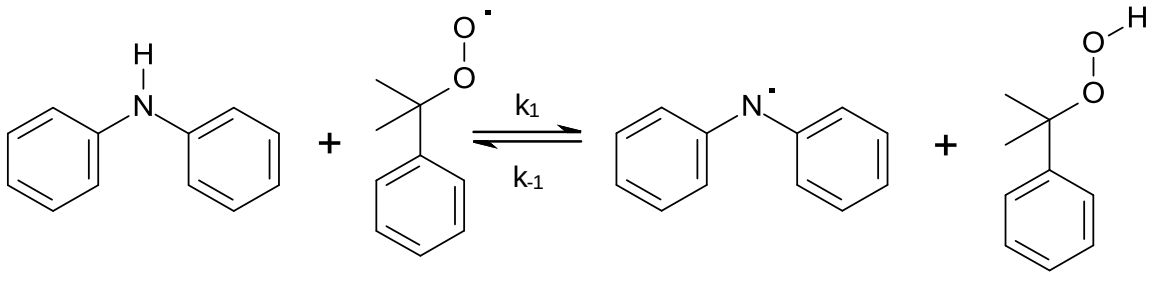

Figure 4.26 – Equilibrium reaction of diphenylamine and cumyl peroxy radicals

However, the position of the reaction equilibrium and therefore the value of the equilibrium constant K is temperature dependent. The Gibbs energy change (G)

indicates whether the forward reaction will be favourable at a certain temperature using the equation:

$$\Delta G = -RT \ln K$$

Equation 4.1 – Calculation of Gibbs free energy kinetically

Gibbs energy can also be expressed in terms of the enthalpy and entropy of reaction, giving information on the temperature dependence of the equilibrium for the reaction:

$$\Delta G = \Delta H - T\Delta S$$

Equation 4.2 – Calculation of Gibbs free energy thermodynamically

A negative ΔG value indicates that the reaction will be spontaneous and therefore favourable. A positive ΔG indicates an unfavourable reaction. Below is a summary of the influence of enthalpy and entropy on ΔG

Table 4.2 – Summary of influence of enthalpy and entropy on gibbs free energy

Favourable reaction?	**ΔH**	**ΔS**
Always	Negative	Positive
At low temperatures (TΔS < ΔH)	Negative	Negative
At high temperatures (TΔS > ΔH)	Positive	Positive
Never	Positive	Negative

4.8.1 Enthalpy of reaction

Using the generalised reaction scheme shown below, literature bond dissociation data was used to estimate the enthalpy of reaction.

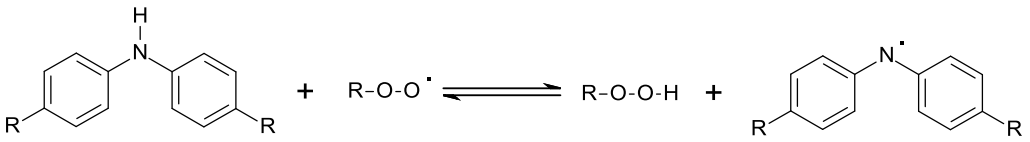

Figure 4.27 – General reaction scheme of substituted diphenylamine antioxidant with alkyl peroxy radicals

Squalane oxidation can produce primary, secondary or tertiary alkyl hydroperoxides. The predominant peroxide of squalane oxidation is the tertiary one as the tertiary hydrogens in branched hydrocarbons such as squalane and pristane are 15 ± 1 times more reactive than the corresponding secondary hydrogens[120] and so the enthalpy of reaction of the tertiary species will be of the greatest relevance to this work.

Calculation of the enthalpy of reaction can be achieved using the equation below using experimental bond dissociation energies (D).

$$\Delta H = D(AnN - H) - D(ROO - H)$$

Equation 4.3 – Calculation of enthalpy of reaction (ΔH)

The enthalpy change for the reaction between alkylated diphenylamine and 1°, 2° and 3° alkyl hydroxyl radicals was found to be exothermic (and therefore favourable) as shown in Table 4.3. It is not assumed that using a shorter alkyl chain on the antioxidant changed the bond dissociation energy significantly compared to ODPA.

Table 4.3 – Bond dissociation energies of antioxidant and alkyl hydroperoxides with experimental errors.

Species	Bond dissociation energy (D) kJ mol^{-1}	ΔH kJ mol^{-1}	Reference
$(4\text{-}CH_3C_6H_4)_2N\text{-}H$	361.1± 3.6	-	[155]
$CH_3CH_2OO\text{-}H$	376.8 ± 8.4	-15.7 ± 9.1	[156]
Tetralin Hydroperoxide	368	-6.9	[157]
Cumene hydroperoxide	368.2 ± 8.4	-7.1 ± 9.1	[158]

4.8.2 Entropy of reaction

Experimental values of entropy (S) for the reaction in Figure 4.13 were not available and so were calculated using the computational software Gaussian 09W, using the method outlined in section 2.5. The entropy change for the reaction was calculated using the formula:

$$\Delta S = S(\text{Products}) - S(\text{Reactants})$$

Equation 4.4 – Reaction entropy calculation

The entropy changes for 1°, 2° and 3° alkyl hydroxyl radicals was found to be negative (Table 4.4). As the enthalpy change of the reaction is also always negative (Table 4.3), the forward reaction will be favourable at low temperatures (where the enthalpy change will dominate) but will become unfavourable at high temperatures (where entropy will dominate).

Table 4.4 – Entropy change of reaction of antioxidant with alkyl peroxy radicals as shown in Figure 4.20

Species	**ΔS J K^{-1} mol^{-1}**
$(4\text{-}CH_3C_6H_4)_2NH$	-
1°	-12.14
2°	-15.21
3°	-16.32

4.8.3 Gibbs energy from enthalpy and entropy results

Combining the entropy and entropy results, the Gibbs free energy change for the reaction can be calculated. A negative Gibbs energy value indicates that the reaction is spontaneous. Using the equation in Equation 4.5, the temperature at which $\Delta G = 0$, and therefore stops being favourable, can be calculated.

$$\Delta G = \Delta H - T\Delta S$$

Equation 4.5 – Gibbs free energy change calculation from enthalpy and entropy data

Because data was available to calculate the enthalpy of reaction, the experimental results used can also be compared against the theoretical results obtained from Gaussian. All of the entropy results obtained were theoretical from Gaussian.

Table 4.5 – Summary of enthalpy and entropy values and the temperature at which the forwards reaction becomes unfavourable

Species	ΔH kJ mol^{-1}	ΔS J K mol^{-1}	T °C at which ΔG = 0
1° - Experimental	-15.7 ± 9.1	-12.14	1292 ± 750
Theoretical	-10.8		617
2° - Experimental	-6.9	-15.21	180
Theoretical	-8.2		266
3° - Experimental	-7.1 ± 9.1	-16.32	162
Theoretical	-2.4		-126

There is a clear difference between the primary alkyl peroxy radical and the secondary and tertiary ones, with the reaction between the primary radical with aminic antioxidant being favourable at all realistic temperatures. For secondary and tertiary radicals, the crossover temperature occurs under piston ring conditions (180 °C for secondary and 162 °C for tertiary) which could prove highly problematic when this antioxidant is used in automotive lubricants. This is in agreement with the crossover temperature of 178 °C reported in Figure 4.19 above which ODPA begins to behave unexpectedly. Although these figures support the previous results that the backward reaction will dominate when at equal concentrations under piston ring conditions, it should be noted that the large error range associated with the enthalpy results will significantly alter the temperature at which G = 0. For example, an enthalpy value of -8.23 kJ mol^{-1} was calculated in this work using Gaussian for the secondary peroxy radical. This difference of just 1.33 kJ/mol (experimental Vs theoretical) is enough to change the temperature at which ΔG = 0 from 180 ºC to 268 ºC and therefore, outside the temperature range measured in this work. The difference between experimental enthalpies and theoretical enthalpies is shown in Table 4.5. For further calculations, experimental results were used when

possible as these have more scientific credibility. Due to the experimental error quoted in measuring the bond dissociation energies there is a significant range in the temperature at which ΔG = 0. For tertiary alkyl peroxy radicals, the quoted value of 162 °C supports the experimental work done in this chapter but is not conclusive.

4.9 Equilibrium constant of the alkyl peroxy radical reaction with ODPA

Using the ΔG values calculated at various temperatures thermodynamically, the equilibrium constant K, can be calculated by rearrangement of Equation 4.6:

$$\Delta G = -RT \ln K$$

Equation 4.6 – Gibbs free energy calculation from equilibrium constant

To give:

$$K = \exp -\frac{\Delta G}{RT}$$

Equation 4.7 – Equilibrium constant calculation from Gibbs free energy

Using the enthalpy and entropy data of Table 4.5 and the corresponding Gibbs free energy values between a temperature range of 273 and 593 K, equilibrium constant

values were calculated using Equation 4.7. By plotting the equilibrium constant data against temperature as an Arrhenius plot (ln K against 1/T), the temperature dependence of the reaction can be determined. This however, can only be an estimation as only two of the products and reactants can be quantified. The other two are radical species which could not be quantified.

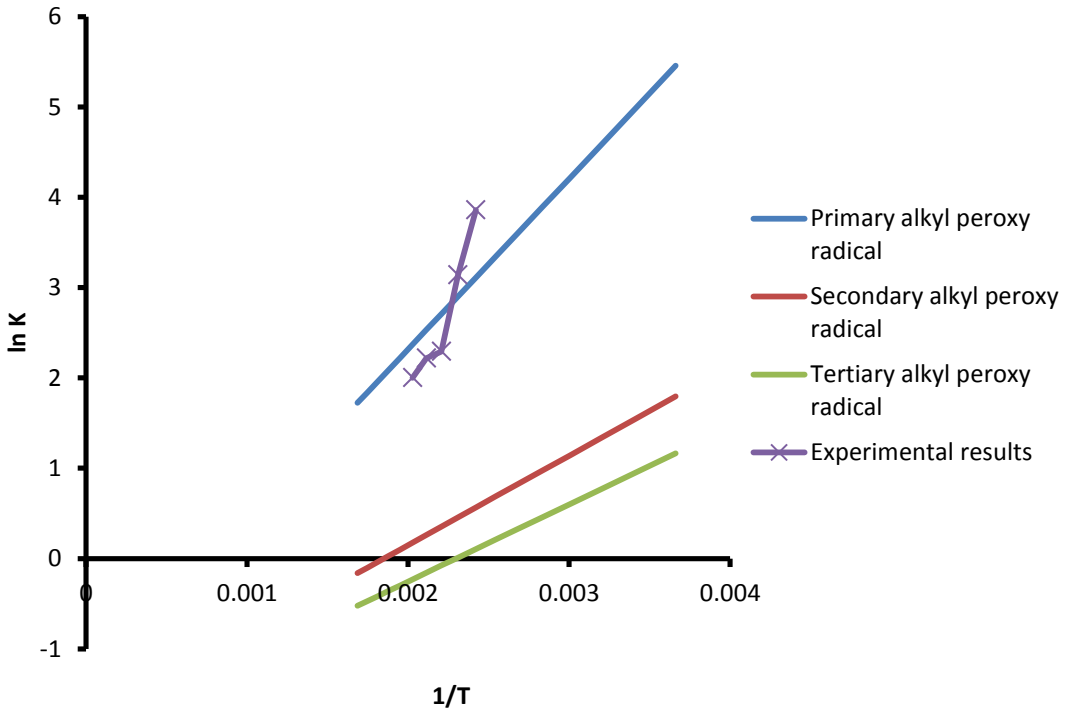

Figure 4.28 – Graph of K Vs T of theoretical and experimental results

At lower temperatures, the value of K is high and so the formation of products (alkyl hydroperoxide and aminyl radical) is favoured, but as temperature increases, the formation of products becomes less favourable as the backwards reaction rate increases. When ln K is plotted against 1/T, the value of ln K falls below 0 (indicating a K value of less than 1) for secondary and tertiary radicals in and around piston ring conditions. For tertiary radicals, this was calculated as 162 °C. For secondary radicals, the temperature is around 267 °C. At this point, the reverse reaction becomes favourable.

This point can also be described as the ceiling temperature and is the transition temperature above which another reaction will begin to dominate. This type of reaction is common in the automotive industry. Two of these reactions and their ceiling temperatures are summarised in Table 4.6.

Table 4.6 – Examples of ceiling temperatures of reactions

Reaction	Ceiling temp °C	Reference
$R\cdot + O_2 \rightarrow ROO\cdot$	624	[13]
$OHPP\cdot + NO_2 \rightarrow OHPP\text{-}NO_2$	197 ± 51	[159]

4.10 The effects of peroxide decomposers on the lifetime of radical scavenging antioxidants

In order to further test the hypothesis that the presence of alkyl hydroperoxide is linked to the activity of ODPA, reactions were carried out using a peroxide decomposer. If ODPA can work in the presence of a peroxide decomposer resulting in a synergistic effect this will imply that the peroxides are the root cause of the inactivity of ODPA.

4.10.1 Selecting a suitable peroxide decomposer

Fully formulated engine oils inhibit oxidation by the use of a combination of both radical scavenging antioxidants and hydroperoxide decomposers such as ZDDP, alkylsulfides, alkylpolysulfides and other metal dithiophosphates[7].

The use of hydroperoxide decomposers such as ZDDP was deemed not suitable as ZDDP can act as a radical scavenger as well as a hydroperoxide decomposer[64,74] which could overcomplicate the experimental analysis.

Common peroxide decomposers used extensively in applications such as hair dye products are iron and copper based. Attempts to use iron sulphate and iron stearate were unsuccessful as they were both insoluble in squalane.

As triphenylphosphine (TPP) has previously been used in this work in Chapter 3 to quantify the concentration of hydroperoxide by decomposing the peroxide to form TPPO and an alcohol (Figure 4.29), TPP was used as a peroxide decomposer in the oxidation of squalane at high temperatures. TPP is a suitable choice as it has a boiling point of 377 °C and flash point of 180 °C so can be used under piston ring conditions without significant volatile loss. It is also soluble in alkanes such as squalane. As well as decomposing peroxides, phosphites such as TPP can also act as chain breaking antioxidants as shown in Figure 4.29.

$(Ph)_3P + ROOH \rightarrow (Ph)_3P{=}O + ROH$

$(Ph)_3P + ROO\cdot \rightarrow [ROOP\cdot(Ph)_3] \rightarrow (Ph)_3P{=}O + RO\cdot$

$(Ph)_3P + RO\cdot \rightarrow [ROP\cdot(Ph)_3] \rightarrow (RO)(Ph)_2P + PhO\cdot$

$PhO\cdot + ROO\cdot \rightarrow$ Inactive Products

Figure 4.29 – The reactions of the phosphite triphenylphosphine with alkyl hydroperoxide, alkyl peroxy radicals and alkoxy radicals[160,161,162,163]

The ability of TPP to act as both a radical scavenger and a peroxide decomposer should make TPP a good antioxidant.

4.10.2 The peroxide decomposer TPP as an antioxidant

Using 0.5% w/w[3] (a typical treat rate for secondary antioxidants) of TPP in squalane at 180 °C showed that TPP can prevent oxidation of squalane for about 35 minutes. Although this is about the same duration as 0.5 % OHPP, due to the lower molecular weight of TPP they cannot be directly compared. As TPP is a peroxide decomposer and not a radical scavenger, it has a different mode of action. Unlike radical scavengers (where almost no oxidation of squalane occurs until the antioxidant is consumed), some low level oxidation occurs throughout the duration of the experiment represented by a slight drift in oxygen concentration during the reaction. This is due to the fact that the chain steps of squalane autoxidation are not inhibited by a peroxide decomposer.

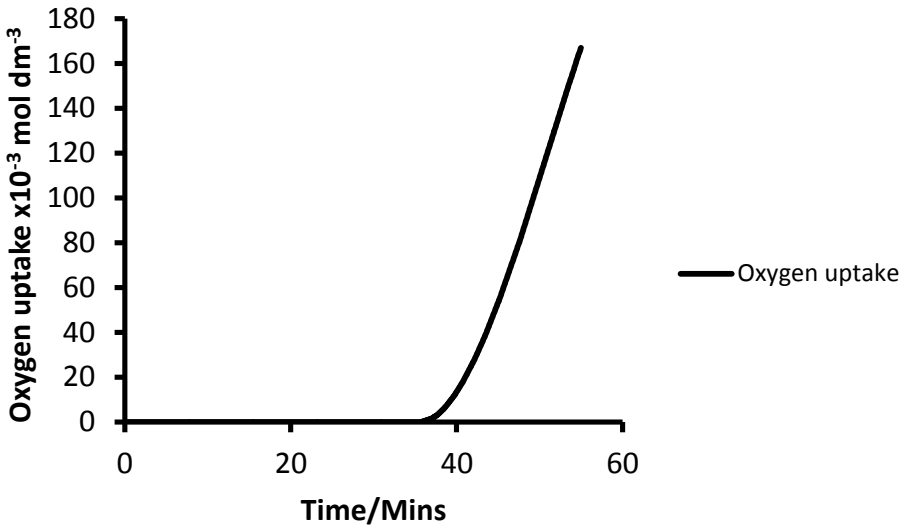

Figure 4.30 – Induction period of 0.5 % TPP at 180 °C

4.10.3 ODPA and peroxide decomposer together

When added to an antioxidant, a peroxide decomposer such as TPP showed synergstic properties as the two component system lasted far in excess of the sum of the individual components. [139,164,165] This was true for both phenolic and aminic antioxidants. As all previous reactions in this work with the aminic antioxidant ODPA suggested that it stops working in the presence of peroxide, then the addition of a peroxide decomposer helped indicate how good an antioxidant it could potentially be and how they were likely to behave in a fully formulated engine oil. If current trends continue and Zn, P and S levels are reduced further then ODPA may be left exposed as peroxide decomposing additive levels such as ZDDP are reduced. The phenolic antioxidant

OHPP mixed at a concentration of $7.5x10^{-3}$ mol dm^{-3} with 0.5% w/w TPP had an induction period for just over 4 hours. ODPA at a concentration of $7.5x10^{-3}$ mol dm^{-3} with 0.5% w/w TPP had a significantly longer induction period and prevented autoxidation for 8 hours. Although when used in a one additive system individually, the phenolic antioxidant OHPP outperformed the ODPA, when used in conjunction with a peroxide decomposer, the ODPA TPP mix performed significantly better. This turn around in antioxidant longevity could be attributed to the presence of TPP which kept the levels of peroxide low.

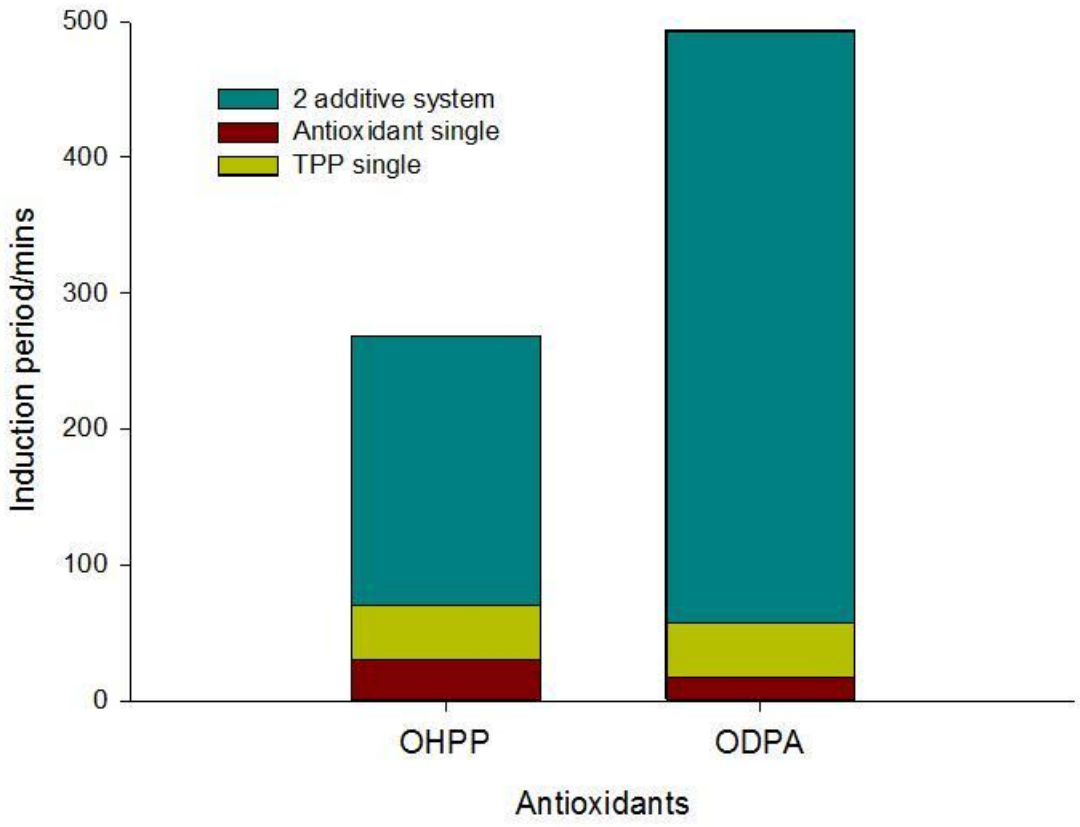

Figure 4.31 – Synergistic properties of peroxide decomposer and antioxidant compared to the sum of the individual component lifetimes at 180 °C

A repeat of the aminic antioxidant and TPP reaction was done with samples taken every 2 hours. The samples were then divided into two. One portion was diluted in toluene in the normal way for GC analysis (Section 2.2.7), the other in toluene that contained additional TPP to a concentration of 1 mol dm^{-3}. Any excess peroxides that remained unreacted in the sample should be decomposed by the excess TPP when diluted for GC analysis. The TPPO peaks of the two samples could then be compared to determine peroxide levels in the sample. The second run lasted 500 minutes (8 ¼ hours), an almost identical induction period to the previous run. During this time the concentration of aminic antioxidant varied very little. The TPP concentration steadily fell until it was consumed after 8 hours (Figure 4.32). The hydroperoxide concentration in the reaction is very low for the first four hours and begins to climb steadily as the TPP concentration declines. Once the TPP is consumed at the 8 hour mark, there is nothing preventing peroxide levels from increasing. 15 minutes after the TPP is consumed is the end of the induction period indicated by oxygen uptake. This is similar to the length of time it takes for ODPA to stop working in a single antioxidant component system, suggesting that the activity of ODPA is closely linked to the concentration of peroxide in the reaction. By decomposing the peroxide (and therefore removing a product), the equilibrium is shifted favouring the forwards reaction.

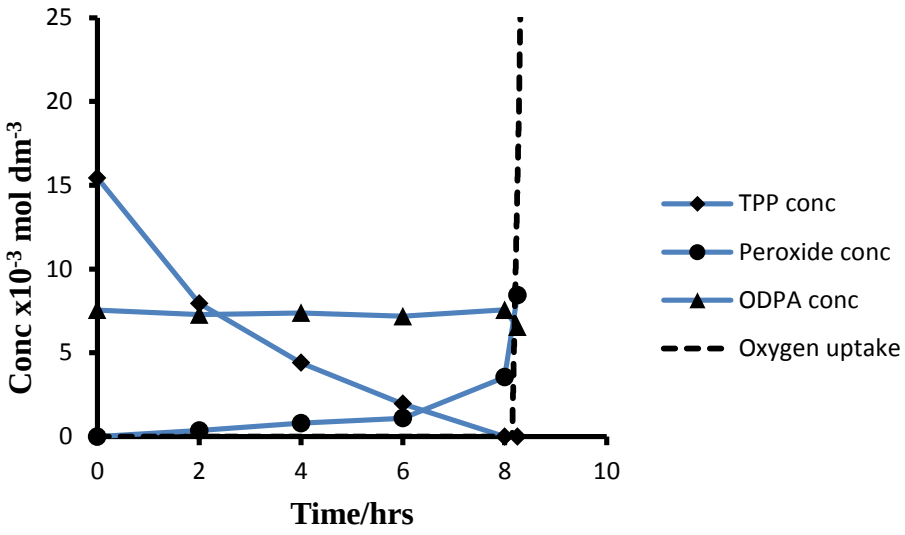

Figure 4.32 – TPP, ODPA and hydroperoxide concentration during induction period

The synergistic effect of radical scavenging antioxidant has been well documented,[166,59,60] with a wide range of peroxide decomposers giving the synergistic effect. Of more significance is the 10 fold increase (52 minutes to 495 minutes) in the lifetime of ODPA compared to just a 4 fold increase (65 minutes to 260 minutes) for OHPP. This large difference in activity results in ODPA going from being an inferior antioxidant compared to OHPP in a single additive system to a superior antioxidant in an antioxidant, peroxide decomposer system. This suggests the removal of peroxide allows the ODPA to act as a radical scavenger without being inhibited and that in the right circumstances with the right base fluid, ODPA will be a superior antioxidant to OHPP.

4.11 Conclusions

4.11.1 ODPA oxidation results

When used in a single additive system in squalane, ODPA performs less well than OHPP at preventing autoxidation at all temperatures tested between 160 and 220 °C. This observation is contrary to previously reported work that aminic antioxidants can prevent base oil oxidation for longer than phenolic antioxidants. [6,13,138,136,137,138]

During the induction period, while the base fluid is protected, ODPA produces one intermediate species detectable by GC. This product was found in small concentrations of approximately 4 x10 $^{-5}$ mol dm^{-3} and is believed to occur via a rearrangement of the antioxidant structure which is reversible, resulting in negligible consumption of the antioxidant or effect on its performance.

4.11.2 Critical concentration of ODPA

It was found that the inhibition of ODPA did not occur at a certain critical concentration below which the antioxidant stopped working. This was demonstrated using small concentrations of ODPA, which still gave some antioxidant performance when tested at 180 ºC.

4.11.3 Peroxide quantification

To test the theory that the effectiveness of ODPA is adversely affected by alkyl hydroperoxides, the concentration of these species was quantified during oxidation. It was discovered that there is a greater increase in peroxide concentration when compared to OHPP. The rate of formation of peroxides in squalane was significantly higher than that seen in n-dodecane at the same temperature, also using oxygen.[143]

4.11.4 The effect of alkyl hydroperoxides on ODPA

In this chapter, it has been shown that alkyl hydroperoxides have a negative effect on the activity of the aminic antioxidant ODPA. Not only does the concentration of the peroxides increase at a faster rate when ODPA is used compared to that of OHPP, the peroxide also has the effect of stopping the antioxidant from working (Figure 4.21). This phenomenon appears to be temperature dependent with the concentration of peroxide at which ODPA stops working varying widely over a 60 ºC temperature range. At higher temperature such as 220 ºC, ODPA immediately stops working. So much so that the induction period is similar to that of squalane that contains no antioxidant.

The failure of ODPA to work as an antioxidant has been attributed to the presence of alkyl hydroperoxides, which promotes the backwards reaction between itself and aminyl radicals, which reform the starting ODPA antioxidant and alkyl peroxy radicals. The

temperature at which the reverse of the reaction between ODPA and alkyl peroxy radicals becomes favourable is lowest for tertiary radicals as this has the least exothermic forwards reaction. This occurs under piston conditions in the region of 160 – 180 °C, according to the results in this work. This is a potentially significant consequence to the motor oil industry, particularly with the drive to produce oils with lower amounts of catalytic converter poisoning substances, such as phosphorus, sulfur and zinc, resulting in lower levels of secondary antioxidants such as ZDDP. Without the peroxide decomposers, any ODPA in the oil may not work effectively, resulting in oil oxidation and potential engine seizure.

4.11.5 Thermodynamics and equilibrium constant of reaction

When using a base oil that does not contain tertiary hydrogens, ODPA appears to act as expected under piston ring conditions, with the antioxidant protecting the base oil until the antioxidant has been consumed. Primary and secondary alkyl peroxy radical reacted with ODPA was found to be favourable under piston ring conditions and this could be the reason why ODPA is unaffected in a system using a base oil, with only primary and secondary hydrogens such as n-dodecane. This goes on to protect the base oil from oxidation until it has been entirely consumed, as seen in the studies by Ekechukwu *et al.*[143] This is not only supported by thermodynamic properties, it is also supported by the Jensen[50] antioxidant mechanism (Figure 4.24) which does not work for tertiary alkyl radicals.

Although the calculations showing the temperature at which the forwards reaction between alkyl peroxy radicals and ODPA becomes unfavourable support the experimental results as the ODPA stops working at similar temperatures to those obtained by calculation (Table 4.5 and Figure 4.22), these calculations are not conclusive due to the error associated with the experimental results for enthalpy used in the Gibbs free energy calculations.

Due to the relatively small enthalpy change of the reaction, slight variations had a large effect on the ceiling temperature of the reaction. However, it is reasonable to say that primary radicals are unaffected .

4.11.6 The effect of peroxide decomposers on antioxidants

Although a relatively large synergistic effect was observed between OHPP and TPP of around 4 times the sum of the two individual components, this was significantly smaller than the synergistic effect observed between ODPA and TPP, which was in excess of eight times longer than the sum of the two individual components. By removing the species thought to be responsible for the poor performance of ODPA, it has been shown that ODPA has the potential to be a much better high temperature antioxidant that it appears in the presence of alkyl hydroperoxides.

4.11.7 Subsequent work on aminic antioxidants

It is possible that the poor performance observed with ODPA is limited specifically to this antioxidant due to the relatively high N-H bond dissociation energy of the ODPA compared to the O-H bond dissociation energy of the hydroperoxides formed during squalane oxidation, which results in an exothermic reaction which becomes unfavourable at high temperatures. The next chapter aims to assess other aminic antioxidants with a variety of N-H bond strengths and substituent groups and compare their activity with that of ODPA. The work from Chapter 5 will then be compared and contrasted with the findings in this chapter.

Chapter 5

The Antioxidant Properties of Selected Aminic Antioxidants

5.0 The Antioxidant properties of other aminic antioxidants under Piston Ring Conditions

5.1 Introduction

Following on from the poor performance of octylated diphenylamine (ODPA) at temperatures between 180 and 220 °C, the work described in this chapter aims to assess other aminic antioxidants to attempt to establish what properties are required to make a good antioxidant when used at temperatures, similar to those seen under piston conditions, using a base fluid which contains tertiary hydrogen atoms e.g. squalane. The antioxidants used in this chapter are a variety of aminic antioxidants currently used commercially in an automotive lubricant, aromatic amines available commercially and the synthetic modification of a commercially available aminic antioxidant, in an attempt to improve their antioxidant properties and increase the induction period when added to squalane.

5.1.1 Previous work

Previously published work with antioxidants such as N-phenylnaphthalen-1-amine (PAN) and alkylated N-phenylnaphthalen-1-amine (PANA) has shown that these antioxidants have excellent antioxidant properties at high temperatures between 180 and 220 °C.[135,136] These antioxidants have been found to prevent oxidation for a longer

period than both phenolic antioxidants and ODPA at a similar concentration in a single additive system.[136]

In addition, diphenylamine antioxidants, which contain a heteroatom bridge such as sulfur, as found in phenothiazine, have also been found to be excellent antioxidants[64,167] Previous work on phenothiazines found that they outperformed ODPA, and phenolic antioxidants[139] but not significantly. Compared to ODPA, the phenothiazine increases the induction period by approximately an additional 15 %.[139]

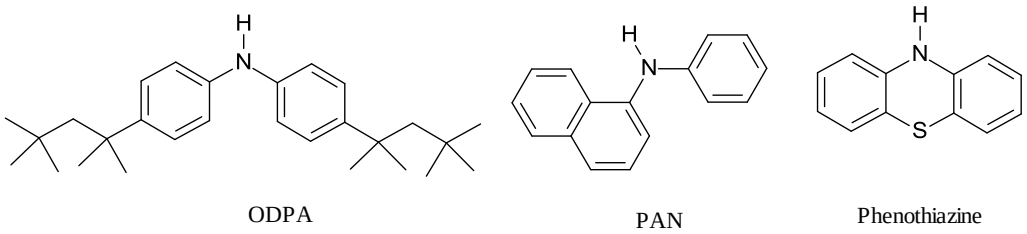

Figure 5.1 – Structures of ODPA, PAN and phenothiazine

5.2 Bond dissociation energies of the N-H bond in diphenylamines

In Chapter 4, it was concluded that the surprisingly poor antioxidant properties of ODPA at elevated temperature was due to the significance of the reverse reaction between alkyl peroxy radicals and aminic antioxidant at high temperatures. This was caused by the near equivalence of the N-H bond dissociation energy in ODPA to the O-H bond dissociation of tertiary alkyl hydroperoxide, meaning that at sufficiently high temperatures, the reaction was reversible.

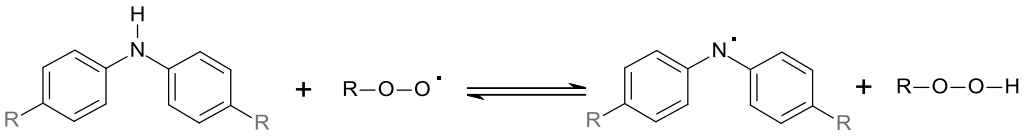

Figure 5.2 – Recap of the reaction between aminic antioxidant and alkyl peroxy radicals

To further test this theory, a literature search was conducted to determine the range of N-H bond dissociation energies of para substituted diphenylamines. If antioxidants could be found which have lower N-H bond dissociation energy, then this should prevent base oil oxidation for longer, as the forwards reaction would be favourable at higher temperatures.

In Chapter 4, it was concluded that an enthalpy change of ~7 kJ mol^{-1} in the reaction between the N-H of ODPA and tertiary alkyl peroxy radicals was insufficient to prevent the backwards reaction becoming favourable above ~160 ºC

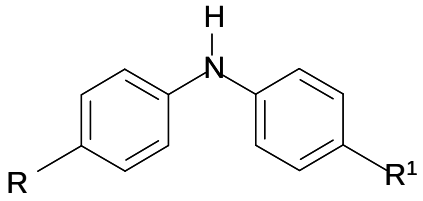

Figure 5.3 – Diphenylamine and para substituent positions

To keep the antioxidant as close to ODPA as possible (and eliminate other possible factors relating to performance), only para substituted aminic antioxidants were included.

Table 5.1 – N-H bond dissociation energies of para substituted diphenylamines R, R^1= H unless otherwise stated (from Figure 5.3)

Substituent(s)	N-H BDE kJ mol^{-1}	Reference
R=R^1=H	364.2 ± 0.5	58
R= H, R^1= Me	363.6 ± 1.0	49
R=R^1= Me	361.1 ± 1.5	155
R=R^1= t-butyl	357.0 ± 0.5	58
R=R^1=OMe	348.1 ± 0.5	58
R=H, R^1=OMe	358.2 ± 1.0	49
R=H, R^1=NO_2	372.9 ± 0.5	58
R=R^1=Br	368.6 ± 1.0	49
R= H, R^1= F	371.5 ± 1.5	155

From this data, the lowest N-H bond dissociation energy is that for the dimethoxy substituted diphenylamine, 4-methoxy-N-(4-methoxyphenyl)aniline (DPAOMe) as the OMe groups have a +M effect, lowering the N-H bond dissociation energy further than the +I effect of alkyl groups.

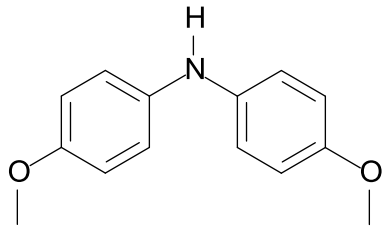

Figure 5.4 – Structure of 4-methoxy-N-(4-methoxyphenyl)aniline (DPAOMe).

The N-H BDE of 348 kJ mol^{-1} for DPAOMe is significantly lower than both the N-H BDE of ODPA[155] and also the O-H BDEs of alkyl peroxy bonds.[156,158,168] If the problems associated with the poor performance of ODPA are associated with the reversible reaction between aminyl radicals and alkyl hydroperoxide, as stated in Chapter 4, DPAOMe should be a good high temperature antioxidant. Using the same computational software and method as Chapter 4, the entropy changes between DPAOMe and alkyl peroxy radicals were calculated to assess the thermodynamics of the reaction. The results showed that the forward equilibrium reaction between DPAOMe and alkyl peroxy radicals should be favourable for all types of alkyl peroxy radical at temperatures associated with automotive lubricants.

Table 5.2 – Comparison of thermodynamic data of ODPA and DPAOMe with alkyl peroxy radicals

Antioxidant	**Peroxy radical type**	**ΔH kJ mol^{-1}**	**ΔS J K^{-1} mol^{-1}**	**T/°C at which ΔG = 0**
ODPA	1°	-15.7± 9.1	-12.14	1292 ± 750
DPAOMe	1°	-19.0	0	N/A
ODPA	2°	-6.9	-15.21	180
DPAOMe	2°	-16.5	-8.04	1779
ODPA	3°	-7.1 ± 9.1	-16.32	162
DPAOMe	3°	-10.6	-9.14	887

5.3 Autoxidation of DPAOMe in squalane

To test the theoretical data obtained from Gaussian in this work and other experimental results, oxidation reactions were done using DPAOMe at 180, 200 and 220 ºC, measuring the induction period of the reaction containing DPAOMe in squalane.

5.3.1 Oxidation of DPAOMe under piston ring conditions

Between 180 and 220 °C, ODPA was not fully consumed by the end of the induction period. To assess the influence of the lower N-H BDE of DPAOME on antioxidant lifetime, its antioxidant concentration was also measured throughout the induction period. The DPAOMe was difficult to dissolve in squalane, due to the substitution of branched alkyl groups for more polar OMe groups. This reduced solubility in the non-polar squalane and so the mixture had to be heated to 90 ºC.

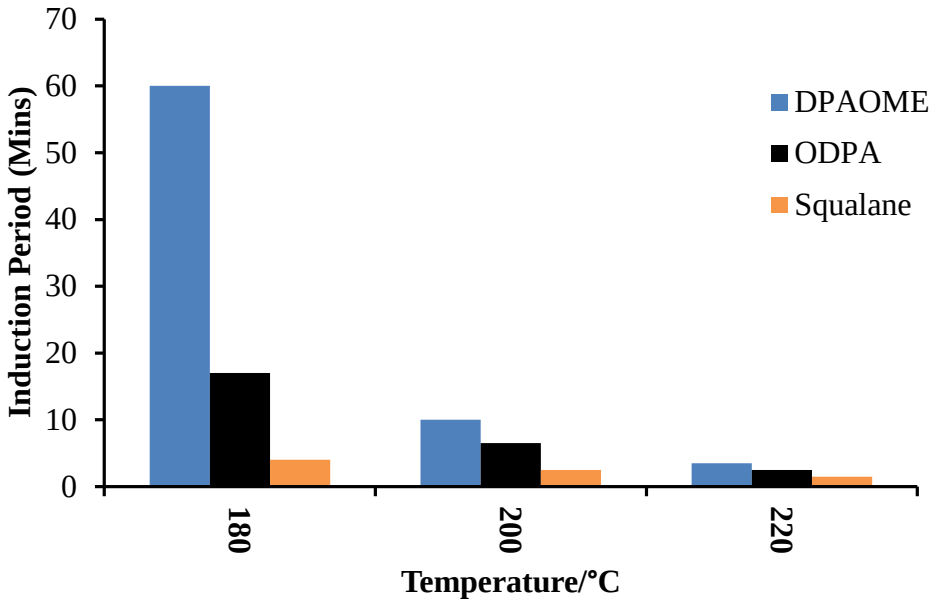

Figure 5.5 – Induction periods of DPAOMe in squalane compared to ODPA squalane and squalane without antioxidant from 180 to 220 °C

DPAOMe proved to be a very good high temperature antioxidant. When compared to ODPA (Figure 5.5), the induction period for DPAOMe was approximately 1 hour at 180 ºC which was over three times more than the 17 minute induction period of ODPA. At 200 °C, the induction period when using DPAOMe was 10 minutes, compared to 6.5 for ODPA. At 220 °C, DPAOME still had a longer induction period than ODPA but was relatively poor, lasting only 3.5 minutes.

5.3.2 Concentration of DPAOMe during the induction period

The problems with the comparative ineffectiveness of ODPA at elevated temperatures reported in Chapter 4 correlated with the presence of relatively high levels of antioxidant still being present at the end of the induction period. To test this with DPAOMe, samples were taken during the induction period and analysed by GC. At the end of the induction period, all of the antioxidant had been consumed, consistent with DPAOMe having a much lower N-H BDE than ODPA and so is not affected by the build-up of peroxide under piston ring conditions.

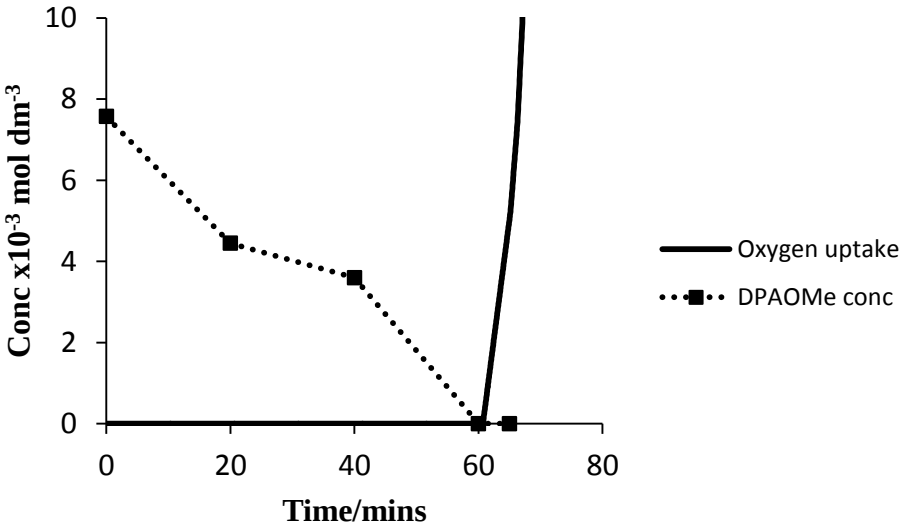

Figure 5.6 – DPAOMe concentration and oxygen uptake during the induction period of an oxidation run at 180 °C

As the antioxidant performed well, it appears that the thermodynamic calculated data for the two aminic antioxidants is approximately correct and, in the presence of tertiary alkyl peroxy radicals (produced during squalane oxidation), ODPA is affected by

having a significant reverse reaction for the reaction between it and tertiary alkyl peroxy radicals, while DPAOMe does not have a significant reverse reaction .

5.3.3 DPAOMe and peroxide decomposer in squalane

It has also previously been described in Chapter 4 of this work that the addition of a peroxide decomposer to ODPA can rectify the problem associated with alkyl peroxy radicals and produce a strong synergistic effect, which is in agreement with other previous work.[166,169] To test this further, DPAOMe was used in a two additive component system and compared against the results of ODPA from Chapter 4.

When ODPA was mixed with triphenylphosphine (TPP) in Chapter 4, a synergistic effect was found where the combination of the two additives together lasted longer than the sum of the individual runs separately. This was also tested for DPAOMe (Figure 5.7) using the same concentrations of 7.55 $x10^{-3}$ mol dm^{-3} primary antioxidant (DPAOMe) and 1.6 $x10^{-2}$ mol dm^{-3} of secondary antioxidant (TPP).

.

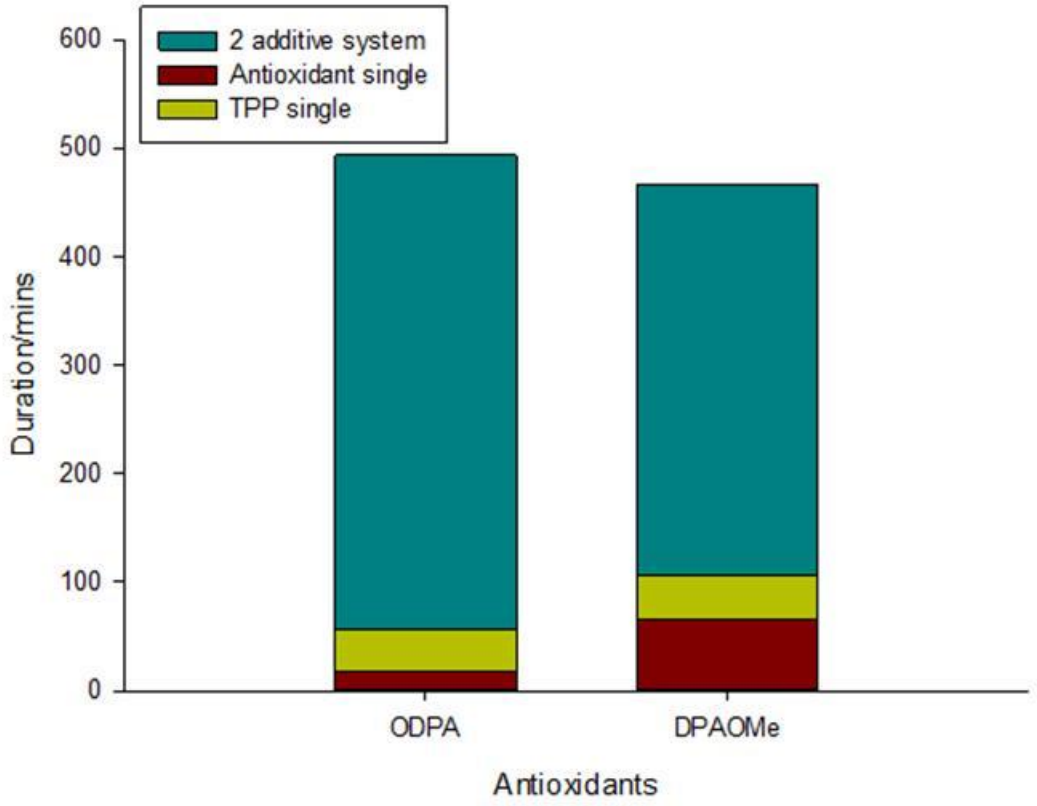

Figure 5.7 – Synergistic properties of peroxide decomposer and the antioxidants ODPA and DPAOMe and the individual components at 180 ºC

As observed with ODPA, when DPAOMe was used together with TPP peroxide decomposer as expected, a synergistic effect was observed.[59] However, the duration of the induction period for DPAOMe was slightly shorter than that of ODPA, despite the sum of the individual components when run as separate reactions being far greater than those of ODPA.

The close proximity of the induction periods for ODPA with TPP and DPAOMe with TPP is supportive of the theory that removal of peroxides by TPP allows ODPA to work as efficiently as other aminic antioxidants such as DPAOMe and that the inhibiting

factor in the poor performance of ODPA is the presence of alkyl hydroperoxides, as suggested in Chapter 4.

5.4 PANA type antioxidant

As well as para substituents, other groups can also reduce the N-H bond dissociation energy of aminic antioxidants.[148,170] Although these cannot be directly compared against ODPA, they still play a significant role in lubricant antioxidants commercially. An example of these are phenyl-alpha-naphthylamines (PANA) antioxidants.

Alkylated N-phenylnaphthalen-1-amine (PANA) type antioxidants are known to be excellent antioxidants at high temperatures,(130 – 180 ºC).[135,136,137] The commercially available antioxidant N-[4-(1,1,3,3-tetramethylbutyl)phenyl]naphthalen-1-amine (OPANA) shown in Figure 5.8 contains one octylated aromatic ring, as found in ODPA, but it also contains a naphthalene ring on the other side of the central amine group. This change in structure allows analysis of the impact of the addition of a naphthalene ring system to an aminic antioxidant.

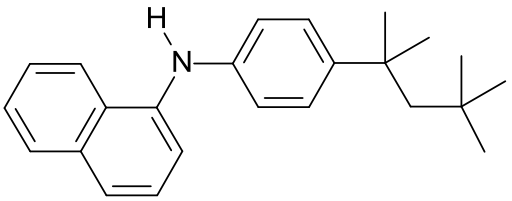

Figure 5.8 – Structure of N-[4-(1,1,3,3-tetramethylbutyl)phenyl]naphthalen-1-amine (OPANA)

5.5 Oxidation reactions of OPANA under piston ring conditions

Due to the lower molecular weight of OPANA to ODPA and OHPP, only 0.312 %wt was used to achieve an equivalent concentration of 7.55 x10^{-3} mol dm^{-3}, which was the standard concentration used to compare antioxidants. The OPANA was tested at 180, 200 and 220 ºC as shown in Figure 5.9.

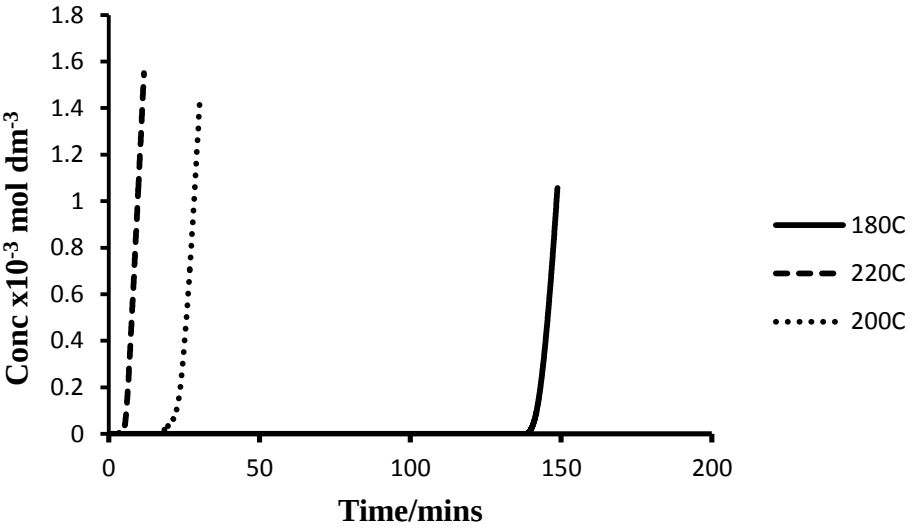

Figure 5.9 – Oxygen uptake of 7.55 x10^{-3} mol dm^{-3} concentration of OPANA in squalane between 180 and 220 ºC

At 180 ºC, OPANA gave excellent protection to the squalane, lasting far longer than any other antioxidant discussed so far in this work. At this temperature, the antioxidant prevented oxidation for 145 minutes compared to 17 minutes by ODPA and 30 minutes by OHPP. This was also the case at 200 and 220 ºC, with OPANA preventing oxidation for 15 minutes at 200 ºC and for 7 minutes at 220 ºC. This observation at 220 ºC was of particular significance as ODPA, OHPP and even DPAOMe at this temperature provided little antioxidant protection to the base fluid. This is consistent with the findings of previous work.[135] However, the difference in activity was much wider in this study which could be caused by the different type of base oil chosen, which does not contain tertiary hydrogens. This will result in a favourable reaction between alkyl peroxy radicals and antioxidant at higher temperatures because of the larger ΔH of the reaction, compared to that of tertiary alkyl peroxy radicals with antioxidants.

5.6 Intermediate product formation during oxidation reactions of OPANA at high temperatures

Previous studies have identified dimer products of PAN (the non octylated version of OPANA), using GPC analysis by detection of a peak at approximately twice the molecular weight to the starting antioxidant.[136] The proposed structures of these intermediates appear to be predicted by studying the mechanism by which PAN reacts, rather than analytic interpretation. The work reported here analyses products using GC and GC-MS in an attempt to gain additional information about the structure of OPANA intermediates and hence the reaction mechanisms by which they react. The OPANA

antioxidant had a retention time by GC close to that of squalane when using a 5 % -phenyl 95 %-dimethylpolysiloxane column (Figure 5.6), which could be problematic for intermediate analysis as they could easily be masked by the much larger squalane peak. GC analysis was also done using the more polar 35 % -phenyl 65 %-dimethylpolysiloxane column to separate the non-polar squalane and polar OPANA but no intermediate peaks were found in this region of the GC trace.

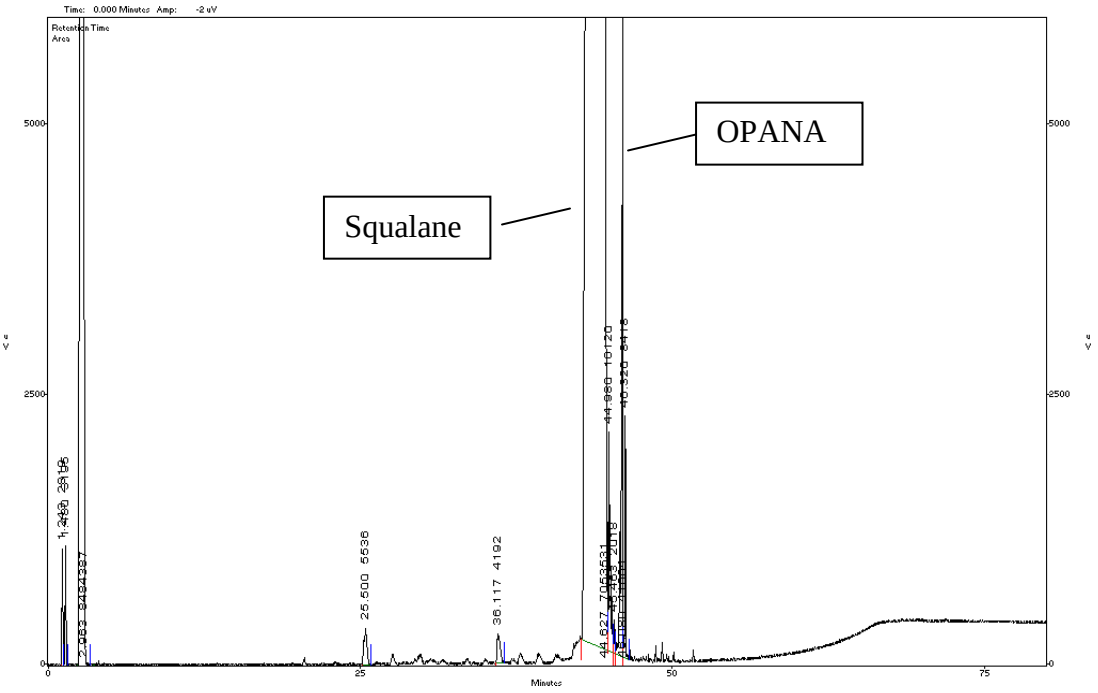

Figure 5.10 – GC-FID chromatogram of OPANA in squalane starting material using a 5 % -phenyl 95 %-dimethylpolysiloxane column

In samples taken during oxidation, a new intermediate peak with a longer retention time was observed in GC analysis. To analyse this further, a short 15 m column (identical to the DB5-HT column in every aspect except length) and a higher maximum GC profile temperature of 400 °C (increased from the standard 360 °C) were used. This was sufficient to get enhanced peak data on the intermediate but unfortunately, the shorter

column also had the effect of reducing the gap in retention time between the squalane and the OPANA and so the antioxidant peak became almost incorporated into the squalane peak between 22 and 23 minutes. When using the short column, three intermediate peaks were detected by GC. These are labelled (in order of retention times lowest to highest): D1, D2, D3.

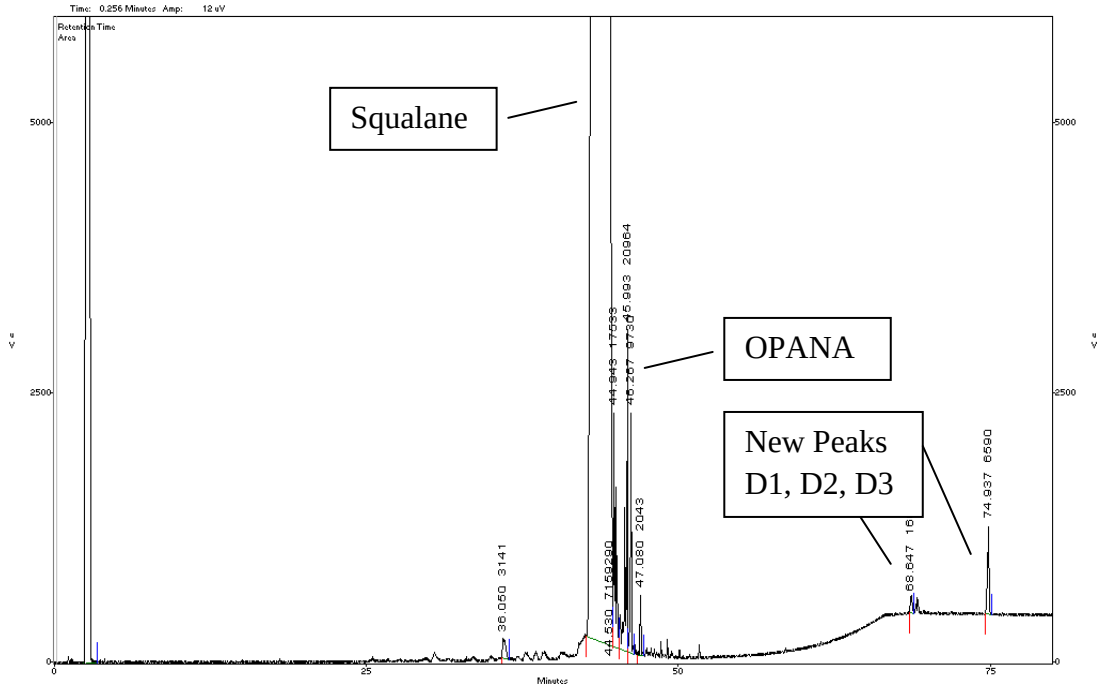

Figure 5.11 - GC trace of OPANA in squalane after 1.5 hours at 180 °C

5.6.1 Product quantification

The products identified by GC-FID were quantified and plotted against the OPANA concentration and the oxygen uptake of the reaction. The concentration of OPANA and intermediates is shown in Figure 5.12 with antioxidant concentration on the left axis and intermediate concentration on the right

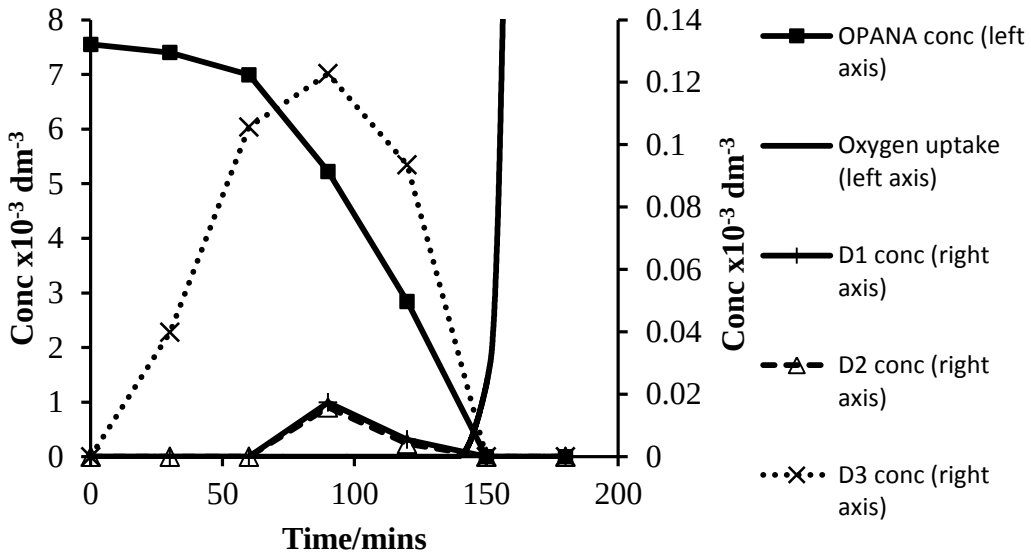

Figure 5.12 – OPANA and intermediate concentration over time at 180 °C

During the oxidation reaction, the intermediate concentration increased as the OPANA concentration fell, indicating possible formation from the OPANA starting material and due to the high retention time of the peaks, these were believed to be dimers of the starting OPANA as seen in previous work by GPC.[136] The concentration of these intermediates was much higher than intermediates previously seen in other antioxidants. After half an hour, the antioxidant concentration had fallen by 0.15 mol dm^{-3}. Of this, 53 % of the antioxidant that had reacted produced intermediate species. This amount fell steadily until after 120 minutes, when only 4 % of the total antioxidant that had reacted was detected as intermediate species, as shown in Table 5.3.

Table 5.3 – Percentage of antioxidant going on to form intermediates

Time/mins	OPANA total concentration loss mol dm^{-3}	Intermediates combined concentration mol dm^{-3}	% of antioxidant forming intermediate
0	0.00	0.00	N/A
30	0.15	0.04	53.4
60	0.55	0.11	38.1
90	2.32	0.16	13.4
120	4.70	0.10	4.4
150	7.53	0.00	0.0
180	7.53	0.00	0.0

5.6.2 Product identification

To confirm the structure of the intermediates, GC-MS analysis was carried out using the same short column and operating conditions as those used in GC analysis. Unfortunately, the maximum temperature attainable in the transfer line between the GC and MS was 250 °C, meaning that the high retention time intermediates which were eluted at 400 °C condensed in the transfer line and were not observed by the mass spec. To help solve this, the concentration of the antioxidant was increased to 1 % and the reaction and analysis was repeated. This was sufficient to obtain spectra of one of the intermediates. The two smaller intermediates determined by GC were still not attainable by GC-MS and so their structures could only be speculated on due to the high retention times observed by GC.

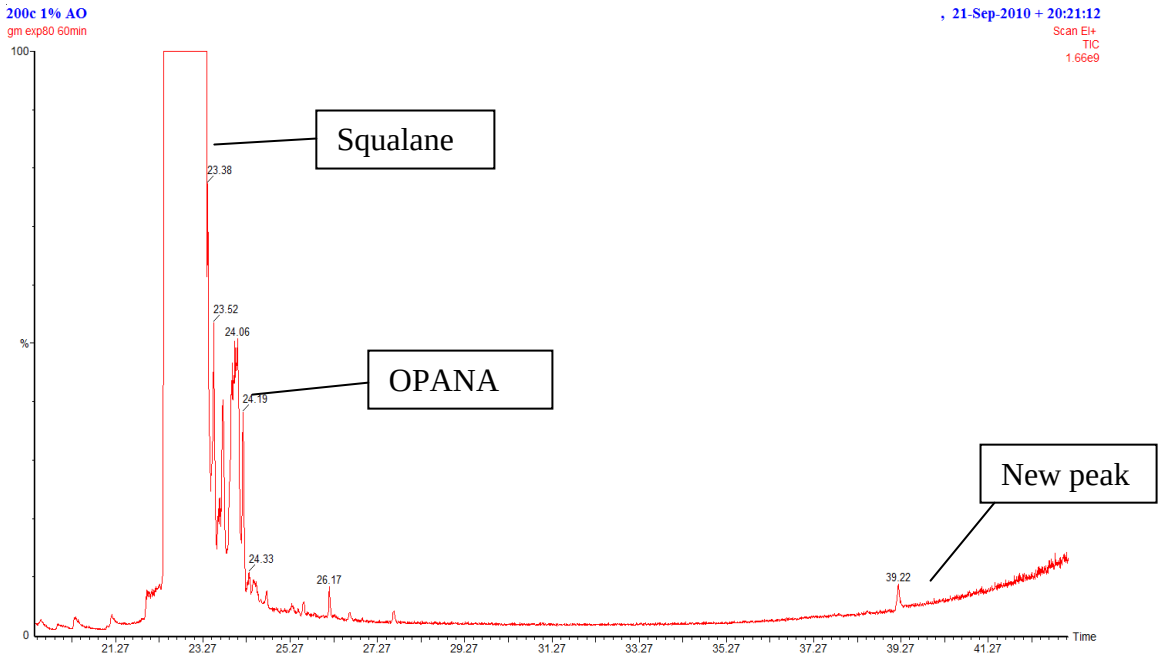

Figure 5.13 – GC trace from the GC-MS analysis

The OPANA antioxidant has the formula $C_{24}H_{29}N$ and a calculated mass of 331.47.

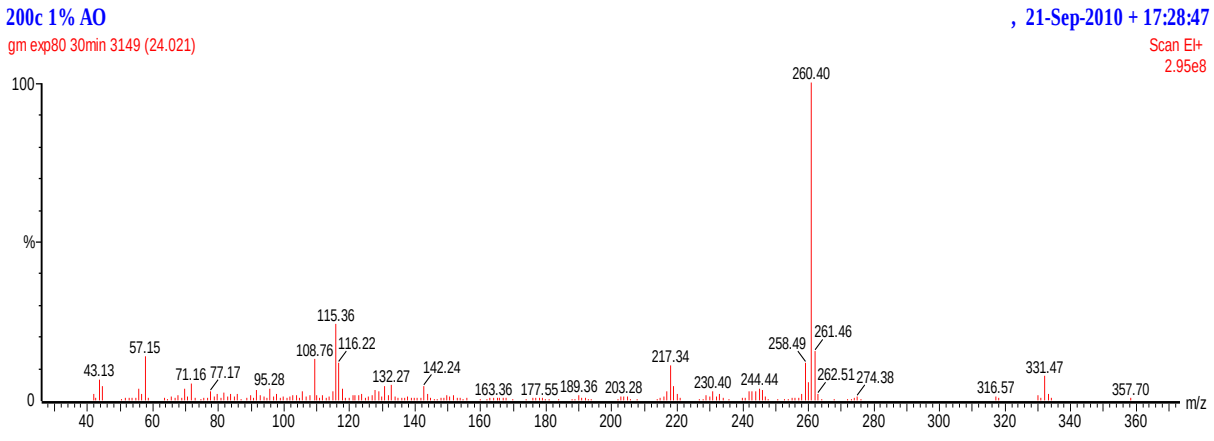

Figure 5.14 – Mass spectra analysis of OPANA

The intermediate peak has a mass ion peak at 660.93. This is consistent with dehydro dimer formation of the antioxidant as this is the mass of double the antioxidant minus 2 with formula $C_{48}H_{56}N_2$. Other significant peaks include 259 ($C_{19}H_{17}N$) and 207 ($C_{16}H_{11}N$).

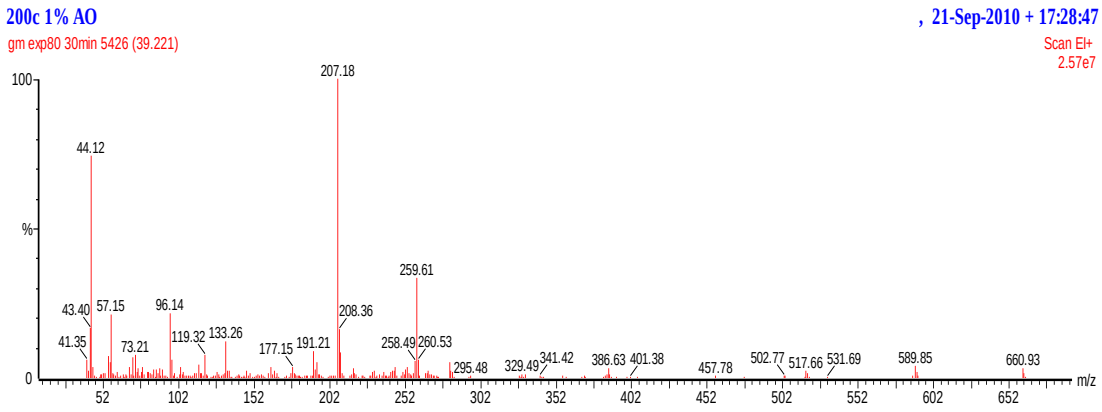

Figure 5.15 – Mass spectra of intermediate species of ODPA oxidation

OPANA will most likely initially react by abstraction of hydrogen from the nitrogen. The three most stabilised (inductively) and therefore likely resonance structures for OPANA are shown in Figure 5.16.[171] The mechanism of dimer formation will occur by a termination step between two radicals which are formed by abstraction of the hydrogen atom of the N-H bond of ODPA by an alkylperoxy radical. This could occur by N-N, C-N or C-C coupling.[136]

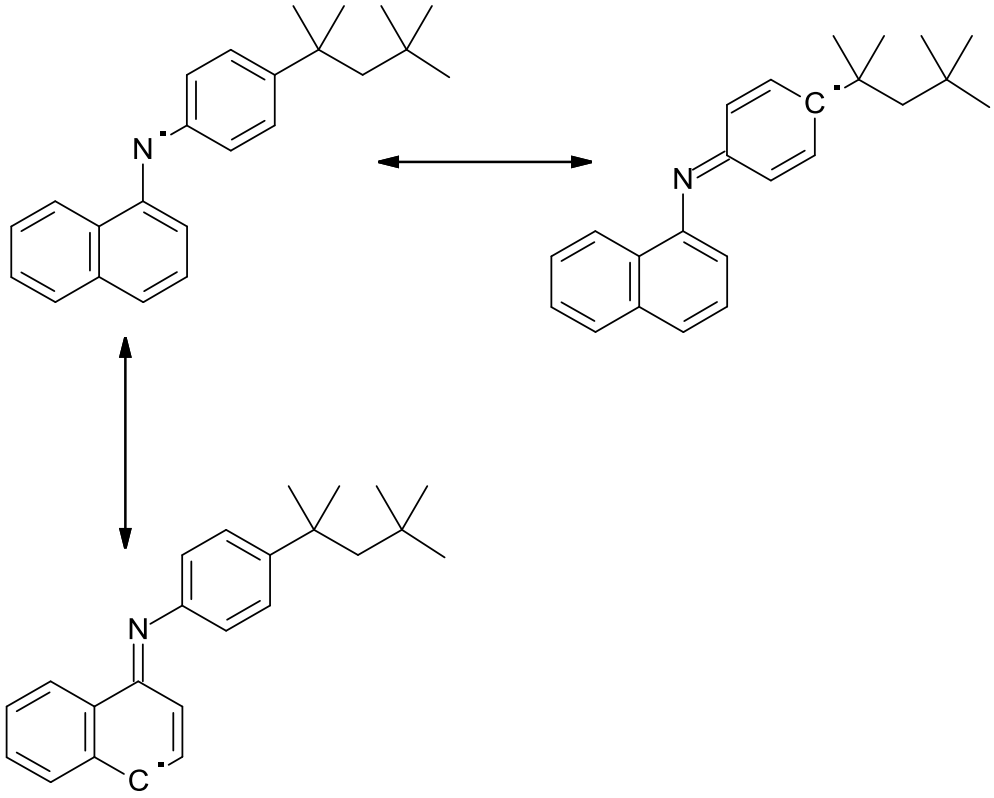

Figure 5.16 – Possible resonance structures of OPANA radical

The three intermediate peaks seen by GC will correspond to three different dimers. This is more substantial than the findings in previous work of Mousavi,[136] who was unable to identify different dimer structures. The proposed dimer structures were based upon the fact that the principle attack of alkyl peroxy radicals on OPANA is on the naphthyl ring[172] and so logically, the dimer structures are more likely to involve these naphtyl ring radicals. Although the identity of the most prominent dimer was not found, it was established that three varieties of dimer are created by OPANA.

The presence of the dimer species makes the fact that OPANA lasts longer than previously tested antioxidants surprising as the aminyl radical formed after abstraction

of the hydrogen of the N-H bond will simply dimerise after consuming a single alkyl peroxy radical and not the multitude of radicals implied by mechanisms such as the Denisov cycle.[53] This combination of two antioxidant radicals implies a highly stable radical with the ability to exist for longer periods of time allowing it to dimerise. Although the OPANA antioxidant appears to be converted to an inactive species by forming the dimer, it is still consumed whilst in the dimer form and after 150 minutes, no intermediates species were detected.

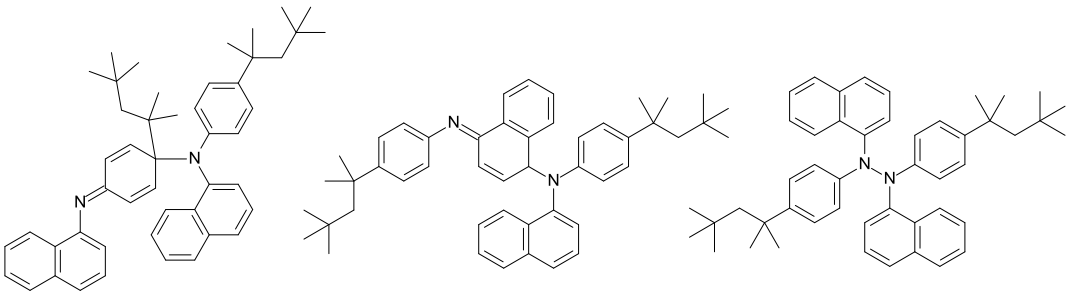

Figure 5.17 – Some possible products by radical-radical combinations of the resonance structures of OPANA

5.7 Comparison of diphenylamine with mononaphthalene - monophenyl antioxidants.

The highly conjugated structure of the OPANA reduces the N-H bond dissociation of the molecule when compared to that of ODPA.[173] When calculated using Gaussian following the same method used in Chapter 4, this was found to be 348 kJ mol^{-1} for OPANA, which is significantly lower than that of OPDA (361 kJ mol^{-1}) and the same as

DPAOMe. This means that like the DPAOMe, the calculated thermodynamics implies that the reaction between OPANA and alkylperoxy radicals will be favourable and not reversible at all attainable temperatures for all types of alkyl peroxy radical.

Although OPANA and DPAOMe have the same N-H bond dissociation energy, OPANA lasts significantly longer than DPAOMe. One theory of why this occurs is that antioxidants containing a naphthalene ring work by a different mechanism.[135]

To test these theories, the level of alkyl hydroperoxide was monitored throughout an OPANA reaction at 180 ºC. Initially, the levels of alkylhydroperoxide remained low but after around an hour, these levels began to increase with the concentration of alkyl hydroperoxide overtaking the concentration of antioxidant after 120 minutes. Shortly after this at approximately 150 minutes, the induction period ended as oxygen uptake increased substantially.

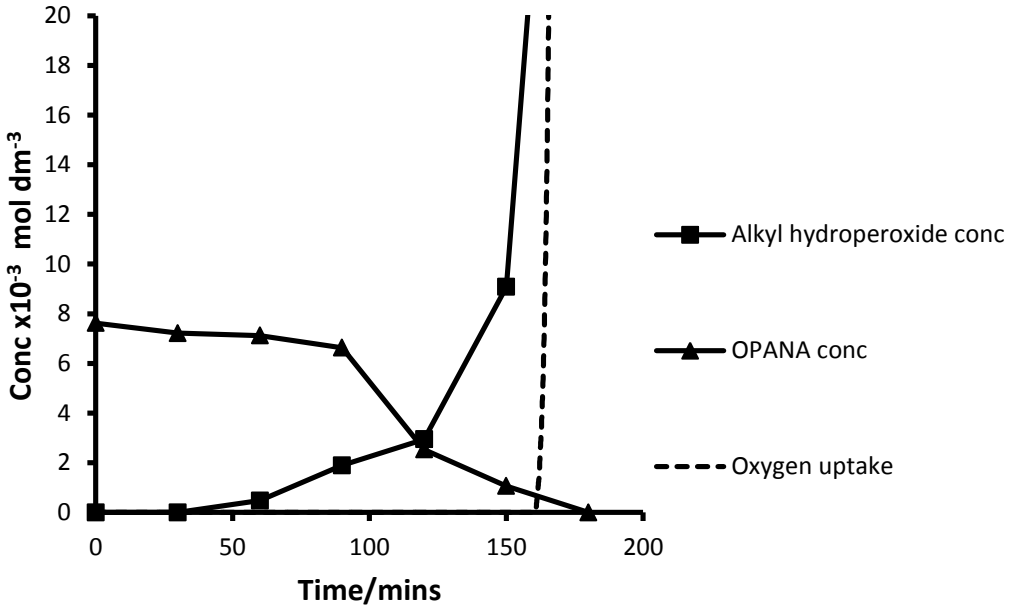

Figure 5.18 – Alkyl hydroperoxide concentration and antioxidant concentration of OPANA in squalane at 180 ºC

When compared to previous antioxidants tested, OPANA, like ODPA, did not appear to decompose alkyl hydroperoxides for the entire induction period, with alkyl hydroperoxide concentration increasing after an hour. Initially, the build-up of alkyl hydroperoxide is slow and starts to increase at around half way through the induction period for both the aminic antioxidants. In contrast, the phenolic antioxidant OHPP appeared to inhibit alkyl hydroperoxide concentration for the whole duration of the induction period.

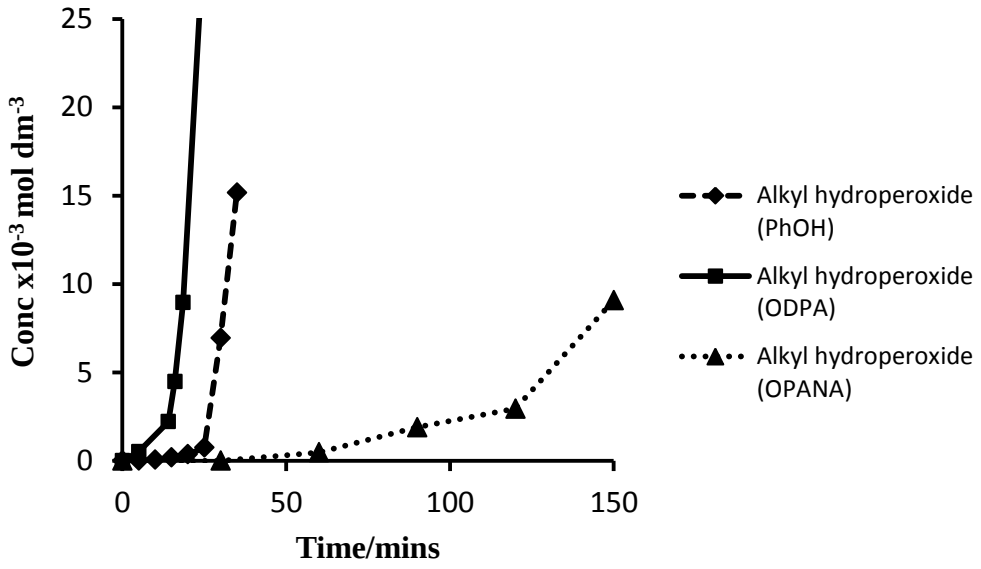

Figure 5.19 – Comparison of alkylhydroperoxide build up in OHPP, ODPA and OPANA

Behaviour of peroxide decomposition by primary antioxidants is something that has previously been observed in both phenolic[174] and aminic antioxidants,[140,175,176] although no mechanism has been proposed. With OPANA, alkyl hydroperoxide levels are low for approximately 1 hour. This slow build-up of peroxide in the reaction suggests that it is not forming alkyl hydrogen peroxide in the first place or the alkyl hydrogen peroxide is being removed by decomposition. As peroxide levels do rise during the reaction, the most plausible explanation for this was proposed by Hunter et al[135] who suggest that PAN type antioxidants inhibit oxidation by a different mechanism to conventional antioxidants. The initial donation of the labile hydrogen to an alkyl peroxy radical ($ROO^{\cdot}$) does not lead to the formation of alkyl hydroperoxide (ROOH), it instead leads to the formation of an olefin and oxygen.[136]

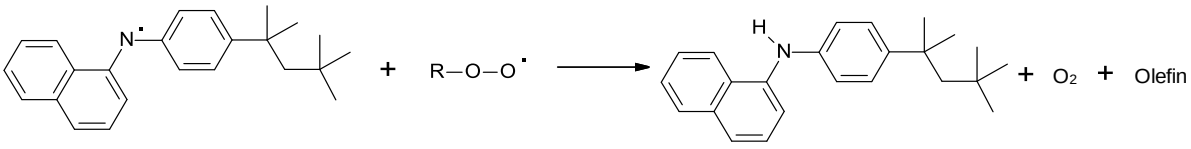

Figure 5.20 – Reaction of OPANA with alkyl peroxy radicals[136]

The activity of OPANA, despite the presence of alkyl hydroperoxide (1 hour onwards), is supporting evidence that the lower bond dissociation energy of the N-H bond in OPANA, compared to that in OPANA means that at piston temperatures (180 – 220 °C), the forwards reaction between OPANA, and alkyl peroxy radicals in favourable for all types of alkyl peroxy radicals (represented by a negative Gibbs free energy). As the bond dissociation energy for the N-H bond in OPANA is 6 kJ mol^{-1} lower than the N-H bond in ODPA, the reaction between OPANA and alkyl peroxy radicals will always be exothermic. Using a tertiary alkyl hydrogen peroxide as an example which has an O-H bond dissociation energy of 368 kJ mol^{-1}. With ODPA, as previously stated in Figure 5.2, this will be exothermic by 7 kJ mol^{-1}, whereas with OPANA this reaction will be exothermic by 11 kJ mol^{-1}. This difference of 4 kJ mol^{-1} means that the reaction between ODPA and alkyl peroxy radicals will become unfavourable under piston ring conditions, whereas with OPANA, the reaction will continue to be favourable above those temperatures seen in an engine.

5.8 Dinaphthalene aminic antioxidants

As the substitution of a naphthalene ring for a phenyl ring had such a large increase on the induction period, antioxidants were tested which contained two naphthalene ring systems to see if the induction period could be further increased.

Of the three dinaphthylamine structures that are available commercially (shown in Figure 5.15), N-(1-naphthyl)naphthalene-1-amine (NANA1) was chosen as this resembled the naphthenic system of OPANA with the hydrogen in the para position to the N-H group available. The 2,2 version (NANA2) was also tested to assess the influence of the para position on antioxidant lifetime, as it is known from previous work on phenolic antioxidants that the resonance stabilized phenoxy radical has significant electron density in the para position of the molecule and is the basis for formation of antioxidant intermediate species such as 2,6-ditert-butyl-1,4-benzoquinone.[130]

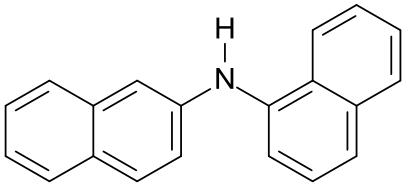

N-(2-naphthyl)naphthalen-1-amine

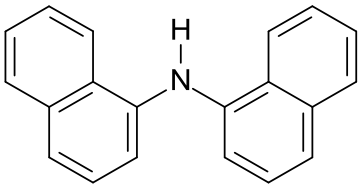

N-(1-naphthyl)naphthalen-1-amine

NANA1

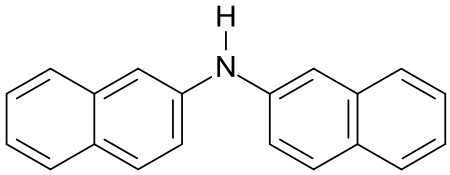

N-(2-naphthyl)naphthalen-2-amine

NANA2

Figure 5.21 – Three structures of dinaphthalene aminic antioxidants

Due to the lack of hydrocarbon chains on these antioxidants, they were significantly less soluble in squalane than the previous antioxidants used. Because of this, the antioxidants had to be heated at 120 °C for 10 minutes, instead of the usual 60 °C, to get them to dissolve. To minimise consumption of antioxidant, the heating was undertaken under a nitrogen atmosphere. However, this was just a precautionary measure. Even at 120 °C, in the presence of oxygen, it would be several hours before significant consumption of the antioxidant would occur.[127]

5.8.1 Autoxidation of dinaphthalene antioxidants in squalane

Autoxidation using NANA1 and NANA2 were compared at temperatures between 180 and 220 °C, as shown in Figure 5.22.

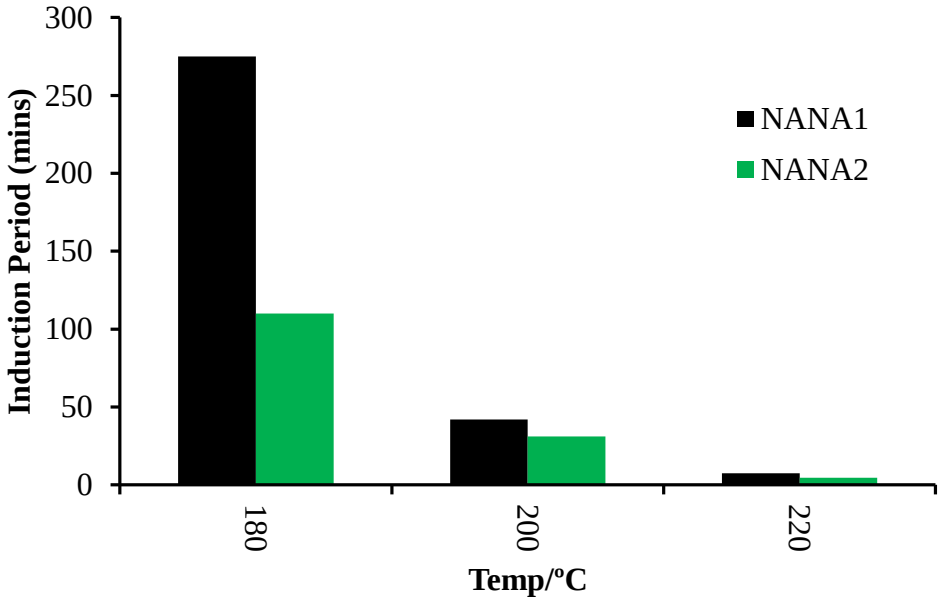

Figure 5.22 – Induction periods of NANA1 and NANA2 between 180 and 220 °C

Autoxidation at 180 °C showed that the NANA1 structure of the antioxidant was significantly better than OPANA when used at the equivalent concentration (7.55 x10^{-3} mol dm^{-3}) and lasted for 260 minutes (Figure 5.21), compared to 150 minutes for OPANA (Figure 5.5). At 200 and 220 °C, this trend continues for NANA1 lasting 42 minutes at 200 °C and 7.5 minutes at 220 °C, compared to 17 and 3.5 minutes for OPANA.

Runs using the NANA2 version suggest that the position of the amine group on the naphthalene ring is also important as this antioxidant only lasted for 120 minutes which is worse than both NANA1 and OPANA. Availability of the para position on the aromatic ring seems important to antioxidant activity. One intermediate product was identified for NANA1. No intermediate species were identified for NANA2.

5.8.2 Identification of intermediate species for NANA1.

When using NANA1, samples taken during the reaction show a colour change from very slight pink colour to orange, to a bright red, before turning yellow a few minutes after the antioxidant is consumed.

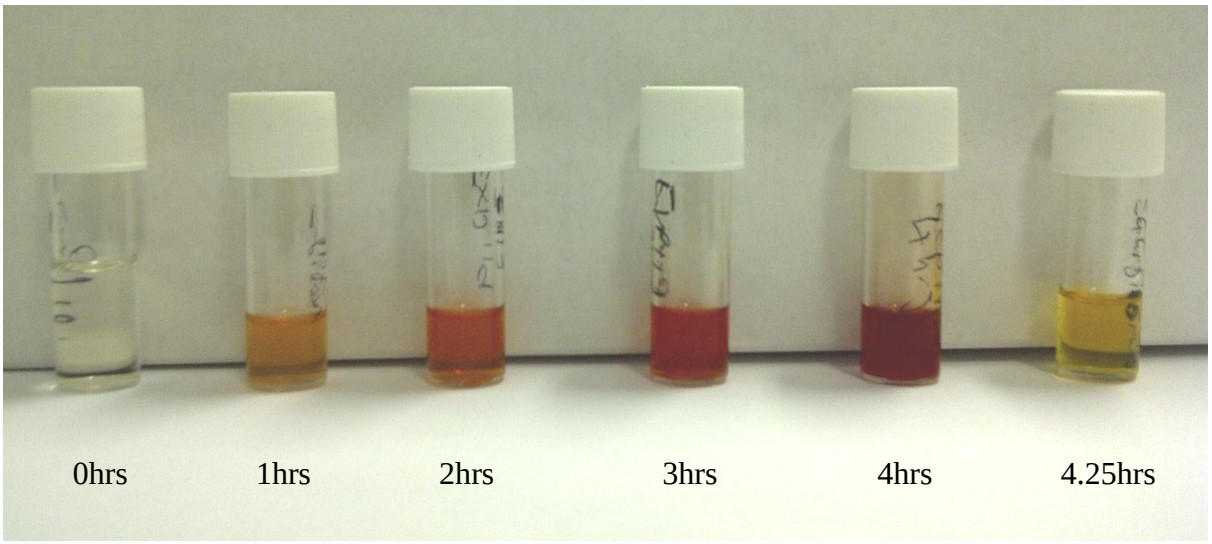

Figure 5.23 – Colour changes during a N-(1-naphthyl)naphthalene-1-amine run

GC-MS analysis of these samples showed a new product peak (termed NANA1OH) which was only observed in the 3 and 4 hour samples and may be responsible for the red colour seen in the sample as the peak up to 4 hours.

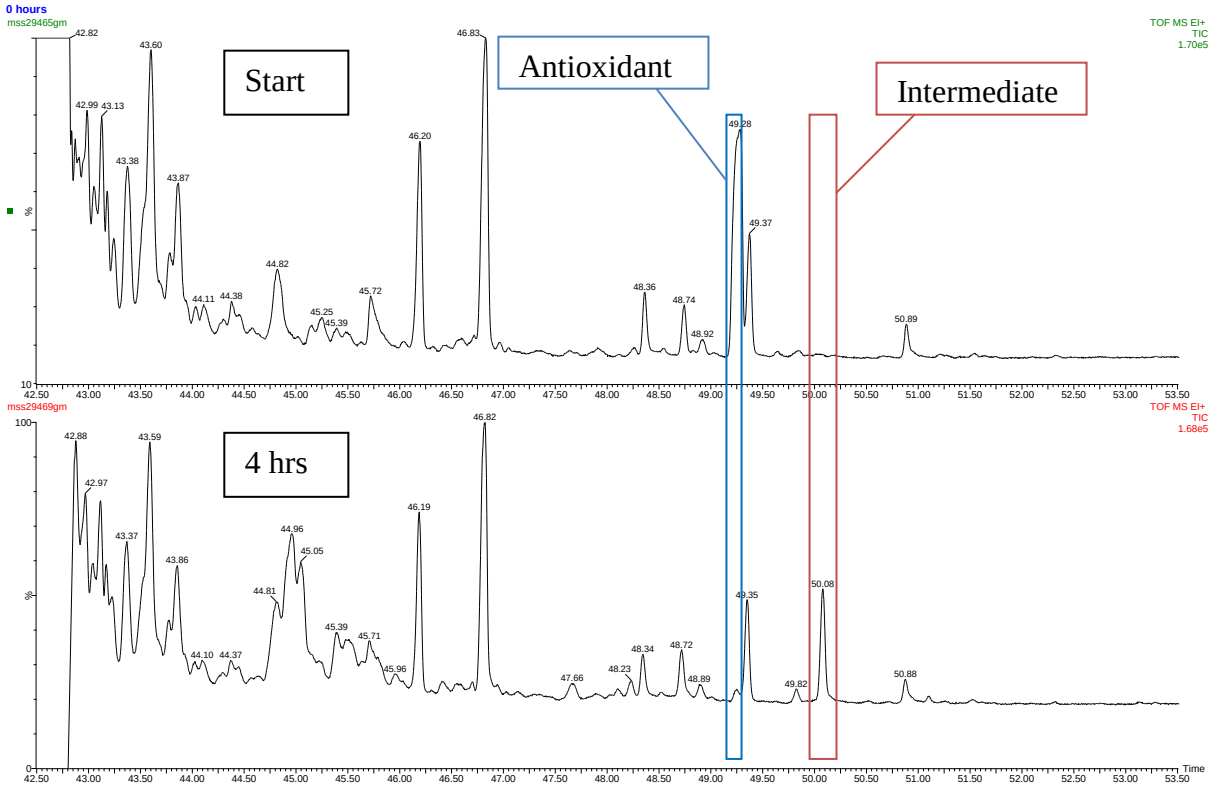

Figure 5.24 – NANA1 sample at the start of the reaction and after 4 hours

The mass spectra of naphthalene shows peaks of large intensity at -1 to the mass ion. Because the starting antioxidant contains two naphthalene rings, the mass spectra has significant fragments at -2, as well as -1 to the mass ion peak. The +1 peak is also of a higher intensity than would be expected from a structure with just one naphthalene ring system such as OPANA. The antioxidant has a molecular ion peak of 269.

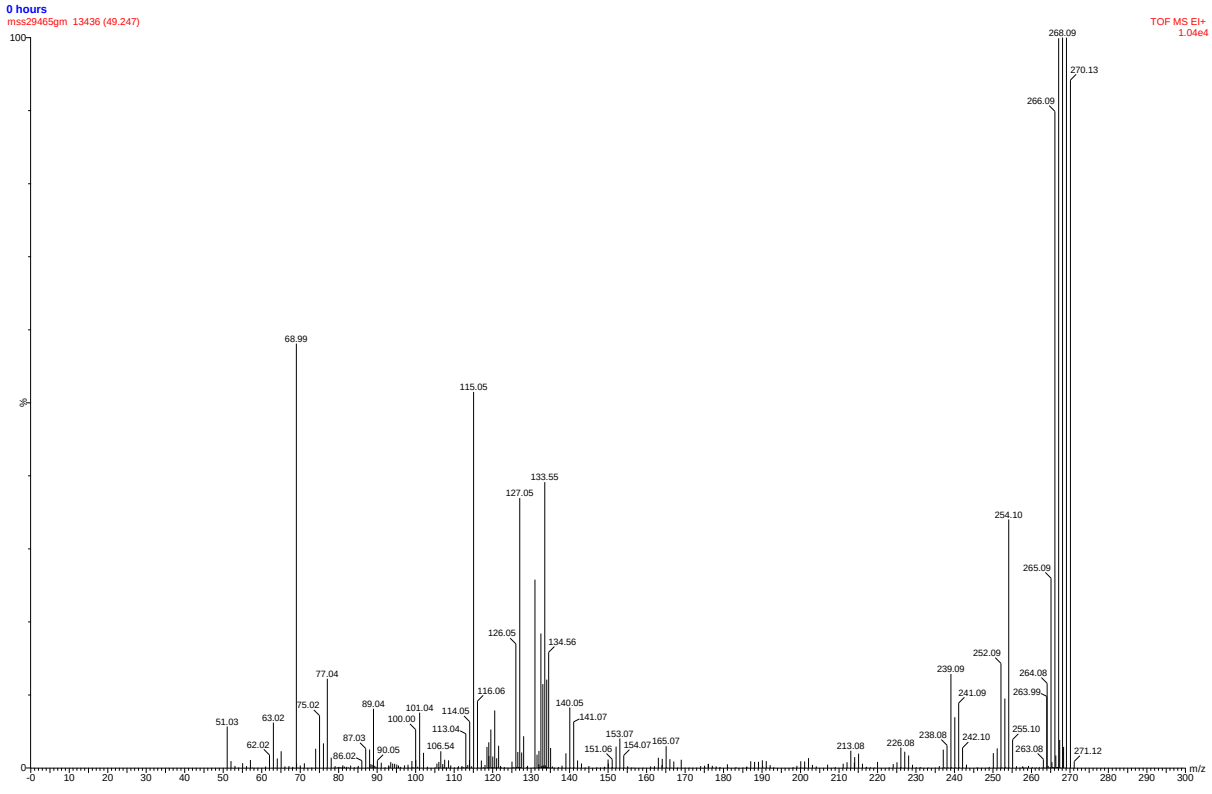

Figure 5.25 – Mass spectra of starting antioxidant

The mass spectrum of this new peak had a molecular ion of 285, which is +16 to the starting antioxidant, indicating the addition of an oxygen atom. It showed the characteristic double naphthalene ring fragmentation pattern with a large -2 peak to the mass ion but has a smaller mass ion peak than the starting antioxidant, which is characteristic of an alcohol containing species.[123] There is a second much smaller naphthalene fragmentation pattern around m/z 267. This is -18 to the mass ion peak and is likely to be due to loss of water from the intermediate, also suggesting there is an O-H group on the intermediate peak.[124,177] The peak at 254 is also present in the starting antioxidant but at a lower intensity. In the starting antioxidant, this is a loss of 15 which is observed in substituted cyclic structures.[177] In the product, this is a loss of 31 (CH_2=OH^+), resulting in a structure with the same formula as the fragment of 254 in the starting antioxidant. If the product was from the N-OH dinaphthylhydroxylamine this

peak should not be present and the product spectra would be expected to contain a -15 peak (as seen in the starting antioxidant). The peak at 218 could be accounted for by $[C_{16}H_{12}N]^{+}$ [178] which also suggests the O-H group is on the aromatic ring and not formed on the nitrogen via a nitroxyl radical.

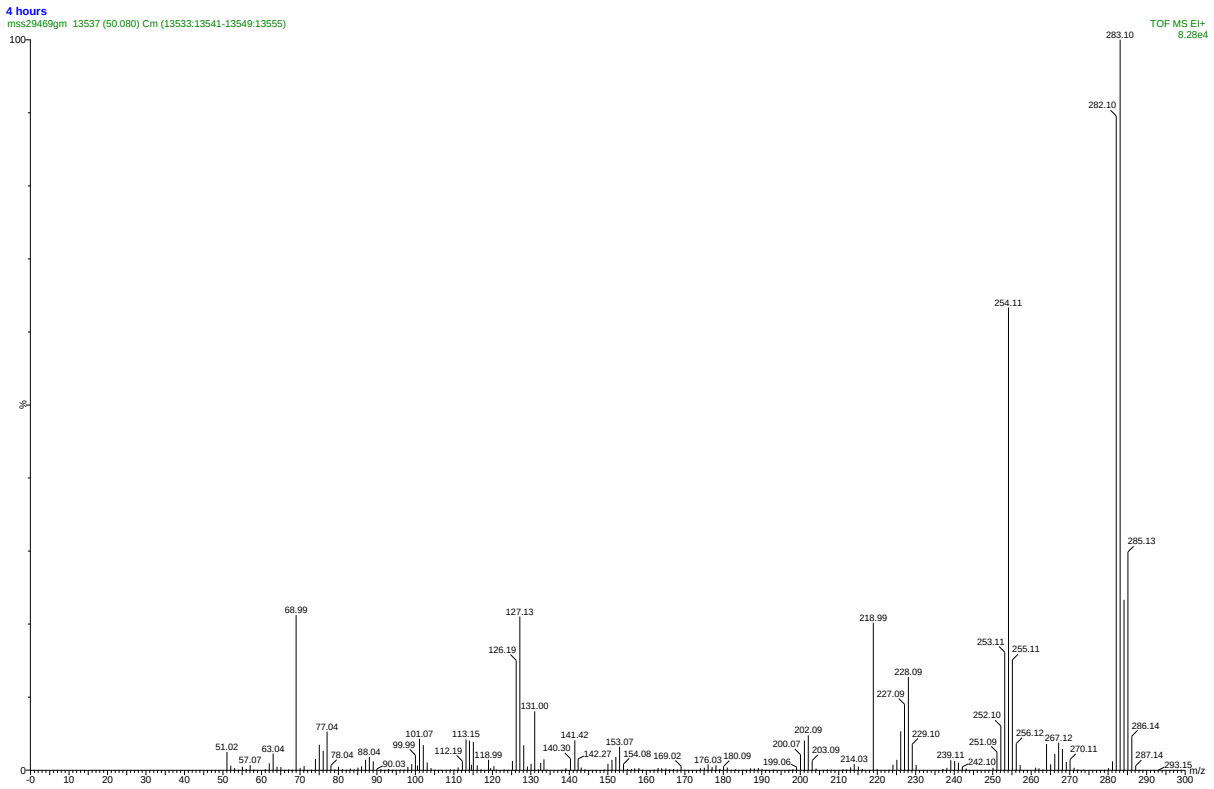

Figure 5.26 – Mass spectra of new intermediate peak at 50.08 minutes

A possible route for the formation of the intermediate could occur via abstraction of the labile hydrogen of the N-H bond (Figure 5.27 step 1). The resonance structure or the resulting intermediate can react with oxygen or an alkyl peroxy radical, which will decompose to ultimately form an alcohol group. The alcohol group addition to the para position to the nitrogen atom of the naphthalene ring coincides with the findings of Mousavi[136] and Pospisil[172] who suggest that this carbon radical is sufficiently stable to react with other radicals such as alkyl peroxy radicals or it reacts with itself in the formation of dimers.

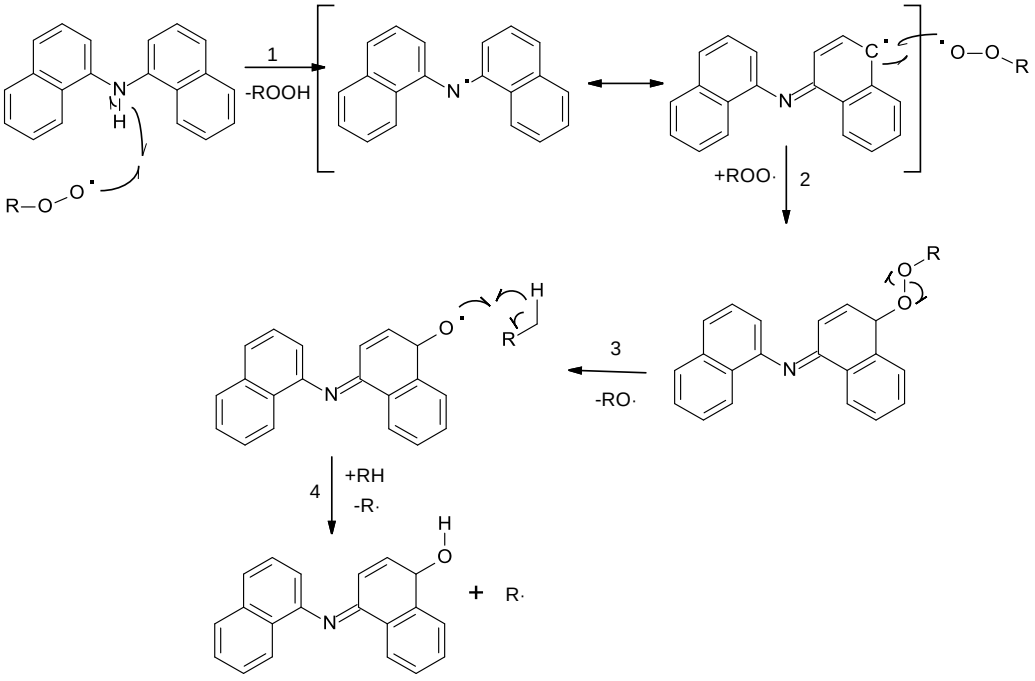

Figure 5.27 – Proposed mechanism for the formation of (4E)-4-(1-naphthylimino)-1H-naphthalen-1-ol (NANA1OH)

5.9 Induction period and N-H bond dissociation energy correlation

In this work, it has been demonstrated in Section 5.3, that by changing the substituents of diphenylamine type antioxidants, the induction period can be increased approximately three fold (ODPA Vs DPAOMe). This can be explained by the interaction between alkyl peroxy radicals and aminic antioxidant, as previously explained in Section 5.2 and Chapter 4.

The induction period of an aminic antioxidant can also be increased by substituting phenyl rings for naphthalene. This has a greater effect than changing the substituents, as although moving from ODPA to OPANA only reduces the N-H bond dissociation energy by 8.3 kJ mol^{-1} (compared to 14.9 kJ mol^{-1} between ODPA and DPAOMe), the induction period is increased by 9 fold. The substitution of the second phenyl ring for a naphthalene ring has the same effect again, reducing the N-H bond dissociation energy by a further 10.1 kJ mol^{-1} and increasing the induction period 15 fold compared to ODPA.

However, if naphthalene rings are added in the 2 position, the N-H bond dissociation energy slightly increases by 1.6 kJ mol^{-1} compared to ODPA but the induction period still increases 6 fold.

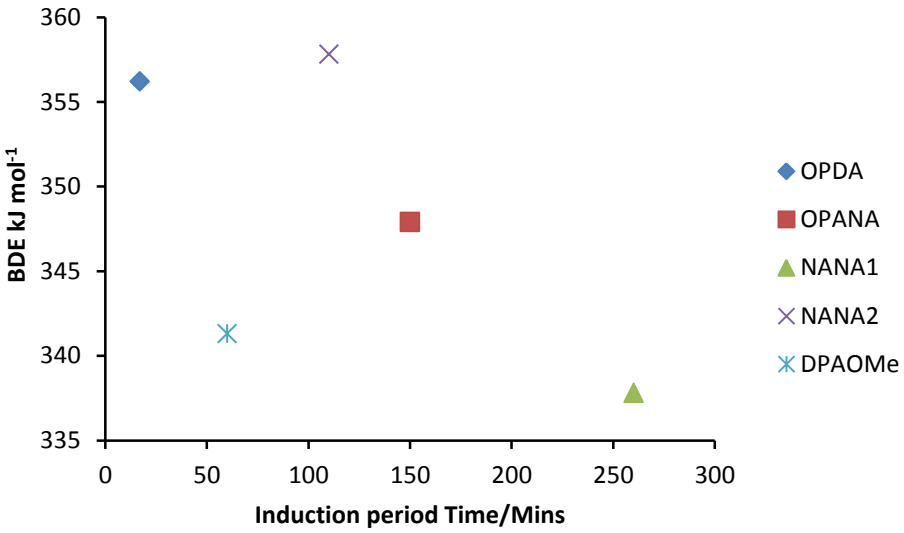

Figure 5.28 – Correlation plot between N-H bond dissociation energy and induction period of aminic antioxidants tested

As the N-H bond dissociation energy for NANA2 is higher than that of ODPA, the reaction between NANA2 and alkyl peroxy radicals will be less exothermic than the reaction between ODPA and alkyl peroxy radicals. Therefore, the reverse reaction will become favourable at even lower temperatures than observed with ODPA. Despite this, NANA2 has the ability to prevent oxidation for a considerable period of time. This could again be explained by the ability of the naphthalene ring containing aminic antioxidants to work via a different mechanism, as proposed in PAN by Hunter et al[135] and Mousavi et al,[136] as outlined in Figure 5.20. The findings of previous works were specific to OPANA (which has a 1-naphthalene ring system) but it is possible that this mechanism is applicable to both the 1-naphthalene structures and the 2-naphthalene structures. If this is the case, NANA2 will have the same problems as ODPA due to the high N-H bond dissociation energy but will last longer than ODPA because of the slower build up of alkyl hydroperoxide.

Although peroxide decomposition by the antioxidant was not apparent for ODPA in this work, according to Capp and Hawkins[140] the rate of peroxide decomposition by amines occurs in the order tertiary > secondary > primary. This can be linked to the N-H bond dissociation energy as tertiary amines in this work contained substituents with a +I effect on the nitrogen, reducing the N-H bond dissociation energy.

As alkyl groups get bigger or have an increased resonance stability, the lone pair of electrons on the nitrogen will become more available, making the nitrogen a stronger nucleophile and more likely to interact with peroxides.[179] Because of this, secondary antioxidants with naphthalene rings could be better peroxide decomposers than those

with phenyl rings. Although this hypothesis explains the behaviour seen in this work, there is no direct comparison of the peroxide decomposing properties of naphthalene vs. phenyl substituted amines.

5.10 Heteroaromatic aminic antioxidants

To further assess the performance of aromatic amines as secondary antioxidants as well as primary, two antioxidants which each contained two heteroatoms were compared. These were phenothiazine and phenoxazine.

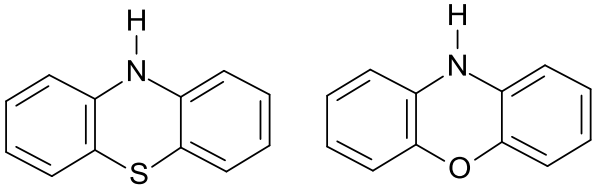

Figure 5.29 – Structures of phenothiazine (left) and phenoxazine (right)

The bond dissociation energies for the N-H bonds of these molecules are known to be 332 kJ mol^{-1} for phenothiazine and 323 kJ mol^{-1} for phenoxazine.[65,101,148,180]. This is considerably lower than any other aminic antioxidant previously tested in this work and is even lower than the O-H bond dissociation energy of OHPP and other phenolic antioxidants such a Vitamin E[101,181] and so are unlikely to be affected in the same way

as ODPA which has an N-H bond strength comparable to that of the O-H bond strength of tertiary alkyl hydroperoxides. When using sulfur as a heteroatom these compounds (with the general formula R_2S), are known to have the ability to decompose peroxides to non-radical species.[19,20, 35,182,183,184]

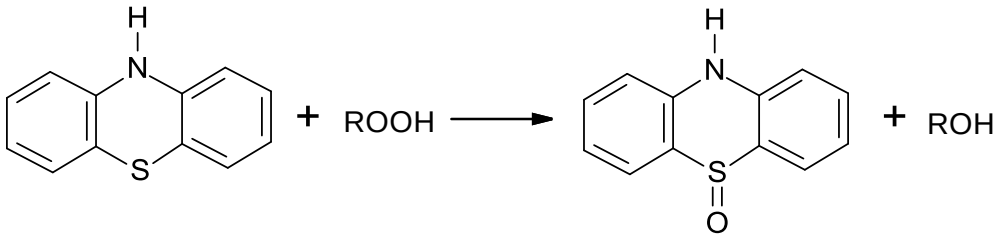

Figure 5.30 – Reaction of phenothiazine with alkyl hydroperoxide

In addition to this mechanism, organosulphur compounds can act as a peroxide decomposer via an electron transfer from the sulfur[167,184,185,186] This ultimately forms non-radical products upon decomposition of the peroxide bond.

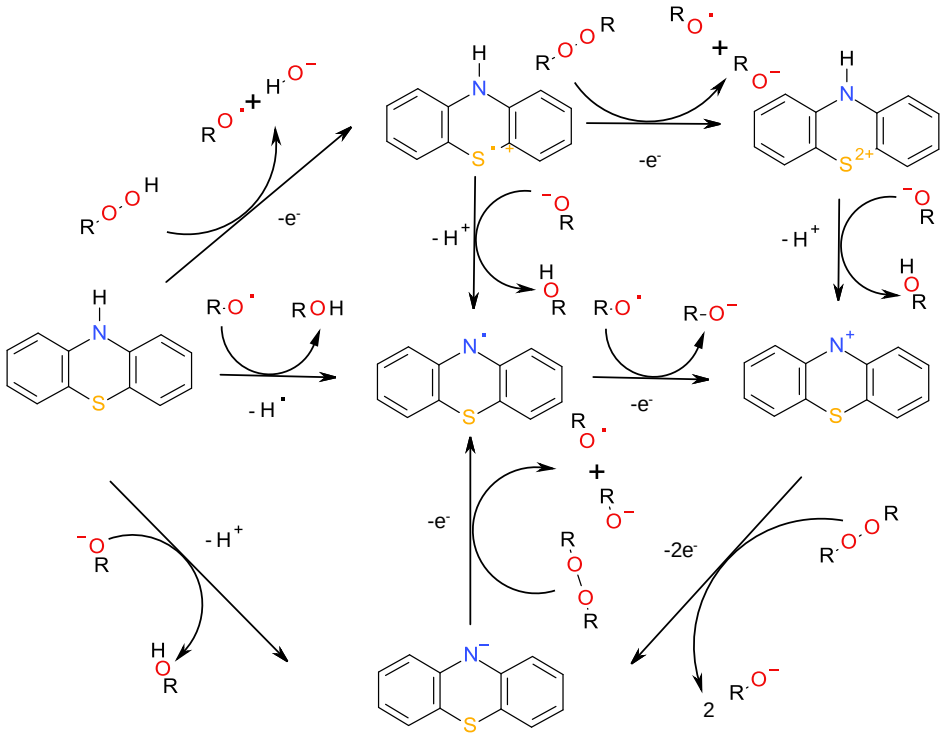

Figure 5.31 – Mechanism of peroxide decomposition by phenothiazine [35,184,186 187,188]

5.10.1 High temperature oxidation of phenothiazine and phenoxazine

Using the same concentration of 7.55 x10 $^{-3}$ mol dm^{-3} in squalane, these antioxidants were tested at 180, 200 and 220 °C. Again like other antioxidants which were not alkyl substituted, the solubility of these antioxidants was relatively poor[189] and so a temperature of 90 °C under nitrogen was required to dissolve the antioxidants in squalane.

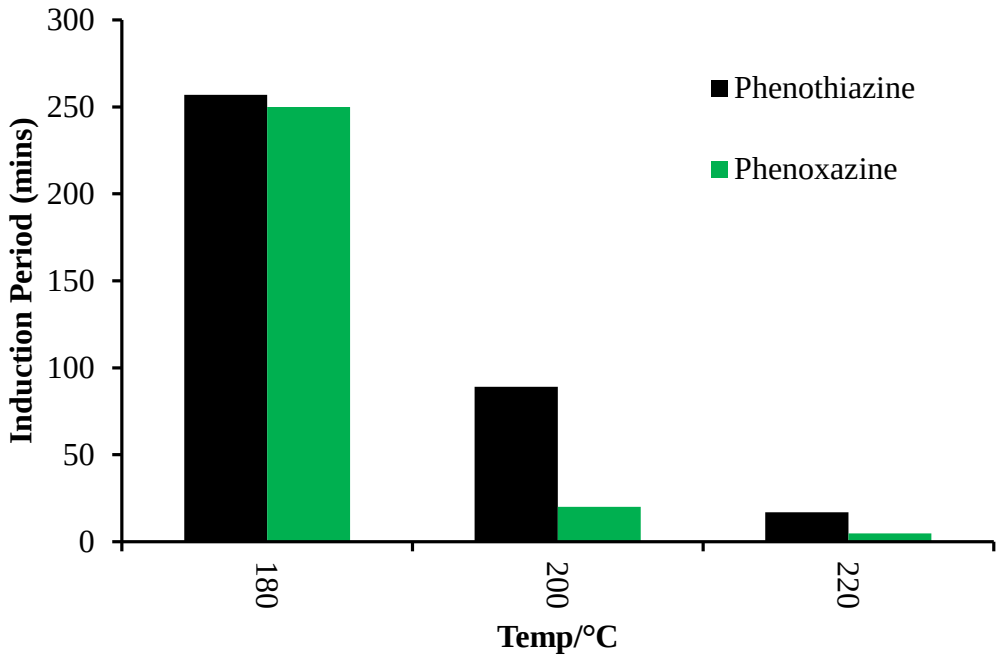

Figure 5.32 – Induction periods of phenothiazine and phenoxazine between 180 and 220 °C

Despite having a lower N-H bond dissociation energy, phenoxazine has a shorter induction period than phenothiazine due to the electon transfer mechanisms. The difference between the two is negligible at 180 °C, with both antioxidants lasting approximately 250 minutes. Above this temperature, phenoxazine lasted 20 minutes at 200 °C and just 5 minutes at 220 °C. In comparison, phenothiazine lasted 89 minutes at 200 °C and 17 minutes at 220 °C. The induction periods for phenothiazine are close to that seen for NANA1 and far in excess of other phenyl aminic antioxidants. The large difference between phenothiazine and phenoxazine at 200 and 220 °C is explained by the rate of oxidation and therefore, the rate of peroxide formation at these very high temperatures.[127] Previous work has indicated that only phenothiazine could efficiently decompose peroxides at the high rates of formation observed at high temperatures.

The 250 minute induction period observed for phenothiazine at 180 °C is 15 times longer than the 17 minute induction period seen with ODPA. As stated earlier, previous work by Becker et al[139] states the difference between ODPA and phenothiazine of just 15 %. Possible reasons for this substantial difference are the lower temperature of 130 °C used by Becker and also the base oil used was a vegetable oil instead of squalane, as used in this work. This base oil will contain no tertiary hydrogen groups. Both of these factors support the findings of Chapter 4 that at high temperatures, ODPA will be a much poorer antioxidant than anticipated in base fluids such as squalane due to the reverse of the equilibrium reaction between ODPA and alkyl peroxy radicals becoming, dominant resulting in the inactivity of ODPA.

This ability of sulfur bridged antioxidants to increase the induction period compared to the non-sulfur bridged counterparts at high temperatures is in agreement with previous findings at 60 °C using azobisisobutyronitrile (AIBN) as an initiator.[190] The increase to induction period achieved by introducing a sulfur bridge to aminics makes phenothiazine structures a possibility when designing new antioxidants. To overcome the insolubility issues of phenothiazine in non-polar media, any new antioxidants will also have to contain alkyl groups such as tert-butyl or tert-octyl.[191] The presence of a sulfur atom in an antioxidant will contribute very little to sulfur emissions of a vehicle, as it has been found that around 99 % of the sulfur found in emissions from diesel engine exhausts originates from the fuel.[85] Although levels of elements such as sulfur and phosphorus are legislatively controlled, these elements are still present in automotive lubricants, despite their propensity to poison exhaust catalytic converters.[192]

5.11 New antioxidant synthesis and induction period

Using the results from the antioxidants previously tested, a synthesis was carried out using the commercially available OPANA to see if the induction period of this antioxidant could be increased by the incorporation of a sulfur atom bridge into the structure (Figure 5.33). Although NANA1 was the aminic antioxidant with the highest induction period, it was not viable to react this with sulfur due to the high cost of the starting antioxidant.

5.11.1 Synthesis of the new antioxidant (SOPANA)

The synthesis was based on the method of phenothiazine synthesis from diphenylamine [193,194,195] and also the reaction with PAN used in the synthesis of dyes.[196,197] The synthesis was a one pot reation consisting of 16.5 g of OPANA, 3.2 g of sulfur (1:2 molar ratio OPANA:sulfur) and 0.15 g of iodine catalyst. It was done as a molten blend and no solvents were used at a temperature of 200 °C for 1 hour. Purification of the crude product mixture was achieved by dissolving the antioxidant in ethanol and filtering off the excess sulfur and then by column chromatography, as detailed in Chapter 2 to remove any unreacted material.

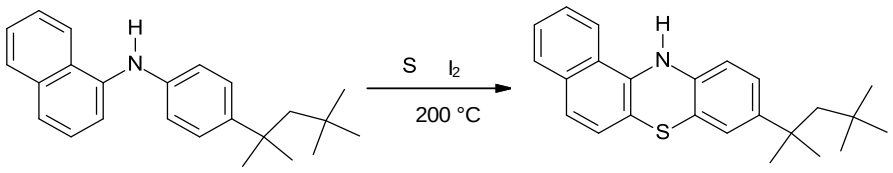

Figure 5.33 – Synthesis of the novel aminic antioxidant

The crude product material prior to column chromatography contained a mixture of three species when analysed by GC. After column chromatography (as outlined in Chapter 2), the material contained 2 species when analysed by GC and GC-MS. The ratio of these products was calculated as 90:10.

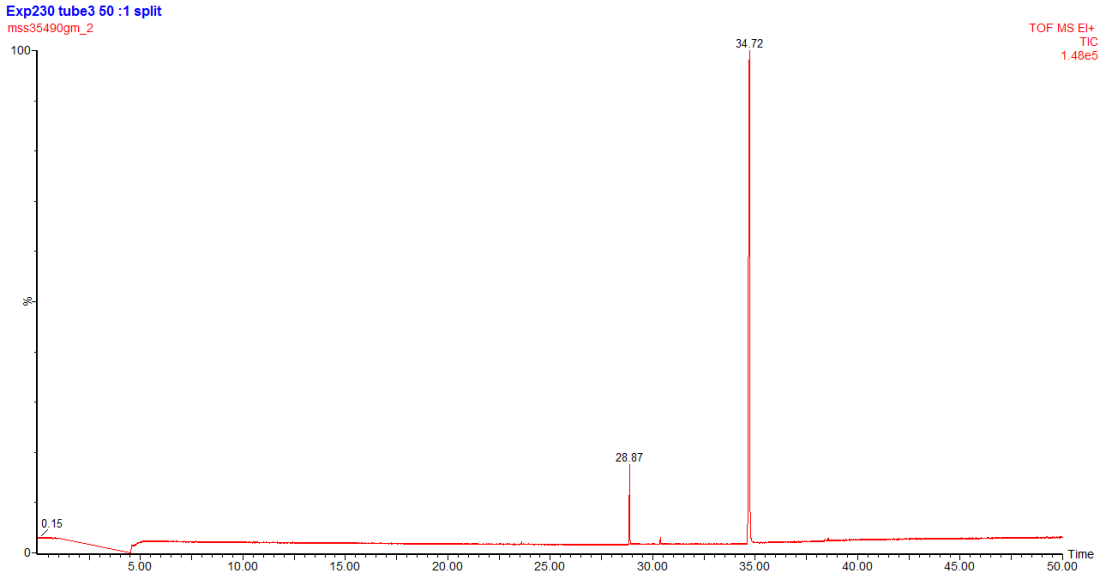

Figure 5.34 – GC-MS of SOPANA synthesis material post column purification

These products were identified as (1,1,3,3-tetramethylbutyl)-12H-benzo-α-phenothiazine (SOPANA) (90%) and benzophenothiazine (10%), which is the non-octylated version of SOPANA by GC-MS. As the benzophenothiazine did not contain an alkyl chain, it did not have the fragmentation pattern associated with branched alkyl substituted aromatic rings.[122] Benzophenothiazine also had a loss of 32 which can be

attributed to loss of sulfur. The SOPANA was +30 to the starting antioxidant (loss of two hydrogens replaced by a sulfur bridge).

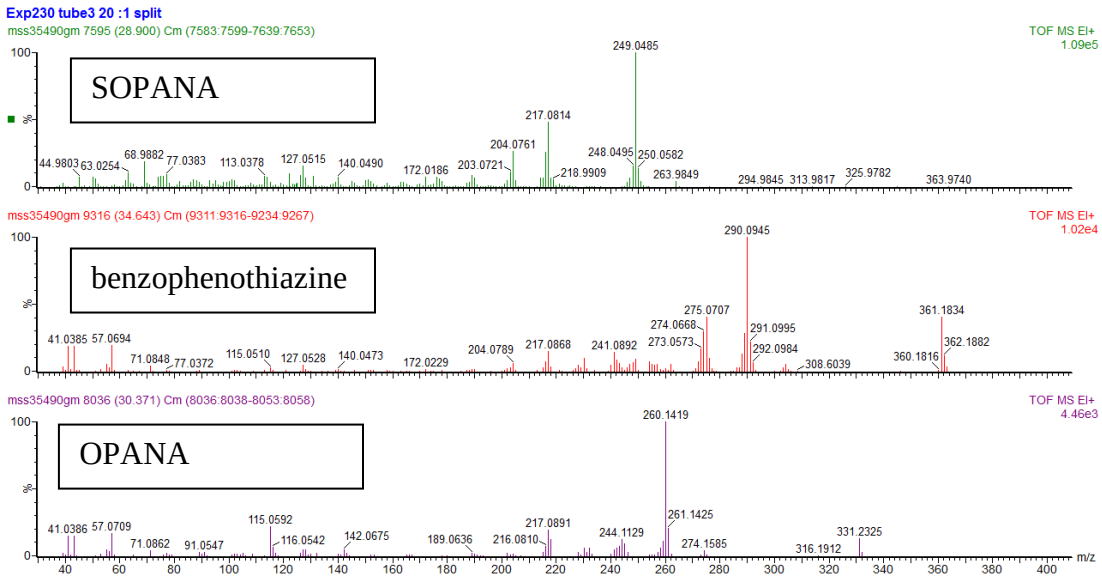

Figure 5.35 – Mass spectra of SOPANA and benzophenothiazine

When compared to the formula mass, the measured accurate mass of the SOPANA and benzophenothiazine had a negligible ppm difference in comparison with the typical accuracy of the mass spectrometer (20ppm) comparable to that of the OPANA starting material.

Table 5.4 – Accurate mass spectroscopy of OPANA, SOPANA and benzophenothiazone

Name	Formula	Formula Mass	Measured Mass	ppm difference
OPANA	$C_{24}H_{39}N^+$	331.2299	331.2325	7.9
SOPANA	$C_{24}H_{39}NS^+$	361.1864	361.1834	-8.3
Benzophenothiazine	$C_{16}H_{11}NS^+$	249.0486	249.0460	-10.4

The mechanism by which the benzophenothiazine product is formed is unknown. The overview of the SOPANA synthesis is summerised in Figure 5.36

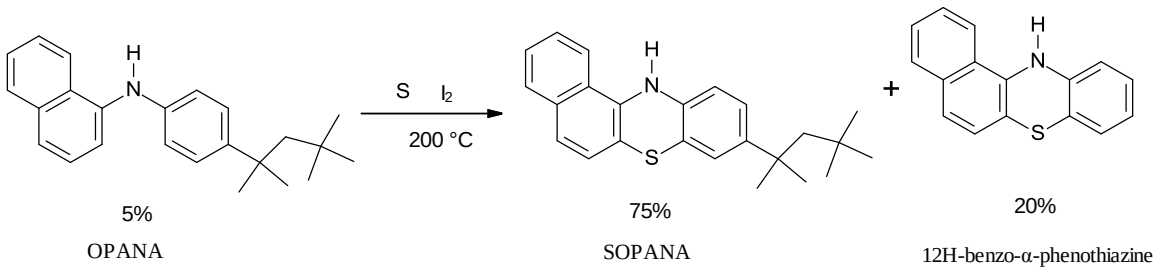

Figure 5.36 – Ratios of material obtained from the reaction of OPANA with sulfur

5.11.2 High temperature oxidation of SOPANA

Using the purified material, oxidation reactions of the synthesised SOPANA material in squalane were carried out using the same concentration as all other previous antioxidants tested.

The induction period for SOPANA was measured at 180, 200 and 220 °C. Results suggest that the addition of the sulfur atom increased the induction period when compared to OPANA. At 180 °C, the induction period increased from 150 to 210 minutes. Although this is an increase on OPANA, the performance was not as good as for phenothiazine (250 minutes), which was unexpected. The reason for this is surprising as both the phenothiazine and SOPANA samples contained the same number of moles of antioxidant and therefore the same amount of N-H and sulfur groups. At 200 ºC, the induction period was also longer than OPANA, lasting 38 minutes compared to 15 minutes respectively. At 220 °C, no increase in induction period was observed with SOPANA lasting 7 minutes, which is the same as OPANA.

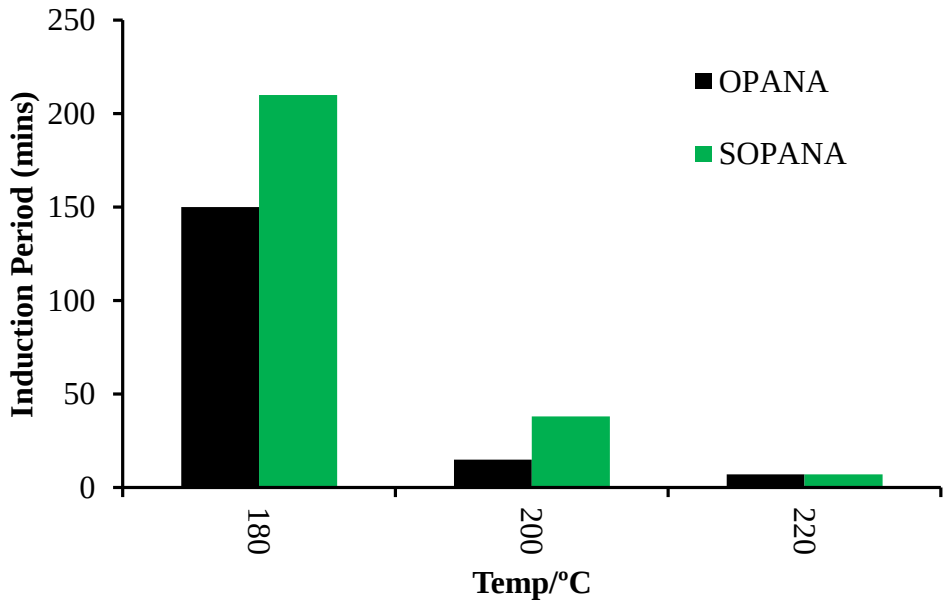

Figure 5.37 – Induction periods of SOPANA compared to OPANA at 180, 200 and 220 °C

The induction period of a similar product was previously measured by Murphy *et al*[167] but this antioxidant had the naphthalene ring in the 2 position and not the 1 position (in relation to the N-H group), which has been shown in this work to make a huge difference to the induction period. It also did not contain an alkyl chain. In addition, the work by Murphy also was not harsh enough to discriminate between antioxidants such as PAN and ODPA with phenothiazine, as all these antioxidants protected the base fluid until the end of the test which was of set duration.

5.12 Conclusions

It has been show in this work that there is a significant difference between aminic antioxidants, depending upon their structure (and influence this has on the N-H bond dissociation energy) and also the presence of peroxide decomposing elements such as sulfur.

After testing several aminic antioxidants, there are several patterns which have emerged from this work done which help to explain how aminic antioxidants behave as antioxidants in a hydrocarbon base fluid at elevated temperatures. The first is that for diphenylamine type aminic antioxidants, N-H bond dissociation energy is critical to the behaviour of the antioxidant. By sufficiently lowering this bond dissociation energy, the induction period of the antioxidant can be increased significantly, as shown in Figure 5.5.

The second structural performance relationship is the presence of naphthalene rings in the antioxidant.

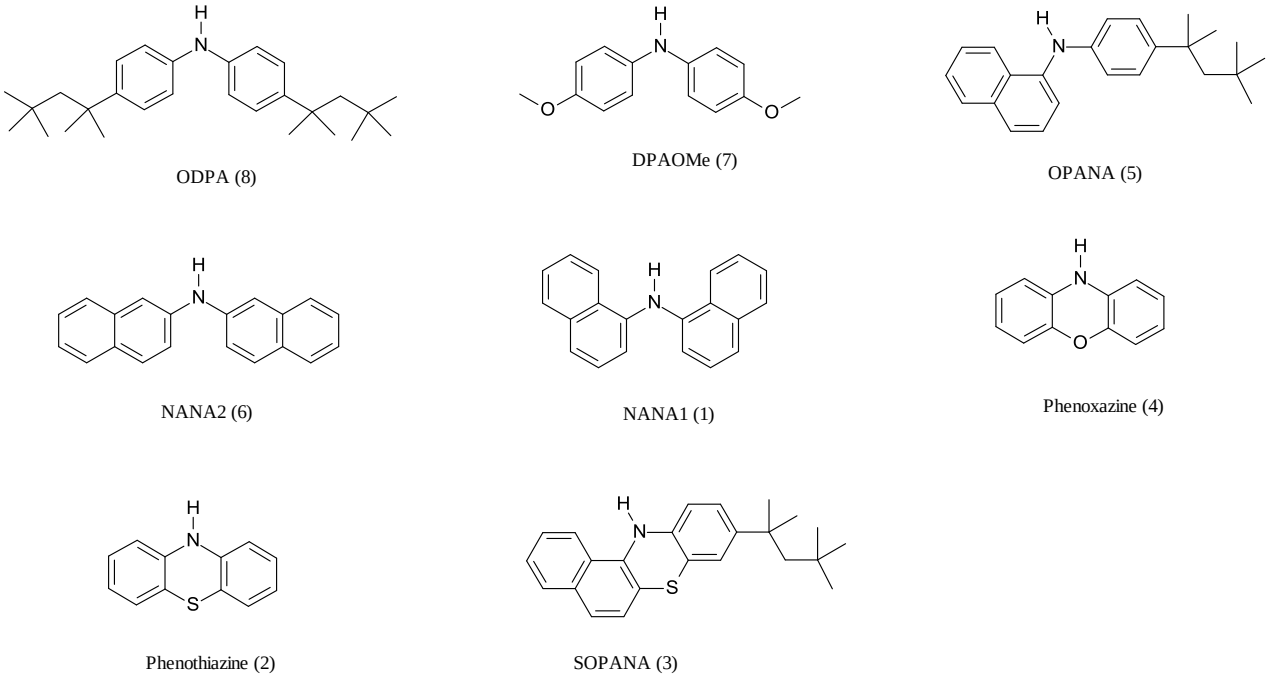

Figure 5.38 – Recap of the aminic antioxidants used in this work and their abbreviations and induction period ranking in brackets when used in squalane at 180 ºC

In Chapter 4, it was concluded that ODPA was a poor antioxidant at elevated temperatures (ie >180 ºC) because of the similarity of the N-H bond dissociation energy to the O-H bond dissociation energy in tertiary alkyl hydrogen peroxides, resulting in the backwards reaction between ODPA and alkyl peroxy radicals becoming significant. It has been shown in this chapter that by reducing the N-H bond dissociation via changing the substituent groups of ODPA from tert-octyl groups (361 kJ mol^{-1}) to

methoxy groups (348 kJ mol^{-1}), the induction period can be greatly increased (Figure 5.5). It also results in the antioxidant being consumed before the end of the induction period occurs, as the backwards reaction between DPAOMe and alkyl peroxy radicals does not become prominent even at high temperatures. For DPAOMe, the induction period ends and the base fluid autoxidation starts only when there is no significant amounts of DPAOMe remaining, consistent with the reaction between the aminyl radical and hydroperoxide for this antioxidant not being significant.

By adding triphenylphosphine (TPP) to DPAOMe, the induction period was increased significantly to almost 8 hours, compared to 1.5 hours for the sum of the induction periods. Despite DPAOMe lasting for much longer than ODPA in a single additive system, the two antioxidants performed equally well (around 8 hours) when combined with a peroxide decomposer. By removing peroxides from the system using TPP, ODPA goes from a poor performing antioxidant to one which is comparable with other diphenylamine type antioxidants, such as DPAOMe, providing further evidence that it is the alkyl hydrogen peroxide presence that hinders the effectiveness of ODPA as an antioxidant.

Bond dissociation energy is not the only factor in assessing what makes a good aminic antioxidant. OPANA, which has a higher N-H bond dissociation energy than DPAOMe, outperformed DPAOMe significantly. As both of these antioxidants have a N-H bond dissociation energy which is low enough not to be adversely effected by the presence of alkyl hydroperoxides, the increased induction period may be associated with the presence of the naphthalene ring and the proposed different mechanism by which this

can operate.[135,136] The substitution of the second phenyl ring for a naphthalene ring (NANA1) also significantly increased the induction period compared to OPANA (which only has one naphthalene ring system).

The orientation of the naphthalene rings was found to be highly significant to the duration of the induction period. NANA2, which is also made up of two naphthalene rings systems (in the two position), is a relatively poor antioxidant in comparison with NANA1 and only has an induction period greater than ODPA and DPAOMe. A phenyl, naphthalene combination where the naphthalene is in the 1 position is superior to NANA2. NANA2 also had an unexpectedly high N-H bond dissociation energy.

A new analytical method for detection of antioxidant dimers has been undertaken for this work which uses GC-MS instead of GPC analysis. The advantages of this method are that multiple peaks can be separated for dimers, showing the differences in the ways in which the radicals can combine. This method does require some further work as only one of the three peaks observed by GC could be obtained by GC-MS due to the high GC retention times of this material (Figure 5.11).

The addition of a heteroatom to a diphenylamine structure had a strong effect on the induction period. The addition of an oxygen atom to produce phenoxazine had little impact upon the induction period but the addition of sulfur to produce phenothiazine produced an antioxidant with the second longest induction period. The reason for the

high induction period of phenothiazine was the ability of the sulfur atom to change its oxidation state and decompose peroxides to non-radical species.

The synthesis of the sulfur bridged aminic antioxidant SOPANA was successful, yielding a high proportion of the desired product (75 %). The by-product which was an un-octylated SOPANA. The mechanism for the synthesis of this material is unknown.

Overall, it has been demonstrated that aminic antioxidants will prevent autoxidation until they have been consumed, with the exception of ODPA. The potential problems associated with this type of antioxidant is of particular significance because of the reduction of phosphorus containing species such as ZDDP, which could leave antioxidants such as ODPA with insufficient secondary antioxidant protection.

5.13 Future work

If a cheaper source of NANA1 could be found, a synthesis could be done reacting it with sulfur, as this could then be compared with SOPANA and NANA1 to see if a combination of two sets of naphthalene rings and a sulfur atom could further increase the induction period.

Using the same aminic antioxidants tested in this work, experimental work could be done to assess the peroxide decomposing properties of these antioxidants using methods similar to those of Capp and Hawkings.[140]

A limitation of the flow reactor and base oil used in this work is that this is only an approximate representation of an engine environment. As an engine oil contains many other additives besides antioxidants, it should be established if any other additive will interact negatively with any of the antioxidants tested in this work. The squalane used in this work is highly non-polar. There is also the possibility that some antioxidants may not be soluble in fluids such as a mineral base oil or synthetic base oils such as esters. The next step would be to test antioxidants for their longevity in a fired engine.[198] It is possible to use squalane in an engine[199] but to protect the engine, dispersant must also be used. This is still fairly similar to the formulation used in this work and would be a good starting point for future work.

A. Appendix to Chapter 3

Mass spectra of acid used in steglich esterification showing decarboxylation.

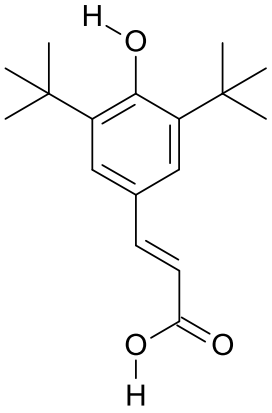

Figure A1 – Structure of (E)-3-(3,5-ditert-butyl-4-hydroxy-phenyl)prop-2-enoic acid (hydroxycinnamic acid)

The mass spectra of the acid used in the synthesis of hydroxycinnamate was used to help interpret mass spectra of intermediate products.

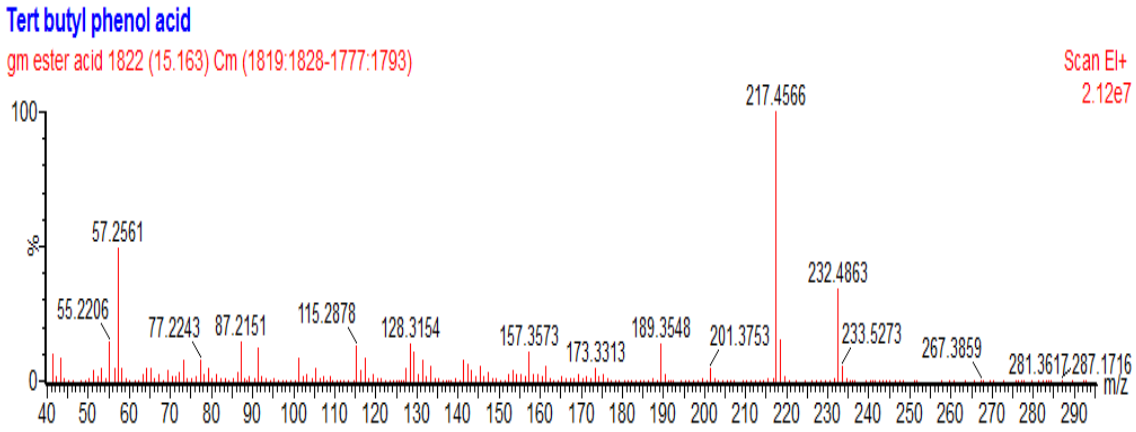

Figure A2 – Mass spectra of (E)-3-(3,5-ditert-butyl-4-hydroxy-phenyl)prop-2-enoic acid (hydroxycinnamic acid)

As observed with the hydroxycinnamate from synthesis and from autoxidation, the hydroxycinamic acid (which has a molecular weight of 276) did not have a mass ion peak at 276. This is due to the decarboxylation mechanism detailed in Chapter 3 resulting in loss of CO_2 and a m/z of 232.

Analysis of products from lead dioxide reaction

A sample of approximately 1ml containing phenolic antioxidant at a concentration of 1.5M dissolved in dichloromethane (DCM) was mixed with a few milligrams of lead dioxide and placed in the ESR cavity. The signal lasted for approximately 1 hour before starting to fade. The concentration of these radicals was found to be approximately 50 μm. The same was attempted using an aminic antioxidant instead of a phenolic one.

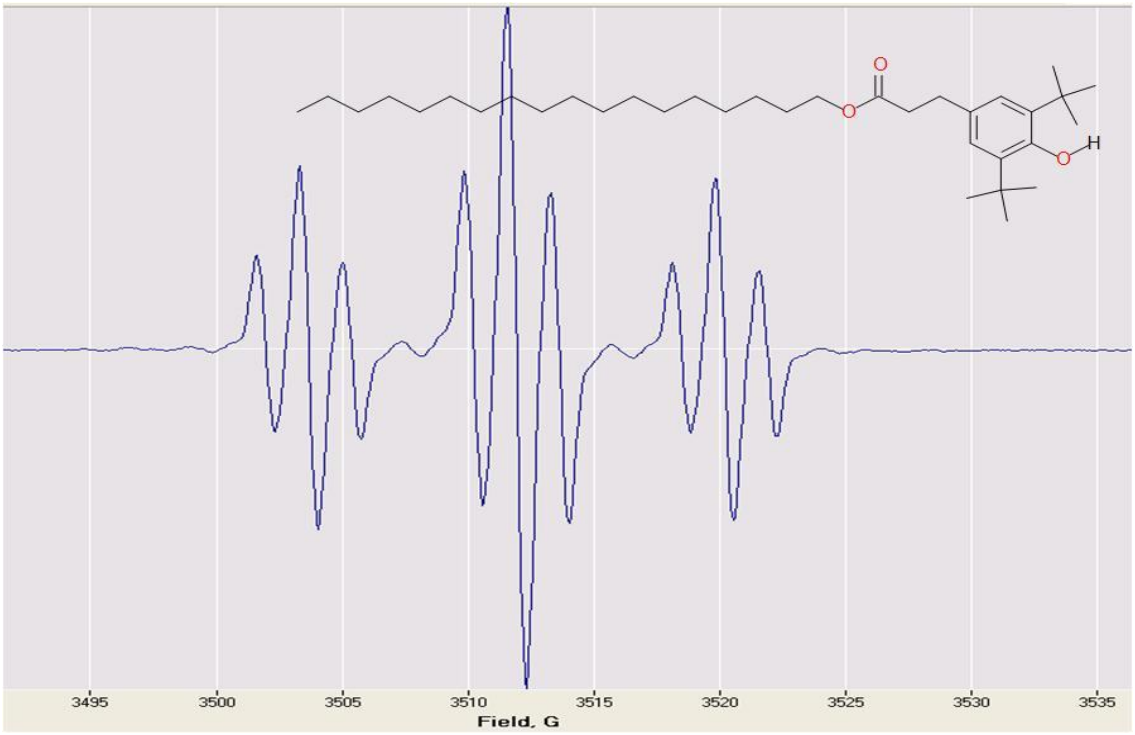

Figure A3 – ESR signal of octadecyl 3-(3,5-ditert-butyl-4-hydroxy-phenyl)propanoate (OHPP) in DCM reacted with lead dioxide

GC-MS of this produced several product peaks which

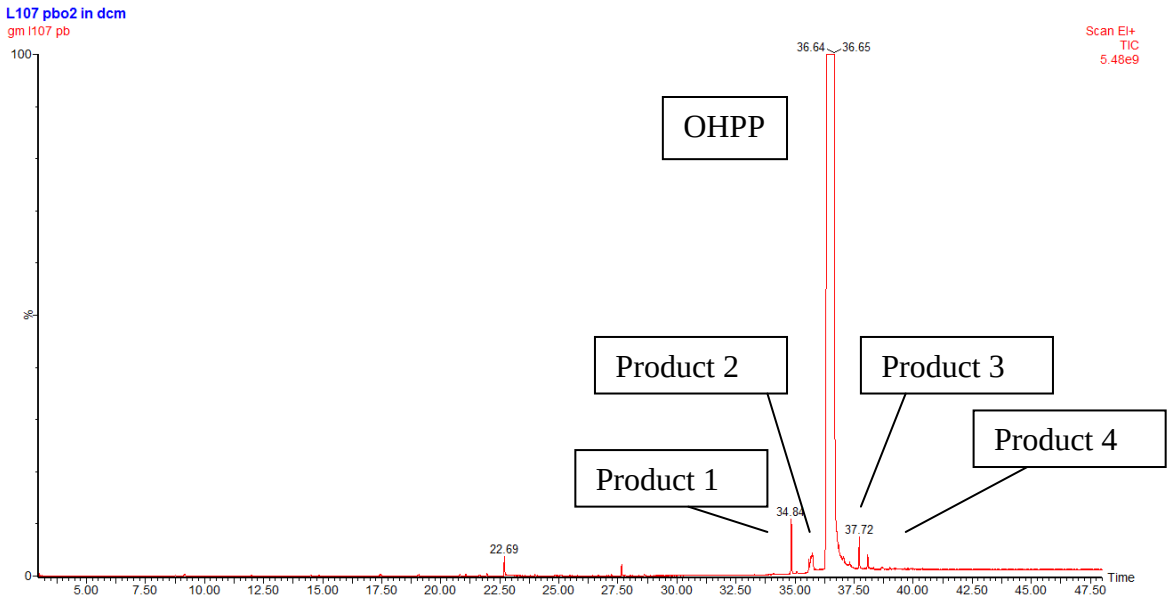

Figure A4 – GC trace of OHPP in DCM reacted with lead dioxide

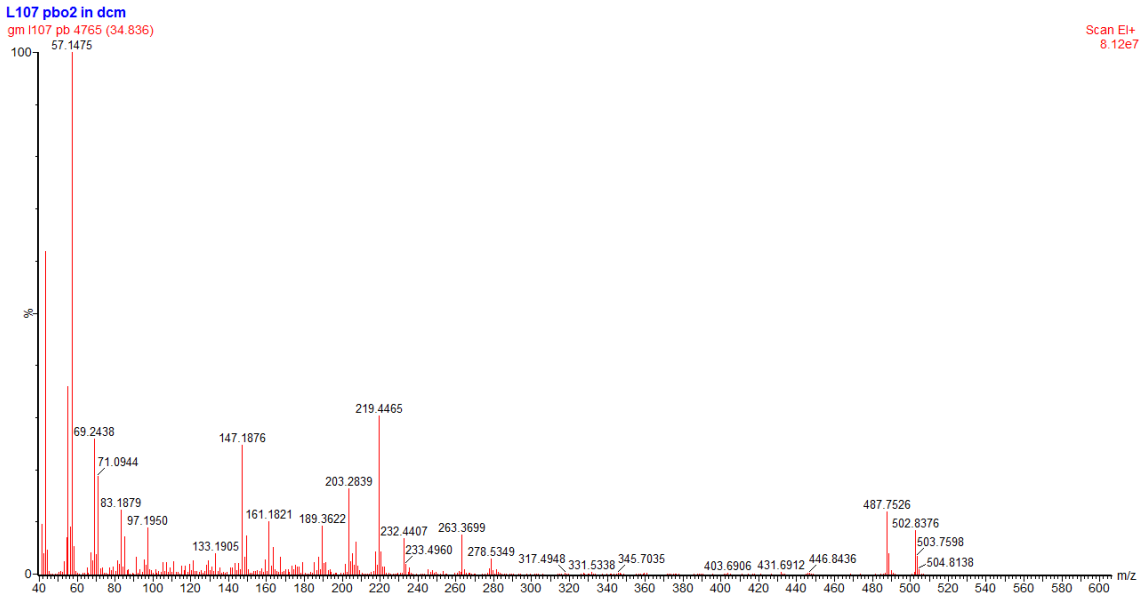

Figure A5 – Product 1

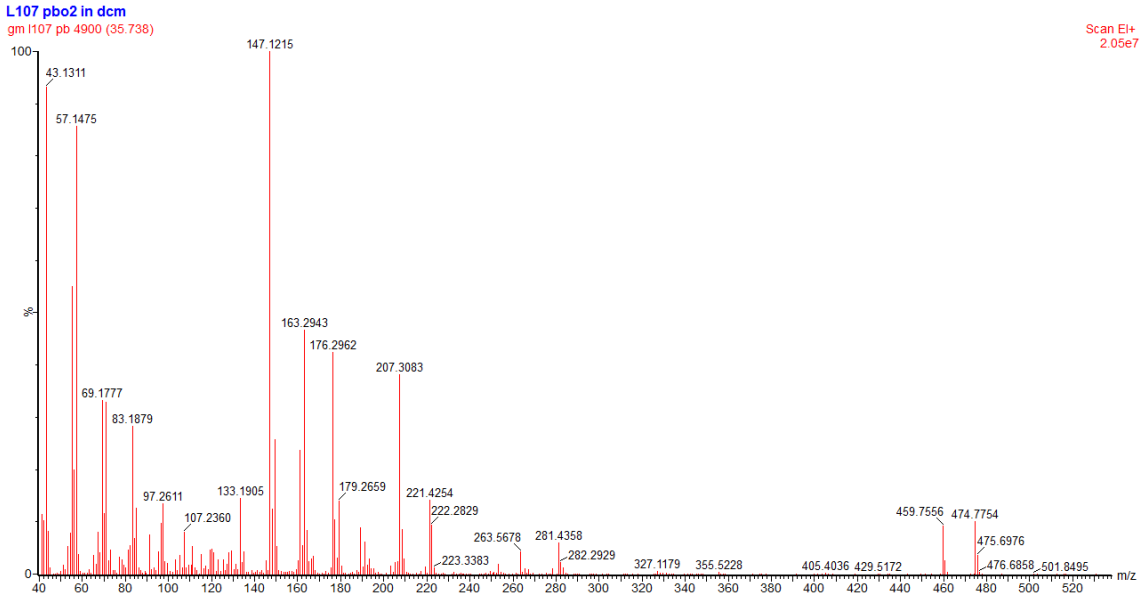

Figure A6 – Product 2

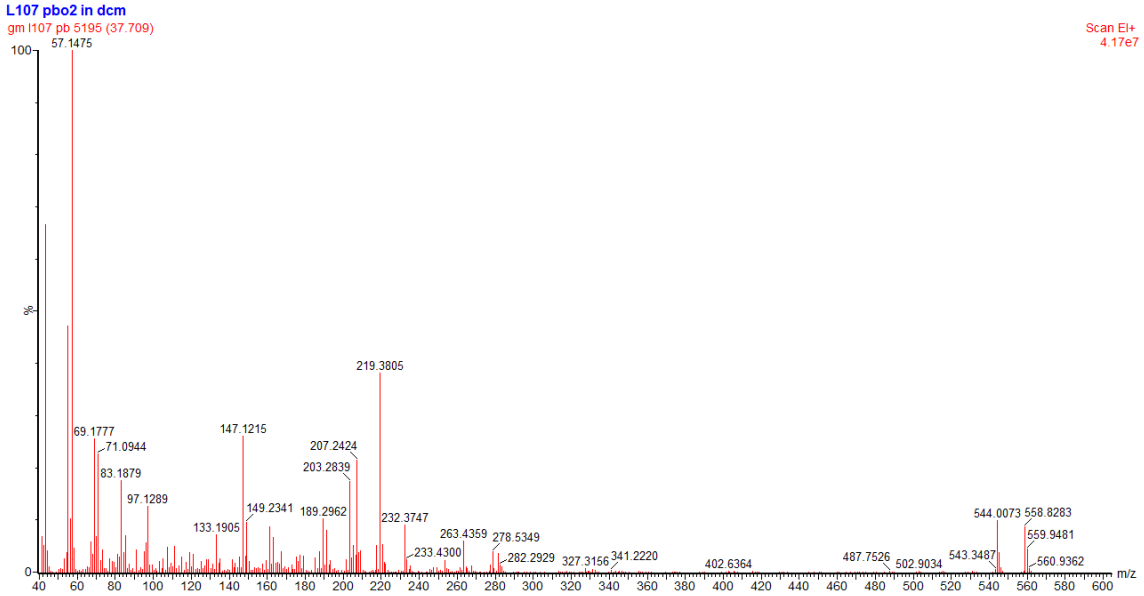

Figure A7 – Product 3

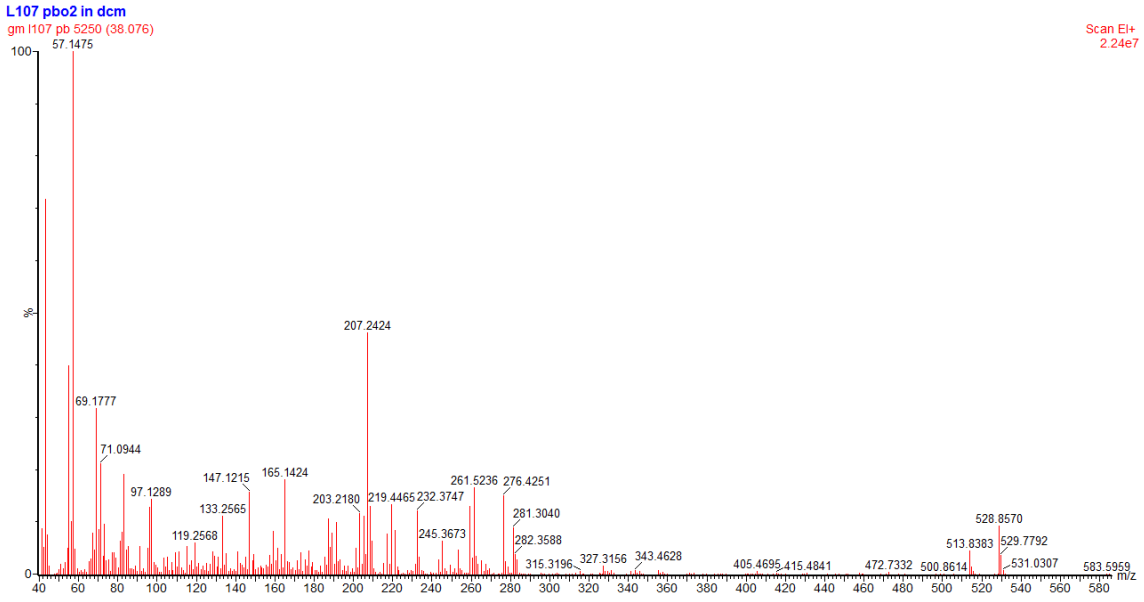

Figure A8 – Product 4

Products using lead dioxide were not representative of an automotive engine and were done to obtain sample ESR spectra for OHPP.

Ester reaction using enzyme calaylst

An attempt to synthesis hydroxycinnamate using the enzyme catalyst Novozyme L435 gave poor yields.[200]

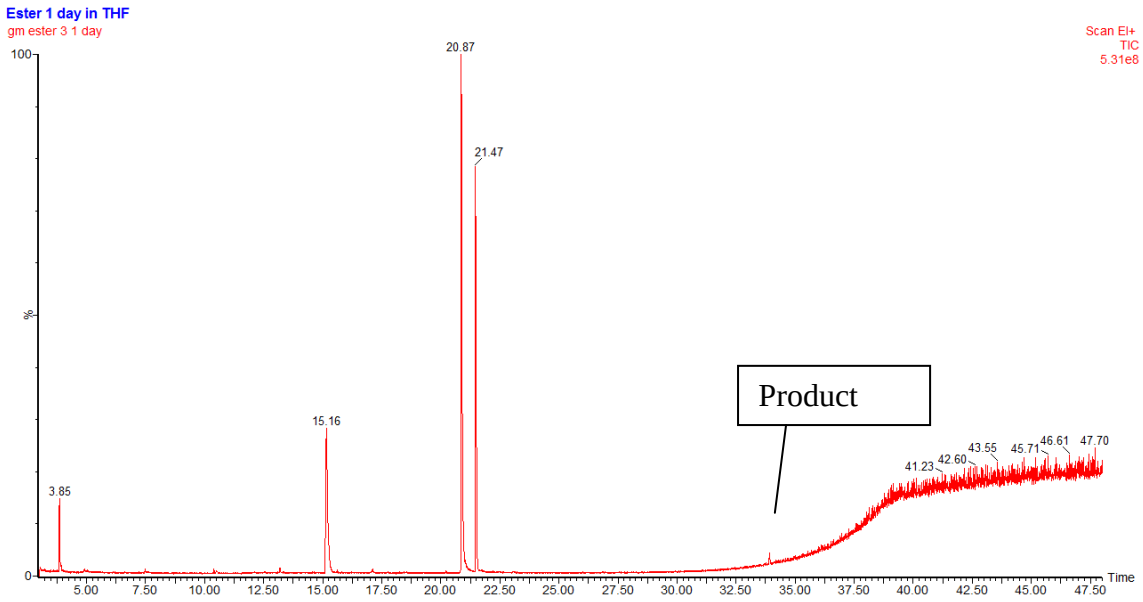

Figure A9 –hydroxycinnamate synthesis using Novozyme L435

B Appendix to Chapter 4

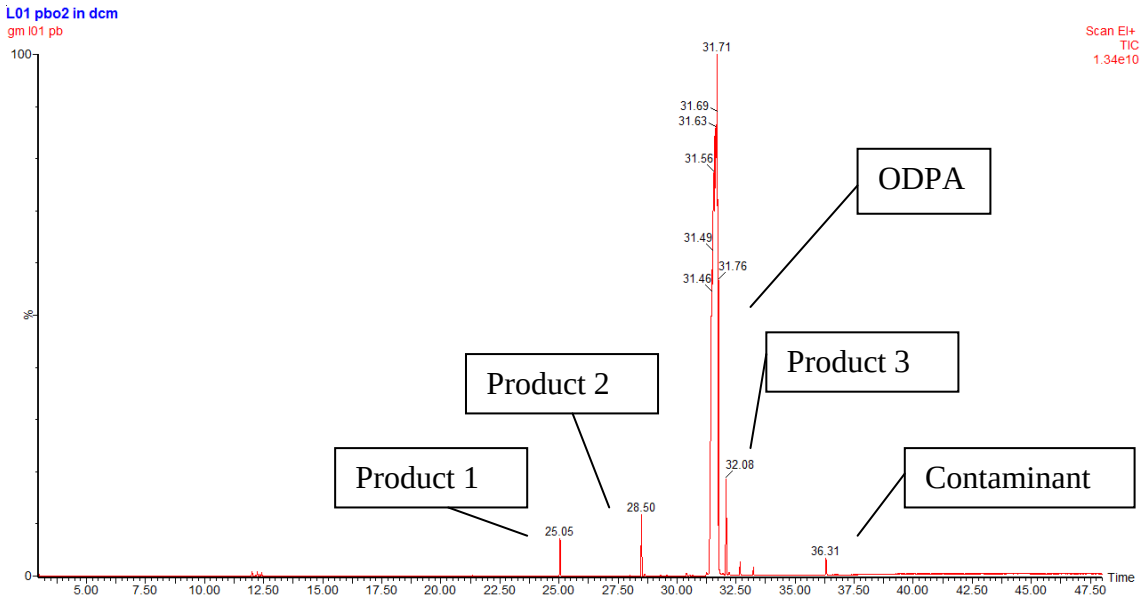

Figure B1 - GC trace of ODPA in DCM reacted with lead dioxide

Three products were identified and one contaminant (left on the column from the OHPP analysis). Product 3 had the same fragmentation pattern as the autoxidation product ODPAP.

Figure B2 – Product 1

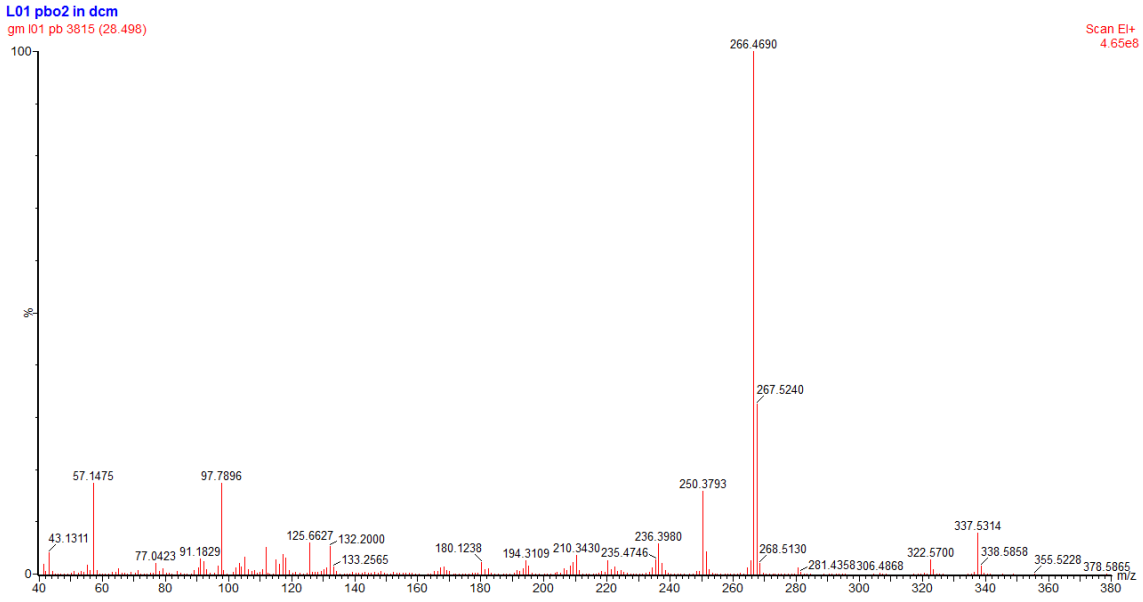

Figure B3 – Product 2

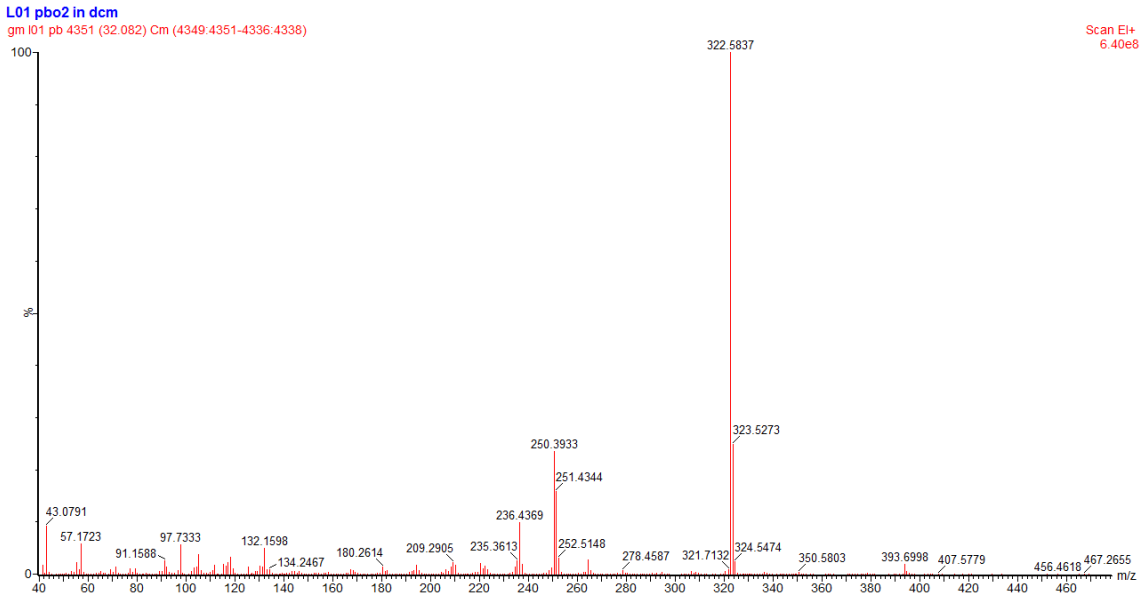

Figure B4 – Product 3

References

[1]Packer, J. E., Slater, T. F. and Willson, R. L., *Nature*, 1979, **278**, 5706, 737-738

[2]Machlin, L. J. and Bendich, A., *The FASEB Journal*, 1987, **1**, 6, 441-445

[3]Rudnick, L. R., *Lubricant Additives Chemistry and Applications 2nd edition*, CRC Press, 2009

[4]Lansdown, A. R., *Lubrication and Lubricant Selection*, Professional Engineering Publishing, 2004

[5]Rasberger, M., *Chemistry and Technology of Lubricants 3rd Edition*, Springer, Dordrecht, 2010

[6]API, *Engine oil licensing and certification system 2007, Appendix E, API Base Oil Interchangeability Guidelines*, API 1509, March 2007

[7]Rizvi, S. Q., *Lubrication Engineering*, 1999, **55**, 4, 33 - 39

[8]Speight, J. G., *The Chemistry and Technology of Petroleum*, CRC press, New York, 2006

[9]Taylor, R. J. and McCormack, A. J., *Industrial & Engineering Chemistry Research*, 1992, **31**, 7, 1731-1738

[10]Miller, S. J. and Zakarian, J. A., *Industrial & Engineering Chemistry Research*, 1991, **30**, 12, 2507-2513

[11]Ingold, K. U., *Chemical Reviews*, 1961, **61**, 6, 563-589

[12]Bateman, L. and Morris, A. L., *Transactions of the Faraday Society*, 1953, **49**, 1026-1032

[13]Curran, H. J., Gaffuri, P., Pitz, W. J. and Westbrook, C. K., *Combustion and Flame*, 1998, **114**, 1–2, 149-177

[14]Benson, S. W., *The Journal of Physical Chemistry*, 1996, **100**, 32, 13544-13547

[15]Benson, S. W., *Thermochemical Kinetics*, Wiley, New York, 1968

[16]Bolland, J. L. and Gee, G., *Transactions of the Faraday Society*, 1946, **42**, 236-243

[17]Russell, G. A., *Journal of the American Chemical Society*, 1957, **79**, 14, 3871-3877

[18]Van-Sickle, D., *Journal of Organic Chemistry*, 1972, **37**, 755 - 760

[19]Scott, G., *Polymer Degradation and Stability*, 1985, 10, 97 - 125

[20]Jensen, R. K., Korcek, S., Mahoney, L. R. and Zinbo, M., *Journal of the American Chemical Society*, 1979, **101**, 25, 7574-7584

[21]Jensen, R. K., Korcek, S., Mahoney, L. R. and Zinbo, M., *Journal of the American Chemical Society*, 1981, **103**, 7, 1742-1749

[22]Pfaendtner, J., *Industrial & Engineering Chemistry*, 2008, 47, 2886 - 2896

[23]Diaby, M., Sablier, M., Negrate, A. L. and Fassi, M. E., *Journal of Engineering for Gas Turbines and Power-Transactions of the ASME*, 2010, **132**, 3,

[24]Diaby, M., Sablier, M., Negrate, A. L., Fassi, M. E. and Bocquet, J., *Carbon*, 2009, **47**, 355 - 366

[25]Hammond, C. J., Lindsay-Smith, J. R., Nagatomi, E. and Stark, M., *New Journal of Chemistry*, 2006, **30**, 741 - 750

[26]Boozer, C., Hammond, G., Hamilton, C. and Sen, J., *Journal of the American Chemical Society*, 1955, **77**, 3233 - 3237

[27]Bickel, A. F. and Kooyman, E. C., *Journal of the Chemical Society (Resumed)*, 1956, 2215-2221

[28]Walker, J. A. and Tsang, W., *The Journal of Physical Chemistry*, 1990, **94**, 8, 3324-3327

[29]Denisov, E. T., *Russian Journal of Physical Chemistry*, 1995, **69**, 4, 563 - 571

[30]Tsang, W., *Journal of the American Chemical Society*, 1985, **107**, 10, 2872-2880

[31]Seakins, P. W., Pilling, M. J., Niiranen, J. T., Gutman, D. and Krasnoperov, L. N., *The Journal of Physical Chemistry*, 1992, **96**, 24, 9847-9855

[32]Jorma, A. S. and Irene, R. S., *Journal of the Chemical Society, Faraday Transactions*, 1997, **93**, 9, 1709-1719

[33]Denisov, E. and Afanas`ev, I., *Oxidation and Antioxidants in Organic Chemistry and Biology*, CRC, 2005

[34]Bolland, J. L. and Have, P. T., *Transactions of the Faraday Society*, 1947, **43**, 201-210

[35]Burton, A., Ingold, K. U. and Walton, J. C., *Journal of Organic Chemistry*, 1996, 61, 3778 - 3782

[36]Bateman, L., *Quarterly Reviews, Chemical Society*, 1954, **8**, 2, 147-167

[37]Denisov, E., *Kinetics and Catalysis*, 2006, **47**, 5, 662-671

[38]Sajus, L., *Oxidation of Organic Compounds*, 75, *Kinetic Data on the Radical Oxidation of Petrochemical Compounds*, AMERICAN CHEMICAL SOCIETY, 1968

[39]Pedersen, C. J., *Industrial & Engineering Chemistry*, 1956, **48**, 10, 1881-1884

[40]Al-Malaika, S., *Polymer Degradation and Stability*, 1991, **34**, 1-3, 1-36

[41]Jensen, R., Korcek, S., Zinbo, M. and Johnson, M., *International Journal of Chemical Kinetics*, 1990, **22**, 1095 - 1107

[42]Mahoney, L. R., Korcek, S., Hoffman, S. and Willermet, P. A., *Industrial & Engineering Chemistry Product Research and Development*, 1978, **17**, 3, 250-255

[43]Ohkatsu, Y. and Nishiyama, T., *Polymer Degradation and Stability*, 2000, **67**, 313 - 318

[44]Yamada, F., Nishiyama, T., Yamamoto, M. and Tanaka, K., *Bulletin of the chemical society of Japan*, 1989, **62**, 11, 3603 - 3608

[45]Le-Tutour, B. and Guedon, D., *Phytochemistry*, 1992, **31**, 4, 1173 - 1178

[46]Zhu, Q., Zhang, X.-M. and Fry, A. J., *Polymer Degradation and Stability*, 1997, **57**, 43 - 50

[47]Lucarini, M. and Pedulli, G., *Chemical Society Reviews*, 2010, **39**, 2106 - 2119

[48]Mahoney, L. R. and DaRooge, M. A., *Journal of the American chemical society*, 1975, **97**, 16, 4722-4731

[49]Bordwell, F. G., Zhang, X.-M. and Cheng, J.-P., *Journal of Organic Chemistry*, 1993, **58**, 6410-6416

[50]Jensen, R. K., Korcek, S., Zinbo, M. and Gerlock, J. L., *Journal of Organic Chemistry*, 1995, **60**, 5396 - 5400

[51]Thomas, J., *Journal of the American Chemical Society*, 1960, 82, 5955 - 5956

[52]Berger, H., Bolsman, T. A. B. M. and Brouwer, D. M., *Developments in Polymer stabilisation, Catalytic inhibition of hydrocarbon autoxidation by secondary amines and nitroxyls*, Elsiver, London, 1983

[53]Denisov, E., *Polymer Degradation and Stability*, 1989, **25**, 209 - 215

[54]Denisov, E. T. and Khudyakov, I. V., *Chemical Reviews*, 1987, **87**, 1313 - 1357

[55]Thomas, J. and Tolman, C., *Journal of the American Chemical Society*, 1962, **84**, 2930 - 2935

[56]Bolsman, T., Blok, A. and Frijns, J., *Journal of the Royal Netherlands Chemical Society*, 1978b, **97**, 12, 313 - 319

[57]Varlamov, V. T., *Seriya Khimkheskaya,*, 1988, **8**, 1750-1755

[58]Varlamov, V. T. and E. T. Denisov, *Russian Chemical Bulletin, International Edition*, 1990, **39**, 4, 657 - 662

[59]Chao, T. S., Hutchison, D. A. and Kjonaas, M., *Industrial & Engineering Chemistry Product Research and Development*, 1984, **23**, 1, 21-27

[60]Gatto, V., Moehle, W., Schneller, E., Burris, T., Cobb, T. and Featherstone, M., *Journal of ASTM International*, 2007, **4**, 7, 1 - 13

[61]Sharma, B. K., Perez, J. M. and Erhan, S. Z., *Energy & Fuels*, 2007, 21, 2408 - 2414

[62]Shanks, D., Al-Maharik, N., Malmström, J., Engman, L., Eriksson, P., Stenberg, B. and Reitberger, T., *Polymer Degradation and Stability*, 2003, **81**, 2, 261-271

[63]Chakraborty, K. B. and Scott, G., *Polymer Degradation and Stability*, 1979, **1**, 1, 37-46

[64]Colclough, T. and Cunneen, J. I., *Journal of the Chemical Society (Resumed)*, 1964,

[65]Korcek, S., Johnson, M., Jensen, R. and Zinbo, M., *Industrial & Engineering Chemistry Product Research and Development*, 1986, **25**, 4, 621-627

[66]Spikes, H., *Tribology Letters*, 2004, **17**, 3, 469 - 489

[67]Scott, R. (2003). Lubricating oil composition. Infineum. USA Patent. **US2003/0162674A1**.

[68]Fujita, H. and Spikes, H. A., *Tribology Transactions*, 2005, **48**, 4, 567-575

[69]Jones, R. B. and Coy, R. C., *A S L E Transactions*, 1981, **24**, 1, 91-97

[70]Fujita, H., Glovnea, R. P. and Spikes, H. A., *Tribology Transactions*, 2005, **48**, 4, 558-566

[71]Topolovec-Miklozic, K., Forbus, T. and Spikes, H., *Tribology Letters*, 2007, **26**, 2, 161-171

[72]Fuller, M., Yin, Z., Kasrai, M., Bancroft, G. M., Yamaguchi, E. S., Ryason, P. R., Willermet, P. A., et al., *Tribology International*, 1997, **30**, 4, 305-315

[73]Barnes, A. M., Bartle, K. D. and Thibon, V. R. A., *Tribology International*, 2001, **34**, 6, 389-395

[74]Burn, A. J., *Tetrahedron*, 1966, **22**, 7, 2153-2161

[75]Willermet, P. A., Carter, R. O., Schmitz, P. J., Everson, M., Scholl, D. J. and Weber, W. H., *Lubrication Science*, 1997, **9**, 4, 325-348

[76]Emanuel, N. M., Maizus, Z. K. and Skibida, I. P., *Angewandte Chemie International Edition in English*, 1969, **8**, 2, 97-107

[77]Punniyamurthy, T., Velusamy, S. and Iqbal, J., *Chemical Reviews*, 2005, **105**, 6, 2329-2364

[78]Waynick, J. A., *Energy & Fuels*, 2001, **15**, 6, 1325-1340

[79]Sarin, A., Arora, R., Singh, N. P., Sarin, R., Malhotra, R. K., Sharma, M. and Khan, A. A., *Energy*, 2010, 2333 - 2337

[80]Taylor, R. I., Mainwaring, R. and Mortimer, R. M., *Mechanical Engineering*, 2005, **219**, 1 - 16

[81]Taylor, R. I. and Evans, P., *Journal Engineering Tribology*, 2004, **218**, Part J,

[82]Qian, Z., Liu, H., Zhang, G. and Brown, D. J., *Knowledge-based intelligent information and engineering systems, Temperature Field Estimation for the Pistons of Diesel Engine 4112*, Springer, 2006

[83]Mahoney, L. R., Otto, K., Korcek, S. and Johnson, M. D., *Industrial & Engineering Chemistry Product Research and Development*, 1980, **19**, 1, 11-15

[84]Piock, W., Hoffmann, G., Berndorfer, A., Salemi, P. and Fusshoeller, B., Strategies Towards Meeting Future Particulate Matter Emission Requirements in Homogeneous Gasoline Direct Injection Engines, *SAE International*, 2011,

[85]Froelund, K. and Yilmaz, E. Impact of Engine Oil Consumption on Particulate Emissions.

[86]de Saint Laumer, J.-Y., Cicchetti, E., Merle, P., Egger, J. and Chaintreau, A., *Analytical Chemistry*, 2010, **82**, 15, 6457-6462

[87]Scanlon, J. T. and Willis, D. E., *Journal of Chromatographic Science*, 1985, **23**, 333 - 340

[88]Hicks, R., *Organic and Biomolecular Chemistry*, 2007, **5**, 1321 - 1338

[89]Yamazaki, T. and Seguchi, T., *Journal of Polymer Science*, 1997, **35**, 2431 - 2439

[90]Taimr, L. and Pospisil, J., *Polymer Degradation and Stability*, 1984, **8**, 67 - 73

[91]West, Z. J., Zabarnick, S. and Striebich, R. C., *Industrial & Engineering Chemistry Research*, 2005, **44**, 10, 3377-3383

[92]Stein, R. A. and Slawson, V., *Analytical Chemistry*, 1963, **35**, 8, 1008-1010

[93]Frisch, M. J. T., G. W.; Schlegel, H. B.; Scuseria, G. E.; Robb, M. A.; Cheeseman, J. R.; Scalmani, G.; Barone, V.; Mennucci, B.; Petersson, G. A.; Nakatsuji, H.; Caricato, M.; Li, X.; Hratchian, H. P.; Izmaylov, A. F.; Bloino, J.; Zheng, G.; Sonnenberg, J. L.; Hada, M.; Ehara, M.; Toyota, K.; Fukuda, R.; Hasegawa, J.; Ishida, M.; Nakajima, T.; Honda, Y.; Kitao, O.; Nakai, H.; Vreven, T.; Montgomery, Jr., J. A.; Peralta, J. E.; Ogliaro, F.; Bearpark, M.; Heyd, J. J.; Brothers, E.; Kudin, K. N.; Staroverov, V. N.; Kobayashi, R.; Normand, J.; Raghavachari, K.; Rendell, A.; Burant, J. C.; Iyengar, S. S.; Tomasi, J.; Cossi, M.; Rega, N.; Millam, J. M.; Klene, M.; Knox, J. E.; Cross, J. B.; Bakken, V.; Adamo, C.; Jaramillo, J.; Gomperts, R.; Stratmann, R. E.; Yazyev, O.; Austin, A. J.; Cammi, R.; Pomelli, C.; Ochterski, J. W.; Martin, R. L.; Morokuma, K.; Zakrzewski, V. G.; Voth, G. A.; Salvador, P.; Dannenberg, J. J.; Dapprich, S.; Daniels, A. D.; Farkas, Ö.; Foresman, J. B.; Ortiz, J. V.; Cioslowski, J.; Fox, D. J. Gaussian 09, Inc., Wallingford CT, 2009.,

[94]Jonsson, M., *The Journal of Physical Chemistry*, 1996, 100, 6814 - 6818

[95]Jursic, B. S., *Journal of Molecular Structure (Theochem)*, 1996, 366, 103 - 108

[96]Jursic, B. S. and Martin, R. M., *International Journal of Quantum Chemistry*, 1996, **59**, 495 - 501

[97]Chandra, A. K. and Uchimaru, T., *International Journal of molecular Sciences*, 2002, 3, 407 - 422

[98]Bakalbassis, E. G., Lithoxoidou, A. T. and Vafiadis, A. P., *The Journal of Physical Chemistry A*, 2003, **107**, 41, 8594-8606

[99]Varlamov, V. T. and Krisyuk, B. E., *Russian Chemical Bulletin*, 2004, **53**, 8, 1609-1614

[100]Alexanderov, A. L. and Marchenko, E. P., *Kinetics and Catalysis*, 1995, **36**, 825 - 830

[101]Gomes, J. R. B., Ribeiro da Silva, M. D. M. C. and Ribeiro da Silva, M. A. V., *The Journal of Physical Chemistry A*, 2004, **108**, 11, 2119-2130

[102]Wasson, J. I. and Smith, W. M., *Industrial & Engineering Chemistry*, 1953, **45**, 1, 197-200

[103]Breese, K. D., *Polymer Degradation and Stability*, 2000, **70**, 89-96

[104]Bagheri, V., Moore, L., Digiacianto, P. and Sanchezrivas, M. (2011). Low Viscosity Oligomer Oil Products, Process And Composition. USA.

[105]Pipiraite, P. P., *Teoreticheskaya i Eksperimental'naya Khimiya*, 1990, **27**, 2, 170 - 178

[106]Mahoney, L. R. and DaRooge, M. A., *Journal of the American chemical society*, 1970, **92**, 13, 4063-4067

[107]Denisov, E. T., *Polymer Degradation and Stability*, 1995, 49, 71 - 75

[108]Kajiyama, T. and Ohkatsu, Y., *Polymer Degradation and Stability*, 2001, **71**, 445 - 452

[109]. "Phenolic Antioxidant - IRGANOX® L 107." from http://www.performancechemicals.basf.com/ev/internet/lubricants/en/content/lubricants/products/antioxidants/irganox_l_107.

[110]Pilar, J., Rotschova, J. and Pospisil, J., *Macromolecular Materials and Engineering*, 1992, **200**, 147 - 161

[111]Pospíšil, J., Habicher, W. D., Pilar, J., Nespurek, S., Kuthan, J., Piringer, G. O. and Zweifel, H., *Polymer Degradation and Stability*, 2002, 77, 531 - 538

[112]Pospíšil, J., Nešpůrek, S. and Zweifel, H., *Polymer Degradation and Stability*, 1996, **54**, 1, 7-14

[113]Pospíšil, J., Nešpůrek, S. and Zweifel, H., *Polymer Degradation and Stability*, 1996, **54**, 1, 15-21

[114]Ershov, V., Volod'kin, A. and Bogdanov, G., *Russian Chemical Reviews*, 1965, **32**, 2, 75 - 93

[115]Hemmingson, J. A. and Leary, G., *Journal of the Chemical Society, Perkin Transactions 2*, 1975, **0**, 14, 1584-1587

[116]Richard, J. P., *Journal of the American chemical society*, 1991, **113**, 12, 4588-4595

[117]Thompson, J. A., Bolton, J. L. and Malkinson, A. M., *Experimental Lung Research*, 1991, **17**, 2, 439-453

[118]Lewis, M. A., Graff Yoerg, D., Bolton, J. L. and Thompson, J. A., *Chemical Research in Toxicology*, 1996, **9**, 8, 1368-1374

[119]Monakhova, T. V., Bogaevskaya, T. A., Shlyapnikov, Y. A., Il'ina, E. A. and Masagutova, L. V., *Infern. J. Polymeric Mater*, 1999, **43**, 249 - 260

[120]Stark, M. S., Wilkinson, J. J., Smith, J. R. L., Alfadhl, A. and Pochopien, B. A., *Industrial and Engineering Chemistry Research*, 2011, **50**, 817 - 823

[121]Kulik, T. V., Barvinchenko, V. N., Palyanytsya, B. B., Lipkovska, N. A. and Dudik, O. O., *Journal of Analytical and Applied Pyrolysis*, 2011, **90**, 2, 219-223

[122]Krokhin, A., *Russian Chemical Bulletin, International Edition*, 1975, **24**, 10, 2334 - 2337

[123]McLafferty, F. and Turecek, F., *Interpretation of Mass Spectra*, University Science Books, 1993

[124]Friedel, R. A., Shultz, L. and Sharkey, A. G., *Analytical Chemistry*, 1956, **28**, 6, 926 - 934

[125]Kingston, D. G. I., Hobrock, B. W., Bursey, M. M. and Bursey, J. T., *Chemical Reviews*, 1975, **75**, 6, 693 - 730

[126]Blanksby, S. J. and Ellison, G. B., *Accounts of Chemical Research*, 2003, **36**, 4, 255-263

[127]Wilkinson, J. (2006). The Autoxidation of Branched Hydrocarbons in the Liquid Phase as models for understanding Lubricant Degredation. York, University of York. **PhD Thesis**.

[128]Steglich, W. and Neises, B., *Angewandte Chemie International Edition in English*, 1978, **17**, 522 - 524

[129]Klemchuk, P. P. and Horng, P.-L., *Polymer Degradation and Stability*, 1991, **34**, 333 - 346

[130]Arstad, B., Nicholas, J. B. and Haw, J. F., *Journal of the American chemical society*, 2004, **126**, 9, 2991-3001

[131]Gatto, V. J., Elnagar, H. Y., Moehle, W. E. and Schneller, E. R., *Lubrication Science*, 2007, 19, 25 - 40

[132]Lai, J. (1996). Synthetic Lubricant Antioxidant from Monosubstituted Diphenylamines. USA Patent, B F Goodrich. **5,489,711**.

[133]Holt, B. (1972). Alkylated Diphenylamines as stabilizers. CIBA. USA, CIBA. **3,655,559**.

[134]Mahoney, L. R., Korcek, S., Willermet, P. A., Jr, E. J. H., Jenson, R. K., Zinbo, M., Kandah, S. K., et al., Time-Temperature Studies of High Temperature Deterioration Phenomena in Lubricant Systems: Synthetic Ester Lubricants., *Ford Motor Company Internal Report*, 1979a,

[135]Hunter, M., Klaus, E. E. and Duda, J. L., *Lubrication Engineering*, 1993, **49**, 6, 492 - 498

[136]Mousavi, P., *Industrial and Engineering Chemistry Research*, 2006, 45, 15 -22

[137]Duangkaewmanee, S. and Petsom, A., *Tribology International*, 2011, **44**, 266 - 271

[138]Gatto, V. and Grina, M. A., *Lubrication Engineering*, 1999, **55**, 1, 11-20

[139]Becker, R. and Knorr, A., *Lubrication Science*, 1996, **8**, 95, 95 - 117

[140]Capp, C. W. and Hawkins, E. G. E., *Journal of the Chemical Society (Resumed)*, 1953, 4106-4109

[141]Ingold, K. U. and Puddington, I. E., *Industrial & Engineering Chemistry*, 1959, **51**, 10, 1319-1324

[142]Varlamov, V. T. and Denisov, E., *Bulletin of the Russian Academy of Sciences*, 1987, 36, 1607 - 1612

[143]Ekechukwu, A. D. and Simmons, R. F., *Journal of the Chemical Society, Faraday Transactions 1: Physical Chemistry in Condensed Phases*, 1988, **84**, 6, 1871-1878

[144]Mahoney, L. R., *Journal of the American Chemical Society*, 1967, **89**, 8, 1895-1902

[145]Ischuk, Y. and Butovets, V., *NLGI Spokesman*, 1991, **55**, 4, 133 - 138

[146]Homma, H., Kuroyagi, T., Izumi, K., Mirley, C. L., Ronzello, J. and Boggs, S. A., *IEEE Transactions on Power Delivery*, 2000, **15**, 2, 796-803

[147]Alfadhl, A. (2008). The Behaviour of Antioxidants in Automotive Engine Oils. York, University of York. **PhD Thesis**.

[148]Lucarini, M., Pedrielli, P., Pedulli, G. F., Valgimigli, L., Gigmes, D. and Tordo, P., *J. Am. Chem. Soc.*, 1999, **121**, 11546 - 11553

[149]Maillard, B., Ingold, K. U. and Scaiano, J. C., *Journal of the American chemical society*, 1983, **105**, 15, 5095-5099

[150]Sedlář, J., Petrúj, J., Pác, J. and Zahradničková, A., *European Polymer Journal*, 1980, **16**, 7, 659-662

[151]Heller, H. J. and Blattmann, H. R., *Pure and Applied Chemistry*, 1973, **36**, 1, 141-162

[152]Bartlett, P. D. and Nozaki, K., *Journal of the American chemical society*, 1947, **69**, 10, 2299-2306

[153]Sheikina, N. A., Petrov, L. V. and Psikha, B. L., *Petroleum Chemistry*, 2006, **46**, 1, 34 - 40

[154]Kerr, J. A., *Chemical Reviews*, 1966, **66**, 5, 465-500

[155]MacFaul, P. A., Wayner, D. D. M. and Ingold, K. U., *The Journal of Organic Chemistry*, 1997, **62**, 10, 3413-3414

[156]Benson, S. W., *Journal of the American Chemical Society*, 1965, **87**, 5, 972-979

[157]Mahoney, L. R., Ferris, F. C. and DaRooge, M. A., *Journal of the American chemical society*, 1969, **91**, 14, 3883-3889

[158]Griva, A. P. and Denisov, E. T., *International Journal of chemical kinetics*, 1973, **5**, 5, 869-877

[159]Pochopien, B. A. (2013). Interactions of Antioxidants with NOx at Elevated Temperatures. York, University of York. **PhD Thesis**.

[160]Ingold, K. U., *Accounts of Chemical Research*, 1969, **2**, 1, 1-9

[161]Schwetlick, K., König, T., Rüger, C., Pionteck, J. and Habicher, W. D., *Polymer Degradation and Stability*, 1986, **15**, 2, 97-108

[162]Bauer, I., Habicher, W. D., Korner, S. and Al-Malaika, S., *Polymer Degradation and Stability*, 1997, **55**, 2, 217-224

[163]Al-Malaika, S., Goodwin, C., Issenhuth, S. and Burdick, D., *Polymer Degradation and Stability*, 1999, **64**, 1, 145-156

[164]Krishnamoorthy, P. R., Vijayakumari, S. and Sankaralingam, S., *IEEE Transactions on Electrical Insulation*, 1992, **27**, 2, 271 - 277

[165]Liston, T. (1980). Synergistic Antioxidant Lubricating Oil Additive Composition. USA Patent, Chevron. **4,200,543**.

[166]Kennerly, G. W. and Patterson, W. L., *Industrial & Engineering Chemistry*, 1956, **48**, 10, 1917-1924

[167]Murphy, C. M., Ravner, H. and Smith, N. L., *Industrial & Engineering Chemistry*, 1950, **42**, 12, 2479-2489

[168]Mahoney, L. R., Mendenhall, G. D. and Ingold, K. U., *Journal of the American chemical society*, 1973, **95**, 26, 8610-8614

[169]Howard, J. A., *Rubber Chemistry and Technology*, 1974, **47**, 4, 976-990

[170]Yamamura, T., Suzuki, K., Yamaguchi, T. and Nishiyama, T., *Bulletin of the chemical society of Japan*, 1997, **70**, 2, 413-419

[171]Pospíšil, J. and Nešpůrek, S., *Polymer Degradation and Stability*, 1995, **49**, 1, 99-110

[172]Pospíšil, J., *Advances in Polymer Science*, 1995, **124**, 87

[173]Denisova, T. G. and Denisov, E., *Petroleum Chemistry*, 2000, **40**, 141-147

[174]Batten, J. J. and Mulcahy, M. F. R., *Journal of the Chemical Society (Resumed)*, 1956, 2948-2959

[175]Morsi, S. E., Zaki, A. B., El-Shamy, T. M. and Habib, A., *European Polymer Journal*, 1976, **12**, 7, 417-420

[176]Morsi, S. E., Zaki, A. B. and El-Khyami, M. A., *European Polymer Journal*, 1977, **13**, 11, 851-854

[177]Kühne, H. and Hesse, M., *Mass Spectrometry Reviews*, 1982, **1**, 1, 15-28

[178]Bernabei, M., Secli, R. and Bocchinfuso, G., *Journal of Microcolumn Separations*, 2000, **12**, 11, 585 - 592

[179]Gambarjan, S., *Berichte der deutschen chemischen Gesellschaft (A and B Series)*, 1925, **58**, 8, 1775-1778

[180]Pratt, D. A., DiLabio, G. A., Valgimigli, L., Pedulli, G. F. and Ingold, K. U., *Journal of the American chemical society*, 2002, **124**, 37, 11085-11092

[181]Denisova, T. G. and Denisov, E. T., *Russian Chemical Bulletin, International Edition*, 2008, **57**, 9, 1858 - 1866

[182]Denison, G. H. and Condit, P. C., *Industrial & Engineering Chemistry*, 1945, **37**, 11, 1102-1108

[183]Denison, G. H. and Condit, P. C., *Industrial & Engineering Chemistry*, 1949, **41**, 5, 944-948

[184]Zabarnick, S. and Mick, M. S., *Industrial & Engineering Chemistry Research*, 1999, **38**, 9, 3557-3563

[185]Low, H., *I&EC Product Research and Development*, 1966, **5**, 1, 80-86

[186]Adam, W., Hückmann, S. and Vargas, F., *Tetrahedron Letters*, 1989, **30**, 46, 6315-6318

[187]Donkers, R. L., Maran, F., Wayner, D. D. M. and Workentin, M. S., *Journal of the American chemical society*, 1999, **121**, 31, 7239-7248

[188]Zhu, X.-Q., Dai, Z., Yu, A., Wu, S. and Cheng, J.-P., *The Journal of Physical Chemistry B*, 2008, **112**, 37, 11694-11707

[189]Strange, H. O., McGrath, J. J. and Pellegrini, J. P., *I&EC Product Research and Development*, 1967, **6**, 1, 33-35

[190]Nishiyama, T., Yamaguchi, T., Fukui, T. and Tomii, K., *Polymer Degradation and Stability*, 1999, **64**, 1, 33-38

[191]Salomon, M. F. (1986). N-Substituted thio alkyl phenothiazines. USA, The Lubrizol Corporation. **4785095**.

[192]Kroger, V., *Topics in Catalysis*, 2007, **42 - 43**, 409 - 413

[193]Smith, N. L., *The Journal of Organic Chemistry*, 1950, **15**, 5, 1125-1130

[194]Fitton, A. O. and Smalley, R. K., *Practical Hetrocyclic Chemistry*, Academic Press, London, 1968

[195]Silva, G. A., Costa, L. M. M., Brito, F. C. F., Miranda, A. L. P., Barreiro, E. J. and Fraga, C. A. M., *Bioorganic & Medicinal Chemistry*, 2004, **12**, 12, 3149-3158

[196]Okafor, C. O., *Dyes and Pigments*, 1985, **6**, 6, 405-415

[197]Okafor, C. O., *Dyes and Pigments*, 1986, **7**, 4, 249-287

[198]Stark, M. S., Gamble, R. J., Hammond, C. J., Gillespie, H. M., Smith, J. R. L., Nagatomi, E., Priest, M., et al., *Tribology Letters*, 2005, **19**, 3, 163 - 168

[199]Lee, P. M., Priest, M., Stark, M. S., Wilkinson, J. J., Lindsay-Smith, J. R., Taylor, R. I. and Chung, S. (2006). Lubricant Degradation, Transport and the effect of extended oil drain intervals on Piston Assembly Tribology. IMechE 50th Anniversary Conference. Tribology 2006: Surface Engineering and Tribology for Future Engines and Drivelines, 12 - 14 July. London.

[200]Stamatis, H., Sereti, V. and Kolisis, F., *Journal of the American Oil Chemists' Society*, 1999, **76**, 12, 1505-1510